



**HAL**  
open science

# Somatosensory gating for brain-computer interfaces using vibro-tactile stimulations

Jimmy Petit

► **To cite this version:**

Jimmy Petit. Somatosensory gating for brain-computer interfaces using vibro-tactile stimulations. Signal and Image Processing. Université de Lille, 2022. English. NNT : 2022ULILB051 . tel-04207062

**HAL Id: tel-04207062**

**<https://theses.hal.science/tel-04207062>**

Submitted on 14 Sep 2023

**HAL** is a multi-disciplinary open access archive for the deposit and dissemination of scientific research documents, whether they are published or not. The documents may come from teaching and research institutions in France or abroad, or from public or private research centers.

L'archive ouverte pluridisciplinaire **HAL**, est destinée au dépôt et à la diffusion de documents scientifiques de niveau recherche, publiés ou non, émanant des établissements d'enseignement et de recherche français ou étrangers, des laboratoires publics ou privés.

UNIVERSITY OF LILLE  
DOCTORAL SCHOOL MADIS

# DOCTORAL THESIS

in partial fulfilment of the requirements for the degree of  
DOCTOR OF THE UNIVERSITY OF LILLE

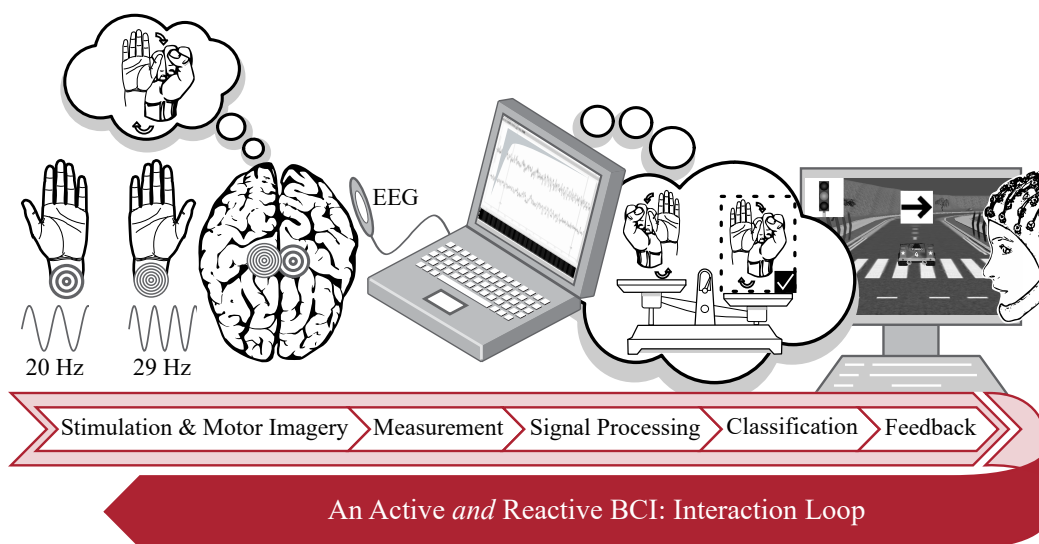
Specialisation:

SIGNAL AND IMAGE PROCESSING

by

JIMMY PETIT

## SOMATOSENSORY GATING FOR BRAIN-COMPUTER INTERFACES USING VIBRO-TACTILE STIMULATIONS



Publicly defended the 6th of December 2022 in front of the doctoral committee composed of:

- |                         |   |                        |
|-------------------------|---|------------------------|
| Mr. Ouriel Grynszpan    | Professor, LISN,<br><i>Université Paris-Saclay</i>  | (Reviewer)             |
| Mr. Fabien Lotte        | Research Director (HDR), Inria Bordeaux Sud-Ouest / LaBRI,<br><i>Université de Bordeaux</i> | (Reviewer)             |
| Mr. Arnaud Delval       | Professor Dr., Département de Neurophysiologie Clinique,<br><i>Université de Lille</i>      | (President & Examiner) |
| Ms. Andrea Kübler       | Professor Dr., Institut für Psychologie,<br><i>Julius-Maximilians-Universität Würzburg</i>  | (Examiner)             |
| Mr. José Rouillard      | Associate Professor (HDR), CRISAL,<br><i>Université de Lille</i>                            | (Co-Supervisor)        |
| Mr. François Cabestaing | Professor, CRISAL,<br><i>Université de Lille</i>  | (Co-Supervisor)        |

UNIVERSITÉ DE LILLE  
ÉCOLE DOCTORALE MADIS

# THÈSE DE DOCTORAT

pour obtenir le grade de  
DOCTEUR DE L'UNIVERSITÉ DE LILLE

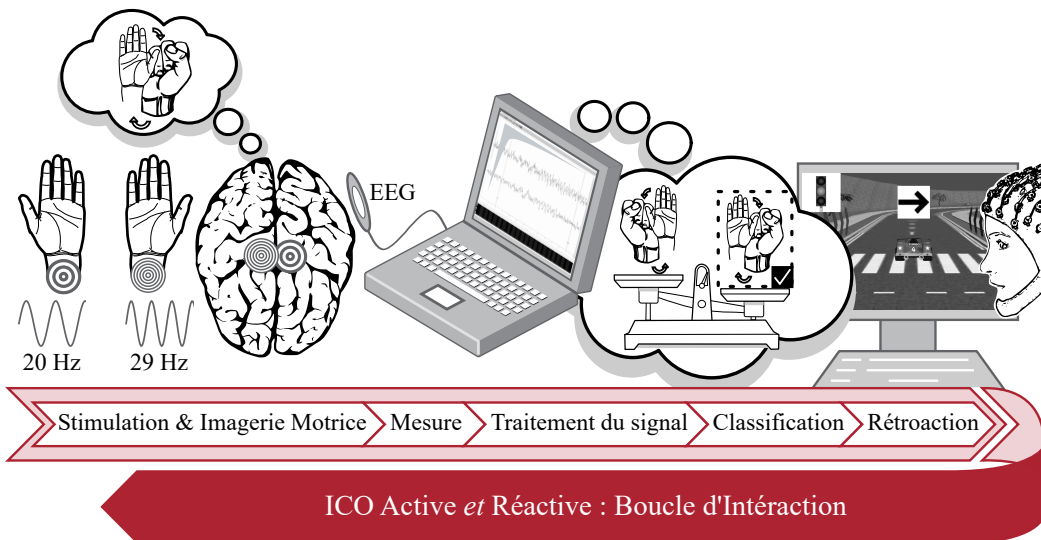
Spécialité :

TRAITEMENT DU SIGNAL ET DES IMAGES

par

JIMMY PETIT

## FILTRAGE SOMESTHÉSIQUE POUR DES INTERFACES CERVEAU-ORDINATEUR UTILISANT DES STIMULATIONS VIBRO-TACTILES



Thèse soutenue publiquement le 6 décembre 2022 devant le jury composé de :

M.	Ouriel Grynszpan	Professeur, LISN, <i>Université Paris-Saclay</i>	(Rapporteur)
M.	Fabien Lotte	Directeur de Recherche (HDR), Inria Bordeaux Sud-Ouest / LaBRI, <i>Université de Bordeaux</i>	(Rapporteur)
M.	Arnaud Delval	Professeur Dr., Département de Neurophysiologie Clinique, <i>Université de Lille</i>	(Président & Examineur)
Mme.	Andrea Kübler	Professeure Dr., Institut für Psychologie, <i>Julius-Maximilians-Universität Würzburg</i>	(Examinatrice)
M.	José Rouillard	Maître de Conférence (HDR), CRISAL, <i>Université de Lille</i>	(Co-Directeur)
M.	François Cabestaing	Professeur, CRISAL, <i>Université de Lille</i>	(Co-Directeur)

*Dedicated to the one with whom I wish to grow grey hair and  
climb the towering staircase to the distant heights...*



Professor McGonagall turned into a cat.

Harry scrambled back unthinkingly, backpedalling so fast that he tripped over a stray stack of books and landed hard on his bottom with a *thwack*. His hands came down to catch himself without quite reaching properly, and there was a warning twinge in his shoulder as the weight came down unbraced.

At once the small tabby cat morphed back up into a robed woman. "I'm sorry, Mr. Potter," said the witch, sounding sincere, though the corners of her lips were twitching upwards. "I should have warned you."

Harry was breathing in short gasps. His voice came out choked. "*You can't DO that!*"

"It's only a Transfiguration," said Professor McGonagall. "An Animagus transformation, to be exact."

"You turned into a cat! A *SMALL* cat! You violated Conservation of Energy! That's not just an arbitrary rule, it's implied by the form of the quantum Hamiltonian! Rejecting it destroys unitarity and then you get FTL signalling! And cats are *COMPLICATED!* A human mind can't just visualise a whole cat's anatomy and, and all the cat biochemistry, and what about the *neurology*? How can you go on thinking using a cat-sized brain?"

Professor McGonagall's lips were twitching harder now. "Magic."

"Magic isn't enough to do that! You'd have to be a god!"

— *Harry Potter and the Methods of Rationality*,  
Chapter 2 – *Everything I Believe Is False*,  
by Eliezer Yudkowsky, a.k.a. Less Wrong.

## ACKNOWLEDGMENTS

---

I wish to deeply thank the members of the jury for taking part in my PhD Defence and their numerous questions. I have enjoyed the discussions that followed. I want to extend my utmost gratitude to Fabien Lotte and Ouriel Grynzpan, for the precious time they took to review my manuscript and for their comprehensive reports. I want to thank Arnaud Delval, the president of the jury, and thanks to whom we recorded our data in the Hospital of Lille using their great hardware. In addition, I want to deeply thank Andrea Kübler, for having me in her lab for three months during this PhD. It truly was a pleasure.

*Je souhaite également remercier mes directeurs de thèse, José, ta façon de te mettre à la place des relecteurs, tes conseils et ta réactivité, malgré un agenda d'enseignement très chargé, m'ont permis de m'améliorer considérablement au cours de ces trois années, merci beaucoup. Enfin, François, un grand merci pour tout. Ta bonne humeur, ton humour, tes conseils, et ton investissement hors normes : merci pour ces pages de calcul reçues parce que « tes étudiants en TP avançaient tout seuls » à peine avons-nous commencé à regarder la CCA de plus près. Merci aussi pour tout le reste, toutes ces anecdotes et histoires autour de l'université, tous ces repas partagés et ces pauses-café avec les collègues du*

P2. *Merci. Ce fut pour moi un plaisir et un honneur que d'avoir pu préparer ma thèse sous votre tutelle conjointe, merci.*

*Pour rester dans l'environnement recherche, je souhaite également remercier les personnes qui m'ont mis le pied à l'étrier lors de mes premiers stages en BCI à L'INRIA Rennes. Merci à Anatole Lecuyer, Ferran Argelaguet et Hakim Si-Mohammed, le trio d'encadrement de choc. J'ai beaucoup appris grâce à vous ! J'ai encore des souvenirs agréables des discussions scientifiques sur la marche à suivre lors de nos travaux. J'en profite pour remercier chaleureusement Camille Jeunet pour ses précieux conseils à l'époque déjà. Merci à tous.*

*Mes remerciements vont pareillement à toute l'équipe BCI, y compris Hakim qui à rejoins l'équipe il n'y a pas très longtemps (félicitations !). Jean-Marc et Marie-Hélène, merci pour votre honnêteté et tous vos précieux conseils, je garderai longtemps en mémoire notre passage à Paris pour Handicap. Je souhaite également remercier Camille Bordeau et Philémon Berne, vous avez été de merveilleux stagiaires avec qui travailler, merci.*

*Je souhaite également remercier les autres représentants des doctorants, ce fut un plaisir de faire partie du comité d'organisation avec vous, pour organiser nos journées pour les autres doctorant.e.s de l'ED. Je tiens aussi à remercier nos secrétaires de l'ED. Malika, Tram, et Aurore, pour votre aide lors de l'organisation de nos journées, mais aussi votre travail formidable et votre constante bonne humeur. Merci également à Ludovic, pour avoir toujours pris le temps de répondre à toutes mes questions.*

*Merci également aux collègues et amis du P2 rencontrés au début de ma thèse, je pense en particulier à Olivier, Christophe, et Luc, merci pour tous ces bons moments passés au RU, avant toutes les difficultés liées au COVID. Ce furent mes premiers mois lors de la thèse et votre accueil très chaleureux a été pour moi un vrai plaisir.*

*Il est grand temps de remercier tous les amis de « chez sigma ». Barbara, Jérémie, nous n'avons peut-être jamais partagé le même bureau, mais c'était tout comme. Merci pour votre accueil, votre humour, et tous les fous rires. Votre support m'a beaucoup apporté tout au long de ma thèse. Je vous remercie du fond du cœur et je vous dis à bientôt. Pour continuer dans mes supports indispensables lors de ma thèse, Pierre P. : « merci pour tout ». Clémence, merci pour tes précieux conseils lors de la préparation de mes slides, merci pour tes encouragements, ils ont été d'or pour moi. Merci à toute l'équipe, permanents ou non, pour ne citer que quelques noms : Ouafae, Diala, Rony, Maxime, Maxence, Markus, Etienne, Hugo, Jan, Michaël, Pauline, Vincent, PA, Rémi, John, Jenny, Patrick et Pierre C. Je n'oublierai jamais votre accueil, votre bonne humeur, tous nos rires et vos encouragements, ils m'ont beaucoup aidé, en particulier lors de la dernière ligne droite de ma thèse. Merci aux anciens sigmas, tous aussi importants, et qui ont commencé de nouvelles aventures : Solène, Quentin, Anh-Thu, Arnaud, et Xiaoyi. J'ai adoré mon séjour à CRIStAL grâce à vous !*

*En plus de sigma, j'aimerais remercier quelqu'un de très spécial, merci à toi Vénancia, pour toutes ces pauses-café et tes sourires radieux chaque matin, tu es formidable.*

I also wish to thank Matthias and Loïc for helping me so much during my stay in Professor Kübler's lab. Thanks also to my friends and best coworkers Eva and Maria, it was nothing less than a delight to share your office for three months. Thanks also to the many others from the team, you are fantastic, I had such an enjoyable stay thanks to you all! I would also like to deeply thank some of my long-time friends. Annika, Samuel, and Brian, we met during our respective internships at MPI. Now you too are almost finished with your PhD, what an amazing journey! I wish you good luck with yours! Thank you for all the fun and travels we've had so far, I hope to do many more!

*Merci du fond du cœur aussi à Marianne, Hervé et JB pour votre amitié et accueil chaleureux. Merci à toi Olivier, merci pour tout.*

*Finalement, un grand merci à mes frères et mes parents, sans qui je ne serais pas là. Merci.*

A brain–computer interface (BCI) is a system aiming at differentiating various mental states of a user to translate them into commands for an external device. A category of BCI named reactive BCIs uses automatic brain responses from sensory stimulation of the user to differentiate between multiple mental states. An evoked potential is the manifestation, as a temporal variation of the electric potential, of the brain response. Our work focuses on evoked potentials from the somatosensory cortex. It is a component of the somatosensory system, which is the neural structure network that permits, among other things, the perception of skin-related sensations. A mechanical action applied on the skin evokes a specific brain response in the somatosensory cortex contralateral to the stimulation. Scalp electroencephalography (EEG) allows for measuring this response yielding a so-called somatosensory-evoked potential (SEP). When the mechanical action is periodic and maintained, which is the case of a vibration, the SEP is also periodic with the same frequency and is called steady-state SEP (SSSEP).

Specific mental activities, such as attention focusing, modulate the amplitude and/or phase of the SSSEP. This volitional modulation constitutes a significant marker of mental activity commonly used in a BCI exploiting SSSEP. In this thesis, we study a new marker based on the somatosensory gating capacity of the brain. Somatosensory gating is the capacity of the brain to filter out irrelevant or repetitive stimuli received from the somatosensory system, in our case, the mechanical receptor of the skin. The somatosensory gating is a particular case of sensory gating which is more general. The sensory gating can occur with the sight or the hearing as well, but in our work we focus on the somatosensory gating. The latter phenomenon was reported in the literature. For instance, a decrease in the amplitude of an electrically-evoked SSSEP can be observed during a motor imagery (MI) task.

BCIs architectures are often depicted as a loop. In the first step, the user performs a mental task that is supposed to generate a specific brain activity pattern while their brain activity is being monitored. Follows a signal processing step to extract the key characteristics of the aforementioned specific brain activity pattern. A classifier then identifies it among multiple labelled brain activity patterns. Feedback is finally provided to the user based on the classification results. It allows the user to react accordingly and for the loop to start again. In this thesis, we investigate each step of this loop for a BCI combining SSSEP and MI. Indeed, we study the characteristics of SSSEPs and methodological constraints resulting from their usage. We study the theoretical aspects of SSSEPs on synthetic data to identify adequate signal processing for our application. We investigate the human-related aspects of the interaction with our system. We primarily focus on the relationship between the performance of the BCI and the user’s perceived usability or mental workload.

\* an extended abstract in French is available in appendix [d](#). *Un résumé étendu en français est disponible en annexe [d](#).*

Finally, we wish for our system to be usable by individuals with heavy motor impairment, such as in a locked-in syndrome state. The somatosensory approach was selected since it exploits the user's sense of touch, which can be viable for some pathology of locked-in individuals. In addition, contrary to attention focusing which can gather information from a single limb at a time, motor imagery could easily be performed with multiple limbs at once. This property of motor imagery leads us to use a combination of SSSEP and MI as it could increase the number of available commands for our BCI system.

## CONTENTS

---

Dedication	iii
Acknowledgments	iv
Abstract	vii
1 General Introduction	1
1.1 Challenges in BCI	2
1.1.1 Data Contaminations	2
1.1.2 <i>Inter</i> and <i>Intra</i> -Individual Variability	3
1.2 PhD Goal: an Active <i>and</i> Reactive BCI	4
1.3 Scientific Contributions	5
1.4 Chapter-by-Chapter Overview	6
2 EEG-based BCIs Exploiting SSSEPs: a Literature Review	11
2.1 Introduction	12
2.2 Methodology	14
2.2.1 Identification stage	14
2.2.2 Screening stage	15
2.2.3 Inclusion stage	15
2.3 Effects of stimulus characteristics on the evoked potential	16
2.3.1 Methods to elicit an SSSEP	16
2.3.2 SEP and SSSEP characteristics	17
2.3.3 Determination of user-specific frequencies	18
2.3.4 Determination of user-specific frequencies in the literature: main results and comments	20
2.4 SSSEP-based BCI: algorithms and performances	25
2.4.1 Turning SSSEP into a usable BCI command	26
2.4.2 Synthesis of SSSEP-based BCIs: introduction	26
2.4.3 Signal processing and feature extraction	29
2.4.4 Synthesis of SSSEP-based BCIs: main results	32
2.5 Conclusion	37
3 Amplitude Estimation of Sinusoidal Components in EEG-based BCIs	39
3.1 Introduction	40
3.2 Assumptions and signal models	41
3.2.1 Brain sources and EEG measurement channels	41
3.2.2 Signal-to-noise ratio	42
3.2.3 Spatial filtering	43
3.3 Compared algorithms	45
3.3.1 Lock-in Amplifier - LiA	45
3.3.2 Canonical Correlation Analysis - CCA	46
3.3.3 Two-Block Mode A Partial Least Squares - PLS	47
3.4 Comparison on synthetic EEG data	48
3.4.1 Synthetic EEG data	48

3.4.2	Amplitude estimation on synthetic data	49
3.5	Comparison on real EEG data	52
3.5.1	Experimental protocol and real EEG data	52
3.5.2	Amplitude estimation on real EEG data	53
3.6	Discussion	54
3.6.1	Results on synthetic EEG data	54
3.6.2	Results on real EEG data	56
3.7	Conclusion	56
4	KMI for Selective Amplitude Modulation of SSSEP by Gating	59
4.1	Introduction	60
4.2	Rationale	61
4.3	Materials and methods	63
4.3.1	Experimental study	63
4.3.2	Participants	63
4.3.3	Hardware and software	64
4.4	Screening: description	64
4.4.1	Experimental procedure	65
4.4.2	EEG data analysis	66
4.4.3	Frequencies of stimulation selection procedure	67
4.5	Screening: results	68
4.5.1	RAI distributions	68
4.5.2	Selection of frequencies of stimulation	68
4.6	Somatosensory gating: description	69
4.6.1	Experimental procedure	70
4.6.2	EEG data analysis	71
4.6.3	Behavioural questionnaires	72
4.7	Somatosensory gating: results	72
4.7.1	Temporal visualisation of SSSEP's amplitude	72
4.7.2	Behavioural data	73
4.8	Discussion	75
4.9	Conclusion	76
5	Somatosensory Gating Effect: an Online & Offline Classification	77
5.1	EEG Signal Processing and Algorithm	78
5.1.1	Preprocessing, Signal Processing, and Feature Extraction	78
5.1.2	Classification Accuracy Computation	79
5.2	4-Class Classification Results	79
5.3	2-Class Classification Results	81
5.4	Discussion	82
5.5	Conclusion	83
6	Design and Study of Two Applications Controlled by a BCI	85
6.1	Introduction	86
6.2	Application Design	87
6.2.1	Description	87

6.2.2	Definition of “Good” or “Bad” Command: Specific Case of SokoBCI	90
6.2.3	Inertia and “Punitiveness”	90
6.3	Test of the Applications	91
6.3.1	Protocol	91
6.3.2	Behavioural Data - Results	92
6.3.3	Relationship Between Performance and SUS	95
6.3.4	Questionnaire, Comments, and Debriefing Interview - Results	96
6.4	Conclusions, Limitations, and Future Works	97
7	Discussions, Conclusions & Perspectives	99
7.1	Our Contributions & Position in the State-of-the-Art	99
7.1.1	SSSEP characteristics and State-of-the-Art of SSSEP-based BCIs – Chapter 2	99
7.1.2	Algorithm Comparison for Sinusoidal Amplitude Estimation in SSSEP-based BCIs – Chapter 3	100
7.1.3	Somatosensory Gating-related Hypothesis Testing and Measurement of BCI Performances – Chapter 4 and 5	100
7.1.4	Study of User-related Aspects – Chapter 6	101
7.2	Discussions: A long road ahead of us	102
7.3	Conclusions	103
7.4	Perspectives	104
7.4.1	Short-term perspectives: In this PhD we also...	104
7.4.2	Mid and Long-Term Perspectives	105
7.4.3	Last Words	107

## Appendix

A	Individual Screening Procedure Results Visualisations	111
B	Individual Somatosensory Gating Results Visualisations	115
C	Poster	119
D	Résumé étendu – <i>in French</i>	121
E	Protocole EDICOPES – <i>in French</i>	127
	List of Figures	173
	List of Tables	178
	List of Acronyms	181
	Publications	185
	Bibliography	187





Brain–Computer Interface (BCI) is simultaneously an aged concept and a vivid field of research\*. Jacques J. Vidal first conceptualises it in 1973 as a direct brain-computer communication or “utilizing the brain signals in a man-computer dialogue” [106]. The key word being “dialogue”: a mutual exchange of information, which requires some mutual understanding. Modern BCIs are based on the idea that the user and the computer must adapt to each other, the former through continuous training and the latter through adaptive methods and classifier training.

*\* it might sound good, but it is also true for many, many research fields...*

It is only later refined as a communication system in Jonathan R. Wolpaw *et al.* in 2002 [113]. BCI is then defined as a system that allows messages or commands to be exchanged from a user to the world relying only on brain activity as the source of information. As the field of research grows throughout the last half-century, BCIs are often separated into three different categories.

The first one, *active BCIs*, relies on the performance of specific mental tasks. The second one, *reactive BCIs*, uses external stimulations. By stimulating one or more human senses coupled with an attention modulation of the user, the latter can produce discriminative patterns of brain activity. Active and reactive BCIs both aim at giving control of a peripheral device to a user to perform an action through the device such as communicating, moving... The third category, *passive BCIs* [115], aims to monitor a user’s cognitive state, such as stress level or workload, for example. One application of passive BCIs is to adapt the environment or the interface to the state of mind of a patient in real time. Contrary to active and reactive BCIs, the user does not intentionally provoke a command in passive BCIs. In this thesis, we focus on the former two categories of BCIs.

Active BCIs can be subdivided into two main paradigms. The first one is named slow cortical potential-based BCI [9]. It uses cortical activity usually occurring at frequencies lower than 1 Hz\*. In this paradigm, the user is asked to find a mental strategy that voluntarily causes negative and positive cortical potential shifts with respect to a reference period. To this end, they receive feedback on the current trend of their brain activity and have to find a strategy that positively or negatively impacts it. However, this approach requires a very long user training period ranging from several weeks to months [10]. Indeed, the user must adapt intensively to the computer whereas the latter must not. In order to alleviate such drawback, a shift in the paradigm has been investigated.

*\* hence the adjective “slow”*

The second standard paradigm in active BCIs is mental-imagery-based BCI. Pfurtscheller *et al.* in 1997 [82] show that a mental imagery task such as motor imagery (MI) of the limbs creates specific brain activity. During MI involving one upper limb, the authors measure an event-related desynchronisation (ERD)\* contralateral to the limb side. They also measure an event-related synchronisation (ERS)\* shortly after the end of the mental task. In this paradigm, the computer adapts

*\* a decrease of power within a frequency band*

*\* an increase of power within a frequency band*

to the user by selecting the most discriminative frequency band. It is highly user-dependent and has to be calibrated. It usually varies within the  $\alpha$  and  $\beta$ -band\* oscillations [83]. Active BCIs also benefit from several advantages. They can be self-paced, meaning the user can elicit a command whenever they choose. They also do not rely on sight, except sometimes for the feedback. This is an undeniable advantage, especially since the individuals who can benefit the most from BCIs are severely motor-impaired patients, suffering from amyotrophic lateral sclerosis or spinal muscular atrophy for instance. Patients at an advanced stage of the disease often can no longer control their gaze.

\*  $\alpha$ -band  $\approx$   
8 to 12 Hz  
 $\beta$ -band  $\approx$   
12 to 30 Hz

To this day, a vast majority of reactive BCIs paradigms are based on sight. Such is the case of one of the first paradigms: the P300 Speller described by Farwell and Donchin [27]. A matrix of letters is displayed in front of a user. Random rows or columns of letters are highlighted for a short time *e. g.* 125 ms. When the user focuses their gaze on one letter, an event-related potential\* can be measured approximately 300 ms after the highlight onset of the letter. Crossing the information over several iterations allows the chosen letter to be narrowed down.

\* a transient positive  
or negative deflection  
in the measurement.  
A P300 is a positive  
deflection.

Reactive BCIs, such as the one described above, rely on rather precisely defined brain responses which can be easier to identify and measure than in active BCIs. As a result, they have the advantage of not requiring much training while being reliable. However, reactive BCIs vastly rely on sight and therefore work under the hypothesis that the user has control over their gaze. These paradigms are thus unusable for patients who suffer from severe motor impairment and have lost gaze control.

## 1.1 CHALLENGES IN BCI

Brain activity can be measured using electroencephalography (EEG), magnetoencephalography, functional near-infrared spectroscopy, or functional magnetic resonance imaging. EEG is a instrument that can measure the electrical activity resulting from the synchronous activation of a large population of neurons. EEG is the most commonly used tool for measuring brain activity in BCIs since it is affordable and has high temporal resolution.

### 1.1.1 Data Contaminations

One of the first challenges in BCI comes from contaminating sources related to brain activity measurements and signal processing. The most common noise source when using EEG is the contamination from muscle activity or electromyography (EMG) activity. Goncharova *et al.* conclude, in 2003, that frontal and temporal muscles EMG spectra can have a peak of power resembling the  $\beta$  band activity peak in the EEG [33]. The authors observe that the effect has a substantial between-

individuals variability. In addition, it is often more prominent on the EEG's peripheral scalp, near the active muscle. As a result, this confounding factor may impair the performance of mental imagery-based BCI in ecological conditions.

Another source of noise in EEG comes from volume conduction [101]. In a few words, volume conduction arises in the tissues and bones between the source of activity and the electrode. It results in spatial spread of electrical activity from a source of activity on the scalp beneath the electrode. The resulting measurement is an intertwining of close but potentially disassociated sources of activity. Applying a spatial filter can help recover the activity near the electrodes. Current source density filters, also known as surface Laplacian filters, are often used to that end [57, 67].

Lastly, the final issue comes from an overuse of filters. Currently available filters are often hardware-based, placed within the amplifier of the EEG, and software-based, placed in the analysis pipeline of the studied phenomenon. However, causal filters, which allow a real-time compatible implementation of the system, can delay and spread the apparition of some common transient or sustained evoked-potentials and have to be used with care [19].

### 1.1.2 Inter and Intra-Individual Variability

Recurrent challenges in BCI are related to between-individual variability [35] and the within-individual variability [34]. Between-individual variability is mainly eminent in active BCIs. The deliberate pattern of brain activity can be quite specific and very different from individual to individual. For example, as we previously mentioned with the MI of the limb, the most discriminative frequency band can vary greatly between individuals [82].

Within-individual variability refers to changes in one's neurophysiological state that affect the measurements and, possibly, the BCI performance through time. In their work, Grosse-Wentrup *et al.* [34], provide a review of the performance variation in sensorimotor rhythm-based BCI, or SMR-based BCI. SMR refers to the variation of power in the  $\mu$ -band\* over the somatosensory cortex during MI [5]. SMR-based BCIs are examples of active BCIs using MI. Grosse-Wentrup *et al.* observe that the inter-trials accuracy of individuals with good performances is highly variable even within a short time window such as 10 min. Nevertheless, such variability is not limited to EEG-based BCI only.

The authors of [42] use micro electrode arrays\* to model mapping between the somatosensory cortex and regions of the hand. They use electric stimulation patterns delivered to the cortex using a single electrode of the matrix. Additionally, they model mapping between the electrical stimulation pattern of the cortex and somatosensory-related sensations (*e.g.* heat or pressure) on the corresponding hand region.

\*  $\mu$ -band  $\approx$   
7 to 11 Hz

\* matrix of implanted electrodes installed on the cortex, capable of measuring the action potentials from an individual to a small group of neurons.

The authors report the need to perform daily calibrations as the former model can change everyday.

### 1.2 PHD GOAL: AN ACTIVE AND REACTIVE BCI

This PhD is motivated by the desire to provide a BCI to patients with severe motor impairments, potentially without gaze control. Therefore, we aim to combine an active and reactive BCI combining their advantages: not requiring the user's gaze control, based on easy-to-detect automatic brain responses and requiring as little training as possible.

To avoid the disadvantage of a sight-based BCI, we rely on a different sensory system: the somatosensory system. The somatosensory system can be defined as the network of neural structures that allow the perception of touch, temperature, body position, and pain. More precisely, we use an evoked brain response called steady-state somatosensory-evoked potential or SSSEP. SSSEP is the measurement of the increase of activity at the frequency of stimulation used to stimulate the somatosensory system mechanically or electrically. It is located over the primary somatosensory cortex and is contralateral to the stimulation [96, 102, 103]. Even though SSSEP's amplitude depends on the stimulation frequency [60] it has the advantage of being relatively stable through time [12].

To implement an SSSEP-based BCI, we must ask the user to perform a voluntary task that modifies a measurable characteristic of the SSSEP. The standard approach in the literature is to use attention focusing. When the user focuses their full attention on one vibration, the corresponding SSSEP's amplitude increases [32]. However, a natural limitation of this approach is the number of possible commands. Focusing one's full attention on the vibration appears feasible only on one location at a time. So, assuming an ideal scenario, the BCI would be limited by the number of vibro-tactile devices. We propose the use of MI to bypass this limitation. One can imagine performing MI with one or more limbs simultaneously, thus multiplying the number of available commands to map.

In fact, MI is a mental task that may also modulate the amplitude of SSSEPs. The "sensory gating" phenomenon is defined as the capacity of the brain to filter out irrelevant or repetitive stimuli coming from the environment [24]. During actual moves or imagined movements, the somatosensory gating capacity of the brain filters out somatosensory-related information [107]. Therefore, the stimulation perceived from the user's arm could also be reduced by gating, which in turn reduces the SSSEP's amplitude. In addition, as mentioned before, the MI produces an ERD contralateral to the imagined limb shortly followed by an ERS [82]. The effect of the ERD might add up to the gating, which can result, in turn, in a more substantial effect size than both phenomena

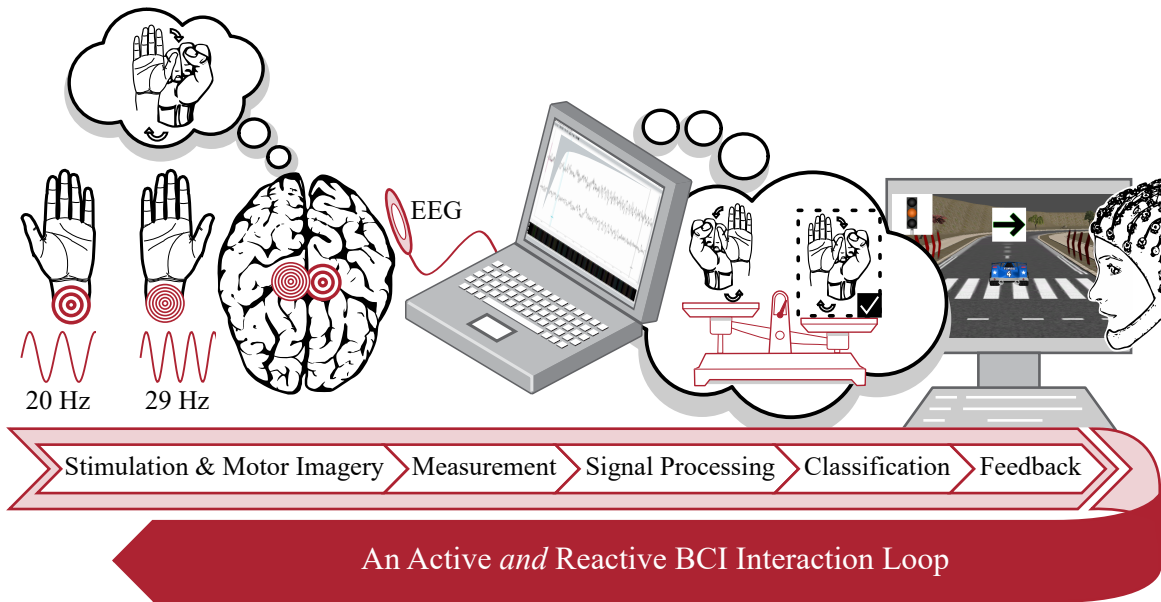


Figure 1.1 : Illustration of the interaction loop of the proposed active and reactive BCI.

alone. We summarise in figure 1.1 our proposed BCI, using the common interaction loop design of online BCI [52].

Finally, considering the above challenges, this combination could mitigate some problems. A reactive BCI benefits from a rather stable feature of interest that is often easier to measure and define. In our case, it is the SSSEP's amplitude. This stability could mitigate some drawbacks of an active BCI, such as the within-individual variability. In turn, the MI could multiply the number of commands of standard SSSEP-based BCI.

### 1.3 SCIENTIFIC CONTRIBUTIONS

This thesis addresses the following questions:

- How to induce an SSSEPs, and what are their characteristics?
- What are the methodological constraints and how to address them when using an SSSEP-based BCI?
- How to estimate an SSSEP oscillation amplitude?
- Can one measure a decrease in SSSEP's amplitude during MI when using simultaneous stimulations?
- If so, is this decrease present only on the imagined limb? In other words, is it contralateral to the limb for which the user imagines a movement while receiving a vibration?
- Is this phenomenon reliable and strong enough for a successful\* BCI implementation limited to a single session?
- Is such a system even acceptable for the user?
- What degree of efficiency has to be achieved to that end?

\* different from a random process beyond reasonable doubt, i. e. better than random.

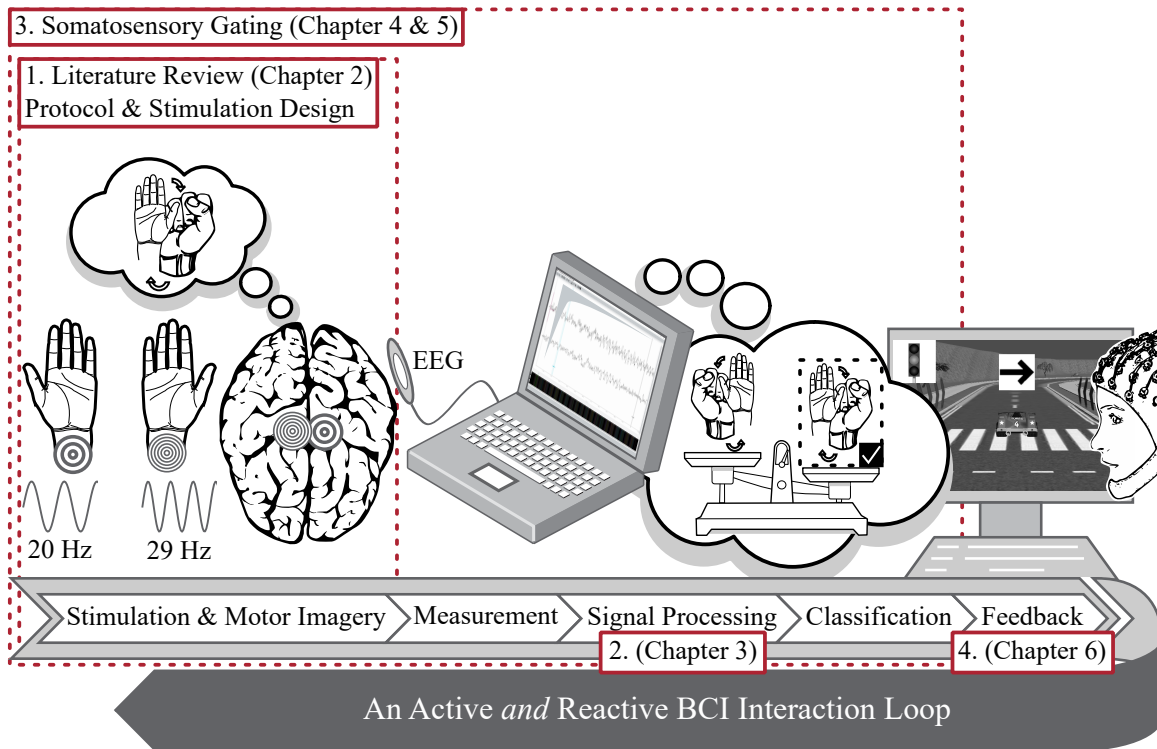


Figure 1.2 : Thesis contributions overview. This figure will be used as a roadmap for this dissertation [43, 75].

We firstly produce a literature review of SSSEPs and their usage in EEG-based BCIs, see contribution 1. in figure 1.2. It allows us to design an experimental protocol and screening procedure to identify the frequency of stimulation to use with our subjects.

Additionally, we contribute to the literature review by studying different signal processing methods. We primarily focus on the problem of estimating a sinusoidal component's amplitude for EEG-based BCI exploiting SSSEP, see contribution 2. in figure 1.2.

We exploit the former results from contributions 1. and 2. by assessing the presence and the effect size of somatosensory gating. We generate gating through MI of one or two limbs while applying simultaneous stimulation on the wrists. In addition, we attempt a first gating-based classification using a simple and standard approach, see contribution 3. in figure 1.2.

Finally, we design and study two BCI applications for our system. In particular, we study the relationship between the BCI performance and the perceived usability of the system, see contribution 4. in figure 1.2.

#### 1.4 CHAPTER-BY-CHAPTER OVERVIEW

We have written an article-based manuscript. On the front page of each chapter, the mention "Related Work" followed by a bibliography



item marks the fact that this chapter results from the insertion of an article submitted to peer review before publication or that we already published during this PhD. We insert the article as faithfully as possible to the original work, may it be published or under review. To standardise the manuscript, we updated the layout of the articles and possibly made the following minor changes to the articles: typos corrections, figure-size management, figures' labels inserted in the text using the word "figure" instead of the journal or conference template preference, and harmonisation of font usage inside the figures.

In the following, we present a chapter-by-chapter summary of the manuscript.

#### *Chapter 2 – EEG-based BCIs Exploiting SSSEPs: a Literature Review*

We review the literature on SSSEP and its usage in EEG-based BCIs. It allows us to describe the main characteristics of SSSEPs. In addition, the analysis of standard calibration protocols allowing the tuning of stimulation to maximise SSSEPs' amplitudes allows us to identify and integrate this procedure into our protocol. Secondly, we present the standard signal processing and data classification algorithms and the obtained classification performance. Additionally, we observe that the profile of the relationship between the frequency of stimulation and the SSSEP's amplitude are highly individual-dependent. Therefore, we insist on the fact that a screening procedure has to be carried out to obtain a stimulation that maximises the SSSEP's amplitude.

The literature also shows that most SSSEP-based BCIs use signal characteristics extracted from spatial information or large frequency band information. Thus, the use of the SSSEPs' amplitude variation in the literature is very scarce. To conclude, the literature review does not allow us to conclude regarding the most efficient algorithm to monitor the SSSEP's amplitude variation.

#### *Chapter 3 – Amplitude Estimation of Sinusoidal Components in EEG-based BCIs exploiting SSSEPs*

In this chapter, we complete the literature review findings by comparing several signal processing methods to estimate the amplitude of a targeted sinusoidal oscillation. We firstly introduce a surface EEG formation model adapted to the specific case of a BCI exploiting SSSEP. Our model considers a mixture of sinusoidal sources of interest and assumes constant volume conduction of the head. Then we measure the amplitude estimation accuracy of signal processing algorithms commonly used in BCI on our synthetic EEG measurements. We extend the comparison to EEG data collected during our experiments. Results show that the current source density spatial filter combined with a simple lock-in amplifier technique is the most efficient out of a small



\* similarly to SSSEP, an SSVEP is an increase of oscillation in the brain activity caused by gazing at flickering stimuli. The oscillation amplitude increases at the stimuli frequency over the occipital lobe.

Laplacian filter and a self-adapting method such as the canonical correlation analysis. The latter is now the gold standard in steady-state *visually*-evoked potentials or SSVEP\*. In particular, we compare the methodological constraints of using SSVEP *vs.* SSSEP.

#### *Chapter 4 – Kinaesthetic Motor Imagery for Selective Amplitude Modulation of SSSEP by Somatosensory Gating*

We describe in detail the protocol set up for the screening procedure and the session aiming to measure the somatosensory gating effect. More precisely, we measure the gating effect in a one- or two-armed MI situation when the subject receives multiple vibro-tactile stimuli. In line with the challenges in BCI about data contamination, we propose a protocol to reduce the noise in the data. We test our primary hypothesis of “selectiveness” of the SSSEP modulation to the MI content. In other words, does the MI performed with the right arm impact only the SSSEP resulting from the same arm? This hypothesis seems necessary to successfully implement a BCI which provides more commands than the number of stimulations sites. Moreover, in this first approach, we want to rely on a simple algorithm that uses exclusively the information from the variations of SSSEPs’ amplitudes.

#### *Chapter 5 – Somatosensory Gating Effect: An Online & Offline Classification Attempt*

This short chapter presents a 4-class classification based on the gating effect alone for the data collected in chapter 4. In other words, we aim to classify MI states using only the SSSEP’s amplitude variation. We use the signal processing method identified in the results from the chapter 3. We also open an investigation on a 2-class classification problem aiming at differentiating the intention of movement, *i. e.* classifying between idle state and any MI state. Finally, numerous leads to improve the classification performance are discussed.

#### *Chapter 6 – Design and Study of Two Applications Controlled by a BCI Exploiting SSSEP*

We propose the design of two BCI applications that differs in two fundamental aspects. The first one is more “punitive” in case of a mistake, and the second one involves inertia. We measure the influence of these factors using a sham feedback-based experimental design. The sham feedback means that the classification performance is simulated to specific values. In this chapter, we introduce a model of the relationship between classification performance and perceived usability. On another note, in Bangor *et al.* [7] work, the authors provide a model

of the relationship between the perceived usability of a system and its acceptability. Our model allows us, by extrapolating from Bangor *et al.* work, to provide a prediction of the classification performance required to achieve an “acceptable” system for each application.

#### *Chapter 7 – Discussions, Conclusions & Perspectives*

Finally, we summarise the contributions of this thesis. Furthermore, we discuss the limitations of our contributions and possible improvements of our work.

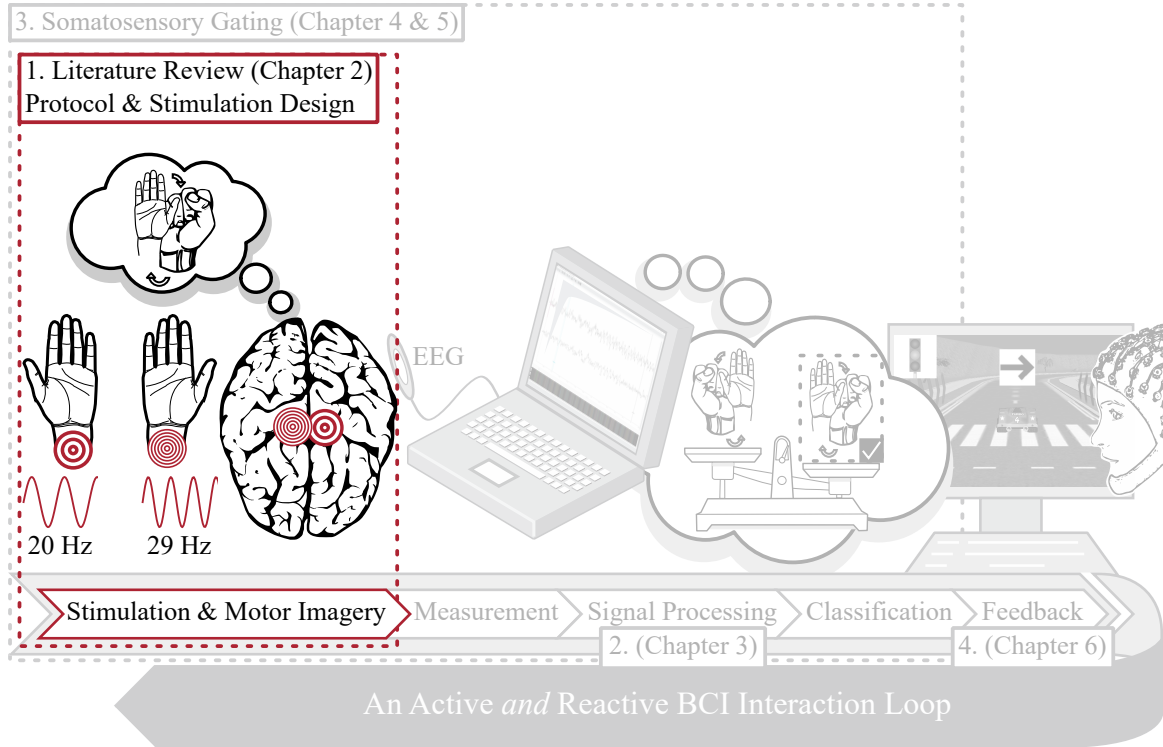
From a more personal point of view, I discuss aspects that I would like to explore further. I also present some aspects of our work done during the PhD but which are not included in this thesis for reasons of coherence of the manuscript. This leads me to discuss the perspectives resulting from this thesis on which I wish to further work.



# EEG-BASED BRAIN-COMPUTER INTERFACES EXPLOITING STEADY-STATE SOMATOSENSORY-EVOKED POTENTIALS: A LITERATURE REVIEW

# 2

## ROADMAP —



In this chapter, we survey the scientific literature on EEG-based BCI exploiting SSSEP. Firstly, we endeavour to describe the main characteristics of SSSEPs and the calibration techniques that allow the tuning of stimulation in order to maximise their amplitude. Secondly, we present the signal processing and data classification algorithms implemented by authors to identify commands in their SSSEP-based BCIs and the classification performance that they evaluated on user experiments. These two steps allow us to highlight the essential elements to design the protocol for our BCI in the rest of this dissertation.

## RELATED WORK —

Jimmy Petit, José Rouillard, and François Cabestaing. “EEG-based brain-computer interfaces exploiting steady-state somatosensory-evoked potentials: a literature review.” *Journal of Neural Engineering* 18.5 (Oct. 2021). Number: 5 Publisher: IOP Publishing, p. 051003. ISSN: 1741-2552. DOI: [10.1088/1741-2552/ac2fc4](https://doi.org/10.1088/1741-2552/ac2fc4)

## 2.1 INTRODUCTION

In EEG-based brain-computer interfaces (BCI) studies, many different paradigms have been proposed, exploiting various markers of mental activity. These markers detect either a volitional modulation of the ongoing brain activity or a specific event elicited by an external stimulus. In EEG signals, the specific brain activity elicited by a stimulation is detected as a small voltage variation immediately following it, called an event-related potential or evoked potential.

The most known evoked potentials used in BCIs are P<sub>300</sub> and steady-state visually-evoked potentials (SSVEP). SSVEPs are quite easy to use as they allow the control of an application by detecting oscillations in EEG signals recorded over the occipital cortex, while the user is looking at visual stimuli flashing at different frequencies. In the same way, periodical beeping sounds, periodical mechanical stimulation of the skin, or electrical stimulation of skin nerves at a constant frequency, elicit steady-state oscillating brain responses, measured respectively by steady-state auditory-evoked potentials (SSAEP) and steady-state somatosensory-evoked potentials (SSSEP).

When the external mechanical or electrical stimulation is applied to the skin, it activates the somatosensory system. In this case, the evoked potential is referred to as a somatosensory-evoked potential (SEP). The stimulation can be either transient or sustained and periodic. After a transient stimulation, specific subcomponents – deflection or inflexion – can be observed in the electrical signal before the brain returns to an “idle” state. Thus, SEP signal analysis is usually performed in the time domain [31]. With a sustained and periodic stimulation, when the time interval between two successive stimuli is too small, the somatosensory system cannot come back to an idle state in between them [64]. Thus, the SEP signal analysis is preferably performed in the frequency domain [32]. More precisely, an increase of power can usually be measured in the SEP signal at the frequency of stimulation or its harmonics. SEPs evoked by a sustained and periodic stimulation are referred to as steady-state somatosensory-evoked potentials (SSSEP). In the rest of the article, a mechanical stimulation of the skin or an electrical stimulation of skin nerves, delivered at a constant frequency, will be referred to as a periodical somatosensory stimulus.

Since the mid-1960s, SEPs have been used as a monitoring tool during neurosurgical procedures or spinal surgery [104]. For example, by stimulating the posterior tibial nerve and by monitoring the SEPs in the somatosensory cortex during spinal surgery, early surgery-related damages to the motor capacity of the patient can be detected [69]. SSSEP have also been used in different clinical applications, for instance to measure the tactile acuity of amputees [97] or as a marker for monitoring cortical processes resulting from a nociceptive and non-nociceptive somatosensory input [23].

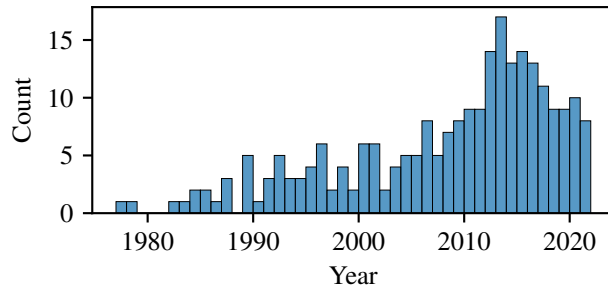


Figure 2.1 : Histogram of the number of publications per year from the PubMed database with the keywords “steady-state somatosensory” in “all fields” the 24th of August 2021.

Figure 2.1 shows an histogram of publications per year reflecting the dynamics of SSSEP-oriented research (from the PubMed database, see section 2.2). After a narrow and centred peak in the number of publications in 2013, the research activity decreases year by year. Despite this apparent lack of interest from the BCI community, we consider that this field is still relevant to study. Indeed, a SSSEP-based BCI exploits a communication channel that is barely used by motor-impaired people. Therefore, we consider that from the user’s point of view, even a small benefit provided by a SSSEP-based BCI using a lost interaction modality is welcome, since the system does not monopolize their sight or hearing.

Additionally, eye fatigue often occurs during the use of SSVEP-based BCI systems and major SSAEP-based BCI systems suffer from low accuracy [86]. Interesting ideas lead to actionable BCIs for certain types of users, for whom audio and visual stimulations cannot be used. For instance, Giabbiconi *et al.* measured, in 2004, that the amplitudes of elicited SSSEPs were modulated by the spatial attention of the subject [32]. It appears that by focusing their attention on the stimulation, the subject could increase the amplitude of SSSEPs.

Extensive literature reviews on non-stationary evoked-potentials, either visually, auditory or somatosensory-evoked, have already been published, for instance [4]. Moreover, a recent literature review on haptics and/or tactile BCIs has also been recently published [28]. Therefore, we limited the scope of our review to research studies in which periodical somatosensory stimuli are used to elicit SSSEP measured by EEG. In section 2 we present how we identified, screened and included articles according to the PRISMA (preferred reporting items for systematic reviews and meta-analyses) methodology [59]. We compare our set of studies to the different references from identified state-of-the-arts while presenting our inclusion and exclusion criteria.

In section 3, we define some specific characteristics of SSSEPs useful for BCI. In order to use SSSEP variations as robust markers in a BCI, one or several optimal stimulation frequencies must be determined. Thus, the notions of frequency of stimulation (FOS) and resonance-like frequencies are presented, as well as techniques for determining user-

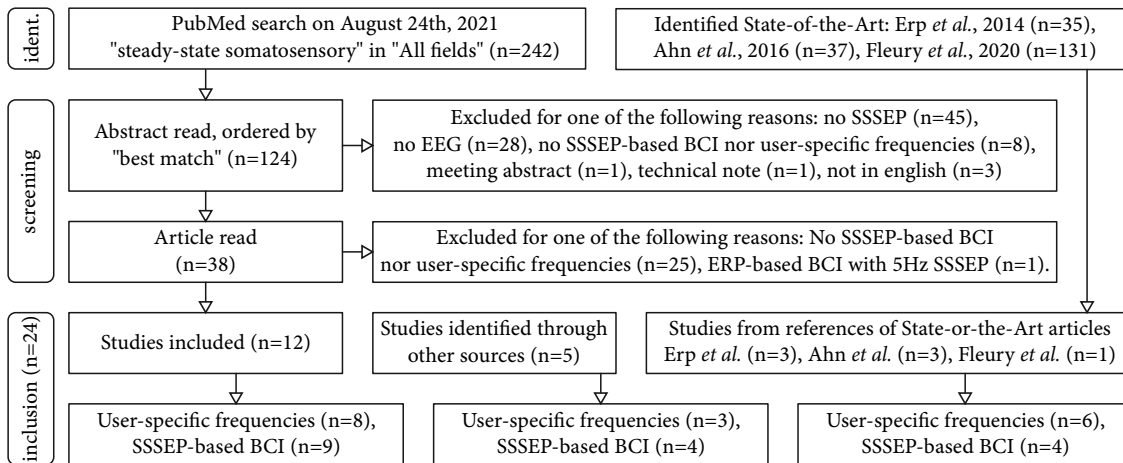


Figure 2.2 : PRISMA-based article inclusion: identification, screening and inclusion stages.

specific frequencies. First synoptical tables (tables 1a and 1b) presents how the selected studies performed a determination of user-specific frequencies, as well as their main results: stimulation location, type of vibration, used FOS or range of FOS, etc.

Section 4 presents the algorithms and performances of SSSEP-based BCIs from the literature. A second pair of tables (tables 2a and 2b) presents the algorithms and the obtained performances. Finally, before the conclusion, we summarize the main results of this SSSEP-based BCI literature review.

## 2.2 METHODOLOGY

In August 2021, we started to review the literature on SSSEPs and SSSEP-based BCIs in accordance to the PRISMA methodology. Figure 2.2 presents our article selection flowchart. More details about the identification, screening and inclusion stages follow.

### 2.2.1 Identification stage

A search on the PubMed database was performed on the 24<sup>th</sup> of August 2021 with the keywords "steady-state somatosensory" in "all fields". This search brought to light 242 items.

Inputs from three state-of-the-art articles were also considered. The first one, chronologically, elaborates on BCIs leveraging the sense of touch [26]. Its scope is broader than ours, since it also includes BCI studies that use a mechanical stimulation of the skin to provide a feedback to the user, or to elicit P300 transient SEPs. The second state-of-the-art article is clearly focused on SSSEP and SSSEP-based BCIs [3]. It ap-

peared relevant to include both articles in the present literature review for two reasons:

- Even though the second state-of-the-art article can be considered conceptually included in the perimeter of the first one, it remains interesting because it analyses an additional two-year of insights on this scientific domain.
- Only one article reference is presented in both state-of-the-art articles, among the 35 presented in [26] and the 37 presented in [3].

A recent survey on the use of haptic feedback for BCI [28] was also analysed, since a short section is dedicated to SSSEP-based BCIs.

### 2.2.2 *Screening stage*

We considered only articles fully written in English, in which measurements were realised using EEG, and presenting either a study of human specific SSSEP characteristics or an SSSEP-based BCI.

The abstracts of the first 124 items, ordered by “best match”, were thoroughly analysed. The analysis showed that 2 items were not research articles, 45 items were not related to SSSEP, 28 used different measurements than EEG, and 8 did not provide insights on an SSSEP-based BCI or a determination of user-specific frequencies. The 38 remaining items were read entirely to assess their eligibility. This second analysis showed that 26 items could not be included since they were describing neither a determination of user-specific frequencies nor an SSSEP-based BCI.

### 2.2.3 *Inclusion stage*

12 articles were included as a result of the screening stage. 5 additional articles, identified during previous searches or corresponding to bibliographical entries of the 12 selected articles, were also included. Finally, 7 additional articles referenced in the state-of-the-art articles were included, ending up with a total of 24 articles studied in our review.

17 articles describe a stimulation, recording and processing procedure that allows the estimation of user-specific characteristics of SSSEPs. These studies are presented and analysed in section 2.3. Section 2.4 is devoted to the presentation of 17 articles that describe an SSSEP-based BCI. 10 studies, that deal with both topics, are presented in the two sections from different points of view.



### 2.3 EFFECTS OF STIMULUS CHARACTERISTICS ON THE EVOKED POTENTIAL

#### 2.3.1 *Methods to elicit an SSSEP*

Historically, in most studies aiming to study SEPs, the latter were elicited by electrical stimulation of peripheral nerves [64, 66, 96]. For instance, a correctly adjusted current flowing between two electrodes placed over the median nerve near the wrist can elicit an SEP. Indeed, the intensity of current pulses is increased until they produce tiny twitches of the thenar muscle, located on the hand palm at the base of the thumb, and simultaneously elicit SEPs [64].

Beside electrophysiological studies, this method of stimulation offers great tools to clinicians for monitoring patient state, for example during delicate spinal chord surgery [69]. However, electrical stimulation of peripheral nerves is reported as unpleasant and elicits SEPs with low amplitude [66, 96]. Therefore, efforts have been made to switch to mechanical stimulation, especially in the context of brain-computer interfacing where the system must be as comfortable to use as possible during long periods.

The nature of the mechanical stimulation is the first aspect to consider when designing an SSSEP-based BCI. In order to elicit an SSSEP, the mechanical stimulation must be sustained and periodical, and several techniques can be used to that end. The first one consists in producing short mechanical pulses, for instance with a moving pin, like the ones used in dot matrix printer heads, in contact with the skin [60]. The shape of this type of stimulation pattern is considered to be identical to the shape of the electrical signal driving the pin, usually a low frequency square wave with a duty cycle of 50%. However, in order to elicit SSSEPs with higher amplitudes, Pacinian corpuscles can be stimulated more efficiently. Pacinian corpuscles are one of the four types of mechanoreceptors of the human skin. Their maximum sensitivity is for a mechanical vibration with a frequency between 200 and 250 Hz [94]. This frequency is way too high to elicit an SSSEP that can be measured on the cortex. Therefore, the mechanical stimulation is actually delivered at a carrier frequency around 250 Hz, but with an amplitude modulated at a much lower frequency [14, 102]. In this case, SSSEPs are elicited at the frequency of the modulation, not of the carrier. This technique is referred to as vibro-tactile stimulation. The amplitude can be modulated either by a square or a sinusoidal function.

In this article, we use the terms short mechanical pulses and vibro-tactile stimulation, both introduced by Müller-Putz *et al.* in 2001 [60]. It is noteworthy to mention that electrical stimulation patterns can also be amplitude-modulated. In this case, similarly to vibro-tactile stimulation, the stimulation current is a high-frequency carrier current whose amplitude is modulated by a low-frequency sinusoidal signal [66].

### 2.3.2 SEP and SSSEP characteristics

The **frequency of stimulation** (FOS) is the frequency of the sustained and periodical somatosensory stimulation eliciting the SSSEP. More precisely, it is either the frequency of short electrical or mechanical pulses or the frequency modulating a carrier stimulation. In the frequency domain, the SSSEP is characterized by a high value, at the FOS, of the power or amplitude of the measured electrical activity.

The **resonance-like frequency** is a term introduced by Müller-Putz *et al.* in 2001 [60]. It is defined as the particular FOS that elicits an SSSEP with the highest amplitude or signal-to-noise ratio, assuming that the stimulation amplitude remains constant. When the SSSEP amplitude *vs.* frequency curve shows several local maxima, the resonance-like frequency is not unique. When this curve does not show a sharp maximum, the resonance-like frequency is sometimes defined as a frequency band [60]. Usually, in an SSSEP-based BCI, at least two FOS are required, one of them being the resonance-like frequency. Other FOS are selected at other local maxima of the amplitude *vs.* frequency curve if they exist, provided that they are different enough from the resonance-like frequency. To achieve this, keeping a minimum difference of 4 Hz [13, 85] or 5 Hz [1, 62] between each FOS is a common practice.

When talking about **latency** several aspects must be taken into consideration. Strictly speaking, when considering the whole causal chain, i.e. from stimulation to human to measurement, the latency is the time between the stimulus onset (the cause) and the SEP appearance in the processed electrical signal (the effect). Hence, the latency encompasses several delays:

- the transport time that is required to transfer the stimulation-related information from the skin to the brain.
- the cortical processing time that encompasses all the delays introduced by following neural pathways within the cortex before SEP appearance.
- the hardware delay, that can be caused by several factors, such as transfer delays in pipeline processing stages after signal sampling, or drifts resulting from lost or artificially inserted digital signal samples in asynchronous communication channels.
- the delays that can be introduced by signal processing techniques, such as narrow bandwidth signal filtering.

These components of the latency cannot be measured separately in practice. For example, the transport time and the cortical processing time are hardly differentiable. A hardware delay, from the computer to the stimulation device, has been measured in a study conducted by Pokorny *et al.* in 2014 [84]. They concluded that this delay, a few

hundreds of microseconds, can be neglected compared to other delays. Finally, delays caused by signal filtering have been known for a long time. The interested reader can refer to an article of De Cheveigné *et al.* in which the authors extensively discuss the implication of filters, either hardware and software, and also suggest delay compensation techniques [19].

In this article, we use the term **total latency** to denote the sum of all delays. In contrast, we use the term **apparent latency**, defined by Regan in [89, 90], to characterize only the physiological part of the total latency. For Regan, the apparent latency is the first derivative of the SSSEP phase with respect to the stimulus frequency, *i. e.* the slope of an SSSEP frequency *vs.* phase plot. One must keep in mind that even the apparent latency cannot be interpreted rigorously from a neurological point of view. Indeed, a long apparent latency can be caused either by a long transport time followed by a short cortical processing time or by the opposite.

From the human-computer interaction (HCI) point of view, minimizing the total latency or at least keeping it constantly below a threshold is of major importance. Indeed, in the context of real-time interaction, the total latency can also be defined as the minimum time it takes for the BCI to detect a user's intention after the stimulation onset.

The **phase difference** is simply the time difference between similar zero crossings (*i. e.* with the same slope sign) of the SEP on the one hand and of the stimulation signal on the other hand, times the FOS and a constant to get an angle-like quantity. It should not be confused with the **phase shift**, as defined by Regan in [90], that is the sum of the phase difference and of the apparent latency, also expressed as an angle.

A schematic definition of apparent latency and phase difference characterizing the onset of a theoretical SSSEP is presented in figure 2.3.

The **time-to-stationarity** can be defined as the duration of the transient response to the periodical somatosensory stimulus, that starts with transient somatosensory-evoked potentials before reaching a steady-state response at the frequency of stimulation. It is assumed that the stimulation remains constant as well as the subject's mental activity, for instance that there is no attention focusing or stimulation triggered mental action. Brickwedde *et al.* measured a time-to-stationarity of 500 ms for a SSSEP evoked by a 20 Hz vibration [15]. Figure 2.4 shows the stabilisation of an SEP into an SSSEP measured by Brickwedde *et al.* [15].

### 2.3.3 Determination of user-specific frequencies

When the skin is stimulated by a periodical somatosensory stimulus, the elicited SSSEP is characterized by measuring the electrical brain activity at the FOS. Many studies have shown that the amplitude and signal-to-noise ratio of the SSSEP are highly dependent on the FOS [12,

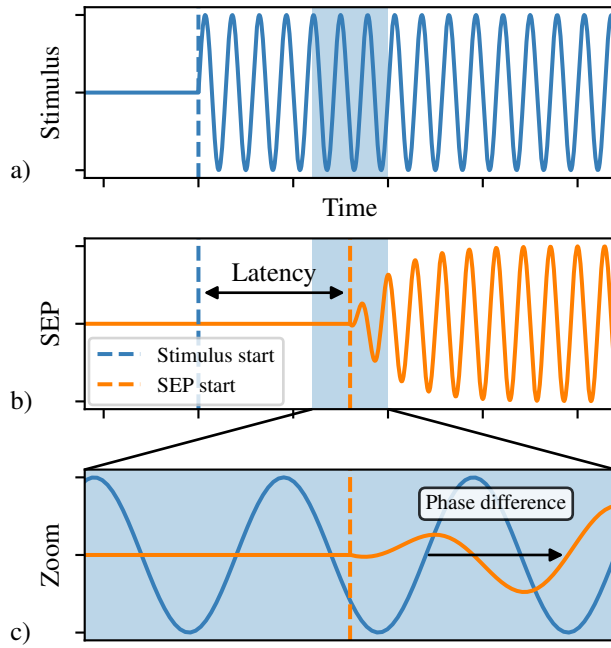


Figure 2.3 : Temporal characteristics of an theoretical SEP reaching its steady-state. (a) The “stimulus” plot is the representation of the periodical somatosensory stimulus amplitude *vs.* time, considered here as a windowed sine function. (b) Representation of an ideal SEP elicited by the stimulus, *i. e.* an amplitude modulated sine function without noise. (c) Zoom on the plots (a) and (b) around the beginning of the SEP. It shows the phase difference between the SEP and the stimulus.

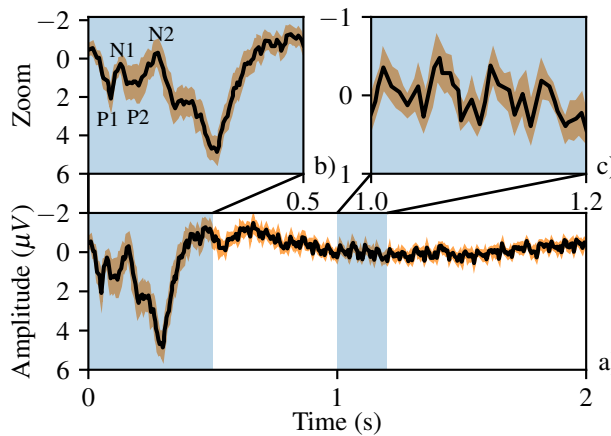


Figure 2.4 : Temporal characteristics of an SEP reaching its steady-state. (a) Grand average over 14 subjects and 40 min of 20 Hz stimulus train on the right index finger for 2 s, with a 5 s inter-trial interval. (b) Zoom on the first half second of the grand average, clear component of the SEP are annotated. (c) Zoom on an SSSEP-established period, 4 periods of the 20 Hz-SSSEP are well visible over 0.2 s of signal. All data is presented from CP1 and as mean  $\pm$  SEM. Figure reproduced with the appreciated authorisation of the authors from [15].

85]. Thus, for each subject and each stimulation position, a specific screening procedure is often performed to estimate the amplitude or signal-to-noise ratio of the SSSEP with respect to the FOS. We refer to this procedure as the tuning curves estimation.

During each trial of the tuning curves estimation procedure, a mechanical stimulation is applied on a given part of the body, with a given FOS, and sometimes for a given duration or shape of amplitude modulation [85]. The tested frequencies, as well as other tested parameters, are usually randomized during the successive trials. Each FOS or stimulation parameter is tested several times, to average the results and increase the measurement precision. This procedure yields one or several tuning curves, that characterize the relationship between the frequency, duration and shape of the stimulation, and the amplitude, power, or signal-to-noise ratio of the SSSEP.

The following two tables summarize the literature describing these procedures. Table 1a presents the methodology of each study regarding the determination of user-specific frequencies. Table 1b presents the results of studies introduced in table 1a. The first 3 columns, present in the two tables, are used as an index: name of the first author, paper reference and stimulation location. The five following columns in table 1a present the methodology, in order: hardware vibrator (Vibrator), surface of the contact area of the vibrator head with the skin (Size), stimulation type and carrier frequency (Stimulation), range and number of tested FOS (FOS or FOS range), and the number of subjects (Subj.) involved in the experiment. The three last columns of table 1b present the main results. The column RLF reports the resonance-like frequency. The next column TC mention if the tuning curves from the determination of user-specific frequencies were reported in their completeness in the study and the last column provides supplementary information when needed.

#### 2.3.4 *Determination of user-specific frequencies in the literature: main results and comments*

In the seminal article published in 1992, Snyder introduces the main physiological characteristics of SSSEPs such as apparent latency, dependence of amplitude to FOS, and spatial location of the stimulus-induced neuronal activity [96]. An EEG setup with 16 channels was used in his experiment, with electrodes over the scalp at locations following the international 10-20 system. The subjects rested their hand (left or right) on top of a rigid plastic spherical shell, with a diameter of 8 centimetres, acting as the vibrator head. Vibro-tactile stimulation, with a carrier frequency of 128 Hz, was used in this experiment. At the maximum amplitude, the vibration head provided a thrust of about 10 Newtons, producing for some subjects a feeling of “rising hand”. Different FOS were tested by Snyder:

- 2 and 3 Hz FOS on 4 subjects;











First author	Ref.	Stimulation Location	Vibrator	Size (cm <sup>2</sup> )	Stimulation	FOS or FOS range (# of FOS)	Subj.
Snyder	[96]		SS	100.5*	Vibration (128 Hz)	2 & 3, 5 to 40 (6), 25 & 27	4 17 13
Tobimatsu	[102]		SS	127*	Vibration (128 Hz)	5 to 30 (9)	10
Tobimatsu	[103]		SS	127*	Vibration (128 Hz)	17 to 30 (6)	8
Müller-Putz	[62]		NP	0.03	Pulses	17 to 35 (10)	5
Wang	[109]		KoP	N/A	N/A	5 to 29 (25)	5 <sup>?</sup>
Breitwieser	[14]		C2	0.45	Vibration (200 Hz)	13 to 35 (12)	14
Ahn	[2]		LRA <sup>?</sup>	0.28	N/A	21 to 25 (5)	8
Ahn	[1]		LRA <sup>?</sup>	0.79	N/A	21 to 25 (5)	16
Breitwieser	[12]		C2	0.45	Vibration (200 Hz)	17 to 35 (10)	9
Pokorny	[84]		C2	0.45	Vibration (200 Hz)	14 to 32 (7)	1
Müller-Putz	[60]		NP	0.03	Pulses	17 to 31 (8)	10
Breitwieser	[13]		C2	0.45	Vibration (237 Hz)	17 to 35 (10)	13
Pokorny	[85]		C2	0.45	Vibration (237 Hz)	17 to 35 (10)	14
Kim	[48]		ERM	0.79	Pulses <sup>2†</sup>	13 to 35 (12)	4 <sup>?</sup>
Kim	[49]		ERM	0.79	Pulses <sup>2†</sup>	13 to 35 (12)	5 <sup>?</sup>
Kim	[50]		ERM	0.79	Pulses <sup>2†</sup>	13 to 35 (12)	12
Kee	[46]		ERM	0.79	Pulses <sup>2†</sup>	13 to 33 (11)	5

Table 1A : User-specific frequencies identifications: Methodology. Legend and Acronyms: Vibration: vibro-tactile stimulation (carrier frequency at X Hz); Pulses: short mechanical pulses; FOS: frequency of stimulation; Subj.: number of subjects; SS: spherical shell; NP: dot matrix needle printer; KoP: Knock-out Pin; C2: C-2 factor; LRA: Linear Resonant Actuator; ERM: Eccentric Rotating Mass; N/A: not available; \*: skin contact assumed to be perfect; †: N/A but likely as in [60], *i. e.* short mechanical pulses; ? : unclear or ambiguous.







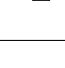





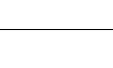




First author	Ref.	Stimulation Location	RLF (body part)	TC	Observations
Snyder	[96]		26 & 40	Yes	40 Hz SSSEP have small amplitude but similar signal-to-noise ratio than 26 Hz-SSSEP. Both hands were stimulated at 25 & 27 Hz.
Tobimatsu	[102]		21	Yes	
Tobimatsu	[103]		21	Yes	Identified RLF for 6 out of 8 subjects. Low-to-none impact of the frequency on the sole-elicited SSSEP. Amplitude of sole-elicited SSSEP are roughly twice lower than hand-elicited SSSEP.
Müller-Putz	[62]		25 to 31	No	
Wang	[109]		N/A	Yes	Tuning curve presented for 1 subject out of 5 subjects, grand average not available.
Breitwieser	[14]		21 & 23	No	Identified RLF for 7 out of 14 subjects.
Ahn	[2]		N/A	No	
Ahn	[1]		22 & 23	No	Identified RLF for 10 out of 14 subjects.
Breitwieser	[12]		N/A	Yes	The TC for each subject highlight how important the inter-subject variability is. Each subject performed two sessions within several weeks (Mean: 28 day, Std: 17.5): the TC between sessions are very similar.
Pokorny	[84]		20	Yes	Irrespective of the wrist.
Müller-Putz	[60]		27 (Left index)	Yes	Low-to-none influence of the frequency on the SSSEP for right index.
Breitwieser	[13]		23 to 27	No	Identified RLF for 9/13 subjects (right index) and 8/13 subjects (left index).
Pokorny	[85]		27	Yes	Irrespective of the index fingertip.
Kim	[48]		17 to 23 (index) 27 to 31 (toe)	No	Irrespective of the index.
Kim	[49]		13 to 25 (index) 29 (toe)	No	Irrespective of the index.
Kim	[50]		17 (index) 27 (toe)	No	Irrespective of the index.
Kee	[46]		13 to 29	No	Irrespective of the toe. Broad distribution of RLF.

Table 1B : User-specific frequencies identifications: Results. Legend and Acronyms: RLF: resonance-like frequency; TC: tuning curve; N/A: not available.



- 5, 7, 11, 17, 26, 40 Hz on 17 subjects;
- and 25 and 27 Hz on 13 subjects.

Firstly, Snyder reports that the SSSEP appeared in the hemisphere contralateral to the stimulated hand on parts of the primary and secondary somatosensory cortex, and on the primary motor cortex. The same locations, when reported, were determined in almost all studies listed in tables 1a and 1b. Besides, Snyders' results show that FOS at 26 Hz and 40 Hz seem to produce SSSEPs with higher signal-to-noise ratios than other FOS. Among those two FOS, the author observed that the amplitude of SSSEP at 26 Hz was greater.

An approximation of the apparent latency, using an estimation of the EEG background noise from the averaged evoked responses, was also calculated. This was performed on a combination of 19 datasets: 13 subjects each-one producing 2 datasets, one per hand, 7 datasets were rejected. The estimated distribution of the apparent latency, over the FOS at 25, 26 and 27 Hz, has a mean of 58.6 ms and a standard deviation of 14.6 ms.

Regarding the resonance-like frequency, in the articles listed in table 1b, two trends can be observed. Tuning curves, *i. e.* amplitude of SSSEP *vs.* FOS, show either a rather flat maximum centred at 27 Hz [13, 60, 85] or more pronounced local maxima centred on lower frequencies such as 17 Hz or 21 Hz [50, 109]. The first trend confirms the results from [96] whereas the other trend confirms the results from [102, 103]. Other determination of user-specific frequencies did not yield tuning curves similar to either trend, such as the one in the article of Breitwieser *et al.* in 2011, that yielded tuning curves with a rather flat maximum centred on a FOS varying from 21 to 35 Hz [14].

In the articles presented in tables 1a and 1b, studies also seem to show that FOS below 20 Hz rarely produce SSSEPs with high amplitudes or signal-to-noise ratios. However, this might be caused by an averaging effect, since in rare subjects, it is useful to test nevertheless these low FOS in the determination of user-specific frequencies procedure, as shown in one article of Breitwieser *et al.* [12]. In their study, they determined the user-specific FOS for all fingertips of the right hand for nine subjects. They used a vibro-tactile stimulation with a carrier frequency at 200 Hz. Each subject performed two sessions within weeks (mean 28 days, standard deviation 17.5 days). Six subjects out of nine had one resonance-like frequency below 20 Hz during one session, for at least one finger. Besides, the results remained rather stable between the two sessions; an ANOVA for repeated measure substantiates this observation. Thus, it seems relevant to assess low frequencies of stimulation as well for determining user-specific frequencies.

Finally, it is noteworthy that in the works of Kim *et al.*, several subjects had already tested a BCI before taking up the main experiment [48–50]. Therefore, across these papers, the resonance-like frequency can be



biased if the same subject performed a similar screening procedure in several successive experiments. Indeed, we know from the work of Breitwieser *et al.* that the resonance-like frequency tends to be stable through time [12]. Their work confirms stability for weeks, but for longer periods this property remains unknown.

It should also be noted that, to the best of our knowledge, the influence of the stimulation location on the total latency has not been reported in the literature.

#### 2.3.4.1 *Force and pressure of stimulation.*

The threshold of human skin sensitivity to mechanical stimulation has been quite studied and known for decades [111]. However, the influence of the intensity of the stimulation on the amplitude of the SSSEP remains unclear. The work of Tobimatsu *et al.* in 1999 provides some insights on this question [102]. However, more recent studies in table 1a and 1b tend to ignore it.

Tobimatsu *et al.* investigated the impact of the stimulation force, measured in Newtons (N), on the amplitude of the SSSEP. They tested different forces, from 0.001 to 0.1 N, for the same FOS at 21 Hz. In the frequency domain, they observed that the mean amplitude of the SSSEP component at the FOS linearly increases with the logarithm of the force up to a plateau, reached at 0.05 N. This trend seems to hold also for the SSSEP amplitude measured at the second harmonic of the FOS, *i. e.* frequency equal to twice the FOS, even though much smaller.

However, for further investigation, the chosen stimulation intensity metric, *i. e.* the force, can be discussed. Indeed, the force controls directly the acceleration of the stimulation pin or head, but it does not take into account the contact surface between this device and the skin. For future studies investigating this influence, we think that it is advisable to use the force as metric, in order to have a comparison point with previous studies, but also the pressure exerted on the skin. This would help taking into account the specificity of the stimulation pin or head, which is important as demonstrated by the variety of devices described by the columns "Vibrator" and "Size" of table 1a. The lack of specificity of the force metric, in fact, may explain a part of the variability observed in the trends mentioned above.

#### 2.3.4.2 *Harmonics of the frequency of stimulation.*

Few studies assess the presence of harmonics of the FOS in the frequency analysis of SSSEPs. In 1996, Noss *et al.* elicited SSSEPs with an amplitude modulated electrical stimulation at 200 Hz [66]. The modulation signal was a pure sine function, *i. e.* with no harmonic content at multiples of the fundamental frequency. However, peaks higher than the baseline were detected in the power spectrum of the SSSEP at frequencies corresponding to harmonics of the FOS. This, according to the

authors, reveals a pronounced non-linearity of the transfer function of the somatosensory system.

In 1999, Tobimatsu *et al.* also performed an harmonic analysis of SSSEPs, but for a mechanical vibro-tactile stimulation [102]. The carrier frequency at 128 Hz was modulated by a sinusoidal signal at frequencies ranging from 5 to 30 Hz. They also report that a peak at twice the FOS can be detected in the power spectrum of the SSSEP, although smaller than the peak at the FOS. What is interesting though, is that the height of the peak at twice the FOS monotonically decreases as the FOS increases.

In fact, a similar phenomenon had already been mentioned by Snyder in 1992. We recall that in his experiments a vibro-tactile stimulation with a carrier at 128 Hz modulated by a sinusoidal FOS was used. Snyder observed that in the power spectrum of SSSEPs elicited by a FOS greater than 11 Hz, the maximum power was localized at the FOS and almost no power increase was detected around its harmonics. On the other hand, in SSSEPs elicited by a FOS lower than 7 Hz, the power increase at twice the FOS was almost as important as at the FOS itself.

It is noteworthy to mention that in the case of vibro-tactile stimulation, if the study of harmonics is considered, the modulation signal should be sinusoidal. Indeed, a modulation signal with a square shape inherently contains the FOS as well as its odd harmonics, but not the even ones. Thus, the second harmonic of the FOS is not present in the vibro-tactile stimulation and therefore cannot produce a response of the somatosensory perception chain. For instance, Breitwieser *et al.* highlighted that no power increase could be found at the second harmonic of a FOS equal to 23 Hz, when using a square modulation signal of a 200 Hz carrier frequency [14].

To summarise, in this section we reviewed research studies in which user-specific frequencies of stimulation are determined. We presented SEP and SSSEP characteristics, and then discussed techniques that aim to determine resonance-like frequencies. SSSEP's amplitude vs. FOS response curve is strongly user-dependant, sometimes flat, sometimes showing one or several sharp maxima. Therefore, precisely identifying user-specific FOS seems essential before implementing an SSSEP-based BCI [12]. Additionally, we observed that the SSSEP's amplitude is positively correlated to the force and pressure of mechanical stimulation, up to a plateau of 0.05 N after which the amplitude of the SSSEP remains stable [102]. We also realised that the influence of the stimulation location on the SSSEP latency and spatial location has been scarcely studied. Further work in this direction seems desirable to gain a better understanding of SSSEPs.

#### 2.4 SSSEP-BASED BCI: ALGORITHMS AND PERFORMANCES

In this section, we focus our review on SSSEP-based BCIs, describing their algorithms and performances, their similarities or at the opposite

their originality compared to other approaches. We firstly discuss the main way to turn an SSSEP into a command usable in a BCI. Secondly, we present and comment on a synthetic table that summarises the methodologies, algorithms and performances of SSSEP-based BCIs. We finally present the most common algorithm described in the literature and compare it to less standard techniques found during our analysis of the state-of-the-art.









#### 2.4.1 *Turning SSSEP into a usable BCI command*

In order to turn the SSSEP, or more precisely one of its characteristics, into a BCI command, it is necessary to specify which mental actions may influence it. In 2004, Giabbiconi *et al.* observed that selective spatial attention towards the hand undergoing a sustained mechanical stimulation modulates the amplitude of the SSSEP elicited by the latter [32]. The authors stimulated the fingertips of the left and right index at 20 and 26 Hz respectively. Subjects were instructed “to attend to the flutter vibration at one finger while ignoring the other”. An increase of the amplitude of the corresponding SSSEP results from this selective spatial attention, although the effect is highly subject dependent. This high between-subject variability motivated the author to use the standard error (SE), which is estimated by dividing the standard deviation by the square root of the number of samples. The authors reported an average increase of 30.6% (SE = 11.2) of the amplitude of the SSSEP elicited in the right hemisphere when the attention was focused on the left index fingertips. Whereas when the attention was focused on the right index fingertips, the average augmentation of amplitude of the SSSEP elicited in the left hemisphere was 27.7% (SE = 11.0). The authors observed that the greatest SSSEP amplitude was measured at frontal electrode locations, contralateral to the stimulated index finger. The first article reporting on an SSSEP-based BCI, in 2006, used this attention focusing mental task [62].

#### 2.4.2 *Synthesis of SSSEP-based BCIs: introduction*

We present and synthesize in tables 2a and 2b the articles describing SSSEP-based BCIs obtained through our literature review. Table 2a presents the methodologies in the experiments, while table 2b presents their main results. The two tables share the first 3 columns, used as an index: name of the first author, paper reference and stimulation location.

In table 2a, four columns present the methodology of each study: was a frequencies screening procedure involved? What task was performed by the subjects? How many subjects were tested? Which algorithms were used? We call “frequencies screening procedure” a user-specific

First author	Ref.	Stimulation Location	Screen.	Task	Subj.	Algorithm		
						Freq.	Spat.	Feat.
Breitwieser	[14]		Yes	AF	14	LAS	CS <sub>BM</sub> (1)	Amp.
Ahn	[2]		Yes	MI   AF <sup>?</sup>	8	wBP	CSP	N/A
Nam	[63]		No <sup>1</sup>	SS <sup>?</sup>	4	wBP + FFT (w+n)BP + FFT	None CSP CSP	SPow. SPow.
Ahn	[1]		Yes	MI & SS MI   SS	16	wBP	CSP	Pow. <sup>?</sup>
Severens	[95]		No <sup>2</sup>	AF <sup>?</sup>	12	FFT	None	SPow.
Müller-Putz	[62]		Yes	AF	5	LAS	CS <sub>BM</sub> (2)	Log. Amp.
Choi	[20]		No <sup>3</sup>	AF	5	wBP + FFT	CS <sub>BM</sub> (2)	Rel. SPow.
Breitwieser	[13]		Yes	AF	13	nBP + LAS	CS <sub>BM</sub> (13)	Log. Amp.
Pokorny	[85]		Yes	AF	15	(w+n)BP + LAS	CS <sub>BM</sub> (13)	Log. Amp.
Zhou	[116]		No <sup>4</sup>	MI	13	wBP + FFT	CSP	SPow.
Yao	[114]		No <sup>5</sup>	MI   SS	11	wBP	CSP	LV
Tao	[100]		wBP + FFT	CS (1)	SPow.			
			wBP + FFT	CS (1)	ISPC			
Kim	[47]		No <sup>6</sup>	SS	3	None FFT	CSP CS (3), CSP	LV SPow. cc LV
			Yes	SS	4	wBP + FFT	CS (3), CSP	SPow. cc LV
			Yes	SS	5	wBP + FFT	CS (3), CSP	SPow. cc LV
						wBP + FFT	CS (3)	SPow.
			Yes	MI   SS	12	wBP wBP + FFT	CSP CS (3), CSP	LV SPow. cc LV
Kee	[46]		Yes	AF	5	wBD + None wBD + PSD	CSP None	LV Pow.

Notes on screeningless SSSEP-based BCI, <sup>x</sup> Material (size), Stimulation Shape:

<sup>1</sup> LRA<sup>?</sup> (0.79 cm<sup>2</sup>), Pulses      <sup>3</sup> LRA (2.5 cm<sup>2</sup>), Vibration (200 Hz)      <sup>5</sup> C10-100 LRA (0.79 cm<sup>2</sup>), Vibration (175 Hz)

<sup>2</sup> Braille Stimulator, Pulses      <sup>4</sup> Electrical stimulation, Pulses      <sup>6</sup> ERM, N/A

**Table 2A : EEG-based BCI exploiting SSSEP: Methods and Algorithms.** All reported works use mechanical stimulation of the skin unless mentioned differently as an observation in table 2b. Legend and Acronyms: BM: bipolar montage; CS ( $x$ ): channel selection  $x$  being the number of kept bipolar channel (if BM) monopolar channel otherwise; cc: concatenate; SPow.: power of selected frequencies (FOS) computed with FFT; Pow.: power computed with FFT; LAS: lock-in amplifier system; Amp.: amplitude output of a LAS; LV: log-variance of spatially filtered data from a CSP; ISPC: inter-stimulus phase coherence; nBP: narrow band-pass filter around stimulation frequencies ( $\pm 1$  Hz); wBP: wide band-pass filters whose range can vary from 16-25 Hz [1] to 8-30 Hz [2]; N/A: not available; \*: irrespective of the paradigms or the algorithms; ? : unclear or ambiguous.









First author	Ref.	Stimulation Location	Accuracy (SSSEP)	Chance L. ( $p = 5\%$ )	Problem	Observations
Breitwieser	[14]		$58.6\% \pm 2.0$	61%	2-class	
Ahn	[2]		$69\% \pm 11$	N/A	2-class	ERD from MI tasks reached an average accuracy of $71\% \pm 10$ .
Nam	[63]		70.0 57.1 75.4	N/A	2-class	Left thumb (22 Hz), right thumb (27 Hz)
Ahn	[1]		$\approx 60\%$	60%	2-class	
Severens	[95]		68%	63.34%	2-class	
Müller-Putz	[62]		min: 66.9% max: 83.9%	N/A	2-class	Accuracy rather stable across days (up to 5 days of experiments)
Choi	[20]		65%	N/A	2-class	Different patterns of stimulation
Breitwieser	[13]		$42.1\% \pm 7.9$	39.8%	3-class	Offline mean accuracy: $48.2\% \pm 7.1$
Pokorny	[85]		$48.6\% \pm 6.2$	40.8% ( $p = 1\%$ )	3-class	9 subjects above chance level, average classification computed with them.
Zhou	[116]		$74.5\% \pm 5.8^\dagger$	N/A	2-class	Classification of right hand MI vs. idle based on the SSSEP's amplitude. Uses electrical stimulations.
Yao	[114]		$72\% \pm 15^*$	N/A	2-class	Left wrist (23 Hz), right wrist (27 Hz)
Tao	[100]		$75.4\% \pm 10.2$ $75.7\% \pm 13.9$ $79.8\% \pm 11.5$	N/A	2-class	Uses electrical stimulations and Inter-Stimulus Phase Coherence (ISPC).
Kim	[47]		76% 80.93%	N/A	3-class	
Kim	[48]		N/A	N/A	3-class	Wheelchair-driving experiment. Identical rhythm of commands between conditions: one every 5 s. Goal reached in average in $35 \text{ s} \pm 2.1$ (joystick) and $101 \text{ s} \pm 27.6$ (SSSEP).
Kim	[49]		N/A	N/A	3-class	Similar to [48].
Kim	[50]		$55\% \pm 6.8^\dagger$ $73\% \pm 11.8^\dagger$ $76\% \pm 12.8^\dagger$	N/A	3-class	
Kee	[46]		$72\%^*$	N/A	2-class	

Table 2B : EEG-based BCI exploiting SSSEP: Performances. All of the reported works uses mechanical stimulation of the skin unless mentioned differently as an observation. Legend and Acronyms: N/A: not available; \*: irrespective of the paradigms or the algorithms; †: extracted from a figure.

procedure aiming to determine the resonance-like frequency, or at least the most efficient FOS, that will be later used in the BCI.

During the literature review, differences in the presentation of the task to the subject have been observed. We categorize the instruction provided to the subject into two categories: selective sensation (SS, stimulation-driven task) or attention focusing (AF, attention orientation-driven task). The instruction given in a SS task is correlated to the sensation produced by the stimulation. For example, the subject can be instructed to “select sensation on the indicated side of their hands as if stimulation on the attended side was stronger than on the unattended side” [114]. Whereas the instruction given in an AF task is focused on the shift of attention expected from the subject. The provided instruction can be: “focus attention on the finger stimulation indicated by the bar (cue)” [62]. We differentiate the instructions provided to the subject based on that difference between SS and AF tasks. Sometimes a small question mark (?) is inserted in table 2a, see column Task, when the authors did not provide enough information to differentiate the instruction type. In addition, some authors implemented a secondary task to help the subject concentrate on the main task. For example, in [62], the authors added a random transient amplitude twitch on the stimulation during some trials, that the subject had to detect and report to the experimenter.

We also sub-categorize the algorithm using three columns. Each column presents the answer to one of three different questions: how was the frequency information of the SSSEP used? How was the spatial information used? And how were the features extracted? Due to the limited amount of data collected during experiments, most of the studies used linear discriminant analysis (LDA) for classification. When the dimension of the extracted feature vector was relatively large, sometimes the “regularized” or “with shrinkage” version of LDA was used. This specific aspect will not be discussed here.

In table 2b, the main results of each study are presented. The classification accuracy (simply called “accuracy” thereafter) is reported, as well as its standard deviation when available. The 95% confidence limits of chance results for the considered classification problem is indicated in the column “chance level” when available [61]. Then a column indicates the type of classification problem, *i. e.* the number of classes that the algorithm was trained to differentiate. Finally, a last column presents the main achievement of the study or provides supplementary information when needed.

### 2.4.3 Signal processing and feature extraction

In this section, we succinctly present the main techniques used in the reviewed articles in order to process the EEG signals and extract significant SSSEP features for further classification. Three categories of data



processing will be considered: estimation of the frequency information contained in EEG signals, use or non-use of spatial information, type and characteristics of classification features.

#### 2.4.3.1 Frequency information

is retrieved from EEG signals with mostly three different approaches: Fourier transform, band-pass filtering or lock-in amplification.

The Fourier transform is the best known method for recovering the frequency information contained in a signal, through projections onto a base of sinusoidal components. Fourier-like transforms implemented in systems requiring real-time processing are usually either the fast-Fourier transform (FFT) [50] or the power spectral density (PSD) estimation [46].

Unlike the other reviewed articles, Kee *et al.* used the power information at all available frequencies in the FFT [46]. The most common approach though is to consider only some frequencies, *e. g.* the FOS and some of its harmonics [95]. The amplitudes or squared amplitudes of the sinusoidal components are then computed and provided as features to the classifier.

Another approach to the estimation of frequency information is narrow band-pass filtering. A narrow band-pass filter can be the first stage to recover the amplitude of a given frequency component of the EEG signal. In order to estimate the power of a signal inside a frequency band, it is common to square the band-pass filtered signal and average the result over time [54]. The authors of [13, 85] followed a slightly different approach, combining a narrow band-pass filter with a lock-in amplifier, technique that will be presented in the next paragraph.

A lock-in amplifier or lock-in amplifier system (LAS\*) computes an estimate of the amplitude and phase of a specific sinusoidal component of a noisy signal. This method is fairly similar to a very narrow and tunable band-pass filter and can be considered as such [62]. In the literature, the amplitude estimation from the LAS is also averaged over a sliding time window of fixed length [62]. Commonly, the logarithm of the averaged amplitude is computed, for conditioning purposes and to obtain a distribution that approximates to normal [62]. Finally, either the averaged amplitude or its logarithm is fed into the classifier as a signal feature. This technique has long been known and frequently used when a single sinusoidal component is targeted in the EEG. Indeed, in a 1966 SSVEP study, Regan *et al.* used the source of stimulation itself, modulated light, with an EEG to implement a physical LAS [88].

\* The acronym LAS is only used in this chapter. We initially followed the terminology from [62]. Later in this manuscript, we use "LiA", a more common acronym for lock-in amplifier system in signal processing.

#### 2.4.3.2 The spatial location

of an SSSEP is well known and stable across subjects. Snyder showed that SSSEP can be principally recorded over the somatosensory cortex located in the post-central gyrus [96]. Moreover, the spatial location can

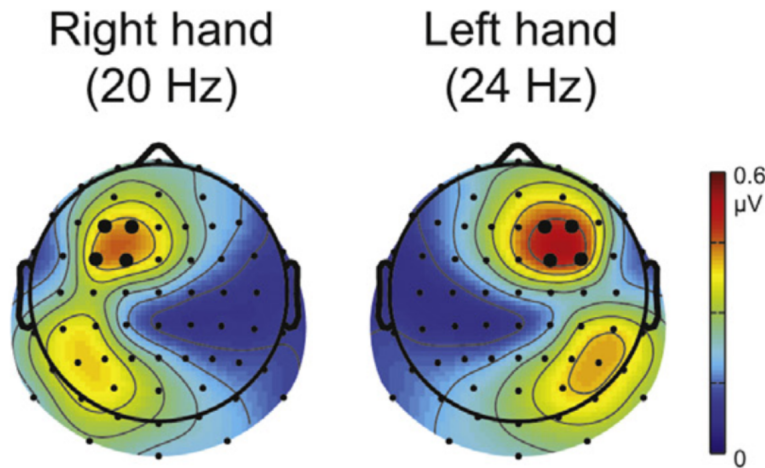


Figure 2.5 : Grand average of SSSEP amplitudes, calculated across subjects and attention-related experimental condition (one-hand attended, one-hand ignored and both-hand attended). Figure reproduced with the appreciated authorisation of the authors from [71].

be refined by building on the sensory homunculus that projects each part of the body onto a precise location of the sensory cortex. Therefore, a straightforward method to take advantage of this precise location is to process only the EEG signal recorded by a specific well-placed electrode. For example, the topomaps of figure 2.5 illustrate the positions of two concurrent SSSEP on the cortex.

For instance, to detect the SSSEP elicited by a mechanical stimulation of the right hand, one can process the signal recorded at location C<sub>3</sub> of the 10-20 international system of electrode placement. The spatial selection of signals of interest, in addition to the use of several FOS, allows SSSEP-based BCIs to provide independent and sometimes simultaneous control channels. This method is commonly used in the literature, we reported it as channel selection (CS) in table 2a.

In order to reduce the noise, some authors use a bipolar montage (BM) [13, 20, 62, 85]. The noise, or more generally a widespread and non task-related cortical activity, is removed by subtracting the signals recorded by two neighbour electrodes located next to the region of interest. For example, in an SSSEP-based BCI, the signal corresponding to a noise-reduced virtual electrode over C<sub>3</sub> is commonly obtained by subtracting the centro-parietal signal recorded at CP<sub>3</sub> from the fronto-central signal recorded at FC<sub>3</sub>. It is worth noting also that the variance of the signal provided by the virtual electrode is lower than the sum of variances of both initial electrodes. More precisely, the variance of the BM signal is the sum of variances of the initial signals minus twice their covariance, the latter being usually high since the electrodes are close to each other. Electrodes with a lower variance are assumed to have a better signal-to-noise ratio. This property actually derives from the principle of “blocking” well known in statistics.



We also noticed that the common spatial pattern (CSP) filtering method was regularly used. CSP is the gold standard spatial filtering technique in motor-imagery-based BCIs (MI) [54]. This algorithm was indeed part of the methodology in all studies that compare SSSEP-based BCIs to MI-based BCI [1, 50, 114]. The CSP algorithm determines spatial filters, *i. e.* weights of a linear combination of EEG signals, that maximize the variance of the resulting signal for one class while minimizing it for the other classes. Here, one class corresponds to the set of signals containing SSSEPs elicited by a specific stimulation, and the other class to the set of all other signals available in the recorded dataset. Typically, most of the studies use 3 pairs of spatial filters computed by the CSP algorithm, *i. e.* 3 filters that maximize the variance of one class and 3 that maximize the variance of the other class. The logarithms of variance of the CSP filtered EEG signals provide the feature vector fed into the classifier, with dimension 6 in the previous example.

#### 2.4.4 *Synthesis of SSSEP-based BCIs: main results*

In all the studies of tables 2a and 2b except one, different limbs were selected for receiving each periodical somatosensory stimulus when more than one was considered. However, in [14], Breitwieser *et al.* implemented a BCI using two fingers of the same hand. The reported average discrimination accuracy between both fingers, across all subjects, was  $58.6\% \pm 2.0$ . This result is below chance level (61%) considering the number of trials and a confidence limit at 95% [61]. However, the attention focusing effect, for one finger *vs.* resting state, both during stimulation, was successfully highlighted. The accuracy related to AF was similar for both fingers, *i. e.* thumb or middle finger, at about  $66.5\% \pm 5.4$ .

Usually, only one of the two stimulation techniques, *i. e.* short mechanical pulses or vibro-tactile stimulation, is used in the presented studies. In [20], Choi *et al.* tested different techniques of stimulation. The accuracy reported in table 2b for this article is the one for the control condition used in their experiment, *i. e.* for a standard vibro-tactile stimulation. Other compared techniques were variations of this vibro-tactile stimulation, with a carrier frequency at 200 Hz amplitude-modulated by non-periodic or periodic signals. One of the tested models was named “random pulses”, in which, during the standard vibro-tactile stimulation, transient random decreases of stimulation amplitude were inserted. Another tested model was named “tic-tic-toc”, in which during the standard vibro-tactile stimulation, a rhythmic train of transient decreases of stimulation amplitude was added. Two out of three pulses were regular pulses (tic) and the other one was much stronger (toc). Once the “toc” was added, the pattern restarted from the first “tic”, during the whole stimulation. This stimulation technique yields a significant improvement of the accuracy ( $p < 0.0001$ , *post-hoc* Tukey tests) compared to the others. The size effect was not reported, but we may deduce from the ex-

periment description that the median accuracy of the tic-tic-toc pattern was around 75%, while the median accuracies of standard vibro-tactile and random pulses were respectively 65% and 70%.

Most of the authors assessed the accuracy of their SSSEP-based BCI in highly controlled conditions. Usually, subjects were seated in front of a screen and performed the same task repetitively. Kim *et al.* followed a different approach [48–50]. Their evaluation framework consisted in driving a wheelchair along a predefined course while avoiding obstacles. The rate of wheelchair commands, one every five seconds, was the same for the tested SSSEP-based BCI and the control condition, *i. e.* a joystick. Three mechanical stimuli were simultaneously provided to the subjects at their right and left index fingertip and at the big toe of the right foot. The subject emitted a command by “concentrating his attention on the vibration stimulus”, task referred to as SS in table 2a. The ending point of the predefined path followed by the wheelchair was roughly 10 m apart from the starting point. Similar performances were obtained within the three studies, the ending point being reached on average twice faster with a joystick than with the BCI.

In tables 2a and 2b, most of the studies involved mechanical stimulation of fingers or, to a lesser extent, wrists. Foot-elicited SSSEPs have been scarcely studied, but we have found an example in the work of Kee *et al.* [46]. The authors asked the subjects to “attend their corresponding feet” when a cue was provided, task referred to as AF in table 1a. This AF task allowed the subjects to discriminate between both feet with an average accuracy of 72.6%.

#### 2.4.4.1 Performance stability of SSSEP-based BCIs.

We already indicated in section 2.3 that user-specific SSSEP characteristics seem to remain stable within a few weeks in between experiments [12]. Here, we aim to provide information about the stability over time of accuracy in SSSEP-based BCIs.

We found only one study that evaluates specifically the accuracy of an SSSEP-based BCI over several days. In 2006, Müller-Putz *et al.* reported an accuracy ranging from 66.9 to 83.9% across subjects on day one of the experiment [62]. Among the five subjects, three performed 4 successive sessions (one per day), and one performed 5 sessions. For each subject, online and offline accuracies were found rather stable from one session to another, except for subject 5 who performed 4 sessions and for whom an increase was observed in online as well as offline accuracies. For this subject, online accuracy increased from 63.8% (day 2) to 71.7% (day 4) whereas offline accuracy increased from 64.4% (day 1) to 75.0% (day 4).

#### 2.4.4.2 Frequency-based detection versus spatial-based detection

is, in the reviewed literature, the mainstream comparison between two algorithms that has been reported.

Kee *et al.* compared the accuracy obtained when using different features, extracted by a CSP or a PSD, in a 2-class classification problem [46]. First of all, in both methods, each EEG signal was filtered by a fourth order Butterworth wide band-pass filter between 0.5 and 40 Hz. This band-pass was introduced to capture specifically the alpha and beta frequency bands. After a frequency screening procedure aiming to assess the resonance-like frequency for each of their subjects, the authors used subject-specific FOS. The results from the frequencies screening procedure shows a broad distribution of resonance-like frequency, across subjects, the resonance-like frequency set was composed of the following FOS: 13, 23, 25, and 29. A PSD estimation computed on EEG epochs, lasting 250 milliseconds and sampled at 125 Hz, yielded a feature vector grouping the powers at 10 frequencies between 4 and 40 Hz.

Thus, although they determined the resonance-like frequency for each subject, the authors did not use it for tuning the parameters of signal processing. Consequently, because of the lack of selectivity, one can wonder if the proposed technique does not detect in fact a fluctuation within the alpha or beta band resulting from the AF task, instead of a specific variation of the SSSEP amplitude induced by AF. For their second method, the authors used the log variance of EEG signals filtered with 3 CSP pairs as classification features. They report similar accuracies for both algorithms, respectively 72.6% for PSD and 72.2% for CSP.

In 2014, Kim *et al.* compared the accuracies of an SSSEP-based BCI for different extracted features [47]. The first tested feature vector groups the log variances of 6 CSP filtered signals. The second tested feature vector gathers CSP-based log variances and several power measurements at specific frequencies determined by a FFT. The power estimation was at least determined at the FOS, but the procedure as well as the parameters of the FFT (window size, sampling frequency) were not reported. Surprisingly, the authors did not compute the FFT on spatially filtered signals, but on raw EEG signals. Performance evaluation was not performed either for feature vectors containing only the powers estimated by FFT. The CSP-based method yields an average accuracy of 76%, whereas the CSP+FFT-based method yields an average accuracy of 80.93%. The experiment was performed on only three subjects, which impairs the statistical significance of results.

In 2018, Kim *et al.* performed an equivalent study, this time on a total of twelve subjects [50]. The accuracy obtained with feature vectors containing only the powers estimated by a FFT was also computed. The CSP and FFT-based methods yield average accuracies of  $73\% \pm 11.8$  and

55%±6.8 respectively. The joint feature vector, including both CSP and FFT attributes, yields an average accuracy of 76%±12.8.

It is noteworthy that, to a lesser extent, one publication also uses phase information [100]. The Inter-Stimulus Phase Coherence is computed using the Hilbert transform and the analytic signal form of the EEG. This signal processing technique increases the accuracy of the proposed system from 75.4% to 79.8%.

#### 2.4.4.3 Comparison and combination of SSSEP-based BCIs with MI-based BCIs.

In tables 2a and 2b, several studies compared the accuracies of an SSSEP-based BCI and a MI-based BCI, such as [1, 2, 50, 114].

In 2014, Yao *et al.* conducted a 4-class experiment (left/right MI and left/right SS). The authors retained 6 combinations of conditions for a 2-class classification task by extracting two different groups of data, for example, right-SS *vs.* left-MI [114]. Four out of the 6 combinations were referred to as hybrid, such as in the previously provided example, when the two considered groups did not correspond to the same modality. The accuracy reported in table 2b is for the non-hybrid combination with only SS. This combination yield an accuracy of 72.6%±14.8, which is comparable to the accuracies of other studies.

For most subjects, using hybrid modalities had a limited impact on the accuracy. However, for two subjects, using hybrid modalities yielded an accuracy increase from 55-60% and 70% to above 90%. It is noticeable that the authors used fixed 23 Hz (left wrist) and 27 Hz (right wrist) FOS and a fixed wide band-pass filter between 8 and 26 Hz, that does not include the right FOS. Feature extraction was performed using 3 pairs of spatial filters computed with a CSP, the log variance of the filtered signals was used. Therefore, we can wonder if this analysis framework does not take mostly into account the spatial information of the left wrist-elicited SSSEP mixed with the influence of attention focusing. Among all combinations, the left SS *vs.* right MI produces the best performance with an average accuracy of 83.1%±10.4.

In 2014, Ahn *et al.* also compared and combined MI and SSSEP-based BCI paradigms [1]. The authors assessed the accuracies for different conditions: MI alone, SS alone, and both mental tasks at the same time. The subject received the same mechanical stimulation during these three conditions. A fourth condition was tested, in which the subject performed a SS task followed by a MI task, but without stimulation. The three conditions with stimulation lead to similar accuracies around 60% while MI without stimulation reached 70%. Actually, this methodology was very similar to the one of Yao *et al.* [114], except that the band-pass filter was different for each condition. The wide band-pass filter was between 16 to 25 Hz for the SS condition and 8 to 15 Hz for the MI without stimulation condition. Every resonance-like frequency identified

during the frequencies screening procedure lies within 16-25 Hz. For each condition, feature extraction was performed using CSP spatial filters, 5 pairs of filters. The vector formed from the power of the filtered signals was fed into the classifier.

In 2018, Kim *et al.* also compared both paradigms [50]. They evaluated an SSSEP-based BCI as well as a MI-based BCI for a wheelchair-driving task. The authors reported that the MI-based BCI was less efficient than the SSSEP-based BCI, with an average path following duration of  $173 \pm 95$  seconds for MI compared to  $102 \pm 26$  seconds for SSSEP. One can notice that with the MI-based BCI, four subjects could not finish the path following task in less than 5 minutes and that in this case a 300 seconds duration of the task was considered for calculating average performance. When these subjects are removed from the list to estimate the average task duration, the latter drops down to  $110 \pm 26$  seconds, which is equivalent to the average duration of the SSSEP-based BCI task.

#### 2.4.4.4 Comparison of SSSEP-based BCI with a somatosensory-evoked P300-based BCI

was very rarely performed in the literature. We report only one study that performed this comparison.

In 2013, Severens *et al.* compared their SSSEP-based BCI with a P300-based BCI in which the P300 was elicited by a transient mechanical stimulation [95]. The SSSEP was elicited by short mechanical pulses, with a 50% duty-cycle control signal. The authors reported that the P300 alone outperformed the SSSEP-based BCI, with an average accuracy of 74% and 60% respectively, after only 2 seconds of recording. With 16 seconds of recording, the respective accuracies increased to 93% and 68%. The SSSEP-based BCI reached this level of accuracy after 4 seconds, and remains stable after that, whereas the P300-based BCI accuracy kept increasing with recording duration. Additionally, the accuracy of the combination of both stimulation, *i. e.* transient twitches and sustained pulsation, does not significantly differ from the one of P300 alone.

However, the differences of performance can be put in perspective from a different point of view. Firstly, the features chosen for SSSEP classification are unusual, since they correspond to the power estimates of EEG signals at the two FOS, 18 and 21 Hz, at two of its harmonics as well as at half of the FOS. EEG was recorded with 64 electrodes, among which the authors performed an outlier detection for each subject, resulting in removing an average of 6.9 electrodes (std 3.8). Anyway, this yields a very large feature vector, with 8 signal powers (at 9, 10.5, 18, 21, 36, 42, 54, and 63 Hz) for each retained electrode. As seen in section 2.3.4.2, other studies tend to demonstrate that powers at harmonics contain little information, especially those produced by FOS

higher than 11 Hz. Moreover, when the stimulation results from short mechanical pulses, *i. e.* from a square signal, there is no information at the second harmonic of the FOS. Therefore, since no prior feature selection is performed before classification, its accuracy can be seriously impacted. This effect may have been counterbalanced by the use of a regularized classification algorithm, but this has not been reported or discussed by the authors.

To summarise, in this section we presented a review of studies describing an EEG-based BCI exploiting SSSEP. We firstly presented the main signal processing and feature extraction techniques reported in the literature. In most studies, features are extracted by a FFT analysis, or by an equivalent technique. Lock-in amplifier systems are also regularly used. Spatial filtering techniques, such as common spatial pattern or channel selection with bipolar montage, can improve SSSEP analysis.

The second part of our review was focused on analysing the performances of the EEG-based BCI exploiting SSSEP. Reported average accuracies, for systems exploiting the stimulation of two distinct upper limbs, varies from 60% to 79.8%, for a 2-class problem. 3-class problems are rarely tackled, and BCI performance shows higher variability, with an accuracy from 42.1% to 80.93%. One study uses SSSEP to reduce the number of false triggering in MI-based BCI [116]. Comparison of SSSEP-based BCI with paradigms other than motor imagery have been scarcely performed, which reinforces our idea that the field should be further explored.

## 2.5 CONCLUSION

In this review, we presented and analysed 24 articles that deal either with the estimation of user specific characteristics of SSSEPs or with the description of an SSSEP-based BCI.

Most studies describing the precise relationship between SSSEP characteristics and stimulation parameters, show that they are highly subject dependant. Due to this strong variability, the frequencies screening procedure, *i. e.* the determination of user-specific FOS, appears as a mandatory stage in any SSSEP-based BCI in order to improve its performance. For instance, the study of Pokorny *et al.* shows that a shift of the FOS by 5 Hz from the resonance-like frequency elicits SSSEPs with an amplitude roughly twice weaker [85]. However, although they are of major interest, the results of the determination of user-specific FOS or the procedure itself are rarely reported in their entirety as can be seen in table 2b.

We also presented 17 studies that describe an SSSEP-based BCI and assess its performance. The reported average accuracy for a 2-class classification problem varies between 60% to 72%, and between 42.1% to 76% for a 3-class classification problem. However, in most of the studies



reporting high average accuracies, experiments were performed with a small number of subjects, which lowers their statistical significance.

Some of the presented studies compare their results to other BCI paradigms. They provide very interesting insights, but again due to the small number of subjects involved in the experiments, no definitive conclusion can be drawn. Paradigm comparison was mostly performed between MI and SSSEP. SSSEP has the advantage of being easier to detect in the EEG, thanks to the use of exogenous stimuli, than MI-related cortical activities. False command triggering, caused by the detection of irrelevant mental activity during MI, can also be mitigated by the use of SSSEP [116].

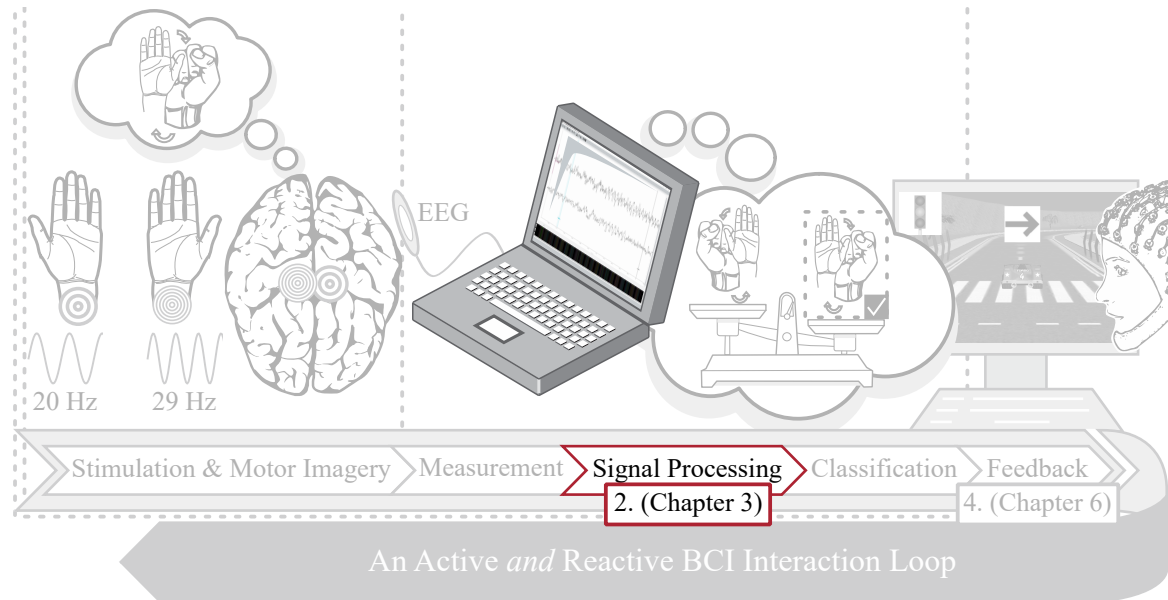
As we stated in the introduction, SSSEP-based BCI uses a modality that is underused or even unused by a person with a motor disability. Hence, SSSEP-based BCIs, that do not monopolize the user's sight or hearing for stimulation or feedback, should be developed and tested for motor-disabled users. All the experiments reported in the reviewed articles were performed on healthy people. However, it has been shown that people who suffer from amyotrophic lateral sclerosis or from other neuromuscular pathologies such as spinal muscular atrophy retain a functional somatosensory system [31, 36]. It offers the hope that future developments of SSSEP-based BCIs will provide these patients with an easy to use interface that does not solicit their visual or auditory system.

After this review, we can also conclude that studies show that SSSEPs characteristics highly depend on the stimulation procedure or device. The use of a standard and validated stimulation unit, conforming with safety standards for medical electrical equipment such as EN 60601-1:2006 [84], might reduce this variability and allow an easier comparison of results from different studies.

Finally, we also lack answers to many questions about SSSEP that initially look rather basic, such as: What is the influence of the stimulation position on the characteristics of the SSSEP, like amplitude or total latency? How long does it take for a SEP to reach its steady-state? Is there a relationship between physical traits of a person and resonance-like frequencies? This research field should be investigated further to gain an in-depth understanding of SSSEPs and pave the way to efficient SSSEP-based BCIs.

# AMPLITUDE ESTIMATION OF SINUSOIDAL COMPONENTS IN EEG-BASED BRAIN-COMPUTER INTERFACES EXPLOITING STEADY-STATE SOMATOSENSORY-EVOKED POTENTIALS

## ROADMAP —



As we observed in our previous chapter, many algorithms handling frequency and spatial information to extract characteristic features of SSSEPs exist in SSSEP-based BCI. We observed some trends in managing spatial and frequency pieces of information. Each trend is most often related to a specific research group. However, our findings do not allow us to conclude regarding the most efficient algorithm, the variability in the classification accuracy being relatively high. It does not hinder our research/implementation since we are more interested in monitoring one sinusoidal component's amplitude variation. Most of the previously presented algorithms do not solely rely on the SSSEPs' amplitude information as a feature for classification. The features are often based on spatial information, or larger frequency bands, or both. Therefore, the information from the SSSEPs' amplitude variation can be unused or mixed with other signal sources. In this chapter, we compare several signal processing methods aiming to estimate the amplitude of a targeted sinusoidal component, *i.e.* the SSSEP, commonly used in the field of EEG-based BCI.

## RELATED WORK (SUBMITTED) —

Jimmy Petit, François Cabestaing, and José Rouillard. "Amplitude Estimation of Sinusoidal Components in EEG-based Brain-Computer Interfaces exploiting Steady-State Somatosensory-Evoked Potentials" (submitted)

## ACKNOWLEDGEMENTS —

We thank our dear colleague Pr. Michael Rudko for his insightful advices on the model and on signal processing techniques, as well as colleagues of the Lille University Hospital for their support during BCI and EEG experiments.



### 3.1 INTRODUCTION

A mechanical action applied on the skin evokes a specific brain response in the somatosensory cortex contralateral to the stimulation. Scalp electroencephalography (EEG) allows measuring this response yielding a so-called somatosensory evoked potential (SEP). When the mechanical action is periodic and maintained (vibration), the SEP is also periodic with the same frequency, and called steady-state SEP (SSSEP) [96].

Specific mental activities, such as attention focusing, modulate the amplitude and/or phase of the SSSEP. This volitional modulation constitutes a significant marker of mental activity potentially used in a brain-computer interface (BCI) [32]. For instance, two vibrations with different frequencies can be simultaneously applied on the left and right wrists. By focusing their attention on one stimulation or the other, the BCI user modulates the amplitude of the corresponding SSSEP, finally resulting in a command sent to the interface.

SSSEP are similar in nature to steady-state visually-evoked potentials (SSVEP) widely used in BCI. In a BCI exploiting SSVEP, several visual stimuli, flickering at different frequencies and/or phases, are simultaneously presented to the user. To send a command through the BCI, the user focuses their attention on one of the visual stimuli. This results in an amplitude increase of the SSVEP at the frequency of target visual stimulation that can be detected by an appropriate signal processing technique.

Despite their similarity, BCIs exploiting SSVEP and SSSEP do not detect exactly the same oscillating markers in EEG signals. Steady-state potentials evoked by visual stimuli do not appear at precisely defined locations in the primary visual cortex. Thus, in BCIs exploiting SSVEP, the aim of signal processing is to find the frequency component with the highest amplitude in many EEG signals recorded over the whole occipital lobe of the brain. To this end, Canonical Correlation Analysis (CCA) is currently considered as the most interesting method, since it yields directly features fed into a classifier that determines the stimulus of interest [18]. In contrast, steady-state potentials evoked by a mechanical vibration are precisely located in the primary somatosensory cortex according to the somatosensory homunculus [73]. Thus, in BCIs exploiting SSSEP, the aim is to measure accurately variations of the amplitude at specific frequencies in a few EEG signals recorded only over the left and right precentral and postcentral gyri of the parietal lobe.

In this article, we compare a basic signal processing method that estimates the amplitude of a specific frequency component, namely the lock-in amplifier (LiA), and more complex techniques used in BCIs exploiting SSVEP, namely the CCA and the partial least squares (PLS) methods. We show that in the specific case of BCIs exploiting SSSEP, the

latter two do not yield any performance improvement over the former despite their greater complexity.

In section 3.2, we introduce a specific model of surface EEG, in which measurement channels are linear combinations of sinusoidal sources — steady-state brain responses to several mechanical vibrations at different frequencies — with additive Gaussian white noises. Then, in section 3.3 we present the amplitude estimation techniques that will be compared later, indicating their similarities as well as their main differences. In section 3.4 the comparison of amplitude estimation techniques is performed on synthetic EEG signals in which a specific sinusoidal component is considered as the source of interest, and all other sinusoidal sources as well as Gaussian noises must be filtered out. Then, in section 3.5, the same comparison is performed on real EEG data, recorded during the second session (attention focusing) of a SSSEP-based BCI experiment (Ethics Committee of Lille University record number: 2020-417-S81). Finally, we discuss the comparison results and conclude.

### 3.2 ASSUMPTIONS AND SIGNAL MODELS

In this section, we introduce the EEG formation model that we use to explain the relationship between EEG signals (measurement channels) and steady-state responses (sources) evoked by the vibrating mechanical stimulation of the user’s skin. We also calculate signal-to-noise ratios, of raw and spatially filtered EEG signals, when a single source is considered as the steady-state evoked response of interest.

#### 3.2.1 Brain sources and EEG measurement channels

We consider that a set of  $N$  vibrating devices, with frequencies  $f_n$ ,  $n = 0, \dots, N - 1$ , stimulate the user’s skin simultaneously. Each device stimulates a well defined part of the skin, evoking a steady-state response in the primary somatosensory cortex at a location corresponding to the somatotopic arrangement [73]. We consider that each response can be modelled as a current dipole source whose amplitude oscillates at the same frequency as the corresponding mechanical stimulation. Very precise models exist that relate the electric activity recorded by a specific EEG electrode to activities of a set of dipoles [25, 68]. In our model, we simply consider that the voltage recorded by an EEG electrode is a linear combination of all dipole amplitudes.

More precisely, let  $e_n$ ,  $n = 0, \dots, N - 1$  denote the cosine signal modelling the dipole source with amplitude  $A_n$ , frequency  $f_n$  and phase  $\phi_n \in [-\pi, \pi[$ , sampled at frequency  $f_e$  to get  $K$  samples

$$e_n[k] = A_n \cos(2\pi f_n k / f_e + \phi_n), \quad k = 0, \dots, K - 1, \quad (3.1)$$

over the sampling window  $K/f_e$ .

The EEG is the set of  $M$  noisy measurement channels  $x_m$  resulting from linear combinations of signals modelling dipole sources:

$$x_m[k] = \sum_{n=0}^{N-1} \delta_{m,n} e_n[k] + v_m[k], \quad k = 0, \dots, K-1, \quad (3.2)$$

where  $v_m[k] \sim \mathcal{N}(0, \sigma_m^2)$  are  $M$  additive white Gaussian noises sampled on the same window as source signals. Each  $\delta_{m,n}$  coefficient weights the influence of the  $n^{\text{th}}$  dipole source in the  $m^{\text{th}}$  measurement channel. When needed, the matrix aggregating all measurement signals  $x_m$  is denoted by  $X$ , a  $K$ -by- $M$  matrix. In some equations, we also use the vector  $\mathbf{x}_m \in \mathbb{R}^K$  regrouping the  $K$  samples of  $x_m$ .

### 3.2.2 Signal-to-noise ratio

Without loss of generality, we consider in the following that the dipole source of interest is  $e_0$ , *i. e.* that the SSSEP amplitude is estimated for the frequency of stimulation  $f_0$ . This implies that other dipole sources  $e_n$ ,  $n = 1, \dots, N-1$  as well as  $v_m$ ,  $m = 0, \dots, M-1$  can be considered as additive noise sources. In the  $x_m$  measurement channel, the meaningful signal is the component created by the  $e_0$  source, given by the samples

$$\delta_{m,0} e_0[k], \quad k = 0, \dots, K-1, \quad (3.3)$$

whereas the noise, *i. e.* all other components, is given by the samples

$$v_m[k] + \sum_{n=1}^{N-1} \delta_{m,n} e_n[k], \quad k = 0, \dots, K-1. \quad (3.4)$$

The power of the meaningful signal defined by (3.3) is the average of its squared samples

$$\frac{\delta_{m,0}^2}{K} \sum_{k=0}^{K-1} e_0[k]^2 = \frac{\delta_{m,0}^2 A_0^2}{K} \sum_{k=0}^{K-1} \cos^2(2\pi f_0 k / f_e + \phi_0), \quad (3.5)$$

which, if the signal period  $1/f_0$  is small enough compared to the sampling window  $K/f_e$ , and as the mean of the squared cosine terms converges to 0.5, can be approximated by

$$\frac{\delta_{m,0}^2 A_0^2}{2}. \quad (3.6)$$

In the following, while evaluating the noise power, *i. e.* the square of (3.4), by “small enough” we mean that the sampling window of length  $K$  must contain enough fully sampled periods of the stimulation frequency  $f_0$  in order to allow the average of non squared cosine terms to decrease toward zero, thus to become negligible.

The power of the noise signal defined by (3.4) is also the average of its squared samples. The  $k^{\text{th}}$  squared sample of the noise is given by

$$v_m[k]^2 + 2v_m[k] \sum_{n=1}^{N-1} \delta_{m,n} e_n[k] + \left( \sum_{n=1}^{N-1} \delta_{m,n} e_n[k] \right)^2. \quad (3.7)$$

The first term of (3.7) is the squared Gaussian noise, so the average of its samples is the noise variance  $\sigma_m^2$ . The second term of (3.7) is the product of samples of the Gaussian noise and uncorrelated samples of a sum of weighted cosine functions. Its average over all samples of the sampling window decreases toward zero if the periods of all stimulation frequencies  $f_n$ ,  $n = 1, \dots, N-1$  are small enough compared to the sampling window  $K/f_e$ .

Finally, the third term of (3.7) can be expressed as the double sum of products of cosine functions:

$$\sum_{n_1=1}^{N-1} \sum_{n_2=1}^{N-1} \delta_{m,n_1} \delta_{m,n_2} e_{n_1}[k] e_{n_2}[k], \quad (3.8)$$

in which each product can be further transformed into the half sum of two cosine functions:

$$\frac{A_{n_1} A_{n_2}}{2} (\cos(2\pi(f_{n_1} + f_{n_2})k/f_e + \phi_{n_1} + \phi_{n_2}) + \cos(2\pi(f_{n_1} - f_{n_2})k/f_e + \phi_{n_1} - \phi_{n_2})). \quad (3.9)$$

If  $1/(f_{n_1} + f_{n_2})$  is small enough compared to  $K/f_e$ , then the average of the first term over all samples can be neglected. When  $n_1 = n_2 = n$ , the second term is equal to one, and therefore the average of the corresponding term of (3.7) over all samples is  $\delta_{m,n}^2 A_n^2 / 2$ . When  $n_1 \neq n_2$ , the average of the second term over all samples can be neglected only when the period  $1/|f_{n_1} - f_{n_2}|$  is small enough compared to  $K/f_e$ . In the expression of the signal-to-noise ratio, in order to neglect terms resulting from the combination of two different frequencies of stimulation, the latter must be different enough.

Under all these assumptions, the signal-to-noise ratio of a measurement channel  $x_m$  is given by

$$\text{SNR}_m = 10 \log_{10} \left( \frac{\delta_{m,0}^2 A_0^2}{2\sigma_m^2 + \sum_{n=1}^{N-1} \delta_{m,n}^2 A_n^2} \right). \quad (3.10)$$

### 3.2.3 Spatial filtering

When considering that the signal of interest is the same in all measurement channels, but that noises are mutually independent, a spatial filtering technique can be introduced in the processing pipeline in order

to increase the final SNR. The spatially filtered signal  $x$  is actually a linear combination of measurement channels given by the samples

$$x[k] = \sum_{m=0}^{M-1} w_{x,m} x_m[k], \quad k = 0, \dots, K-1, \quad (3.11)$$

where  $w_{x,m}$  are the weights characterising the filter. Averaging measurement channels is equivalent to applying a spatial filter with identical weights on all measurements, *i. e.*  $w_{x,m} = 1/M$ ,  $m = 0, \dots, M-1$ .

One can easily express the signal-to-noise ratio of the spatially filtered measurement channels. In  $x$ , the meaningful signal is the sum of components created by the  $e_0$  source, given by the samples

$$\left( \sum_{m=0}^{M-1} w_{x,m} \delta_{m,0} \right) e_0[k], \quad k = 0, \dots, K-1, \quad (3.12)$$

whereas the noise is given by the samples

$$\sum_{m=0}^{M-1} w_{x,m} \left( v_m[k] + \sum_{n=1}^{N-1} \delta_{m,n} e_n[k] \right), \quad k = 0, \dots, K-1. \quad (3.13)$$

Considering the same hypotheses as in section 3.2.2, *i. e.* that the average of non-squared cosine functions decreases toward zero and that stimulation frequencies are different enough one from the other, but also that the  $M$  Gaussian noises are mutually independent, the SNR of  $x$  is given by

$$\text{SNR}_x = 10 \log_{10} \left( \frac{\delta_0'^2 A_0^2}{2 \sum_{m=0}^{M-1} w_{x,m}^2 \sigma_m^2 + \sum_{n=1}^{N-1} \delta_n'^2 A_n^2} \right), \quad (3.14)$$

in which

$$\delta_n' = \sum_{m=0}^{M-1} w_{x,m} \delta_{m,n}, \quad n = 0, \dots, N-1. \quad (3.15)$$

Among spatial filtering techniques, the surface Laplacian has gained a particular interest in the BCI community [57, 67]. Combining a specific measurement channel and some of its spatial neighbours, the surface Laplacian filter helps recovering the influence of sources located near this channel by removing unwanted activities of other sources reaching it because of volume conduction [56].

The filtered measurement channel samples are given by

$$x[k] = x_m[k] - \sum_{m' \in B(m)} w_{m,m'} x_{m'}[k], \quad k = 0, \dots, K-1, \quad (3.16)$$

in which  $B(m)$  is the set of indices of measurement channels neighbouring  $x_m$  and  $w_{m,m'}$  are positive weighting coefficients. In this study, we consider two particular cases of surface Laplacian filters, the so-called "small Laplacian" (SL) and the scalp current density (SCD) estimator.

The SL combines the considered measurement channel  $x_m$  and its four nearest neighbours [56]. Thus,  $B(m)$  is a set of four channel indices and the weights are the inverse of distances — on the scalp — between electrodes, normalised to one:

$$w_{m,m'} = \frac{d_{m,m'}^{-1}}{\sum_{m' \in B(m)} d_{m,m'}^{-1}}, \quad m' \in B(m). \quad (3.17)$$

The CSD filter [45] estimates the current source density through the scalp at one measurement location using a spatial filter equivalent to a surface Laplacian. For this filter, the  $B(m)$  set of indices is the range  $0, \dots, M-1$  except  $m$ , and the weights are determined using the spherical spline interpolation technique proposed by Perrin *et al.* [74]. In order to better control the effect of spatial filtering on the amplitude estimation, we normalise the CSD filter coefficients to get the sum of positive values equal to one, in the same way as for the simple SL of (3.16) [56].

### 3.3 COMPARED ALGORITHMS

In this section, we introduce three signal processing techniques that yield an estimation of the amplitude of a specific sinusoidal component, with frequency  $f_a$ . To this end, the lock-in amplifier (LiA) processes a single signal, whereas the two others — canonical correlation analysis (CCA) and partial least squares (PLS) — process the whole set of EEG measurements.

#### 3.3.1 Lock-in Amplifier - LiA

A lock-in amplifier (LiA) is a homodyne detector followed by a low-pass filter [8]. When the aim is to detect a sinusoidal component in the signal at the analysis frequency  $f_a$ , homodyne detection is just performed by multiplying every signal sample by samples of the cosine and sine functions with frequency  $f_a$ , as follows:

$$\begin{aligned} c[k] &= x[k] \cos(2\pi f_a k / f_e), \text{ and} \\ s[k] &= x[k] \sin(2\pi f_a k / f_e), \\ &\text{for } k = 0, \dots, K-1. \end{aligned} \quad (3.18)$$

In the following, we consider that  $h[l], l = 0, \dots, L-1$  is the finite impulse response of a causal low-pass filter. For the sake of simplicity, we do not take into account side effects, *i. e.* potentially out of bounds

indices in the following equations. Samples of the low-pass filtered homodyne detection signals  $c_h$  and  $s_h$  are given by:

$$\begin{aligned} c_h[k + L - 1] &= \sum_{l=0}^{L-1} c[k + l]h[L - 1 - l], \text{ and} \\ s_h[k + L - 1] &= \sum_{l=0}^{L-1} s[k + l]h[L - 1 - l], \\ &\text{for } k = 0, \dots, K - 1. \end{aligned} \quad (3.19)$$

The amplitude estimation by the LiA of the signal component at frequency  $f_a$  is given by

$$\widehat{A}_{\text{LiA}}(f_a) = 2\sqrt{c_h[k]^2 + s_h[k]^2}, \quad \widehat{A}_{\text{LiA}}(f_a) \in \mathbb{R}^+. \quad (3.20)$$

One can notice that this estimation is obtained for every sample, which allows an estimation of the sinusoidal component's amplitude dynamics.

When the low-pass filter impulse response is a gate function with length  $L = K$ , *i. e.* when  $h[l] = 1/K, l = 0, \dots, K - 1$ , it is straightforward to show that the LiA estimator is strictly equivalent to a discrete Fourier transform.

### 3.3.2 Canonical Correlation Analysis - CCA

The CCA aims at measuring the relationship between two blocks of variables. In BCI exploiting SSVEP, CCA is used to find the maximum correlation between a block of measurements of the cortical activity, usually EEG signal samples, and a block of analysis functions [30, 51]. The sketch of CCA computation, similar to the one proposed in [51] is presented in figure 3.1.

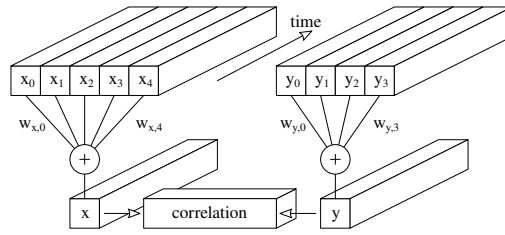


Figure 3.1 : Illustration of CCA computation

EEG measurements correspond to the  $M$  signals  $x_m$  on the left and analysis functions to the  $P$  signals  $y_p$  on the right. The CCA algorithm estimates the weights  $w_{x,m}$ ,  $m = 0, \dots, M-1$ , and  $w_{y,p}$ ,  $p = 0, \dots, P-1$  that maximize the correlation between the two linear combinations [110]. In the following,  $w_x \in \mathbb{R}^M$  and  $w_y \in \mathbb{R}^P$  denote the vectors concatenating respectively the weights of measurements and analysis functions, and  $Y$  denotes the  $K$ -by- $P$  matrix aggregating all analysis functions  $y_p$ .



The linear combinations of signals yielding  $\mathbf{x}$  on one side, and of analysis functions yielding  $\mathbf{y}$  on the other side, can be considered as two projections from high dimensional spaces (respectively  $\mathbb{R}^{K \times M}$  and  $\mathbb{R}^{K \times P}$ ) onto  $\mathbb{R}^K$ :

$$\mathbf{x} = Xw_x, \text{ and } \mathbf{y} = Yw_y. \quad (3.21)$$

With the optimal weights provided by CCA,  $\mathbf{x}$  and  $\mathbf{y}$  are unit vectors and the angle between them in  $\mathbb{R}^K$  is minimum.

In the literature, the correlation coefficients computed by the CCA are most of the time considered only as classification features. The amplitude estimation or relative amplitude estimation (such as in [30]) is usually not performed. Here, in the specific case of BCIs exploiting SSSEP, since amplitude estimation is mandatory, it will be considered as well for CCA.

Like for the *a priori* defined surface Laplacian filters, we normalise the coefficients  $w_{x,m}$ ,  $m = 0, \dots, M-1$  yielded by the CCA in order to get the sum of positive values equal to one. Let  $\gamma$  denote the positive constant by which the coefficients are multiplied to obtain this normalisation. The normalised projection of EEG samples onto  $\mathbb{R}^K$  is now

$$\mathbf{x}' = X\gamma w_x, \text{ and } \|\mathbf{x}'\|_2 = \gamma \|\mathbf{x}\|_2 = \gamma. \quad (3.22)$$

Therefore, in order to keep the same length of both projected vectors in  $\mathbb{R}^K$ , the samples of the analysis functions must also be multiplied by  $\gamma$ . Finally, the resulting linear combination of analysis functions with the weights  $\gamma w_{y,p}$ ,  $p = 0, \dots, P-1$  is the best approximation by CCA of the signal of interest.

In our case, we only use two analysis functions  $y_0$  and  $y_1$ , namely a cosine and a sine function with frequency  $f_a$ . Therefore, the best source approximation obtained from measurement signals is the sinusoidal function with samples:

$$y[k] = \gamma w_{y,0} \cos(2\pi f_a k / f_e) + \gamma w_{y,1} \sin(2\pi f_a k / f_e), \quad k = 0, \dots, K-1, \quad (3.23)$$

from which it is straightforward to show that the searched amplitude is given by

$$\widehat{A}_{\text{CCA}}(f_a) = \gamma \sqrt{w_{y,0}^2 + w_{y,1}^2}. \quad (3.24)$$

### 3.3.3 Two-Block Mode A Partial Least Squares - PLS

CCA is formally equivalent to the Two-Block Mode B Partial Least Squares (PLS) method from the PLS sets of methods [110]. However, since CCA was first described in 1936 by Hotelling [41], but PLS only in 1975 by Wold [112], the name CCA remains commonly used rather than

PLS-W2B. Because of its similarity with CCA, we decided to include also the PLS-W2A in our set of compared estimation methods. For clarity, in the rest of the paper PLS-W2A will be simply named PLS.

The PLS method differs slightly from CCA since it aims at determining the optimal weights  $w_x$  and  $w_y$  that maximise the covariance between  $X$  and  $Y$  [110], rather than their correlation.

With the PLS, the amplitude of the component of interest is estimated using the same method as for the CCA, *i. e.* the normalisation of spatial weights to get a sum of positive values equal to one. The estimated amplitude is denoted by  $\hat{A}_{\text{PLS}}(f_a)$ .

### 3.4 COMPARISON ON SYNTHETIC EEG DATA

In this section, we compare the amplitude estimators on synthetic EEG data obtained using the model described in section 3.2. We first present the synthetic signals, and then the amplitude estimations obtained by the compared methods.

#### 3.4.1 Synthetic EEG data

In this simulation, we consider that sources' activities are evoked by two mechanical stimulations, one on each wrist, with the same amplitudes. During an idle period, the user receives no stimulation and the measurement signals are considered as a baseline. Then, during an active period, the user receives both stimulations and the measurement signals include the corresponding SSSEPs. With the synthetic signals, we want to assess whether the target frequency can be recovered during the active period depending on the SNR.

We consider 64 EEG electrodes located according to the international standardized 10-20 system [92]. The electrodes' positions are those from the "biosemi64" montage from MNE-Python. The sampling frequency is 512 Hz and the sampling window duration is 3.0 s. We consider two steady-state dipole current sources, with frequencies 20 Hz and 25 Hz, located respectively in the left and right somatosensory cortices. The source at 20 Hz is located next to electrode C3 in the left hemisphere and the source at 25 Hz is next to electrode C4 in the right hemisphere. More precisely, both current dipoles are radial, *i. e.* orthogonal to the scalp surface, have the same amplitude, and are located 25 millimeters below C3 and C4 electrodes. The dipoles' frequencies are set with a difference of 5 Hz between them, as it is the common practice to keep this minimum distance between two frequencies of stimulation in SSSEP-based BCI [80]. The signal of interest comes from the source at 20 Hz located below C3. EEG voltages are determined assuming the basic volume conduction model in a homogenous and isotropic conductive sphere [68]. The voltage produced by a source on a given EEG electrode is proportional to the squared distance between it and the middle of

the current dipole, as well as to the cosine of the angle between the dipole axis and the straight line connecting its middle to the electrode. Voltages created by both current sources are finally added up to get the synthetic EEG measurement signals.

According to the model described in section 3.2, independent white Gaussian noises with the same variance are then added to every synthetic EEG channel. Following (3.10), the Gaussian noise standard deviation is fixed at  $6.3 \times 10^{-7}$  V to have a SNR of 1 dB over C<sub>3</sub> when  $A_{0,active} = A_{1,active} = 1 \mu\text{V}$ . To test different SNRs we progressively increase the amplitude of both sinusoids from  $10^{-9}$  V to  $10^{-4}$  V. Two thousand noise realisations are computed for each amplitude level.

In the following comparison of signal processing techniques, we compute the ratio between the amplitudes of the target frequency estimated on two successive measurement windows. The first window, from 0 to 1.5 second, is the idle period, during which amplitudes are set at zero, and the signals have only one component, *i. e.* the Gaussian noise. The second window, from 1.5 to 3.0 seconds, is the active period during which the amplitude of the source of interest and of the other sources are set to a given value.

### 3.4.2 Amplitude estimation on synthetic data

We compare the five amplitude estimation methods listed in table 3.1. Each method combines a spatial filter (see section 3.2.3) and an amplitude estimator (see section 3.3). The impulse response of the low-pass filter of the LiA is as a gate function with the same length as data snippets. Electrode selection is considered as a spatial filter with a unit weight on the selected electrode — here C<sub>3</sub> — and null weights on other electrodes. The Small Laplacian (SL) centred on C<sub>3</sub> combines this measurement channel and channels C<sub>1</sub>, CP<sub>3</sub>, C<sub>5</sub>, and FC<sub>3</sub> according to (3.16). The Current Source Density (CSD) spatial filter estimated at C<sub>3</sub> is normalised in order to have a unit weight on this electrode of interest.

Method	Spatial Filter	Amplitude Estimator
LiA	Selection of C <sub>3</sub>	LiA
SL-LiA	SL centered on C <sub>3</sub>	LiA
CSD-LiA	CSD estimated at C <sub>3</sub>	LiA
CCA	Determined by CCA	CCA estimator
PLS	Determined by PLS	PLS estimator

Table 3.1 : Compared amplitude estimation methods, each one combining a spatial filter and an amplitude estimator

Figure 3.2 shows the evolution of the ratio of amplitudes at target frequency estimated during active and idle periods as the SNR increases.

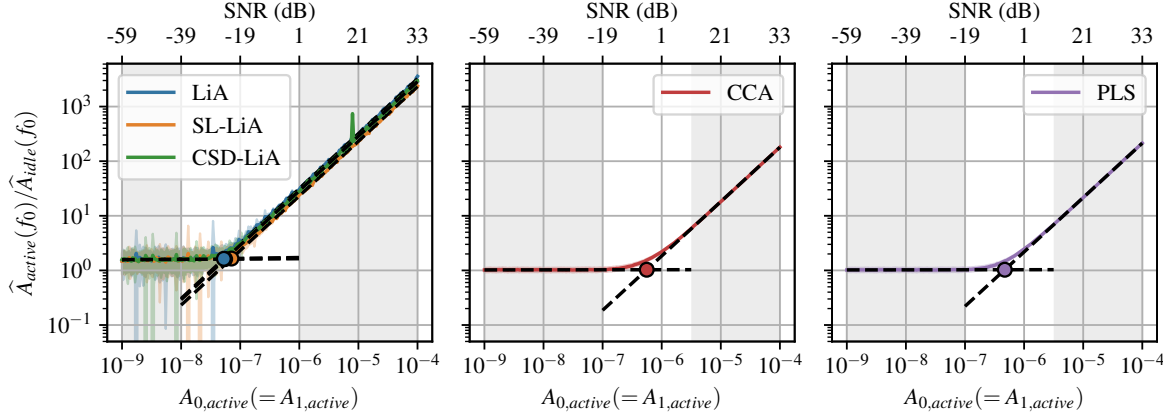


Figure 3.2 : Influence of sinusoids amplitude on the ratio of amplitudes at target frequency estimated during active and idle periods for a fixed Gaussian noise level. The targeted sinusoidal signal has a frequency of 20 Hz and a random phase in  $]-\pi, \pi]$ . The second sinusoidal component, treated as noise in the simulation, is at 25 Hz with a random phase in  $]-\pi, \pi]$ . The Gaussian noise standard deviation is fixed at  $6.3 \times 10^{-7} V$  to have an SNR of 1 dB over  $C_3$  when  $A_{0,active} = 1 \mu V$  – see (3.10). One relative standard deviation is displayed in a colour lighter than the one of the average curve, computed as  $\frac{1}{\ln(10)} \frac{Std(x)}{\bar{x}}$ . The light grey area displays the x-axis interval where the linear regressions are calculated in order to find the divergence point.

For all methods, resulting curves show a plateau near 1.0, in the log scale, for amplitudes lower than  $10^{-8} V$ . It indicates that the target component can not be retrieved in the measurements for such low SNR. As the amplitude increases, each method eventually diverges from the plateau, reaching a linear relationship between the computed ratio and the amplitudes of the sinusoids. The methods that first diverge from the plateau are the LiA-based ones, indicating that they can retrieve the target sinusoid for lower SNRs than the CCA and PLS estimators.

In order to get a quantitative result, we define a divergence point at the intersection of the two asymptotes of each curve, determined by linear regressions in areas coloured in light grey in the figures. The signal amplitudes and SNRs of divergence points of all methods are summarised in table 3.2. All LiA-based methods start to retrieve the target component for a SNR around -23 dB, in contrast to CCA and PLS that need a higher SNR around -5 dB.

Figure 3.3 shows spatial filters determined by the CCA and PLS estimators during the active period for several levels of SNR. For comparison, figure 3.4 shows the fixed spatial filters used in LiA-based estimators, that are independent of the SNR level. The maximum values of all filters are normalised to 1.0 in the two figures, for the sake of comparison.

Method	$A_{0,active}$ (V)	$SNR_{C3}$ (dB)
LiA	$5.3 \times 10^{-8}$	-24.5
SL-LiA	$7.1 \times 10^{-8}$	-22.0
CSD-LiA	$5.6 \times 10^{-8}$	-24.1
CCA	$5.6 \times 10^{-7}$	-4.1
PLS	$4.7 \times 10^{-7}$	-5.5

Table 3.2 : Divergence point for each method, signal amplitude and equivalent SNR.

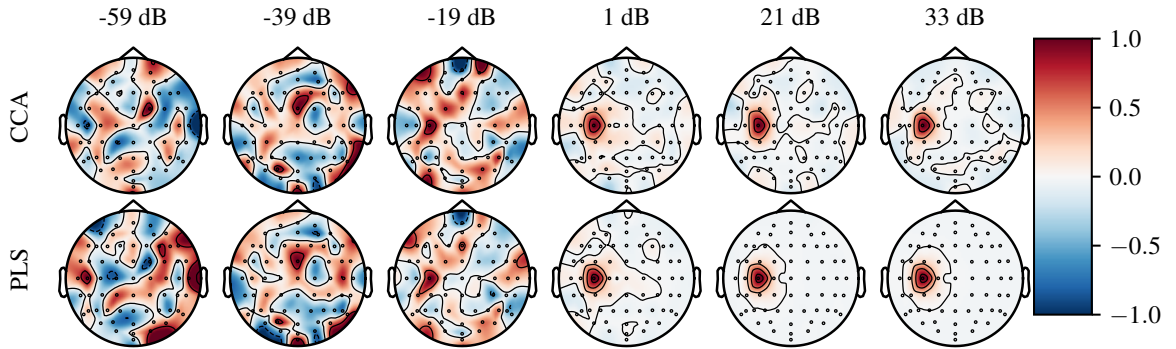


Figure 3.3 : Examples of spatial filters computed by the CCA and PLS as the SNR level increases. They are estimated on a single noise realisation and are normalised to have a maximum coefficient of 1.0.

We can observe that for low SNRs, the filters look random, indicating that neither method can locate the position of the source of interest. As the SNR increases, the PLS yields a filter that seems to converge towards a filter equivalent to the CSD at C3. On the other hand, the CCA also locates the source of interest, but yields a filter that looks less regular, even for very high SNRs. We hypothesise that this is due to the multicollinearity within synthetic signals, that tends to cause numerical instability of the CCA algorithm because of the inversion of a close to singular matrix [110].

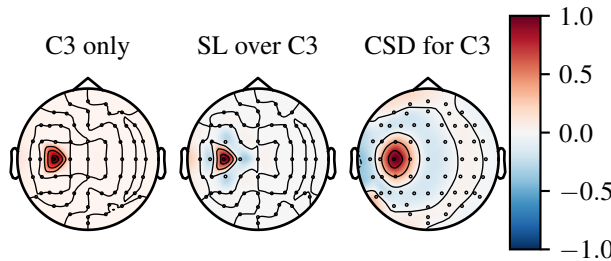


Figure 3.4 : Spatial filters resulting from the electrode selection, Small Laplacian, and computed by the Current Source Density at C3.

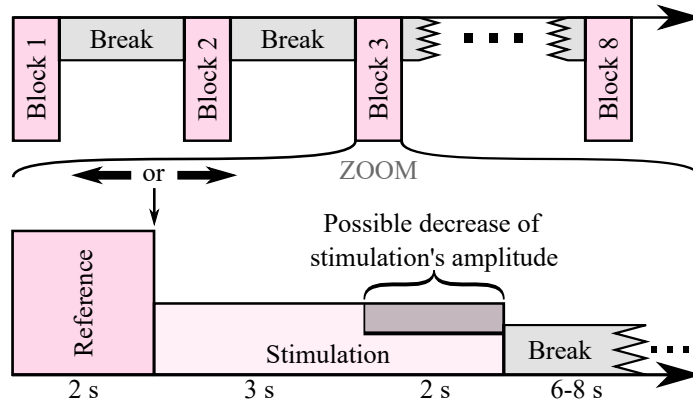


Figure 3.5: Attention Focusing session timeline. Each block lasts approximately 5 minutes. Blocks are interspersed with three-minute breaks. One block consists of 20 trials. One trial contains a 2-second long idle period (no stimulation, idle) and a 5-second long active attention focusing period (with stimulations at different frequencies on both wrists).

### 3.5 COMPARISON ON REAL EEG DATA

In this section, we compare the same amplitude estimators on real EEG data recorded during the experimental validation of an SSSEP-based BCI. We first describe the experimental protocol and recorded EEG data, then the amplitude estimations obtained by the compared methods.

#### 3.5.1 Experimental protocol and real EEG data

Real EEG data used in this section were recorded during the second session of an experimental protocol aiming to validate an SSSEP-based BCI on healthy subjects. This protocol has been approved by the Ethics Committee of Lille University (record number: 2020-417-S81)\*. Ten participants — average age 23.8 years, std: 3.2 years, min: 19, max: 28 — underwent the four experimental sessions of this protocol. Mechanical vibrations were applied on both wrists by C2-tactors<sup>1</sup> powered by a micro-controller connected to the computer hosting the BCI.

The first session of the protocol, called screening, aims to identify the resonance-like frequencies of SSSEPs [62], to choose them as the most effective stimulation frequencies for each participant. The second session of the protocol, called Attention Focusing (AF), aims at measuring the variation in the SSSEP’s amplitude when a subject is focusing their whole attention on one vibration [32]. The timeline of an AF session is presented in figure 3.5.

During the session, the subject seats in front of a computer screen, and wears a 64-channels EEG cap and one C2-tactor on each wrist. At the beginning of a trial, a white cross appears on the screen for 2 sec-

\* the protocol accepted by the ethical comity is available in appendix e

<sup>1</sup> Engineering Acoustics, Inc. (EAI), Casselberry, FL, USA



onds, and the subject has to keep their gaze at it and remain still. Then, stimulation starts on both wrists simultaneously and a white arrow pointing either to the left or to the right, pseudo-randomly, appears on the screen. This arrow instructs the subject about the vibration on which they have to focus their whole attention. The AF periods last 5 seconds, after which the subject is given a break of random duration, between 6 and 8 seconds.

In some trials, during the last 2 seconds of the attention-focusing active period, the amplitude of mechanical stimulation applied on the attended wrist is sometimes decreased by half. The subject has to detect this variation and report it verbally at the end of each trial in which it occurs. This secondary task is required from the subject to maintain their engagement in the experiment [32]. In the AF session, this protocol yields 160 trials per subject: 80 Left-AF and 80 Right-AF, half of which contain an amplitude decrease.

For algorithm comparison, we focus our analysis on the data from the AF session, since the subject receives both stimulations simultaneously. Ideally, these stimulations should yield EEG measurements produced by two sinusoidal sources of activity, located below C3 and C4 electrodes. To compare amplitude estimators, we selected only two subjects among the 10 of the experiment, #6 and #10, for whom the SSSEP were perfectly highlighted in EEG data during the screening session, using a standard methodology [80].

We present only the amplitude estimation of SSSEP's resulting from the stimulation of right wrists, considering the other SSSEP as a noise source. Hence, the analysis is focused on a sinusoidal source located approximately below C3. The idle period is the reference of each trial, whereas the active period is when the stimulation is at its maximum. The frequencies of stimulation of the right wrist (FOSR), are respectively 26 Hz and 23 Hz for subjects #6 and #10. At these frequencies, the probabilities of measuring an increase of SSSEP amplitude during the active period compared to the idle period were respectively 0.875 and 0.9 for subjects #6 and #10.

### 3.5.2 Amplitude estimation on real EEG data

For each method  $m$  in {LiA, SL-LiA, CSD-LiA, CCA, PLS}, we estimate two amplitudes, one during the idle period  $\hat{A}_{m,idle}(f_a)$  (from 0.5 to 1.5 s) and one during the active period  $\hat{A}_{m,active}(f_a)$  (from 3.0 to 4.0 s). The frequency of analysis  $f_a$  is the FOSR. We compute the Relative Amplitude Increase (RAI) using

$$RAI_m(f_a) = \frac{\hat{A}_{m,active}(f_a) * 100}{\hat{A}_{m,idle}(f_a)} - 100. \quad (3.25)$$

A 0% RAI corresponds to no amplitude change between the idle and active periods.



Figure 3.6a presents the mean RAI and the 95% confidence interval (computed with 1000 bootstraps) for both subjects. Results show a strong and significant RAI at the FOSR detected by all LiA-based methods. Among different spatial filters, a trend seems to appear in favour of the CSD-LiA that yields the highest mean RAI compared to LiA and SL-LiA. On the other hand, CCA or PLS estimators fail to detect a similar RAI.

Figure 3.6b shows average spatial filters estimated by CCA and PLS on the 80 right AF trials with the FOSR stimulation. These results partly explain the poor estimate shown in figure 3.6a, since the CCA and PLS do not seem to be able to compute a spatial filter centred on the source of activity.

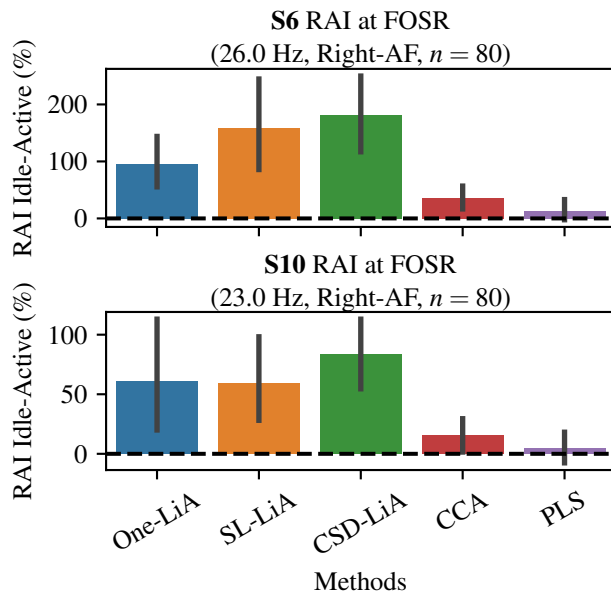
### 3.6 DISCUSSION

Our comparison of signal processing methods aiming to estimate the amplitude of a specific sinusoidal component in EEG measurements was performed on synthetic signals as well as on real data recorded during an experiment. In the following, we first discuss the results in both cases, and then conclude the article.

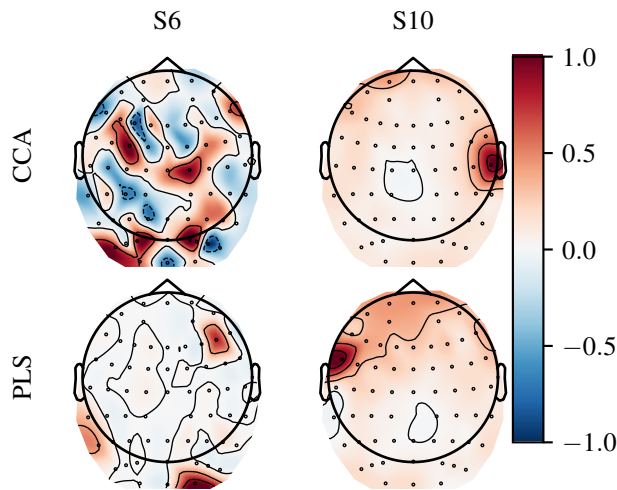
#### 3.6.1 Results on synthetic EEG data

Our simulations have mainly shown that determining a spatial filter with a self-adapting method — like CCA or PLS — has no real interest when the goal is to detect a SSSEP. Indeed, these potentials are precisely located in the somatosensory cortex and therefore *a priori* defined spatial filters proved their efficiency. Using such filters, the LiA displays a capacity to detect the sinusoid of interest when the SNR is greater than  $-23$  dB. On the other hand, CCA or PLS only reach the same performance for signals with a SNR greater than  $-5$  dB, *i. e.* when the amplitude of the target sinusoid is almost ten times greater.

When the SNR reaches the divergence point, spatial filters computed by CCA and PLS become very similar to the CSD large Laplacian, showing again the interest of using a predefined filter. Furthermore, we have also observed that the CCA algorithm can become unstable for high SNRs. This algorithm, which requires inverting a matrix, is known to be unstable when the two blocks of variables show multicollinearity [110]. Although this effect seems to not impair the estimation results for high SNR, one can wonder how it might impact the results obtained by CCA on real high density EEG data. The multicollinearity can be much higher since the noise is also spatially dependent in real EEG data, which our model does not encompass. For these reasons, it seems relevant to study or use the PLS instead of the CCA in such situations.



(a) Estimation of the SSSEP’s RAI during the Attention Focusing on the right wrist. The SSSEP’s RAI are estimated using all methods presented in section 3.4.2, error bars shows 95% confidence interval computed with 1000 bootstraps.



(b) Mean spatial filters for amplitude estimation at FOSR computed by the CCA and PLS (maximum value normalised to 1.0). EEG was recorded using the ANT Neuro waveguard 64 channels EEG cap, which explains the slightly different positioning of electrodes compared to the results on synthetic data. FPz and CPz are the reference and the ground, respectively.

Figure 3.6 : Comparison of amplitude estimators on real EEG data. Legend – RAI: Relative Amplitude Increase, FOSR: Frequency Of Stimulation of Right wrist.

### 3.6.2 Results on real EEG data

Results of the analysis of real EEG data are in line with the results on synthetic data. LiA estimators performed much better than the CCA or PLS ones. For LiA-based methods, the Laplacian filters (SL and CSD) seem to be more efficient than a simple channel selection. It may be explained by the presence of spatially dependant noise in real EEG measurements, which can be swiftly removed by the Laplacian spatial filters.

The observation of spatial filters provided by CCA and PLS — see figure 3.6b — suggests two sources of errors. The first one, highly visible for subject #10, is the presence of artefacts. We did not perform visual artefact removal, the standard approach in EEG data analysis, because the aim of a BCI is to be used in real-life situations, hence signal processing must be able to handle artefacts. The second source of error seems to be caused by the low SNR of EEG. Indeed, the spatial filters computed for subject #6 appear very erratic or irrelevant in regard to the location of the source of activity, similarly to the results for low SNR in figure 3.3 with synthetic EEG data.

### 3.7 CONCLUSION

In BCIs exploiting steady-state visually-evoked potentials (SSVEP), the canonical correlation analysis (CCA) has become the method of reference and many studies have shown its superiority. In this article, we have shown that the CCA, as well as the almost equivalent partial least-squares (PLS) method, are not well suited for amplitude estimation in BCI exploiting steady-state somatosensory evoked potentials (SSSEP).

We have proposed a simple model for EEG synthesis in which a target sinusoidal source is mixed with other non-target sinusoidal sources and white Gaussian noises. Using this model we reproduced, on simulations with synthetic data, the EEG signals that would be recorded in a SSSEP-based BCI when the user receives several vibrating stimuli simultaneously. Each mechanical stimulation produces a SSSEP at the frequency of stimulation at a known location in the somatosensory cortex. Simulation results showed that the Lock-in Amplifier (LiA), used with an integration filter of the same length as the signal snippet (*i. e.* equivalent to the Discrete Fourier Transform at one frequency), combined or not with a spatial filter, performs much better than the CCA or the PLS. The latter two can only identify the target source of interest when its amplitude is an order of magnitude greater.

We extended the methods comparison to real EEG signals from a dataset recorded during a SSSEP-based BCI experiment. Since the goal here was just to compare amplitude estimators, we only used the data of two subjects for whom the SSSEP were clearly evoked. The results are in line with the observation drawn from the simulation. The CCA

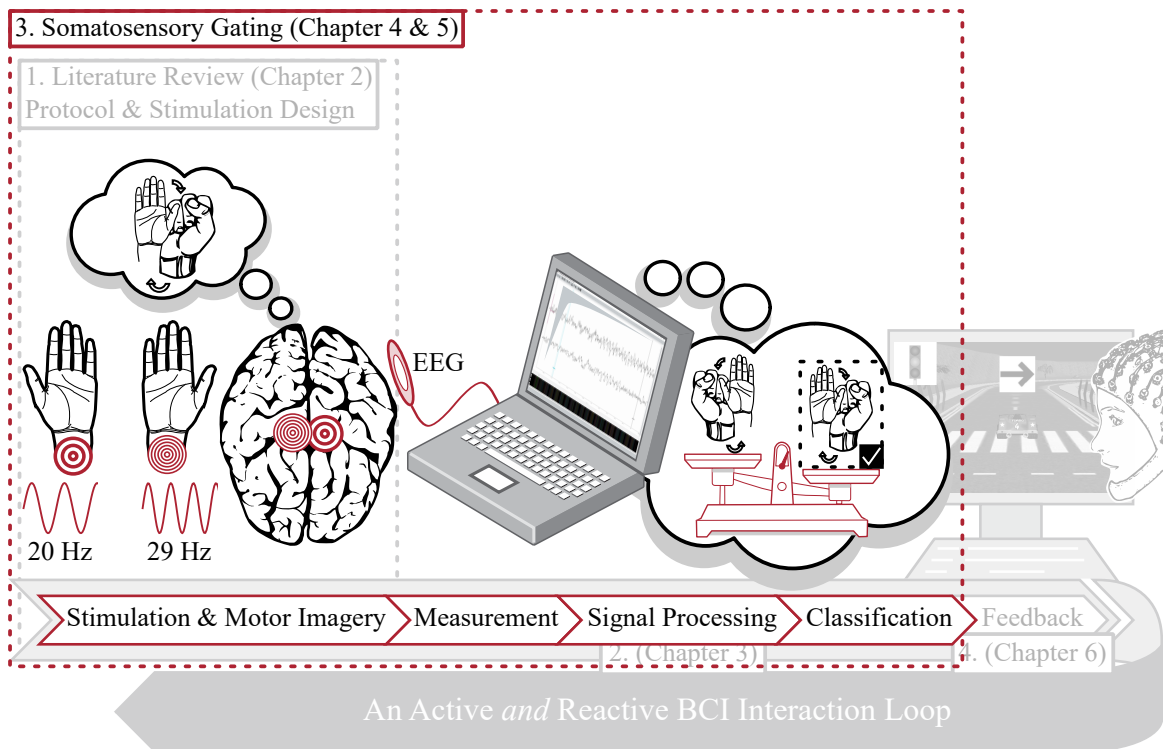
and PLS failed to measure the SSSEP whereas the LiA-based methods could find an amplitude increase during Attention Focusing. Among the three spatial filters, the LiA seems to perform better using the large Laplacian filter, also known as Current Source Density (CSD). This better performance has not been proved on synthetic data. We hypothesise that the presence of spatially correlated noise in real EEG signals — not included in our model — can be removed by the Laplacian filters.

One potential advantage of CCA and PLS methods is that harmonics of the stimulation frequency can be introduced in the set of analysis functions. This could potentially increase their relevance in BCIs exploiting SSSEP if one considers that the brain response to tactile vibrations is not purely linear, and therefore implies the presence of harmonics. Further analysis would then be required, but up to our knowledge, such a method has never been tested in the literature dedicated to BCIs exploiting SSSEP.



# KINAESTHETIC MOTOR IMAGERY FOR SELECTIVE AMPLITUDE MODULATION OF SSSEP BY SOMATOSENSORY GATING

## ROADMAP —



Building on the findings of the two previous chapters – screening procedure for subject-wise frequency of stimulation selection, design of mechanical stimulation, and signal processing method to estimate the SSSEPs' amplitude – we conducted an experiment. In this experiment, we primarily investigate the interaction between SSSEP and MI to assess the “selectivity” in the SSSEPs' amplitudes decrease resulting from MI during simultaneous vibrations on both wrists. For example, we hypothesise that during MI with the right arm, only the amplitude of the SSSEP elicited from vibration on the right wrist will decrease, and not the SSSEP from the left wrist. In this chapter, we focus on the BCI's neurophysiological aspects.

## RELATED WORK (IN PREPARATION) —

Jimmy Petit, José Rouillard, François Cabestaing, and Arnaud Delval. “Kinaesthetic Motor Imagery for Selective Amplitude Modulation of SSSEPs by Somatosensory Gating” (in preparation)

## ACKNOWLEDGMENTS —

The authors would like to thank Philémon Berne, a former intern of the team, who successfully contributed to the work by collecting and digitising some data from the experiments.

#### 4.1 INTRODUCTION

Oscillations in the electroencephalogram (EEG) can be spontaneous, induced or evoked. Induced oscillations occur in relation with an event without phase-locking to the stimulus or the event and are studied via time frequency analysis that combine frequency and time domains. Evoked oscillations also appear after a stimulation but are time and phase-locked to the stimulus. They occur after low frequency sensory stimulation and have been of clinical use to rely on passive neural responses originating from peripheral radicular, brainstem, subcortical or cortical structures (somatosensory evoked potentials, auditory evoked potentials, visual evoked potentials) [87]. They are mainly studied in the time domain (latency, magnitude of the responses). They occur at short latencies after the stimulus. For example, contralateral primary sensory cortex responses occur 20 ms after a stimulation of large fibres at the wrist and mainly reflect passive responses of the nervous system to the stimulation, since they can be recorded even in comatose or anaesthetised subjects. Later responses (long latency evoked potentials) reflect endogenous responses to an event or a context. They can occur before or after the event, for example before moving a hand, or after looking at a signal requiring attention or decision making. They are related to a stimulus in a particular context or to an action and are then called event related potentials (ERP) [55]. They reflect stages of information processing, decision making in large neuronal networks.

ERPs have been used to build brain–computer interfaces (BCI) that acquire brain signals, analyse them, and translate them into commands that are relayed to output devices that carry out desired actions. For example, ERPs frequently used to build BCI include the *bereitschaft* potential [22], a slow negative potential that reflects movement preparation in the supplementary motor area and occurring up to 1.5 s before muscle activation. Induced oscillations are also described as event related desynchronisations or synchronisations in comparison to baseline oscillations in a given frequency range (mainly theta, alpha, beta or gamma bands) [83]. This latter method is used to build BCI and alpha and beta desynchronisations before movement are reliable markers of movement intention [65]. Last, oscillatory EEG activity can also result from high frequency repetitive stimulation that provoke resonance of the EEG activity at the frequency of stimulation (FOS) [90]. These steady-state evoked potentials (SSEP) are therefore a resonance of neural activity with peripheral stimulation and are obtained by repetitive stimuli with a frequency domain analysis. We will focus on these SSEPs.

Indeed, SSEPs are obtained by repetitive visual, auditory, somatosensory stimulations. For example photic stimulation is used as an activation method in clinical EEG recordings [44]. In some cases, even in healthy subjects without abnormal cortical excitability of the occipital cortex, photic stimulation can provoke resonance at the FOS of the back-



ground posterior EEG activity. This reflects that neurons in the visual cortex synchronize their firing to the frequency of photic stimulation. Steady-state visual evoked potentials can be evoked at a large range of frequency, up to 75 Hz [39]. The temporal resonance of the somatosensory system is at an intermediate level between the auditory and visual systems [62]. This temporal resonance of the somatosensory system plays an important role in extracting the stimulus features as neural filters in the temporal domain. Vibro-tactile stimulations are largely used, see [80] for a recent review. Psychophysical experiments have shown that frequency discrimination for vibro-tactile stimulation has a gradual linear increase for the frequency range from 5 – 40 Hz [98]. This discriminative capacity is thought to be mediated by fast-adapting type IMRAs (Meissner corpuscles). Primary somatosensory cortical fast adapting neurons in the monkey discharge in a phase-locked manner in response to the peripheral vibration [98]. EP studies in humans also demonstrated a relationship between stimulus intensity and the magnitude of the evoked response [29]. These findings suggest that the primary somatosensory cortex is therefore selectively tuned to the stimulations.

The effect of attention on early perceptual processes in the visual, auditory and sensory modalities is illustrated by an amplitude modulation of the ERP [37]. This has also been demonstrated for somatosensory steady-state evoked potentials (SSSEP). Giabbiconi *et al.* demonstrated that the amplitude of the SSSEP elicited by vibrating stimuli increases with attention whose topography is the primary somatosensory cortex contralateral to the stimulation [32]. One of the main roles of contralateral somatosensory cortex is also to filter irrelevant signals during a motor behaviour, for example somatosensory signals when a subject imagines a movement or actually moves. For example, somatosensory-evoked potentials are modulated during active movements and this modulation is called a gating phenomenon. The concurrent inputs from nearby cortical areas probably interfere with the modulations by the sensory and motor areas which affect the activity of the sensory tracts. Gating, also called “sensory gating”, can be defined as the neurological processes filtering out redundant or superfluous stimuli from the environment [24]. In the case that interests us, when a person performs a movement with an arm (or imagines doing it), while a vibratory stimulation is applied to this arm, the stimulations perceived on the arm by the subject appear to be reduced by the gating.

#### 4.2 RATIONALE

Tactile BCIs have been scarcely studied in comparison to BCIs exploiting the sight. They often rely on the detection of P300 evoked after one transient tactile stimulation or, less often, on SSSEPs when the stimulation

is sustained with a constant frequency. In our study, we focus on the latter stimulation technique.

A recent literature review provides an overview of the use of SSSEP in a BCI and of identification of resonance-like frequencies relevant for the implementation of such BCIs [80]. A resonance-like frequency is defined as the FOS that yields the SSSEP with the highest relative amplitude increase compared to the reference period [60]. Several resonance-like frequencies can be determined if multiple frequencies of stimulation yield SSSEPs equivalent in terms of amplitude. In [80] two different trends of distribution of resonance-like frequencies have also been summarised: a rather flat maximum centred around 27 Hz or a sharper peak centred on lower frequencies such as 17 or 21 Hz. However, one of the conclusions is that the resonance-like frequency is very different from person to person and that a screening procedure is necessary to determine the specific FOS most adapted to each user.

Additionally, in [80], only BCIs based on the modulation of SSSEPs by attention focusing have been described. To the best of our knowledge, an amplitude variation caused by somatosensory gating has never been used as a marker of mental activity in a SSSEP-based BCI. Only one study describes sustained electrical stimulation of the median nerve and simultaneous motor imagery (MI) [100]. However, the authors do not investigate a potential effect of somatosensory gating in their data. One drawback of the attention-focusing-based BCIs is the intrinsic limitation of the number of discriminable mental states, *i. e.* of possible BCI commands. Indeed, one can hardly focus their attention selectively on several simultaneous stimulations. For instance, when both wrists of a user are stimulated, they can focus their attention either on the left or on the right wrist, but much less easily on both wrists at the same time.

At the opposite, if the sensory gating phenomenon could be used in a SSSEP-based BCI, the user could imagine moving the left arm, the right arm or both arms at the same time, resulting in three possible commands with the same two stimulations. A recent study assesses the instruction to provide to the user in order to produce the strongest somatosensory gating effect [107]. The authors ask subjects to perform either visual MI or kinaesthetic MI tasks. In the former task, the subject must imagine looking at a moving arm, either from a first or third-person point of view. In the latter task, the subject must imagine the visual motion as well as the sensations related to motion, for instance, clothes touching the skin, muscles contractions... In conclusion, the authors observed that kinaesthetic MI produces the strongest gating effect. In addition, the speed of the imagined motion is strongly positively correlated with the size effect of the somatosensory gating.

We hypothesise that subjects performing different kinaesthetic MI tasks (while their both wrists are mechanically stimulated) can selectively (left/right/both) decrease the amplitudes of SSSEPs through somatosensory gating. For example, if this hypothesis is true, then the

SSSEP's amplitude resulting from the left arm stimulation would be the *only* modulated SSSEP, and the SSSEP resulting from the right arm stimulation on the left hemisphere would remain unmodulated. Such a simultaneous stimulation is common in BCIs that exploit attention focusing. Here, we investigate the gating ability under simultaneous stimulation to assess if the somatosensory gating could be exploited in an SSSEP-based BCI. To our knowledge, a BCI exploiting amplitude modulation of SSSEPs by sensory gating has never been described in the literature.

## 4.3 MATERIALS AND METHODS

### 4.3.1 *Experimental study*

This study was conducted between the 11th of October 2021 and the 11th of February 2022 in the Department of Clinical Neurophysiology of the University Hospital of Lille (France). It was promoted by the Centre de Recherche en Informatique, Signal et Automatique de Lille (CRISAL, UMR 9189) and obtained the approval of the ethics committee of University of Lille (record number: 2020-417-S81). The study was conducted in accordance with the Code of Ethics of the World Medical Association (Declaration of Helsinki) for experiments involving humans. Our experimental study included four sessions, but in this article we only consider the screening session [60] and the gating session.

### 4.3.2 *Participants*

All participants are recruited via advertisements on the scientific campus of the University of Lille. Each participant received an information letter describing the aims of the research as well as the description of experimental sessions. All participants gave a written informed consent stating that they took part voluntarily in the study.

A total of  $n = 10$  healthy subjects, 7 males and 3 females, participated in both sessions. No participant met the exclusion criteria: neurological history (epilepsy, stroke, or dementia), pregnancy, person under guardianship or curatorship, major comorbidity considered as a contraindication by the investigator, or administrative impossibility.

Participants are on average 23.8 years old (std: 3.2 years, min: 19, max: 28). We used the 10-item version of the Edinburgh Handedness Inventory [70, 105], soft drink questionnaires [58], and asked questions regarding sleep time habits. Results of the 10-item version of the Edinburgh Handedness Inventory showed a dominance of right-handed subjects with an average laterality quotient of 76 (std: 20.9, min: 44.4, max: 100).

We recorded the sessions with an average of 19 days in between (std: 3.78 days, min: 14 days, max: 24 days). As far as possible, we carried out

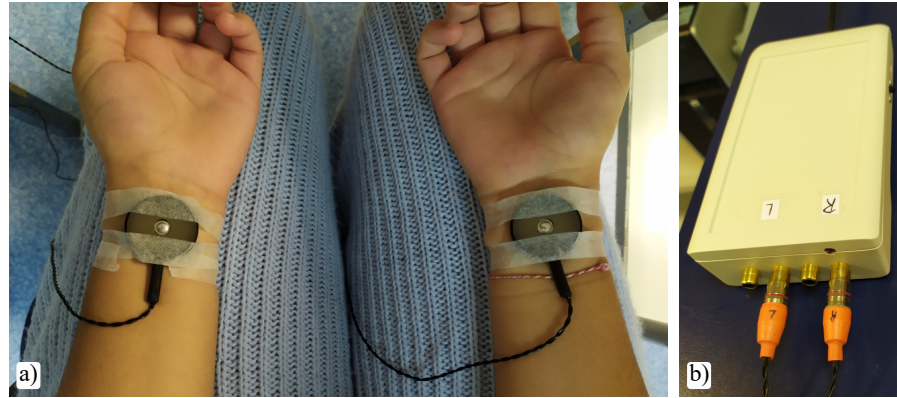


Figure 4.1 : (a) Vibro-tactile factors taped on the subject's wrists. (b) Stimulation box: a micro-controller that powers vibro-tactile factors and connected to a computer.

the second session in the same time slot as the first session, *i. e.* during the morning or the afternoon. This condition could not be met for 3 subjects: #1, #6 and #10.

#### 4.3.3 Hardware and software

Mechanical vibrations are delivered by C-2 Tactors<sup>1</sup> taped over the subject's wrists, see figure 4.1 (a) [84]. Two factors are powered by a single micro-controller connected to, and controlled by, a host computer, see figure 4.1 (b). The micro-controller box design is inspired by the work of Pokorny *et al.* [84]. For more details, the first implementation of our stimulation device is presented in [93]. The stimulation signal is a high-frequency sine-wave, around 275 Hz, close to the resonance frequency of the C-2 Tactor. This signal is amplitude-modulated by a square signal at a lower frequency, varying from 14 to 32 Hz.

EEG is recorded with a waveguard EEG cap of 64 electrodes located according to the 10-20 international system [92]. EEG signals are sampled at 512 Hz by an eego<sup>TM</sup> sports amplifier of ANT Neuro. Data recording and online processing are performed using OpenViBE [91]. During the recordings, all hardware devices are battery-powered to avoid noise potentially produced at 50 Hz by the power network.

Offline signal processing and statistical analysis are performed using the MNE and SciPy libraries of Python.

## 4.4 SCREENING: DESCRIPTION

The literature review highlights the importance of performing a screening procedure with each subject to determine the most effective FOS. During the screening session of our experimental protocol, we test the

<sup>1</sup> Engineering Acoustics, Inc. (EAI), Casselberry, FL, USA

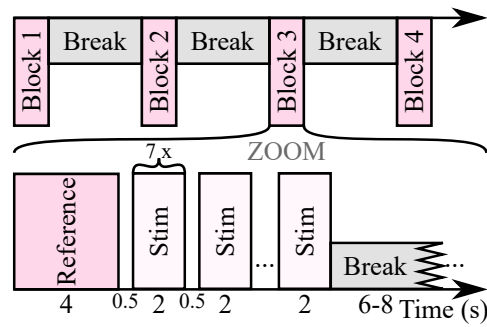


Figure 4.2 : Timeline of the screening session. Each block contains 20 trials and blocks are separated by 3-minute breaks.

following primary hypothesis: “the mechanical stimulation produces an *increase* of oscillatory activity at the FOS in the somatosensory cortex contralateral to the stimulated limb”. The secondary goal of the screening session is also to identify two FOS, one for each wrist, that will be used during other sessions.

#### 4.4.1 Experimental procedure

During the screening session, the subject sits comfortably in front of a table. We assess both wrists, but only one wrist is stimulated during every trial. We also assess seven FOS, ranging from 14 to 32 Hz separated by 3 Hz steps. The combination of both variables yields fourteen experimental conditions denoted by {Wrist  $\times$  FOS}.

Screening EEG data are recorded during four nine-minute recording blocks, interspersed with three-minute breaks. Each block consists of twenty trials, interspersed with breaks of seven-second average duration. One trial starts with a reference period of four seconds followed by a series of seven stimulation periods, each two-second long with half a second breaks in between. We consider that this allows the somatosensory cortex to reach back an idle state in between stimulation periods. One of the fourteen experimental conditions is tested during each trial. The tested conditions sequence is pseudo-random, with only one constraint which is that the same condition is not tested twice in a row. One block of data produces 10 tests per experimental condition, resulting in 40 2-second stimulation recordings for each experimental condition per subject. The flow of a screening session is summarised in figure 4.2.

During the series of stimulation periods, the subject is asked to remain still and avoid blinking or swallowing as much as possible. We instruct the subject to not focus their attention on the vibration. During each recording block the subject listens to relaxation music [99]. The subject chooses the music volume, not too high in order to be comfortable, not too low in order to mask the noise of mechanical vibrators. We also ask

the subject to focus their gaze on a red cross on the wall while keeping their eyes open.

#### 4.4.2 EEG data analysis

EEG data analysis is performed offline. However, we implemented a causal EEG analysis pipeline, in order to make it compatible with a future online implementation since the aim of a BCI is to be used online and in real time.

All the components of the system (stimulation device, computer, EEG amplifier) are battery-powered. Since there is no peak at 50 Hz (power-line frequency in France) in the power spectrum of EEG signals, the latter are only filtered by a causal high-pass filter at 5 Hz [19].

We spatially preprocess EEG signals with a bipolar montage between FC3 and FC4 with CP3 and CP4, respectively, yielding denoised estimates of C3 and C4. It is the standard approach for screening procedures used in the literature [80, 85]. We do not perform further visual artefact removal, although it is a standard approach in EEG data analysis. Indeed, since the aim of a BCI is to be used online, we consider that the tested signal processing pipeline must be able to handle artefacts.

The standard signal processing technique used to identify resonance-like frequencies is the discrete Fourier transform (DFT). The DFT is calculated on the reference period, without stimulation, and during a stimulation period of a trial corresponding to a couple in {Wrist × FOS}. More precisely, for each electrode, we estimate the amplitude of oscillations at the FOS on two analysis windows. The first one, for the reference, is a two-second-long window centred in the reference period (four seconds at the beginning of the trial). The second one, for the stimulation, is a one-second-long window centred on a stimulation period of the trial. The amplitudes estimations from every reference period of a recording block are averaged. Then, we calculate the relative amplitude increase (RAI) of the stimulations for the said block. The RAI at the frequency of analysis  $f_a$  is defined as

$$\text{RAI}_m(f_a) = \frac{\widehat{A}_{m,stim}(f_a) * 100}{\widehat{A}_{m,reference}(f_a)} - 100, \quad (4.26)$$

with  $m$  being the measurement channel, either C3 or C4. A 0% RAI corresponds to no amplitude change between the reference and the stimulation period.

We also propose an alternative referencing method, that we call the non-condition (NC) reference. The idea is to determine a NC reference amplitude for a given frequency of analysis  $f_a$  as the average amplitude of the DFT, of one measurement channel at  $f_a$ , during stimulation periods at a FOS different from  $f_a$ . The RAI for this other referencing method is determined in a similar way, but considering a denominator in (4.26) equal to the NC reference amplitude.



#### 4.4.3 *Frequencies of stimulation selection procedure*

The second objective of the screening procedure is to determine two frequencies of stimulation (FOS), one for each wrist, that elicit the most pertinent SSSEPs for the subject. We search for resonance-like frequencies for each wrist, *i. e.* FOS that produces the maximum RAI [60]. To choose the FOS for one subject, we first look for the resonance-like frequencies from each wrist according to the two referencing methods. Starting from this point, there are multiple possible situations:

1. The resonance-like frequencies of the right and left wrist are 6 Hz apart from each other [96, 102] and are identical across referencing methods.
2. The resonance-like frequencies of the right and left wrist are 6 Hz apart from each other and differ between referencing methods.
3. The resonance-like frequencies are too close to each other, in at least one of the referencing methods.

The first case is the ideal one. The wrists' FOSs for the experiment are simply chosen at the resonance-like frequencies. The second case occurs when one resonance-like frequency on at least one wrist differs for the two referencing methods. In this situation, priority is given to the NC referencing method as we wish to use FOSs that induce SSSEPs with highest amplitudes. For the third case, we take into consideration the spread of the distributions, considering two possible situations:

1. The spread of the distributions is very narrow, *e.g.* most of the power lies within a 6 Hz bandwidth.
2. Distributions appear flat or with a wide distribution centred on a local maximum.

In the rare first case, we decide to choose two FOSs close to each other, *i. e.* separated by only 3 Hz. The second case occurs when a narrow peak is nowhere to be found, *i. e.* when the distribution appears rather flat and every average RAIs lies within other's RAIs error bars. The most suitable FOS, in terms of mean RAI and degree of lateralisation between wrists, is chosen as the FOS for the rest of the experiment. For the second FOS, any frequency 6 Hz apart from the already chosen FOS and with overlapping error bars is a potential candidate. The Reference and NC referencing distribution are investigated to choose the FOS yielding the highest SSSEP's amplitude increase. In addition, priority is not given to frequencies at 14 and 17 Hz, for example when the first chosen FOS is 20 or 23 Hz. Indeed, a visual inspection of the topography at such FOS often shows wide sources of activity unlikely to be related to SSSEP. In some cases, the above criteria are not fully met. An *ad-hoc* expert-based decision is made to select the FOS in order to continue the experiment.



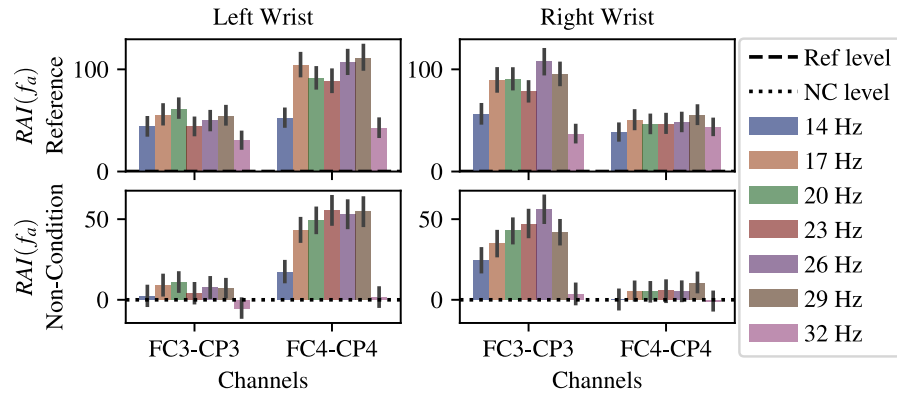


Figure 4.3 : Grand Average of RAI according to two different referencing modes. The first line shows the RAI to the Reference period (*i. e.* without stimulation). The second line shows the RAI to the non-condition (NC) period. Error bars show 95% confidence interval (computing using 1000 bootstraps).

## 4.5 SCREENING: RESULTS

### 4.5.1 RAI distributions

We display the grand average of the RAI distributions in figure 4.3. The left column shows only the condition where the left wrist is stimulated, inversely with the right column. The y-axis scale differs between reference methods, and the error bars show a 95% confidence interval. We expect the SSSEP to be very lateralised. Therefore a large RAI is expected on the electrode contralateral to the stimulation side, whereas a low-to-none is expected on the electrode ipsilateral to the stimulation side.

Table 4.1 shows a statistical analysis performed on the grand average, using the NC reference. The table displays the p-values from a non-parametric one-sample one-tailed Wilcoxon signed-rank test assessing if the expected *increase* of activity caused by the stimulation is statistically significant. The tested hypotheses are the following:

$H_0$ : the distribution of the RAI is symmetric about zero.

$H_1$ : the distribution of the RAI is stochastically larger than a distribution symmetric about zero.

### 4.5.2 Selection of frequencies of stimulation

Figure 4.4 shows the distribution of the RAI to the Reference period and NC condition for subject # 10. Following the selection procedure previously described, for illustration we present the frequency selection only on subject # 10. The diligent reader can find the RAI distributions for every subject in the supplementary information (see appendix a).

FOS (Hz)	Left Wrist		Right Wrist	
	FCE-CP3	FC4-CP4	FCE-CP3	FC4-CP4
14	0.79	$1.5 \times 10^{-4}$	$7.8 \times 10^{-9}$	0.93
17	0.21	$3.6 \times 10^{-24}$	$3.9 \times 10^{-16}$	0.42
20	0.0086	$3.5 \times 10^{-27}$	$2.3 \times 10^{-22}$	0.39
23	0.57	$1.3 \times 10^{-29}$	$7.6 \times 10^{-21}$	0.35
26	0.097	$2.5 \times 10^{-28}$	$1.9 \times 10^{-30}$	0.36
29	0.13	$4.6 \times 10^{-27}$	$1.9 \times 10^{-20}$	0.019
32	1	0.83	0.74	0.94

Table 4.1 : Results from one-sample one-tailed Wilcoxon signed-rank test over the RAI to the non-condition referencing mode. The colour code shows the p-values lower than a risk threshold  $\alpha$  at 0.05, 0.01 and 0.001, with the colour red, orange, and green respectively. The threshold  $\alpha$  is Bonferroni-corrected, so the threshold  $\alpha$  at 0.001 becomes  $7.1 \times 10^{-5}$ , and so on.

We observe a left wrist resonance-like frequency at 17 Hz while at 26 Hz on the right wrist, according to the reference baseline. However, on the NC reference, the resonance-like frequency becomes 23 Hz on the left and right wrists. This situation corresponds to selection procedure's second case. Therefore, between 23 Hz and 26 Hz for the right wrist, the priority goes to 23 Hz. It is, fortunately, also 6 Hz apart from 17 Hz selected for the left wrist. Finally, for subject # 10, we chose a FOS at 17 Hz for the left wrist and a FOS at 23 Hz for the right wrist. The table 4.2 shows the selected FOS for every subject.

Subject Index	1	2	3	4	5	6	7	8	9	10
FOS Left (Hz)	20	29	29	17	17	20	29	20	23	17
FOS Right (Hz)	29	20	26	29	29	26	20	29	17	23

Table 4.2 : Expert-based selection of FOS for each subject based on distribution RAI, statistical test, and visual inspection of the subject-wise topomaps. FOS for subjects in bold are results from the selection procedure.

#### 4.6 SOMATOSENSORY GATING: DESCRIPTION

In the gating session, we investigate if the subject produces a *selective* amplitude modulation of SSSEPs by kinaesthetic MI. For example, in the case of a left arm MI task, we expect to measure a decrease *only* in the SSSEP's amplitude evoked by the stimulation of the left wrist. Therefore, the corresponding RAI should be lower in the MI condition than for no MI. In the case of both arms MI, we expect to measure a

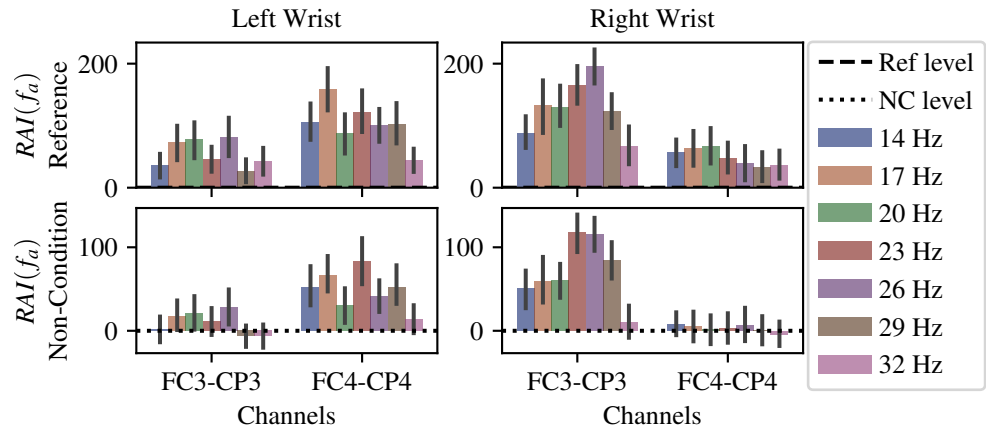


Figure 4.4 : Relative amplitude increase to the Reference period (first row) and non-condition (second row) from the screening procedure of subject #10. Error bars show 95% confidence interval (computing using 1000 bootstraps).

simultaneous *decrease* in SSSEPs' amplitudes. In other words, we test the following primary hypothesis: "Kinaesthetic motor imagery produces selective amplitude modulation of SSSEPs by somatosensory gating".

#### 4.6.1 Experimental procedure

In this session, the subject sits comfortably in front of a table and looks at a computer screen set up in front of them. We record brain activity using an EEG. Both wrists of the subject are stimulated, at their respective FOS, during the stimulation periods. The wrists lie on the subject thighs. The palms face the interior of the thigh or the ceiling, according to the subject's preference. In any case, we want to avoid the stimulation spreading to the thighs, as in the situation where the factor is pressed between the thigh and the wrist.

We use four different experimental conditions, instructed using the following cues:

- Left: a white arrow pointing to the left (kinaesthetic MI of left arm only)
- Right: a white arrow pointing to the right (kinaesthetic MI of right arm only)
- Up: a white arrow pointing at the ceiling (kinaesthetic MI of both arms)
- Circle: a white circle (no MI)

We instruct the subjects to repeat the motion in a loop during the whole duration of the stimulation period. Subjects are informed that the speed of the imagined movement is important, the faster the better. However, we ask them to not overdo it and to not forget the most important part of the task, *i. e.* the "kinaesthetic" feelings of MI.

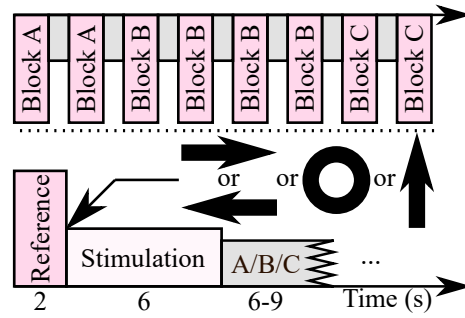


Figure 4.5 : Timeline of the somatosensory gating session. Each block contains 20 trials. Blocks are separated by 3-minute breaks. There are three possible trial types. In trials of A blocks, no feedback is given to the subject before a break lasting from 6 to 8 s. In trials of B blocks, the subject receives sham feedback 1 second before the break. In trials of C blocks, the subject receives a real feedback 1 second before the break.

The session contains eight blocks. Each block lasts about five minutes and includes twenty trials. Each trial starts with a reference of two seconds during which a small white cross appears on the screen. The subject is instructed to keep their gaze on the cross and avoid, as much as possible, muscle artefacts, like blinking or swallowing. After two seconds of reference, the cue for the current trial appears on the screen. The two first blocks are EEG recordings without feedback. During the four following blocks, we add sham feedback for one second at the end of each trial. Sham feedback is a mock feedback, it helps maintaining the subject engaged in the experiment. The artificial accuracy is set to eighty percent of correctness. When the computer correctly classifies the given cue, the cue turns green, otherwise it turns red. For the two last blocks of recording, true online feedback is given to the subject. The chronology of a recording session of gating is given in figure 4.5.

#### 4.6.2 EEG data analysis

For the somatosensory gating session, we use a different signal processing pipeline than for the screening. Indeed, the cortical source of an SSSEP elicited by mechanical stimulation of the wrists, based on the somatotopic arrangement of the brain, is located under the C3 and C4 electrodes [40]. Therefore, we spatially preprocess EEG signals using a current source density filter [45, 57, 67] and then pick up only these two electrodes. Doing so, we aim at maximising the portion of activity related to SSSEP [40].

The SSSEP's amplitude is calculated using a lock-in amplifier (LiA) set up with a low-pass filter with a gate impulse response. The LiA can be regarded as a very narrow tunable filter, which provides amplitude and phase information of a sinusoid component out of a ran-

dom noise [62]. More precisely, amplitude estimation by a LiA with a low-pass filter with a gate impulse response is equivalent to retrieving only one amplitude component out of a discrete Fourier transform. In addition, the LiA has the advantage of providing an estimation of the SSSEP's amplitude throughout time, like a DFT computed over a sliding time window. The RAI of each trial is then computed using a one-second-long analysis window centred on the reference period, as the reference, and every time point of the signal. The resulting time series are then downsampled from 512 Hz to 8 Hz.

#### 4.6.3 Behavioural questionnaires

For the somatosensory gating session, we use the same questionnaires as in the screening session. In addition, we add a measure of the mental workload using the Raw Task Load Index (Raw-TLX), a variant of the NASA Task Load Index [38].

We measure the subject's self-perceived "awakeness", tiredness, mood orientation, and mood intensity using 5-point Likert Scales, before and after the session. The "awakeness" ranges from very unawake (1) to very awake (5). Tiredness ranges from not tired at all (1) to very tired (5). Mood orientation ranges from very negative (1) to very positive (5). Mood intensity ranges from not very low intensity (1) to very intense (5).

On the post-session questionnaire, we also measure the perceived unpleasantness and painfulness using a 5-point Likert Scale. Items range from "Not at all" (1) to "A lot" (5).

### 4.7 SOMATOSENSORY GATING: RESULTS

#### 4.7.1 Temporal visualisation of SSSEP's amplitude

We display the time course of the two SSSEPs, one from each arm, during each experimental condition for subject # 2 in figure 4.6. The peak RAI difference between conditions occurs between  $t = 2$  and  $t = 3$  s, for SSSEP on C4, *i.e.* from the left wrist. On the contrary, the effect is fainter but more steady during the whole stimulation on the SSSEP on C3, *i.e.* from the right wrist.

Table 4.3 shows a statistical analysis of the data extracted over the analysis windows for every subject. Since we are interested in measuring the gating effect, we investigate if the RAI distributions are significantly *lower* in MI conditions than in Circle conditions. We use non-parametric one-tailed Mann-Whitney U-tests comparing each pair of distributions. We test the following hypotheses:

$H_0$ : the distribution of the RAI of both populations are identical.

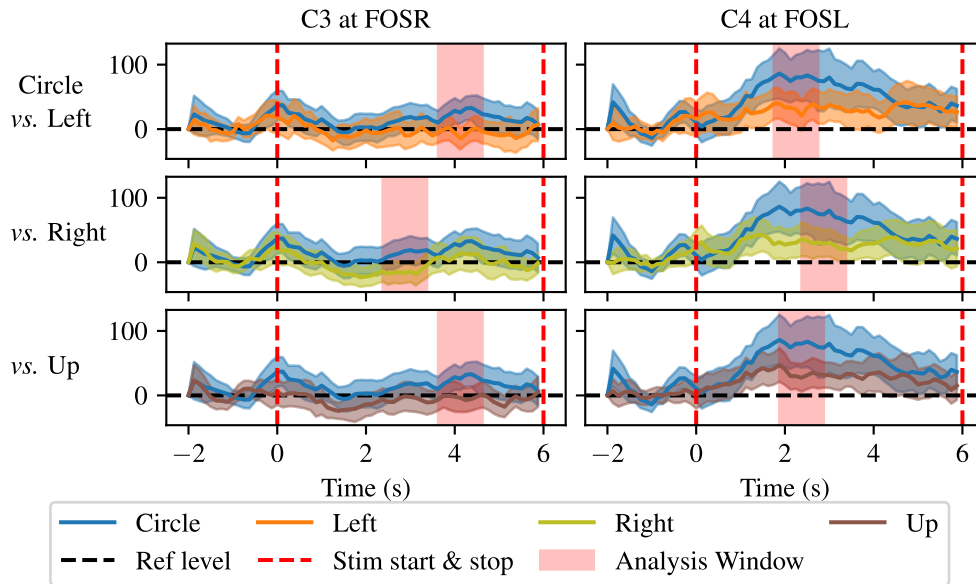


Figure 4.6 : Subject #2: comparison of the average RAI (%) between conditions: Circle *vs.* Right, Left, and Up. Analysis windows are centred around the maximum difference between start and stop of stimulation. Lighter colours show the 95% confidence interval.

$H_1$ : the distribution of the RAI during MI is stochastically lower than in condition Circle.

For subject #2, the statistical analysis shows that the mean RAI differences from C3, over the analysis window, are statistically significant for each comparison. The p-values are equal to 0.0015, 0.006, and 0.0016 for Circle *vs.* Left, Right, and Up, respectively. However, none are statistically significant for the SSSEPs' amplitude difference from C4.

Visualisation of the SSSEPs' amplitude timeline, similar to figure 4.6, are available for every subject in the supporting information, see appendix b.

#### 4.7.2 Behavioural data

The Raw-TLX shows a median score of 52 out of 100 (min: 33, max: 69). The Raw-TLX score indicates the level of mental workload, a high average score meaning that the subject has experienced a high mental workload. The detail scores are given in figure 4.7.

Figure 4.8 shows the evolution of responses to the behavioural questionnaire for both sessions. Results show that the Mood Orientation or the Mood Intensity experienced do not seem to change during the experiments. The self-estimated "awakeness" by the subjects seem stable through the screening session. However, the tiredness increase from a majority of mentions from 1 or 2 to 2 or 3, for the screening session. The most important change seems to happen during the somatosensory

Subj.	Circle vs. Left		Circle vs. Right		Circle vs. Up	
	C3 at FOSR	C4 at FOSL	C3 at FOSR	C4 at FOSL	C3 at FOSR	C4 at FOSL
1	0.38	0.24	0.44	0.29	0.59	0.32
2	0.0015	0.018	0.006	0.04	0.0016	0.033
3	0.006	0.004	0.0034	0.19	0.0021	0.27
4	0.45	0.29	0.32	0.34	0.37	0.093
5	0.11	0.00075	0.2	0.054	0.049	0.035
6	0.16	0.015	0.23	0.2	0.73	0.022
7	0.42	0.21	0.31	0.3	0.35	0.087
8	0.086	0.14	0.084	0.86	0.047	0.54
9	0.00058	0.44	0.04	0.26	0.07	0.41
10	0.06	0.12	0.095	0.11	0.0079	0.029

Table 4.3 : Statistical analysis results: are RAI distributions significantly lower during MI than during idle state? Results from one-tailed Mann-Whitney U-tests over the distributions of RAI within the analysis window shown in figure 4.6. The colour code outlines p-values lower than a risk threshold  $\alpha$  at 0.05, 0.01 and 0.001, with red, orange, and green, respectively. The threshold  $\alpha$  is Bonferroni-corrected, so the threshold  $\alpha$  at 0.05 becomes 0.0083, and so on.

gating session. Most of the subjects report an increase of their tiredness level between before and after the recordings, the majority mentioning a change from 2 to 3 after the recordings. In line with these results, the self-assessed “awakeness” strongly diminishes as well. These results can be explained by the high perceived mental demand and effort felt by the subjects, as can be observed with the Raw-TLX results in figure 4.7.

Finally, each subject reported “Not at all” when asked if vibro-tactile stimulation is unpleasant or painful.

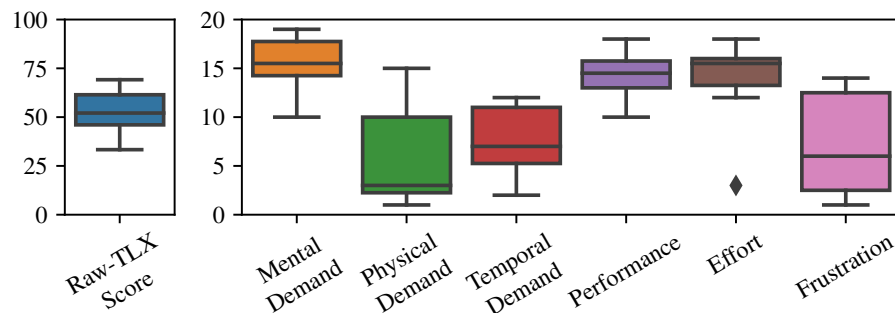


Figure 4.7 : (a) Distribution of the Raw-TLX scores. (b) Distribution of the individual dimension of the Raw-TLX questionnaire.



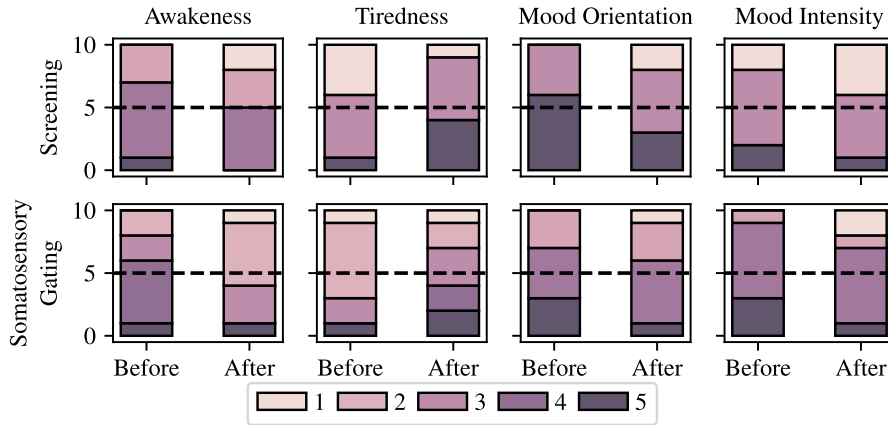


Figure 4.8 : Results from the behavioural data on the 5-point Likert scale item: Awakeness, Tiredness, Mood Orientation, and Mood Intensity, for the screening and somatosensory gating session, before and after the recordings.

#### 4.8 DISCUSSION

When using the Reference period, one can observe that the screening's RAI distributions do not look well lateralised (see figure 4.3). The RAI distributions on the electrode ipsilateral to the stimulation side are not centred on 0%. Thus, the results do not align with the knowledge of somatotopic arrangement [40]. Comparatively, the NC reference method that we propose to use appears much better suited. Indeed, we observe a 0% change in activity on the ipsilateral hemisphere to the stimulated side. We recall that the only difference between the two referencing modes is the presence or absence of a mechanical stimulation unrelated to the to-be-investigated FOS. Therefore, results suggest a large ERD/S caused by the presence of the stimulation, which is no longer an issue with this second way of referencing. These results also motivate using the NC referencing method in choosing the FOS for the second session.

In table 4.1, results show that a FOS at 32 Hz does not seem to produce a SSSEP beyond a reasonable doubt. This result provides comfort in choosing the frequency range tested during the screening session. In addition, the slight increase of activity visible on the side ipsilateral to the stimulation does not appear statistically significant. This result confirms that the measured SSSEPs are well lateralised using the NC referencing method.

SSSEPs are correctly detected for seven subjects out of ten. However, the variability in the measurements sometimes makes the FOS hard to identify following the FOS selection procedure described earlier, even for these subjects. Further work towards an automatic FOS selection process could be interesting. However, since we are interested in measuring the somatosensory gating effect, it is out of the scope of the present work.

Our results from the screening procedure tend to support one of the trends observed in [80]. Indeed, a relatively flat maximum around 26 Hz, irrespective of the stimulated wrist, is observable in figure 4.3. In addition, these results seem more pronounced using the NC reference method.

The NC referencing method appears very interesting in terms of neurophysiology. It highlights the influence of the usage of one specific frequency over the other, *i. e.* the sensitivity of the somatosensory system to a specific frequency. These results differ from those obtained with the standard approach, *i. e.* referencing using a period without stimulation.

From the results in figure 4.6, for subject # 2, we observe that in any MI task, both SSSEPs are lower than in the idle condition. The analysis in table 4.3 substantiates these results and extends it to all subjects. It shows that a statistically significant decrease in SSSEPs amplitude can irrespectively affect the motor imagery content over half of our subjects. As a result, our primary hypothesis about the “selectiveness” of the gating effect can not be confirmed. We hypothesise that a training program, over several MI sessions, could improve these results. Indeed, in MI, it is known that the training effect is essential [10, 43]. Subjects can need several dozens of sessions in order to demonstrate consistent effects.

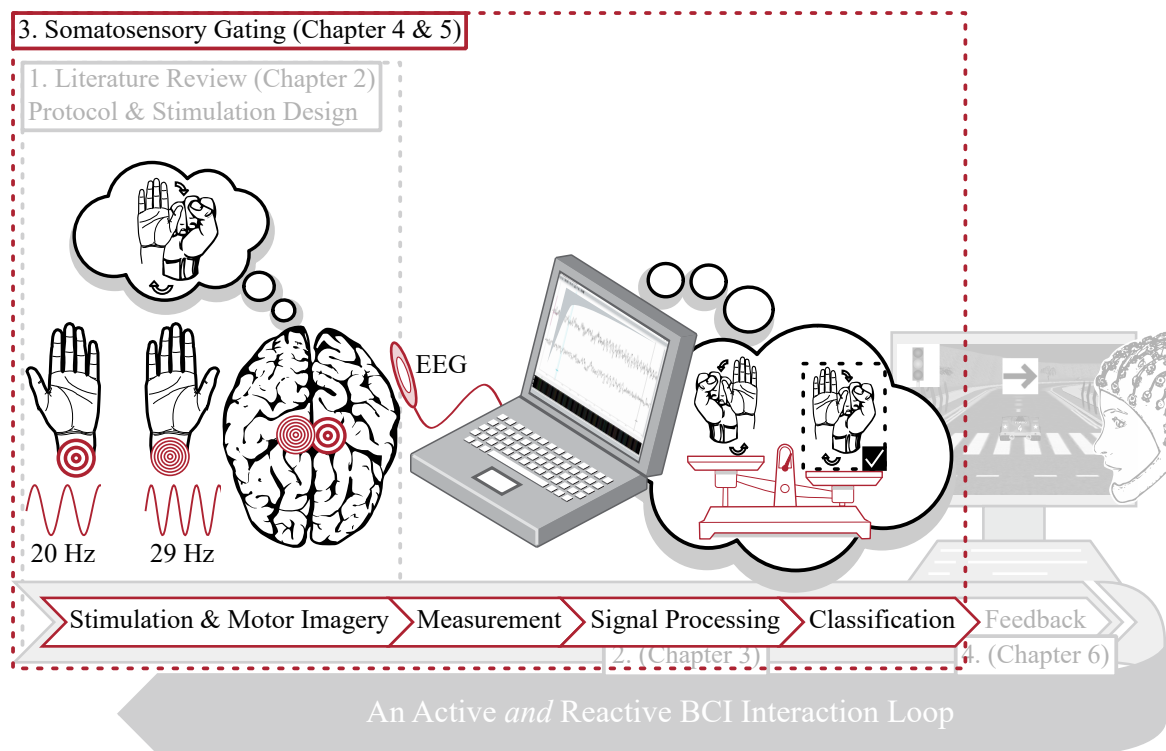
#### 4.9 CONCLUSION

In this work, we proposed a new methodology for referencing the increase of activity, at the frequency of stimulation, evoked by a vibrotactile stimulation of wrists. Our methodology produces a well-lateralised visualisation of the SSSEPs. We also successfully measured the somatosensory gating effect produced by kinaesthetic MI, in a single experimental session. However, our initial hypothesis of lateral “selectiveness” of the decrease produced by MI could not be confirmed by this first experiment.

MI produces event-related desynchronisations (ERD), contralateral to the arm involved in imaginary motion, within the  $\mu$  and  $\beta$  (12 to 30 Hz) frequency bands [82]. But the exact frequency of ERD is very user-dependent and sometimes varies slightly between experimental sessions, which makes the analysis of amplitude variations quite complex. It is also well-known that to operate an MI-based BCI detecting ERDs, user training can take weeks or even months [10, 43].

Using mechanical stimulation at a precisely selected frequency, we obtained a statistically significant effect with half of our subjects in solely one session. In a BCI exploiting this paradigm, signal analysis could be similar to the one used in a standard MI-BCI, except that the frequency of analysis is known *a priori*, and therefore perfectly stable over time. Moreover, we hypothesise that the “selectiveness” of SSSEPs’ decrease might become exploitable after user training.

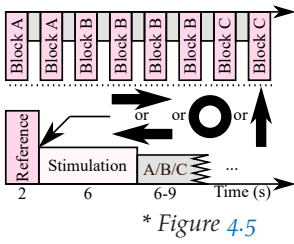
ROADMAP —



As in the previous chapter, we focus on the neurophysiological aspect of our BCI. In this chapter, we aim to present the methodology and results of the classification mentioned in chapter 4. In the somatosensory gating session, an online 4-class classifier provides the user with some online feedback during C-blocks. The feedback informs the subject whether the computer correctly classified the imagined movement based on their EEG.

In addition, we attempt an offline 4-class classification exploiting our results from chapter 3, *i. e.* combining the usage of a CSD and LiA to estimate the SSSEPs' amplitude on the C3 and C4 electrodes. As an additional experiment, we also lower the classification to a 2-class problem. We attempt to identify the intent of movement by distinguishing the "Circle" condition, *i. e.* idle during stimulation, from other kinaesthetic MI conditions, namely "Left", "Right", or "Up".

UNPUBLISHED WORK —



\* Figure 4.5

During C-blocks of the somatosensory gating session\*, we provide online feedback from a 4-class classification algorithm to the user. The classification is based on a lock-in amplifier (LiA) implemented in OpenViBE [91]. For this first classification attempt, we use a simple algorithm present in the literature [20, 62].

We briefly present the algorithm in the following lines. The amplitude of the SSSEP resulting from vibrations on the right wrist is calculated using a LiA over the bipolar montage FC<sub>3</sub>-CP<sub>3</sub>. For the left wrist, the estimation is similar and performed over FC<sub>4</sub>-CP<sub>4</sub>. Logarithms of the estimations are computed. It helps the distribution of data to approximate a normal distribution, also called signal conditioning in [62]. Then, a simple difference is computed between the mean estimation over two observation windows. The first one, lasts two seconds and starts with the Reference period while the second one lasts five seconds and starts one second after the beginning of the stimulations. It results in a two-dimensional vector per trial. The first components measure the change in amplitude at the frequency of stimulation (FOS) of the right wrist, over the bipolar measurement FC<sub>3</sub>-CP<sub>3</sub> and between the reference and stimulation period. The second components do the same, but for the SSSEP resulting from the left wrist stimulation. The classification is performed using linear discriminant analysis (LDA). This short pipeline of analysis is similar to the one proposed by Müller-Putz *et al.* [62]. The measurements of changes using a reference period come from the work of Choi [20].

The online 4-class classification results in an average accuracy ranging from 15% to 35%. With 10 tested trials per class and a 4-class classification problem, any accuracy above 40% is better than a random process with an  $\alpha$  risk at 0.05 [61]. None of the subjects passes this threshold. In this chapter, we aim at performing an offline 4-class classification attempt using an online-compatible processing pipeline. We will also deepen our analysis of the classification errors.

## 5.1 EEG SIGNAL PROCESSING AND ALGORITHM

In this section, we present the preprocessing and signal processing used for the offline classification in our BCI.

### 5.1.1 Preprocessing, Signal Processing, and Feature Extraction

The preprocessing is identical to the one used in the somatosensory gating section of the previous chapter, see section 4.6.2. We remind the reader that the data were recorded using battery-powered components. After inspection of the EEG spectrum, we keep the preprocessing as soft as possible to reduce the alteration of data [19]. Spatial filtering is

performed using the current source density spatial filter, then we select two electrodes of interest: C<sub>3</sub> and C<sub>4</sub>.

For the classification, the SSSEP's amplitude is monitored over C<sub>3</sub> and C<sub>4</sub> continuously. The amplitudes are calculated using a LiA. The SSSEP's amplitude from the vibro-tactile stimuli on the right wrist is calculated on C<sub>3</sub> and *vice-versa* for the left wrist. We compute an RAI using a one-second-long analysis window centred during the reference period, as the reference, and at every time point of the signal. To extract features, we compute an average of the LiA over a one-second-long analysis window starting 500 ms after the beginning of the stimulation. Similarly to the first online classification, it results in a two-dimensional feature vector for each trial.

### 5.1.2 Classification Accuracy Computation

The classification is performed using LDA. This classifier has the merit of not being computationally expensive and compatible with a classification using a small amount of data. For these reasons, the LDA is mainstream in BCI.

The recording of the somatosensory gating session yields 40 trials per class per subject. We perform a dataset train-test split with a 75%-25% ratio, balanced per class. One LDA model is trained using 75% of the data and tested on the 25% remaining unused data points. The accuracy is the proportion of correct classification. We performed this process a thousand times per subject to calculate average accuracy and standard deviation.

To know if the classification accuracy is different than a fair 4-faced coined flip process with reasonable doubt, we use the results from Müller-Putz *et al.* [61]. The authors show that for 10 test-trials per class in a 4-class classification problem, and a risk of error  $\alpha$  at 0.05, the average accuracy should be higher than 40% to be reasonably considered different than a uniform-random process.

## 5.2 4-CLASS CLASSIFICATION RESULTS

Figure 5.1 shows the mean accuracy calculated for each subject. Errors bars show one standard deviation.

To analyse the type of error (*e. g.* false positive or negative, in 2-class problems) in our model, we calculate the average confusion matrices. A confusion matrix shows the relationship between the predicted labels and the ground truth. It allows the visualisation of some classification biases. Figure 5.2 displays the confusion matrix for each subject. To interpret the figure, if the classification is perfect, *i. e.* without any mistakes, then the confusion matrix should be diagonal with a bright yellow on the diagonal and deep blue outside. The maximum possible

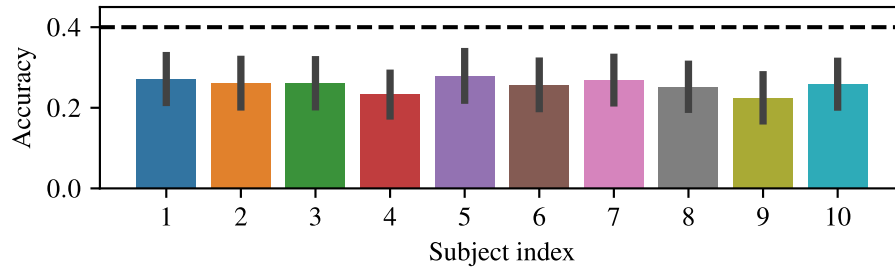


Figure 5.1 : Mean classification accuracy from a thousand train-test split of the dataset with a ratio of 75%-25%. Error bars show one standard deviation. The threshold at 40% represents the chance level for a risk  $\alpha$  at 0.05 for 10 test-trials per class in a 4-class classification problem [61].

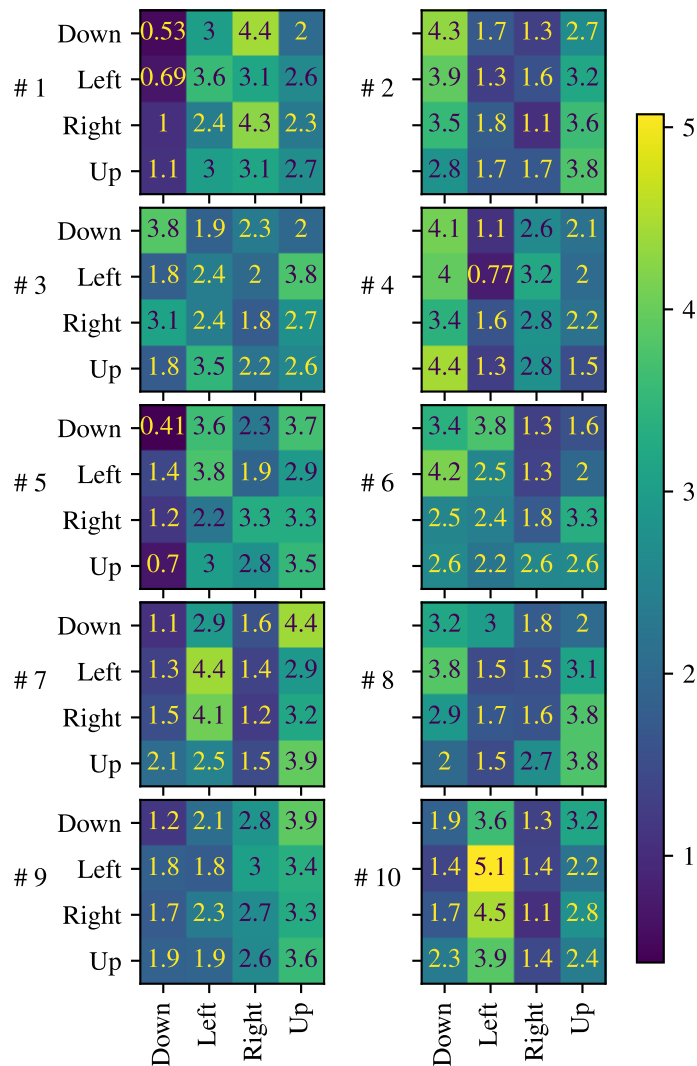


Figure 5.2 : Average confusion matrices from a thousand LDA, for every subject. There are 10 test-trials per class. Predicted labels are displayed on the x-axis while True labels are on the y-axis.

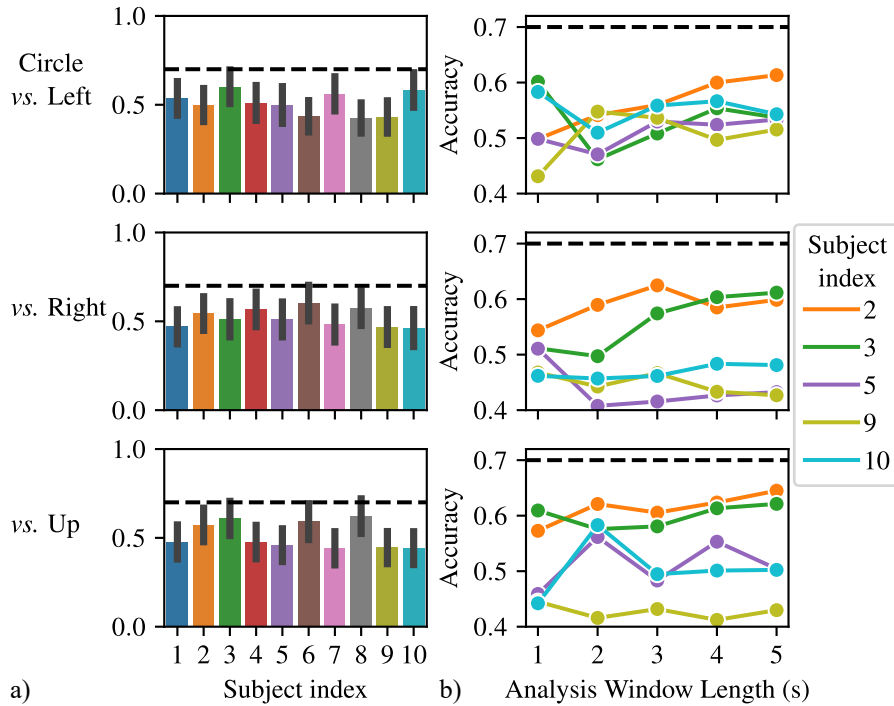


Figure 5.3 : (a) 2-class classifications, from top to bottom: Circle *vs.* Left, Right, and Up. (b) Evolution of the mean accuracy on selected subjects versus a length increase of the analysis window. Error bars show one standard deviation. Chance level is at 70% in these conditions (risk  $\alpha$  at 0.05) [61].

value in a cell is 10, since we have 10 test-trials per class. As a result, the sum of values within a row (*i.e.* True label) is equal to 10.

### 5.3 2-CLASS CLASSIFICATION RESULTS

We extended the first classification attempt presented in the previous section to a 2-class classification. We attempt to classify the movement intention, depending on the MI content: one arm, left or right, or both arms simultaneously, *i.e.* the condition Up. We use the same feature extraction methods. However, we are training the LDA classifiers using only two classes.

We display in figure 5.3, panel (a), the mean accuracy resulting from a one-second-long analysing window starting 500 ms after the beginning of MI. Error bars show one standard deviation. The first row presents the classification results between the 2-class problem: Circle *vs.* Left. The second row presents Circle *vs.* Right, while the third row presents Circle *vs.* Up.

In panel (b), we display the mean accuracy while progressively increasing the length of the analysis window. Nevertheless, we keep its start 500 ms after the beginning of MI. The selected subjects on panel



(b) of figure 5.3, are the ones who show a statistically significant gating effect in chapter 4.

#### 5.4 DISCUSSION

We observe in figure 5.1 that none of the subjects passes the 40% threshold. This observation means that the classifiers yield average accuracies that are not distinguishable from a 4-faced dice roll process, above a reasonable doubt. This result, although unfortunate, confirms the assumptions made in the previous chapter. Indeed, in the previous chapter, we observed that the SSSEP's modulation in untrained subjects seems irrespective of the MI content, *i. e.* left or right arm. Therefore, as shown by the results, a classification based solely on the SSSEP's modulation from somatosensory gating, in the particular context of a 4-class classification, seems unreliable without training.

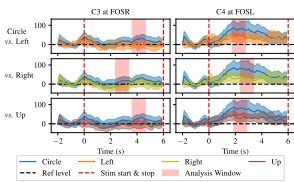
In figure 5.2, the most interesting result is that we can not observe any specific pattern in the matrices. A critical bias, such as having a classifier that always answers "Left", irrespectively of any given input, would constrain the predicted label to the "Left" column. Therefore, the "Left" column would be yellow while the rest would be dark blue. This lack of pattern shows that none of the classes generates many mistakes. Hence, it indicates that the training model seems unbiased toward one class rather than the others.

We notice that the Left condition for subjects # 7 and # 10 seems better classified than the others. For example, in subject # 10, with a coefficient of 5.1, this condition is well classified, on average, in half of its occurrences.

The figure 5.3 (a) shows that none of the subjects passes the threshold of 70%. Therefore, similarly to the 4-class classification, the classification is not better than random. However, one can observe that the standard deviation sometimes crosses the threshold, like in subject # 3 or # 6 in Circle *vs.* Left or Right, respectively. This trend is encouraging for deeper analysis.

On panel (b), we can also observe that subjects # 2 and # 3 seem to benefit from longer analysis windows. Indeed, the mean accuracy from subject # 2 during Circle *vs.* Left increased from 51% to 61%. We can explain these results when observing the SSSEPs' amplitude through time for subject # 2 from chapter 4\*. We can observe that the mean SSSEP's amplitude from C3 is steadily higher in the Circle condition than in any other conditions. Hence, a longer integration window could increase the precision of the estimate and might result in linearly separable RAI distributions.

However, this approach can suffer from slow variations in the RAI estimates. With subject # 2 it seems to work well because the mean RAI does not vary a lot over time for SSSEP on C3. Nevertheless, from SSSEP measured on C4, we can observe that there is only a shorter window



\* Figure 4.5

where the SSSEP during idle seems higher than during motor imagery. Future approaches might investigate voting systems that integrate the classifier's answers every second, which may make classification more robust to such slow variations.

## 5.5 CONCLUSION

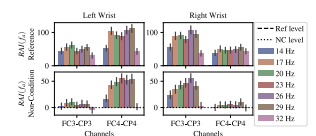
The results presented in this chapter for offline classification were obtained using classification pipelines compatible with online implementation and not computationally expensive. The somatosensory gating effect is not suitable as a marker allowing the implementation of a 4-class BCI, at least when the experiment is performed during a single session. However, as demonstrated in chapter 4, the somatosensory gating can be efficiently measured during a single session of motor imagery. We observed that the SSSEP's amplitude modulation seems irrespective of the motor imagery content, *i. e.* left arm influence *only* the SSSEP from the left wrist. The lack of significant accuracy corroborates that finding and the importance of this hypothesis for a classification algorithm based on SSSEP's amplitude modulation only.

For offline classification, we used a quick-to-reply classification algorithm. That is because in modern BCI, the classification result is expected to be really quick, within a couple of seconds after the start of the task. Hence, our choice was to use only a one-second-long analysis window starting 500 ms after the beginning of stimulation. It could be interesting to investigate the influence of the analysis window's length on the accuracy.

In addition, we aimed at knowing if the SSSEP's amplitude variation caused by gating is large enough to implement a BCI. Hence, our usage of a LiA using a low-pass filter with a unit gate impulse response. The LiA can be regarded as a very narrow tunable filter, which provides amplitude and phase information of a sinusoid component out of a random noise [62]. Our signal processing aims at extracting only the amplitude of the SSSEP.

We observed in the grand average of the screening procedure\* that the presence of the stimulation itself seems to generate an ERS over the high  $\alpha$  and the  $\beta$  band. One can wonder if a feature vector extended to frequency components other than the frequency of stimulation component would lead to better results. Also, the motor imagery is known to generate an event-related desynchronization (ERD) of the  $\beta$  band, during motor imagery, followed by an event-related synchronization (ERS) shortly after [82]. The latter is known as the  $\beta$  rebound. In a future analysis, we could try to detect the presence of this  $\beta$  rebound and investigate its suitability to increase BCI performance.

In the review of literature in chapter 2, we identified multiple leads to improve MI-based BCI exploiting SSSEP. In the work of Tao *et al.* [100], the authors use electrical stimulation and the well-named inter-stimulus



\* Figure 4.3

phase coherence metric (ISPC). Electrical stimulation can produce SSSEPs with higher amplitudes, however, it can be more unpleasant for users than vibro-tactile stimulation.

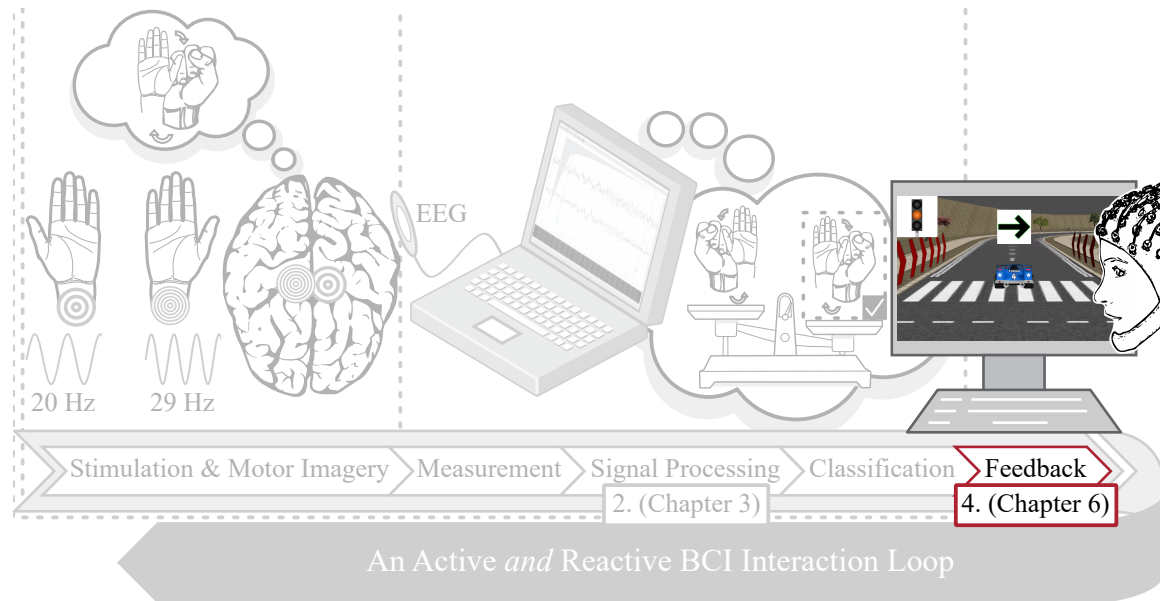
Differently, Kim *et al.* in multiple works [48–50] based their classification on a combination of frequency and spatial features. They mix band power estimates and log variances of multiple common spatial patterns (CSP) filtered signals.

Finally, these observations lead to several possible technologies or methods that could improve significantly our BCI performance: use of electrical stimulation, SSSEP phase-related information (ISPC), spatial feature parameters (CSP), or  $\beta$  rebound shortly after motor imaging. The most promising research lies in the use of vibro-tactile stimulation to facilitate the measurement of ERD during motor imagery in a short-training 2-class BCI.

# DESIGN AND STUDY OF TWO APPLICATIONS CONTROLLED BY A BRAIN-COMPUTER INTERFACE EXPLOITING STEADY-STATE SOMATOSENSORY-EVOKED POTENTIALS

# 6

## ROADMAP —



This chapter focuses on the BCI's Computer–Human Interaction aspects developed in the previous chapters. We tackle the design and study of two applications controlled by this BCI. The applications differ in two characteristics: their inertia, or rhythm of information flow perceived by the user, and the “punitiveness” of the application in case of mistakes. To study the user experience in perfectly controlled conditions, we used a so-called “sham” feedback rather than the real feedback computed by analysing the user’s brain waves. With sham feedback, the BCI provides commands with an *a priori* defined accuracy. Varying the sham feedback accuracy permits the study and modelling of the relationship between the system’s perceived usability and the BCI’s performance.

## RELATED WORK —

Jimmy Petit, José Rouillard, and Francois Cabestaing. “Design and study of two applications controlled by a Brain-Computer Interface exploiting Steady-State Somatosensory-Evoked Potentials.” *Human Interaction & Emerging Technologies (IHIET 2022): Artificial Intelligence & Future Applications*. Vol. 68. ISSN: 27710718 Issue: 68. 2022. DOI: [10.54941/ahfe1002787](https://doi.org/10.54941/ahfe1002787)

## ACKNOWLEDGEMENTS —

We would like to acknowledge Camille Bordeau and Philémon Berne, both helpful interns of the team at the time who contributed to the work presented in this chapter. We would like to thank our colleagues of the Lille University Hospital for their support during BCI and EEG experiments.

## 6.1 INTRODUCTION

We implemented a Motor Imagery-based BCI which provides four commands.

We conducted a user experiment to evaluate our applications over a group of ten healthy subjects. This user experience is the last session of a four-session-long experiment (ethical comity of Lille University, reference: 2020-417-S81). The other three sessions are more focused on studying the neurophysiological aspects of the BCI. Describing these sessions and their results is out of the scope of this paper dedicated to the Human-Computer Interaction aspect.

For the user experiment, we have developed two applications. However, BCI using motor imagery and four different commands tends to have a low accuracy, which greatly improves with a lot of training. Since the users had no time to train themselves, we used sham feedback to simulate various levels of performance [72].

The sham feedback has various advantages compared to testing the real performances of the system:

1. The classifier used by the BCI has already been trained before the user experiment session. However, within one or two weeks between the two sessions, the mental activity may have drastically changed, and it would be likely that the classifier would produce the same output to any given input, resulting in a succession of commands like Turn Left, Turn Left, Turn Left, ... Sham feedbacks avoid locking the user in that situation.
2. A consequence of implementing sham feedback is that we must set the desired command (a "Good" action) for any given state of the application using a combination of level design and instructions. This allows us to then perform an offline relevant test of different classification algorithms and build on a dataset where the number of commands is reasonably balanced. For example, without sham feedback, the subject could be stuck in a state where they must use the same command repeatedly, which seriously unbalances data set.
3. For the user experiment, we use various levels of sham, ranging from 45% to 90%, which allows us to study the relationship between the system accuracy and various measured aspects in the questionnaires, which is not possible otherwise.

The objective of this article is to provide the details of the applications and how we encourage the user to use a balanced number of commands. In addition, we study the effect of the applications and the user experiment on the users themselves using questionnaires investigating fatigue, mood orientation, or mental workload, for example. Finally, we study the correlation between the perceived usability of the system,

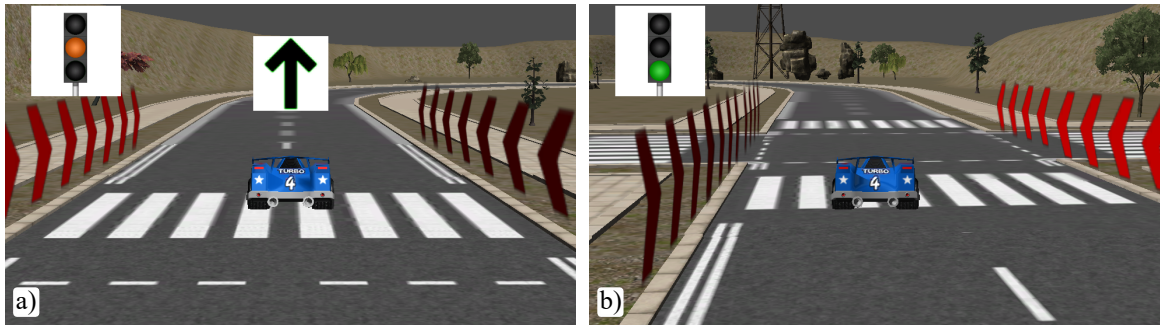


Figure 6.1 : Screenshots of the kart (a) on a straight line (b) at the cross section of the eight shaped.

assessed with a System Usability Scale, and the performance of the system. Therefore, for a given BCI performance, we can predict what mean degree of perceived usability will be achieved, and *vice-versa*.

## 6.2 APPLICATION DESIGN

In this section, we present in detail the applications, to allow their reproducibility. In addition, as our user experiment uses sham feedback, we introduce our definition of “Good” and “Bad” commands in the applications.

### 6.2.1 Description

The first application is a kart-driving application. The kart is controlled with the four available commands provided by the BCI: Move Forward (MF), Turn Left (TL), Turn Right (TR), and Do Nothing (DN). To balance the number of “active” commands, i.e., MF, TL and TR, the kart moves on an eight-shaped road. During a left turn of the road the user is instructed to perform a TL command, and *vice-versa*. In a straight part, the user is instructed to perform the MF command. Instructions are given using a sheet at the beginning of the experiment. A Turning command performs two actions on the kart: the vehicle turns and receives an additional pushing force. Therefore, one TL or TR command will make the kart follow a curved trajectory. To help stay on tracks, semi-transparent walls, with red arrows on them, follow the kart and apply a repulsive force to it as soon as it gets too close to them. Figure 6.1 shows two screenshots of the application. Figure 1 (a) shows the feedback given to the user: the kart moves or gains speed and an image is displayed on top of the kart. The kart is on a straight line, therefore, it has a fixed percentage, like 60%, of doing MF according to the sham feedback. If a “Bad” action must be performed, then the action is randomly and uniformly selected between TL, TR, and DN.





Figure 6.2 : User view at the beginning of a level 2 (Turn Left induced-design).

The second application is a puzzle-solving type of game called SokoBCI, inspired by the game Sokoban (Hiroyuki Imabayashi, 1982). The user controls the movement of a 3D avatar who must plant trees. The user must solve the levels using the smallest number of commands. To balance the number of active commands, one run of the application is composed of 2 levels. The first level is a simple symmetric level that forces the user to use an uneven number of TL and TR commands. During the solving of the first level, the system counts the number of TL and TR commands. Level 2 is chosen to encourage the user to use the command least used during level 1. The actual vision from the user's point of view during level 2 is displayed in figure 6.2. The level designs and the aforementioned process are displayed in figure 6.3, which is a top view of the levels. When the user plants a tree, the tree appears on the red square and the red square turns green. During a run of the application, as soon as the user finishes level 1, the appropriate level 2 appears on the screen and the loop of commands starts again. To give time to the user to think about the best solution, the first command of level 2 is completely ignored by the computer, during a dozen seconds of break.

For both applications, a three-colour light is displayed at the top-left corner of the screen. The green light gives the cue to the user to start the Motor Imagery task to send a command to the BCI. After six seconds, the light turns to orange, indicating the feedback period, during which the kart or the avatar will react accordingly to the given command. After three seconds of feedback, a short break with random duration, between three to four seconds, is given to the subject with the red light.



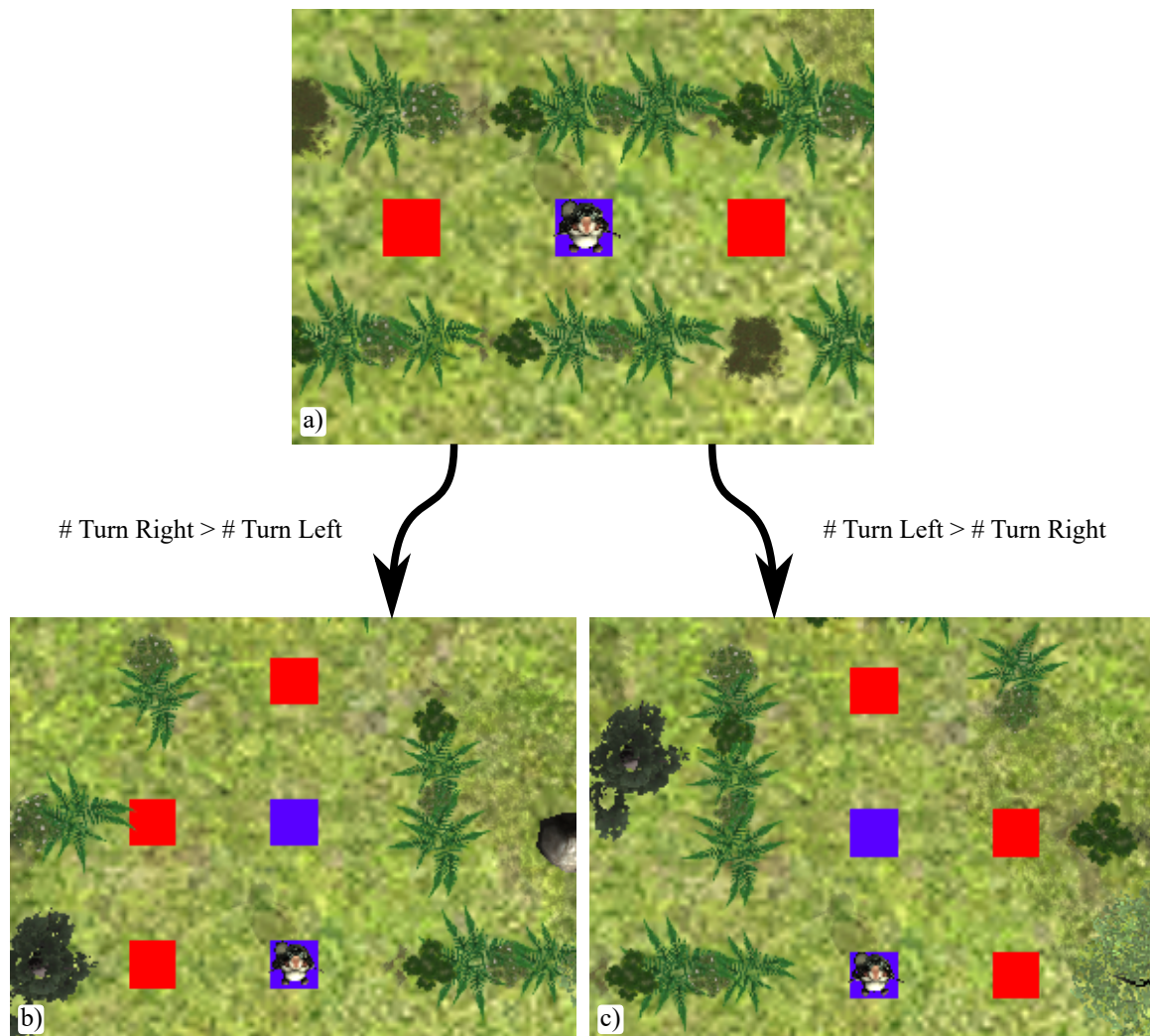


Figure 6.3 : Top view of the SokoBCI levels. (a) shows level 1. Depending on the number of TL or TR used to solve the level 1, one level 2 is chosen (b) or (c). The blue squares show the possible location of the avatar, accessible with the Forward command while facing the proper direction. The red squares show the targets. The user has to orient the avatar towards a target and use the command MF to plant a tree.

### 6.2.2 Definition of “Good” or “Bad” Command: Specific Case of SokoBCI

The description of the Kart driving task is quite clear about the instructions given to the subject. We believe that the definition of “Good” or “Bad” command is straightforward in this case. However, for the SokoBCI it is less clear. In our user experiment, the user is instructed to “use the least number of commands to plant all the trees. If the system does an unwanted action, [example given], you might need to change your initial plan.”. When observing the level design, one can verify that the solution for level one is to rotate once, left or right, and plant a tree, then rotate twice, in the same direction, to plant the second one. In this situation, the commands TL and TR are considered equally “Good” commands, the commands MF and DN, will have the same effect which is leaving the avatar motionless and are “Bad”. However, during the U-turn, the initial rotation will dictate the next choice of the user, the first rotation will be either an error or not, depending on the user’s mental decision. Given the instruction, the user will adjust their mental plan to pursue the rotation, and therefore the “Good” action becomes predictable.

In the first level, the avatar can face four different directions and the tree planting can have four different states (no tree planted, the left tree only, the right tree only, and both trees planted): there are thus twelve ( $4 * (4 - 1)$ ) different possible game states, the game state where all trees being planted being naturally ignored. Four of the game states have two “Good” actions. In the second level, left or right, the avatar can face four different directions, through two different locations, and the tree plantation can have eight different states ( $2^3$  possible situations). Therefore, we have fifty-six ( $4 * 2 * (2^3 - 1)$ ) possible states of the game, of which thirteen states have two simultaneously “Good” actions.

### 6.2.3 Inertia and “Punitiveness”

The first difference between applications is in inertia. Indeed, the kart continues to move forward during the green light period. It is a vehicle that gains momentum by receiving the TL, TR, and MF commands. The user must therefore analyse the road and the speed of the kart to decide when to send the next command, even during the red-light periods which represent the breaks.

The second difference is the punishment for mistakes, which we call “punitiveness”. In the kart application, the semi-transparent walls follow the kart as it moves along the track, pushing the kart in the opposite direction as it gets closer. In this case, even mistakes tend to move the kart forward, however slowly. In the SokoBCI, on the other hand, a mistake can be much more frustrating as the user will have to make a correction move in most cases.

### 6.3 TEST OF THE APPLICATIONS

We conducted a user experiment with a group of ten healthy participants, seven males and three females. The average age of the participants is 23.8 years (std: 3.2 years, min: 19, max: 28). In this section, we present the experimental protocol.

#### 6.3.1 Protocol

The subject sits in front of the computer and fills out a pre-session questionnaire. Then, the experimenter gives an instruction sheet to the subject, who reads it and can ask any questions needed for good comprehension. Afterwards, the experimenter installs the brain-computer interface device on the user, as well as the devices that deliver the mechanical stimulations to the wrists. After this installation step, the proper tests can begin. We start by demonstrating one of the applications, chosen with a pseudo-random order across subjects, we remind the user the objective of the application and the instructions. After that, the user performs four blocks of recording with the application. Each block has a specific accuracy for the sham feedback, the four chosen accuracies are 45%, 60%, 75%, and 90%. The order is also pseudo-random. After four blocks of recordings, the demonstration and test steps are repeated for the other application. The subject has a mandatory break of 3 minutes (minimum) between each recording block.

The subject fills out questionnaires after each block and the experimenter conducts a debriefing interview with the subject at the end of the experiment. The experimenter asks the subject to fill out the questionnaire independently from one block to another. We have three different questionnaires. The first one is about behaviour measurement, the second one is a NASA Task Load Index without the pairwise comparison of the questionnaire's dimensions, called Raw TLX [38], and the last one is the System Usability Scale [16, 17], or SUS. The last two are given to be completed at the end of each block. The first questionnaire is given as a pre-session questionnaire and after the first block, the fourth block (*i.e.* four blocks of the first application), the fifth block and the eighth block (*i.e.* four blocks of the second application), to measure changes in behavioural data during each application.

The Behavioural questionnaire contains four items assessing "Awakeness", Tiredness, Mood Orientation, and Emotion Intensity with a five-point Likert scale. Additionally, a space for comments is left for subjects to express themselves on the application they have just tried. The Raw TLX aims at measuring the mental workload of the application with six items: Mental Demand, Physical Demand, Temporal Demand, Performance, Effort, and Frustration measured on a twenty-point Likert scale. The SUS aims at measuring the usability of the system with a ten-item long questionnaire, also using a five-point Likert scale.

- 1) What did you think of the experiment?
- 2) What did you think about the difficulty to adjust your mental plan to the system's error during the SokoBCI?
- 3) Inform the subject about the sham feedback: what is it about, how is it done, and why we do it.
- 4) Did you ever suspect the sham feedback? [If yes, when?]
- 5) Did you suspect different levels of performance/accuracy?
- 6) Did you discuss about performances during the previous session [which also had sham feedback] with your friend/colleague? [Question optional, question asked only if the friend/colleague also participates in the experiment.]

Table 6.1 : Interview guide for the experimenter

In the debriefing interview at the end of the session, we discuss with the subject different aspects of the whole experiment. Table 6.1 presents the different questions asked, and their order. At the end of the session, some subjects had strong time constraints, which led us to shorten some interviews.

### 6.3.2 Behavioural Data - Results

Results of the Behavioural data analysis are displayed in figure 6.4. We can observe that, "Awakeness", Mood orientation (positive to negative), or Emotion Intensity do not seem to evolve during the session. However, Tiredness tends to increase, indeed the majority mention (the mention that crosses the 50% threshold) became three (out of five) by the end of the session. A few subjects filled out the mention number four during the session too, which they did not at the beginning of the session. To conclude in a few words, the eight blocks of recording seem to cause a little fatigue to the subjects population, additionally, the three other dimensions do not evolve much.

The Raw TLX results are presented in figure 6.5. When observing the distribution of the Raw TLX score against the sham accuracy, no trends seem to appear. No difference can be observed between applications either. However, the individual dimensions of Performance and Frustration are highly inversely proportional to the sham accuracy. It seems to hold for the Effort dimension of the questionnaire too, however to a lesser extent than the previous two dimensions. The subjects seem to have well experienced the difference in the BCI performances and the frustration level diminished as the performance increased, likely caused by the decreasing number of mistakes performed by the system. Interestingly, as the accuracy increases, we measure a difference in

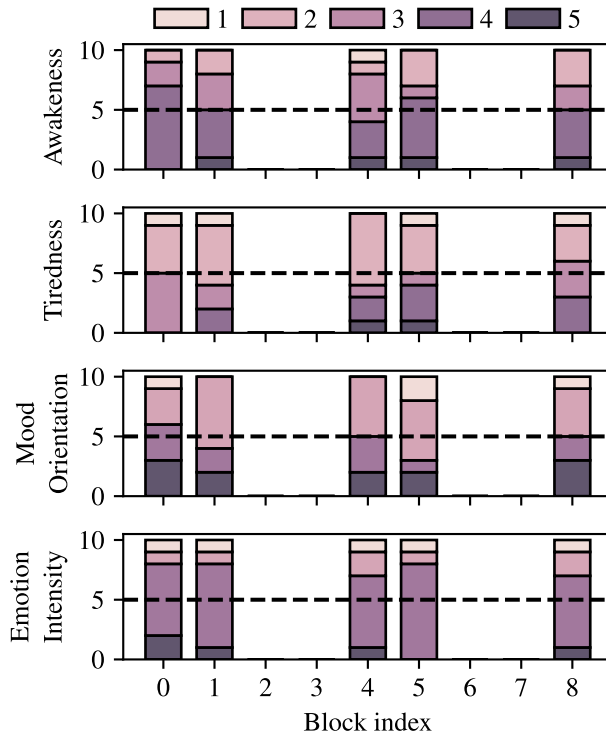


Figure 6.4 : Stacked bar plots showing the distribution and evolution of Behavioural data over the subjects.

Mental Demand between the applications. With sham accuracy at and above 75%, the subjects seem to experience a Kart application more mentally demanding than the SokoBCI application. This is confirmed using a dependent samples t-tests<sup>1</sup>: at 75% a p-value of 0.0012 ( $< 0.05$ ) and at 90% a p-value of 0.019 ( $< 0.05$ ) are computed. At 75%, the mean difference in Mental Demand between the Kart and the SokoBCI is at 2.2 points (std: 1.6) while being at 2.5 points (std: 3.1) at 90% of sham accuracy. This difference can be explained by the difference in inertia between the two applications. In the kart, when the three-colour light is red, the kart is still moving, and the user must think to anticipate the movement of the kart. Additionally, the effect does not occur for low accuracies since multiple errors tend to slow down, or even stop, the kart. Finally, a weak difference between the application in the Frustration level is also observable for the lowest accuracy as the mean and median are systematically higher in the SokoBCI than in the Kart. This could be explained by the “punitiveness” of the SokoBCI, an error being much more costly in this application than in the Kart-driving one.

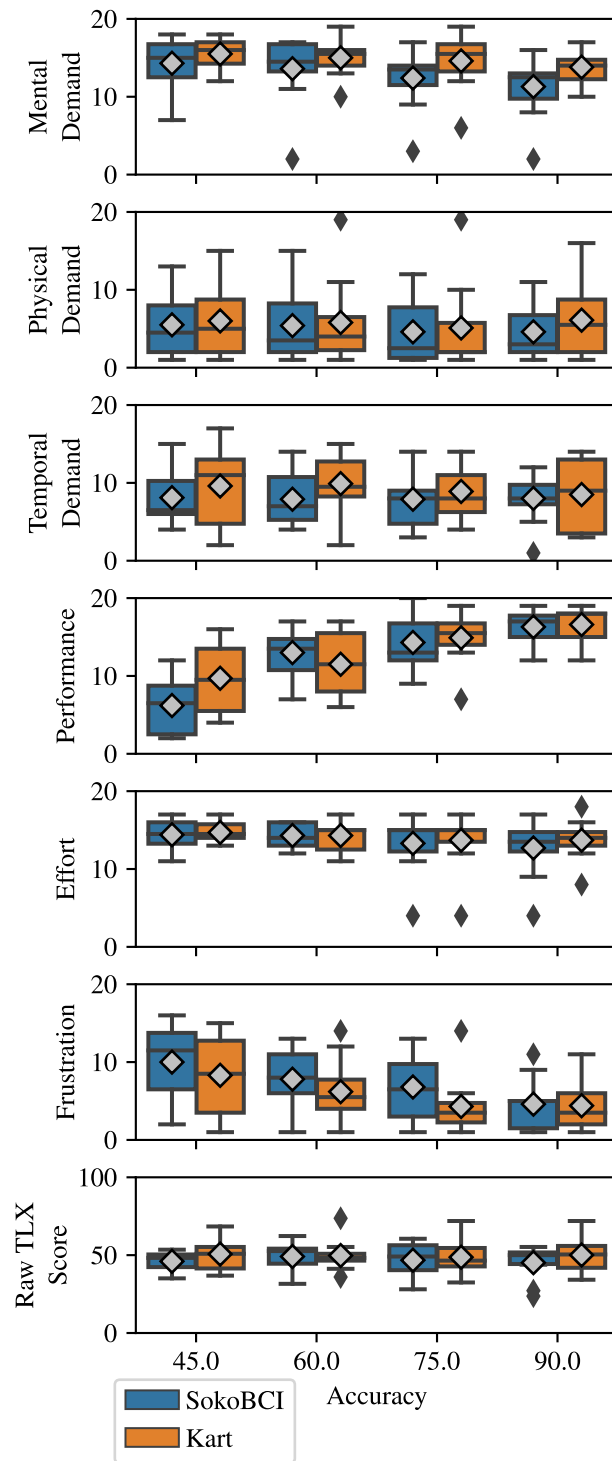


Figure 6.5 : Box plots of the Raw TLX results, grouped by the application type. The six first lines show the individual dimension of the questionnaire, while the seventh line show the score of it.

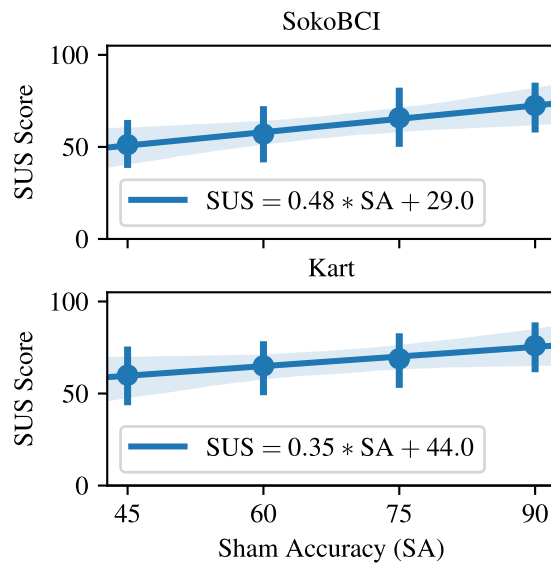


Figure 6.6 : Mean and 95% Confidence Interval, computed by bootstrap, of the SUS Score in regard to sham accuracy.

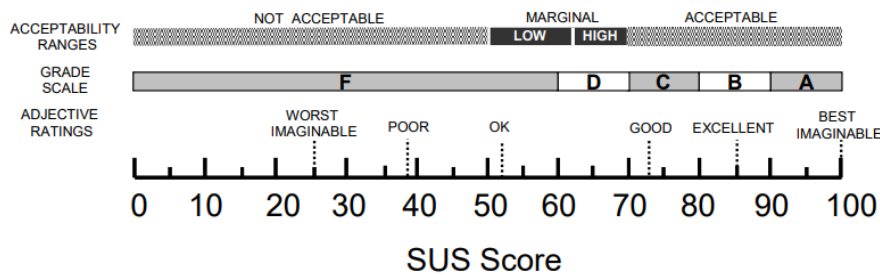


Figure 6.7 : Relationship between the adjective ratings, acceptability scores, and school grading scales, in relation to the average SUS score. From [6].

### 6.3.3 Relationship Between Performance and SUS

Figure 6.6 shows the results of the SUS questionnaires. Firstly, the SUS scores are positively correlated to the sham accuracy.

According to the slope coefficient of linear regression, the effect is stronger in the SokoBCI application than in the Kart. It can be also explained by the higher “punitiveness” of an error in SokoBCI than in the Kart.

Bangor *et al.* added an adjective rating scale to mean SUS scores, see figure 6.7 [6]. In doing so they also provide an interpretation of SUS scores using an adjective, school grading system, or acceptability range from previous works. According to their results, a system would start to be acceptable with a SUS of 70 and everything below had usability

<sup>1</sup> We failed to reject the hypothesis of normality of the four samples using Shapiro-Wilk tests and a rejection threshold of 5%, therefore we assumed the normality of the samples.



issues and is cause for concern. Therefore, using these models, in a BCI with similar features to the SokoBCI, the system would become acceptable with a minimum performance level of 85.4%, whereas a system like the Kart application would need a minimum performance level of 74.3%.

#### 6.3.4 *Questionnaire, Comments, and Debriefing Interview - Results*

Reading the comments and notes during the experimenter's debriefing allowed us to identify four categories of feedback: **Strategy**, the strategy found by the subject to perform the task; **Application Comparison**, the subject expresses some preference toward one application over the other; **Positive Comment**, various adjectives that show the subject's appreciation for the application, the system or the experiment; and **Improvement Tips**, which is a list of things that could be improved to make the applications better.

The commentaries related to session comparison (see Table 6.1 - 1) and the performance of the subject written during the session are ignored, as the subjects did not expect sham feedback. We have translated the comments from French to English as faithfully as possible. Finally, we added context to comments or shortened them, if necessary, when indicated in brackets.

##### 6.3.4.1 *Strategy*

Two subjects spontaneously used the same strategy of Motor Imagery during the SokoBCI. They imagined themselves pulling the antenna of the avatar with one or two arms. For example, subject n°10 writes "The design of the character helped me to visualise the correct movements, I imagined taking the antennas on the head of the character and pulling them (the antenna on the right with the right hand to turn to the right, [etc])".

The subject n°6 comments that he found it easier to focus on the road instead of the kart: "I found it easier to concentrate when I wasn't looking at the vehicle (looking at the road instead) [After Kart 45%].".

##### 6.3.4.2 *Application Comparison*

Subjects 2 and 10 comment about the higher complexity of the SokoBCI over the Kart driving application, subject n°2 writes: "[SokoBCI] is very funny (more than Kart), but more complex too". However, subject n°4 states during the debriefing having more trouble processing the scene and movement while performing the Motor Imagery task: "it's hard to see the game and play at the same time. Acquire information and respond in time, that's difficult."

#### 6.3.4.3 *Positive comments*

Almost every subject commented something positive; the words “fun” or “playful” appeared a lot. The word “fun” was given by six different subjects. Subject n°10 noticed how time seems to pass much faster and subject n°3 highlights the intuitiveness of the system: “It’s fun finally seeing the system working for me. It’s pretty instinctive to use at this point [after SokoBCI at 75%]”. Subject n°8 comments that the experiment was more ecological: “Last session with a concrete application is a bit more playful.”.

#### 6.3.4.4 *Improvement Tips*

Subjects 4, 5 and 8 commented that the inertia of the kart was disturbing them: subject 4 writes “I struggle focusing simultaneously on the stimulations and on the commands to be performed”, and subject n°5 writes: “I struggle to focus simultaneously on the stimulations and on the commands to be performed [during Kart]: really tiring. [In SokoBCI] The character is static during the acquisition [i.e. Green light] so we do not receive information, this helps to focus.”. Interestingly, subject n°7 mentioned that the breathing animation of the avatar in the SokoBCI during the green light was a distraction: “The [IDLE] movement of the avatar are distracting.”.

Subjects 2 and 3 retain some ambiguity on the action to be performed during the Kart as they commented on the questionnaire: “Sometimes, I did not know which movement to imagine. For example: a turn arrives, should I turn by anticipation?” (Subject n°2). In this case, the instruction was repeated, however, the anticipation aspect seems uneasy.

Subject n°4 advised to reduce the duration of the green light periods as it was too long, and subject n°5 advocates for a blue sky in the kart application and wished for a more comfortable EEG headset installation.

## 6.4 CONCLUSIONS, LIMITATIONS, AND FUTURE WORKS

In this paper we presented the design of two applications controlled by a BCI: a kart driving application and a puzzle solving application called SokoBCI. The BCI provides four commands. The applications differs on two main points, SokoBCI is more punitive than the Kart in case of mistakes. Indeed, after a mistake the user must react to provide a corrective command in the SokoBCI, while in the kart, invisible walls on each side of the road push back the kart in the good direction as it gets closer in case of mistakes. Secondly, the Kart’s motion is continuous and partly controlled by inertia while in SokoBCI the avatar steps from its current position to the next one. It means that the kart keeps moving during the Motor Imagery task and the breaks, and therefore that the

user must maintain a significant level of mental activity in the decision-making process to choose the correct command to use.

We evaluated both applications using questionnaires, open written comment and discussions with a group of ten healthy subjects. We observed that some dimensions of the Raw TLX are highly correlated to the performance of the system, like Performance and Frustration, while others don't. In addition, the Mental Demand at high performance of the system, was more important in the Kart than in SokoBCI. It might be explained by the difference in inertia between the application. This was also confirmed by the users in the commentary and discussion.

Additionally, we proposed a model of the relationship between the performance of the BCI and the perceived usability, assessed with an SUS. Firstly, the models show a positive correlation between the variables for both applications. In addition, the correlation was stronger in the SokoBCI than in the Kart. This could be explained by the fact that the SokoBCI is more punitive to the user in case of mistakes. Therefore, one might be concerned by the design choice in the application creation process as it can make an application felt acceptable by the user for a performance level much lower or higher. In our case, we found a ten-point difference in accuracy between the application to reach the acceptability threshold.

One straightforward limitation of this work is the number of subjects included in the experiment, further inclusions are needed to increase the significance of results. Finally, elaborating a more general approach based on characteristics of various application, like inertia or "punitiveness", to model the impact of those application characteristics on the user might be an interesting tool to help in the design of serious games.

#### DATA AVAILABILITY STATEMENT

The data that support the findings of this study are available upon reasonable request from the authors.

In this final chapter, I summarise our contributions described in this thesis. I discuss various aspects of our research work, their limitations, and various areas of improvement. I conclude with the main takeaway of this dissertation and present various perspective works that I wish to pursue or that I find relevant for further research.

### 7.1 OUR CONTRIBUTIONS & POSITION IN THE STATE-OF-THE-ART

This thesis aimed to study and implement a combination of active and reactive BCI to benefit from their mutual advantages. We selected SSSEP as our signal of interest to produce a BCI that does not rely on the user's gaze. MI-based BCI was our natural choice for this combination since it involves the somatosensory system and can provide a new way to voluntarily modulate the amplitude of the SSSEP. The literature presents the standard approach to voluntarily modulate the amplitude of the SSSEP by attention focusing (AF). This new approach could mitigate the limitations of this paradigm, *i. e.* the number of available commands for a given number of vibro-tactile stimulations. Indeed, it seems easier to imagine a movement involving multiple limbs rather than focusing full attention on multiple locations simultaneously.

The literature review drew a broad state-of-the-art of SSSEP-based BCI. Our first observation was that among the rare works that focused on the simultaneous usage of MI and SSSEP, none of them investigated the performance of a BCI using solely the SSSEP's amplitude modulation induced by MI through somatosensory gating. In addition, none of them measured the somatosensory gating in a situation of multiple stimulations. In our work, we tested these two aspects. A second observation was that SSSEP-based BCI using AF showcased in the literature exploited a maximum of three classes. Hence, most of which required three stimulations simultaneously. In this thesis, we investigated the possibility of SSSEP-based BCI providing four commands using only two stimulations by exploiting MI. Our fourth idle condition was added to distinguish between the user's voluntary and coincidental commands, also known as Midas' touch problem.

#### 7.1.1 *SSSEP characteristics and State-of-the-Art of SSSEP-based BCIs – Chapter 2*

Conclusions drawn from the literature review showed that the SSSEP's amplitude highly depends on the frequency of stimulation. In addition, this dependency is also true across individuals, resulting in a not negligible between-individual variability. However, this relationship also seems relatively stable over time for each individual. Hence, this relationship shows a small within-individual variability. This level between

and within-individual variabilities form a methodological constraint that motivated us to include a screening procedure in our protocol.

The state-of-the-art of 2-class SSSEP-based BCIs using AF showed a mean performance that varied from 60% to 72%. The standard deviation associated with the mean performances in the literature was also quite significant, meaning that some subjects showed very poor performance while others did not. Such variability raises the question of BCI's illiteracy rate in this paradigm. Illiteracy can be defined as the proportion of users for which a specific paradigm remains inefficient even after training. However, the state-of-the-art was rather scarce, and we still lack information on this subject.

### 7.1.2 *Algorithm Comparison for Sinusoidal Amplitude Estimation in SSSEP-based BCIs – Chapter 3*

In this chapter, we introduced a model to generate synthetic EEG in line with the knowledge of SSSEP drawn in chapter 2. We compared the performance of the standard algorithm in BCI involving steady-state potentials, such as the steady-state visually-evoked potentials, in addition to SSSEP-based BCI. Our comparison included the lock-in amplifier, the canonical correlation analysis (CCA) and the partial least square (PLS). Using the lock-in amplifier, we tested different spatial filters, such as the current source density (CSD). Our results showed that the lock-in amplifier filter combined with a CSD demonstrated the highest efficiency for the synthetic data and a subset of the EEG data from our experiments. These results consolidated our choice to use these methods in the rest of this work.

### 7.1.3 *Somatosensory Gating-related Hypothesis Testing and Measurement of BCI Performances – Chapter 4 and 5*

This chapter resumed the hypothesis testing involving questions about somatosensory gating. Our primary hypothesis was that somatosensory gating induced by kinaesthetic motor imagery (KMI) is measurable in the context of multiple vibro-tactile stimulations. KMI is a type of MI where the subject is asked to perform MI and add to it the sensation related to the skin, such as the rubbing of clothes when moving, muscle contractions... Our secondary hypothesis was that the KMI selectively induces a decrease in SSSEP's amplitude. In other words, if one has both wrists stimulated and is performing KMI with the left arm, does the SSSEP's amplitude elicited by the stimulation on the left arm diminish?

The experiment results showed that a gating effect could be measured on C3 or C4 irrespectively of the KMI content. Therefore, the experiment results seemed to substantiate our primary hypothesis while rejecting our secondary hypothesis. Additionally, we attempted a 4-class classification of the SSSEPs' amplitude into four commands\*. For the

\* as a reminder: KMI with left or right arm, KMI with both arms simultaneously or none. The latter being an idle state.

implementation, we restrained our algorithm to real-time compatible ones, quick-to-answer algorithms, and we only used SSSEPs amplitude as a discriminative feature. In addition, our objective was to mediate with as many common challenges in BCI as possible. For example, we used a minimum amount of filters and battery-powered components to reduce data contamination as much as possible.

The results of the 4-class classification showed that none of the subjects demonstrated high enough performance to be distinct from a random process beyond a reasonable doubt. These results can be explained by the fact that our secondary hypothesis is not sustainable. Indeed, left or right-arm motor imageries do not produce selective modulation of the gating. Therefore, their effect can not be differentiated based solely on the SSSEPs' amplitudes variation. However, our results showed a statistically significant decrease in SSSEP amplitude between idle and KMI conditions for half of the subjects. This result is very encouraging as it was obtained in a single session. In addition, it demonstrated that the SSSEP's amplitude is a relevant discriminative feature for future research.

In chapter 5, we also evaluated a 2-class classification algorithm to assess our position with respect to the state-of-the-art AF-based BCIs using SSSEP\*. We adopted an approach that was compatible with a real-time implementation and solely used the SSSEP's amplitude modulation as the source of information. Our result showed that classification accuracy ranged between 40.0% and 65.2% among subjects. These results are not above the chance level. However, as the results for some subjects lies within the range 60% to 72%, the performances of 2-class AF-based BCI exploiting SSSEP, this new alternative combination appears relevant for future further investigations.

Finally, it is known that in MI-based BCI the training of the user plays an important role and is often necessary to reach a reliable performance of the BCI [43]. We hypothesise that our system could also benefit from training the users. More precisely, the hypothesis of "selectiveness" might become sustainable after training as the MI-related brain activity becomes more conspicuous in the data.

#### 7.1.4 Study of User-related Aspects – Chapter 6

In this last contribution, we investigated different human-related aspects when interacting with our system. We developed two applications controlled by our system. Both applications aimed at controlling a moving object on a 2D surface in a 3D world. They differed in their interactions. The first one, a kart-control application named Kart, had inertia. Indeed, the kart moved as if powered by a series of impulsions, similar to a hand-propelled wheelchair. The second application was a puzzle-solving application named SokoBCI\*. In this application, the control was discrete and was rather punitive in case of mistakes. Indeed,

*\* during AF trial, the subject was asked to focus their whole attention on one vibration instead of the other, resulting in an SSSEP's amplitude increase.*

*\* it was inspired by the game Sokoban from Hiroyuki Imabayashi.*



the user had to provide a corrective command in case of mistakes, contrary to the kart where walls pushed it back on track if it drifted away from it. In this experiment, we were particularly interested in the perceived usability of the system, measured by the system usability scale [16, 17].

As we exposed the user to different levels of performance of our BCI using sham feedback, it allowed us to propose a linear model of the relationship between the BCI performance and the SUS scores. Building on this model and extrapolating from the work of Bangor *et al.* [7], we concluded that Kart and SokoBCI should operate at a mean performance level of 74.3% and 85.4%, respectively, to be “acceptable”. This is a not negligible 10-point difference! First and foremost, the commonly admitted 70% of accuracy over which a BCI is usable seems adequate as long as the application is not too “punitive”. At least for applications based on controlling a movable object on a 2D surface in a 3D world. Additionally, these results can provide guidelines for designing a BCI application depending on the desired objective, like making it more or less challenging...

Camille Jeunet observes in her work [43] that to improve one’s learning capacity, the training task should be adaptable and slowly increase in difficulty. The training should be done in a motivating learning environment. In addition, multi-modal, explanatory and supportive feedback can contribute to one’s learning capacity. With our work, we hope to have contributed to improving future BCI training programs. Indeed, video game-like applications can be expected to be more fun to train with and provide a motivating learning environment. Finally, applications proposed to users can be disclosed following an increasing “punitiveness” curve to ease training.

## 7.2 DISCUSSIONS: A LONG ROAD AHEAD OF US

In this thesis, we hope to have contributed to the joint improvement of MI and SSSEP-based BCI. However, like many scientific work, it has its limits. In this section, we discuss the limitations of our work.

A straightforward limitation of this work is the number of subjects. We benefit from a 4-sessions protocol and recruited only ten subjects to participate in the whole experiment. However, the number of participants remains relatively small. Therefore, we limit the various statistical analyses in our work to subject-level analysis. Our initial objective was to recruit 20 participants. We identified different factors contributing to this reduced number of subjects.

Some technical aspects of the work slowed down the study of SSSEP, in a more general context. Contrary to SSVEP, where programming a flickering stimulus using a screen is quite easy, the use of specifically designed hardware to produce a vibro-tactile stimulation takes a longer time to implement and a rare set of abilities. This difference might



explain the scarcity of studies involving SSSEP / SSSEP-based BCIs compared to SSVEP-based BCIs or MI-based BCIs.

Another factor is the recruitment of subjects. Indeed, participants have to voluntarily come to the hospital for four recording sessions, each lasting about two to three hours. The lack of financial gratification made recruiting harder. Shortening the screening time by merging sessions should be investigated for future work.

Lastly, our deeply experimental thesis was not spared by the different restrictions associated with the pandemic.

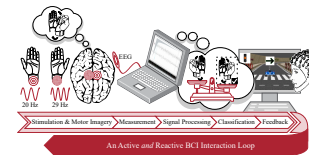
### 7.3 CONCLUSIONS

In this thesis, we designed and studied a combination of active and reactive BCI. We proposed a combination of SSSEP and MI. As described in the introduction, they should, in theory, interact well. Our work focuses on multiple aspects of the interaction loop of the BCI\*.

Indeed, our experimentation on signal processing allowed us to identify an algorithm to use when measuring the amplitude of an SSSEP on synthetic and real EEG data. In addition, we tested two hypotheses related to the combination of SSSEP and MI. Our results demonstrated that a gating effect could be successfully measured in a single session of kinaesthetic MI. In the ecological conditions of our system, *i. e.* without outlier removal, short-term classification output and real-time compatible implementation, the mutual influence of brain pattern in the combination seems unsuccessful for a 4-class implementation of the BCI. However, one knows the importance of training subjects in MI-based BCI [43]. In addition, our experiment also demonstrated statistically significant somatosensory gating effects on the SSSEPs' amplitude by kinaesthetic MI in a single session. These results on untrained users are highly encouraging for future research on 2-class SSSEP and MI-based BCI.

In this dissertation, we hope to have demonstrated the advantages of a combination between SSSEP and MI. However, to reach a reliable and efficient BCI, there is still a long road ahead of us. With our work, we have contributed by shedding light on a few interrogations and providing some answers. We hope to have shown that SSSEP is a very interesting evoked potential to work with and would greatly benefit from more attention from the community.

To this day, SSSEP is indeed scarcely studied. In the literature review, we found only a couple dozen papers\* investigating SSSEP-based BCI. None of them reported work involving motor-disabled patients. Patients with amyotrophic lateral sclerosis or spinal muscular atrophy retain a functional somatosensory system [31, 36]. Thus, they may benefit from a SSSEP-based BCI system. Indeed, involving the somatosensory system does not obstruct the field of view, which is a plus in the context of displacement in general, as in wheelchair-controlled by BCI, for



\* Figure 1.1

\* combining journals, conferences and workshops

example. Also, the cortical area of interest is located at the top of the head, an area largely available for placing electrodes on patients who use wheelchairs whose heads rest on the head cushion. Thus, the electrodes would not be pressed on the cushion, which reduces the amount of noise in the EEG.

#### 7.4 PERSPECTIVES

This section presents different aspects I wish to dive into in the short future. In addition, I present some ongoing projects as they also represent short-term perspectives. I finish this dissertation with a few last words about future work I wish to pursue and its motivation.

##### 7.4.1 *Short-term perspectives: In this PhD we also...*

*... aim to contribute to Open Science*

We intend to publish the source code and the data supporting all our findings. We worked in collaboration with our laboratory data protection representative since the early stages of this thesis. It results in thorough compliance of our work with the European General Data Protection Regulation (GDPR).

It impacted several of our experimental protocols: the one submitted to the university ethical comity, the one for the control group, and the one to the *comité de protection des personnes*, for a group of patients with a spinal muscular atrophy\*. Therefore, the questions of consent form and anonymisation have been settled.

\* not included on the manuscript as it is currently pending.

In the consent form, we explicitly mentioned that the document matching the subject's name to their subject ID would be deleted three months after their last sessions. After this period, the data will switch from pseudo-anonymised to anonymised and become shareable on public databases.

*... measure the attention focusing effect on SSSEPs' amplitude*

Our experimental protocol initially had four sessions. Session number two of our protocol was dedicated to measuring the impact of attention focusing on the SSSEPs' amplitude. This session, combined with the data collected during session three, the somatosensory gating, should allow us to compare the performances between these paradigms.

In future work, I wish to analyse the data recorded during this session and compare results to the state-of-the-art. We might be able to answer questions such as: what is the proportion of subjects who presents measurable attention focusing effect but not a gating effect? Would that be a suitable alternative for people who do not produce a significant gating effect?

*... investigate different hardware*

During this PhD, in agreement with my directors, I reached out to professor Andrea Kübler to perform a three-month research stay at the Institute of Psychology at the University of Würzburg. Our project was to investigate the measurement of SSSEP using standard hardware and new around-the-ear hardware. The latter, named cEEGrid, is a relatively affordable EEG system that provides disposable flexible patches to stick around the ears. The patches contain ten EEG electrodes each and are connected to a small amplifier attached to the collar of the subject's garment.

We proposed a 2-sessions protocol. The first one aims at screening subjects to identify one FOS with the maximum RAI across wrists. In this session, we want to assess the possibility of using around-the-ear EEG to measure SSSEPs. The second session assesses the capacity of the BCI to discriminate between an idle state and an attention focusing on the vibration state. In other words, we will assess the capacity of such BCI to be used as a brain switch. Additionally, we hypothesised that the increase of activity resulting from the attention focusing could help enable or facilitate the measurement of SSSEP using the cEEGrid.

As I am writing these lines, recordings are still ongoing, and I wish to provide soon some answers to the different hypotheses tested with a large group of subjects.

#### 7.4.2 *Mid and Long-Term Perspectives*

*Recruitments methodology improvement*

When combining my experiment from internships and this PhD, I had the opportunity to collaborate and conduct experiments involving BCIs within four laboratories. Two laboratories were in France, INRIA Rennes and the CRISAL in Lille. The other two were in Germany. It was the Max Planck Institute of Tübingen and the Institute of Psychology in Würzburg. I have observed differences in the methodological approaches I wish to integrate into my future research.

For me, the most striking difference was the recruitment of participants. In Germany, students can participate in experiments to earn ECTS credits or financial gratifications. In some cases, it is even mandatory for the students to receive a few credits by participating in experimental studies as part of their *curriculum*. To accommodate this recruitment, laboratories often have a public website or database to publish an announcement about the recruitment for a new study. Participants (not only students) are also paid for their time in many experiments. Both of these facts facilitated my recruitment and enabled me to obtain participants from a more comprehensive demographic range, particularly regarding age.

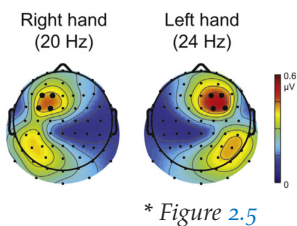
In France, I recruited mainly by canvassing colleagues and friends. It resulted in a pool of participants consisting mainly of students in a narrow age range. The existence of a website and database to recruit in the German universities where I worked did not prevent me from asking friends and colleagues to participate, of course, but it mitigated this drawback.

I believe having a demographic of participants with a large variety of profiles, especially in terms of age, is relevant when investigating the performance and human-related aspects of a communication and control system such as BCIs. I wish to contribute to creating a local or national volunteer database for experiments in France.

### *Spatial Filter Analysis Extension*

In our contribution 2., we studied multiple signal processing methods related to estimating sinusoidal oscillation amplitude in spatially dependent multiple sinusoidal oscillations and spatially independent Gaussian noise. Resulting from these works, we use a CSD and selective electrode based on *a priori* neurophysiology knowledge in chapter 4 and 5. Indeed, we used the mapping between electrode position and cortex location from Hamon *et al.* [40] and the known somatotopic arrangement.

Bipolar montages were not included in this first comparison. In the literature, the bipolar montage, usually between electrodes anterior and posterior to C3 and C4, is also noticeable as a spatial filter. Under the electro-to-cortex mapping and somatotopic arrangement, its efficiency is somehow challenging to predict. On the other hand, when observing the SSSEPs topography provided in figure 2.5 from [71]\*, one can observe that their grand averaged SSSEPs are well located around the FC line of electrodes and contralateral to the stimulated side. However, these results are somewhat limited and not confirmed in other literature. Nevertheless, a bipolar montage between an electrode within the source of activity (FC3) and without (CP3) might be efficient in such topography as the signal contribution lies within one electrode and therefore is resilient to subtraction. In addition, if the two electrodes have a substantial covariance, explained by spatially dependent noise sources, the difference can decrease the variance on the bipolar electrode\*.



\* Figure 2.5

\* see chapter 2, section 2.4.2, for more information about the principle of “blocking” in statistics.

### *Explore Different Neuromarkers*

In this thesis, we focused on the SSSEPs amplitude as the principal source of information and investigated related hypotheses. However, we knew from the work of Pfursheller *et al.* that an ERD occurs during MI, followed by an ERS shortly after [82]. The combination between MI and SSSEP may also benefit from the ERD/ERS neurophysiological marker from MI.

Therefore, I wish to extend the feature space to other frequency bands and spatial features, doing so might increase the reliability of the combination.

#### *Task Design Improvement for Somatosensory Gating*

Nowadays, the classification in BCI happens within a couple of seconds after the beginning task, especially in reactive BCIs [18]. In our somatosensory gating session, we use longer durations of MI as we are especially interested in the gating effect. However, in the prospect of implementing an efficient BCI, it could be interesting to assess the performance of the same BCI using swift motion. Indeed, we know from Voisin *et al.* [107] that the speed of the imagined movement is positively correlated to the gating effect.

Thus, a future experiment involving an SSSEP-based BCI exploiting gating by MI could be to ask our subject to imagine performing an especially fast motion, such as punching through the computer screen. The speed of the movement should increase the gating effect [107]. Additionally, as the cue occurs, this instruction would be performed only once per trial instead of repeating the imagined motion during the stimulation duration as it was done in our protocol.

Finally, we can also hypothesise that imagining an intense sensation, such as the pain of one's fist punching a screen, may increase the gating effect. It also could shorten the stimulation duration and increase the number of repetitions per subject. Hence, increasing the statistical power of our analysis and might even benefit from a stronger gating effect.

#### 7.4.3 *Last Words*

Recently, a friend of a patient with ALS came to us, looking for a gaze-free BCI. Indeed, he is suffering from severe motor impairment, and to this day, he is capable of contracting one remaining muscle on the inside of the thigh. The communication device available for him is a detector tapped to his thigh that rings a bell when he contracts his muscle. With this simple device, this person can still communicate with his mother, who helps him on a daily basis. Complex communication is possible between them. Indeed, her mother spells out some letters, and he rings the bell to select a letter to compose a message.

Our work was only preliminary in a very exploratory field, and without ongoing clinical trials, we cannot do much for potential users like him. We redirected him to a specialised clinician and new technology platform\*. Unfortunately for this person, a vast majority of assistive technology on the market relies on sight. To this day, there is not a single gaze-free BCI working as a brain switch to allow this person to ring a bell when needed.

\* these are technological platforms that can offer technical solutions designed explicitly for one's disability with the help of occupational therapists.

In this PhD and this dissertation, we wish to have demonstrated the potential benefit of our proposed BCI for patients like him. Especially in future works, I wish to investigate brain switches in general, and more precisely, I wish to explore the potential performances of our combination as a brain switch.

## APPENDIX





# INDIVIDUAL SCREENING PROCEDURE RESULTS VISUALISATIONS

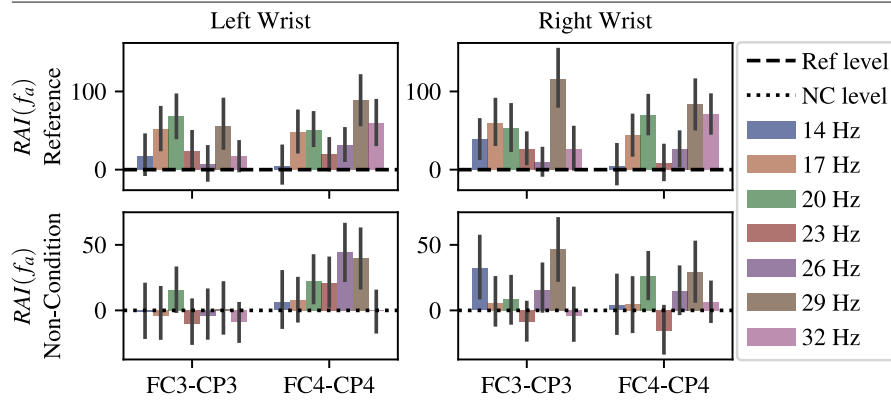


Figure A.1 : Results for subject # 1.

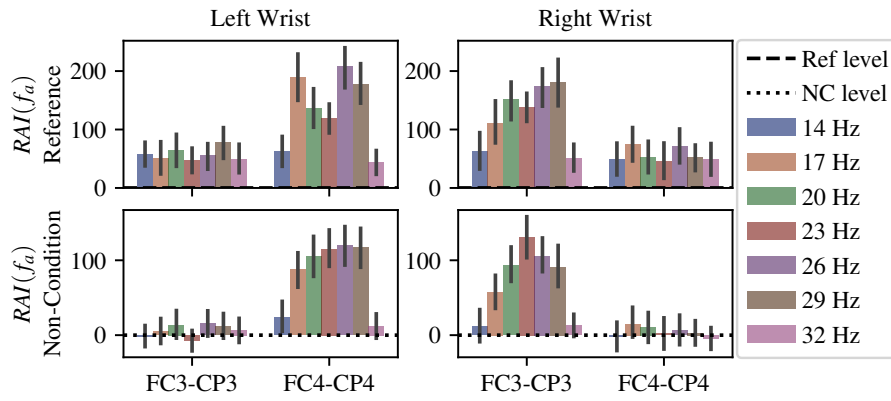


Figure A.2 : Results for subject # 2.

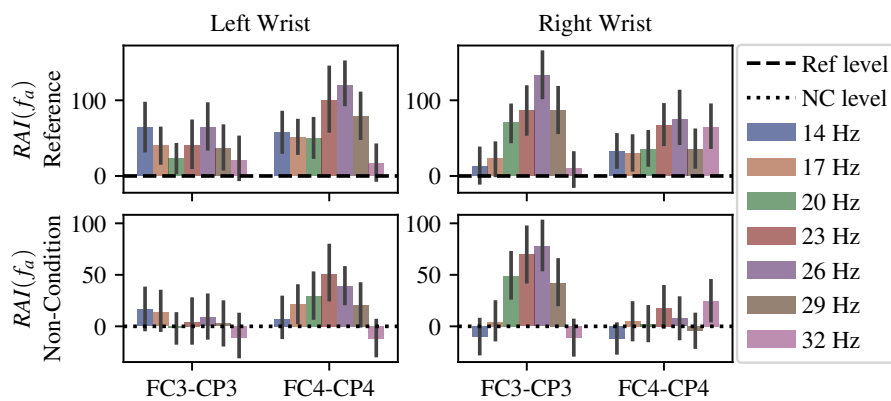


Figure A.3 : Results for subject # 3.

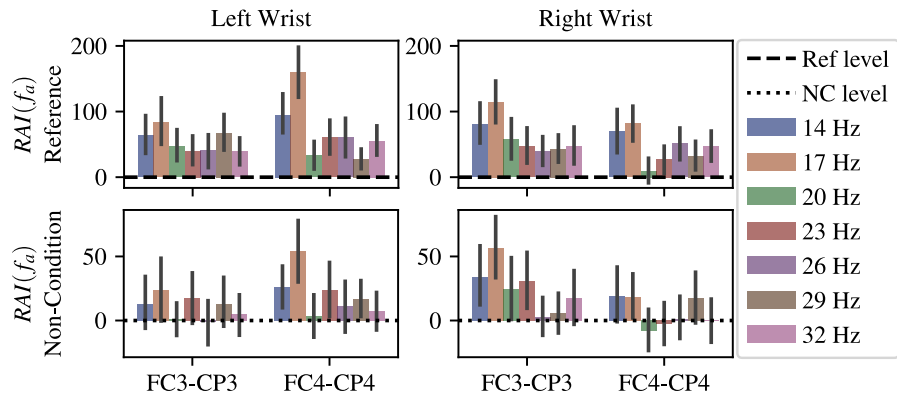


Figure A.4 : Results for subject # 4.

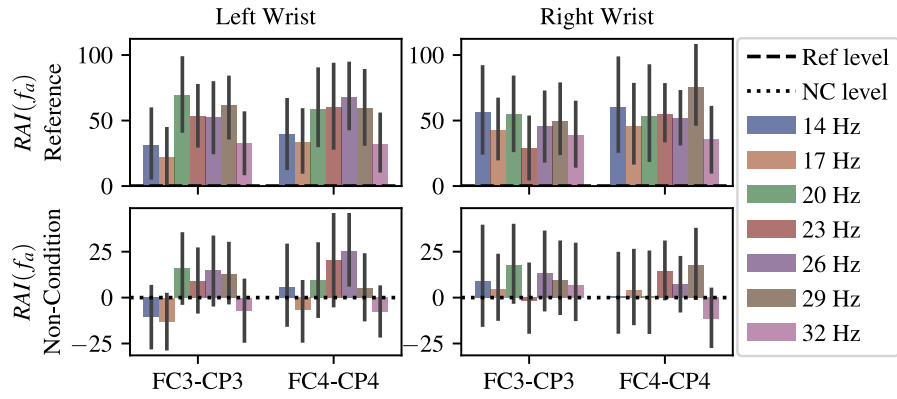


Figure A.5 : Results for subject # 5.

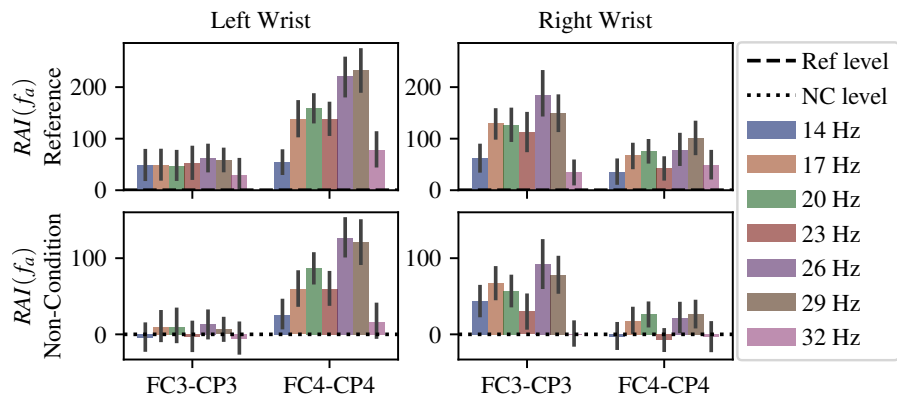


Figure A.6 : Results for subject # 6.

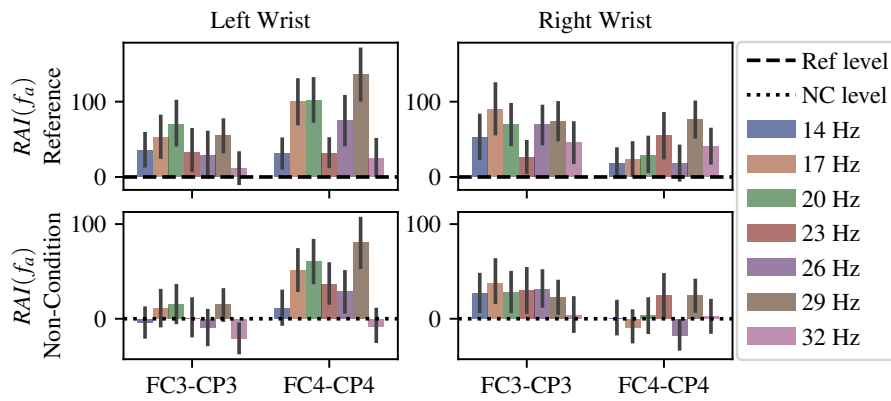


Figure A.7 : Results for subject # 7.

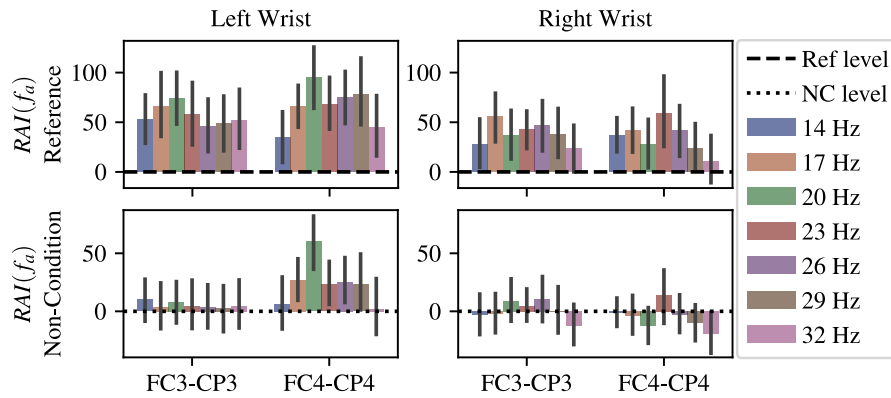


Figure A.8 : Results for subject # 8.

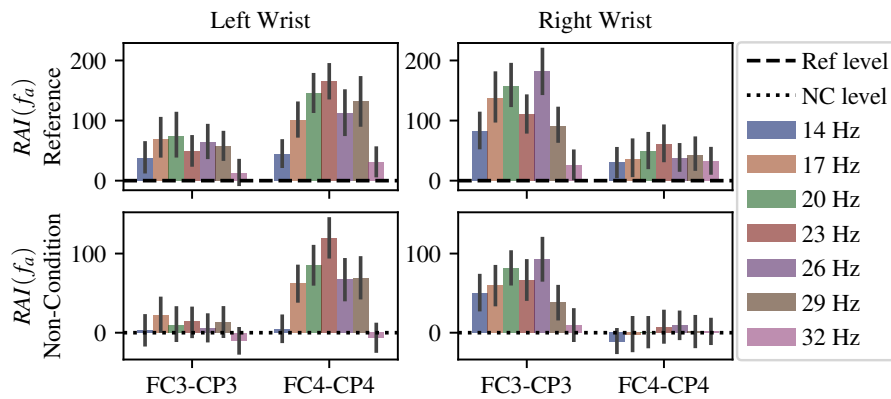


Figure A.9 : Results for subject # 9.

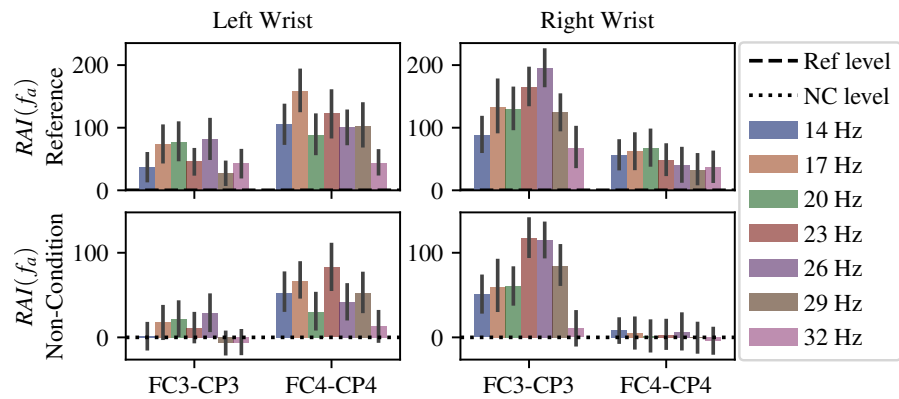


Figure A.10 : Results for subject # 10.

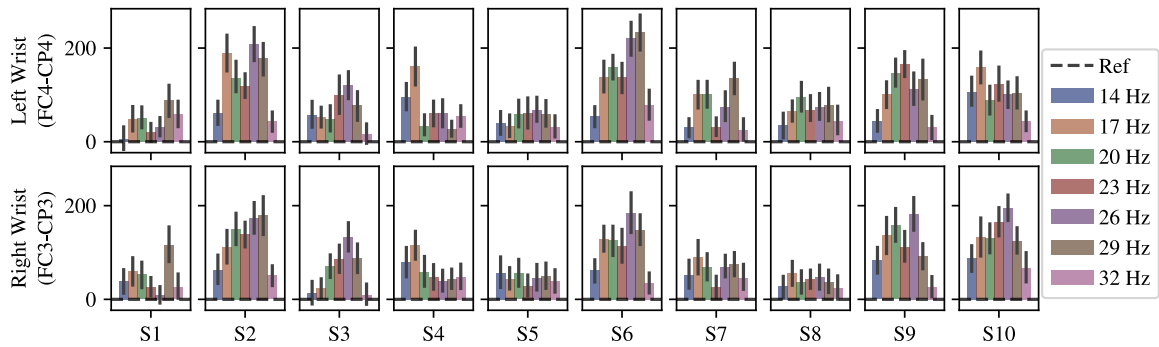


Figure A.11 : Results from all subjects for easier comparison. Reference to **Reference period**. It displays only the electrodes contralateral to the stimulation side.

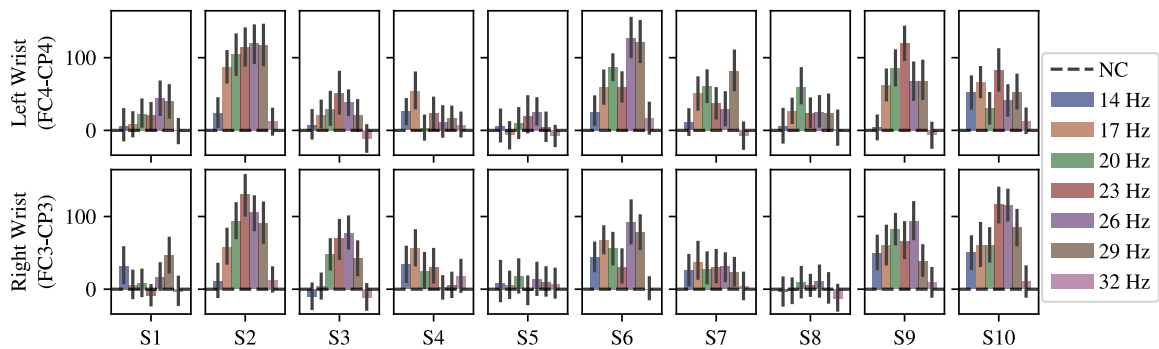


Figure A.12 : Results from all subjects for easier comparison. Reference to **Non-Condition period**. It displays only the electrodes contralateral to the stimulation side.

INDIVIDUAL SOMATOSENSORY GATING RESULTS  
VISUALISATIONS

B

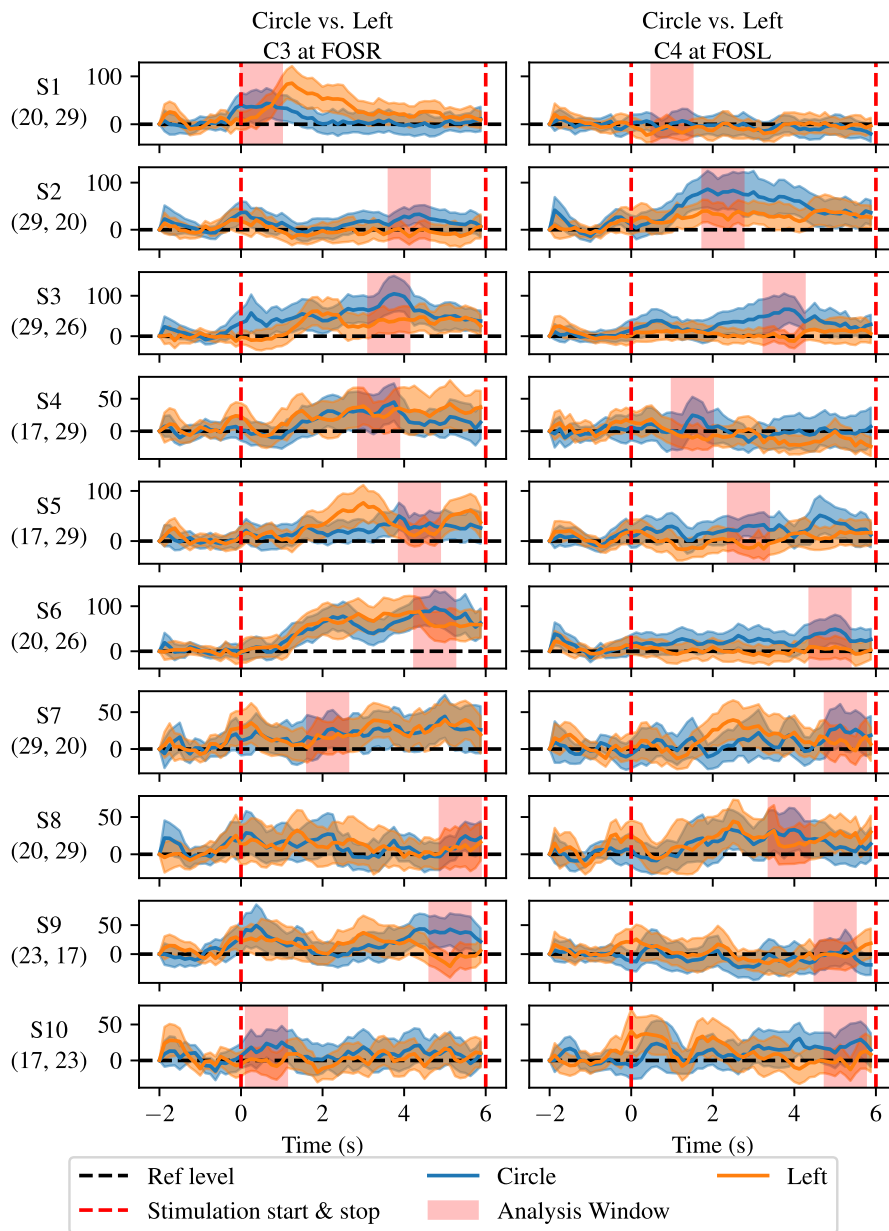


Figure B.1 : Comparison of the average relative band power increase (%) of Circle condition against Left condition. Identical y-scale between conditions for each subject. FOS are reminded in parenthesis (FOS on left wrist, FOS on right wrist). The analysis window is centred around the maximum difference between the start and end of stimulation.

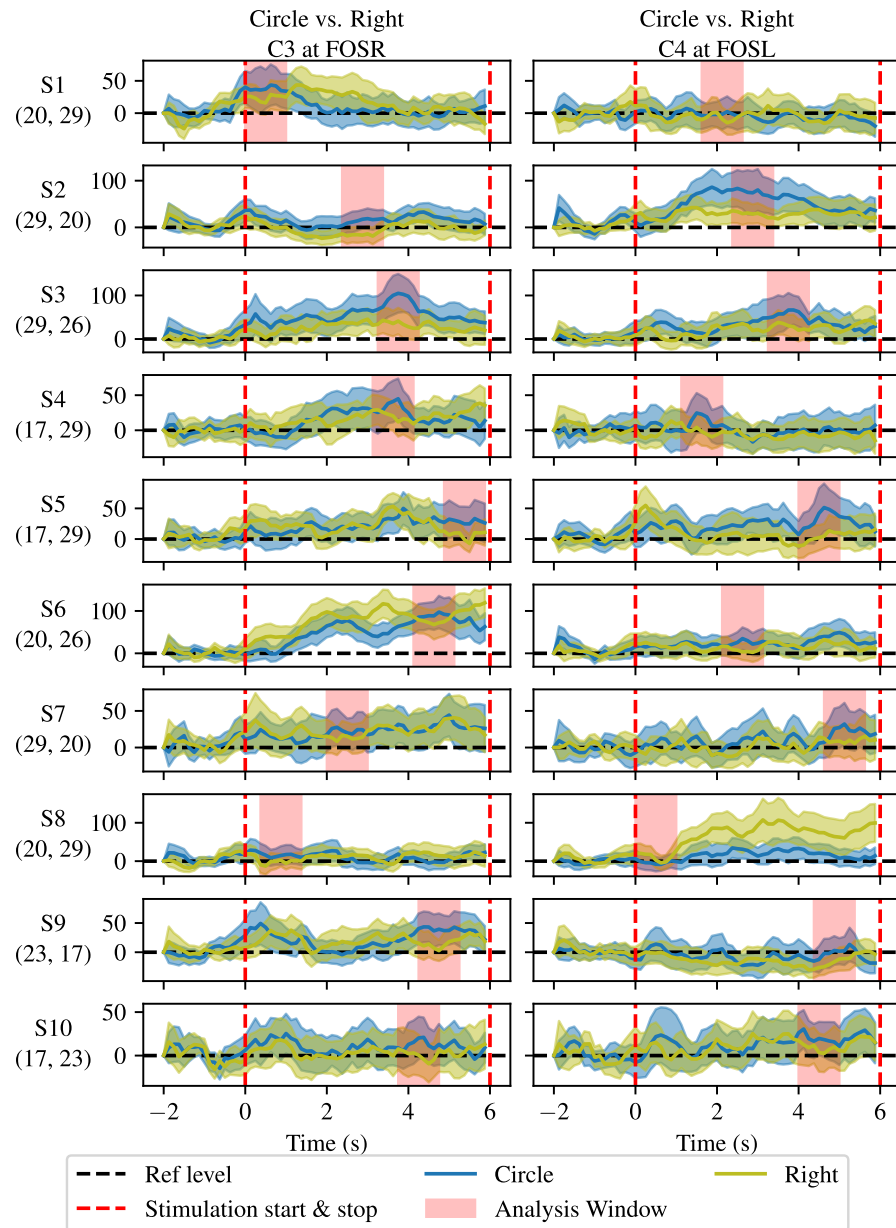


Figure B.2 : Comparison of the average relative band power increase (%) of Circle condition against Right condition. Identical y-scale between conditions for each subject. FOS are reminded in parenthesis (FOS on left wrist, FOS on right wrist). The analysis window is centred around the maximum difference between the start and end of stimulation.



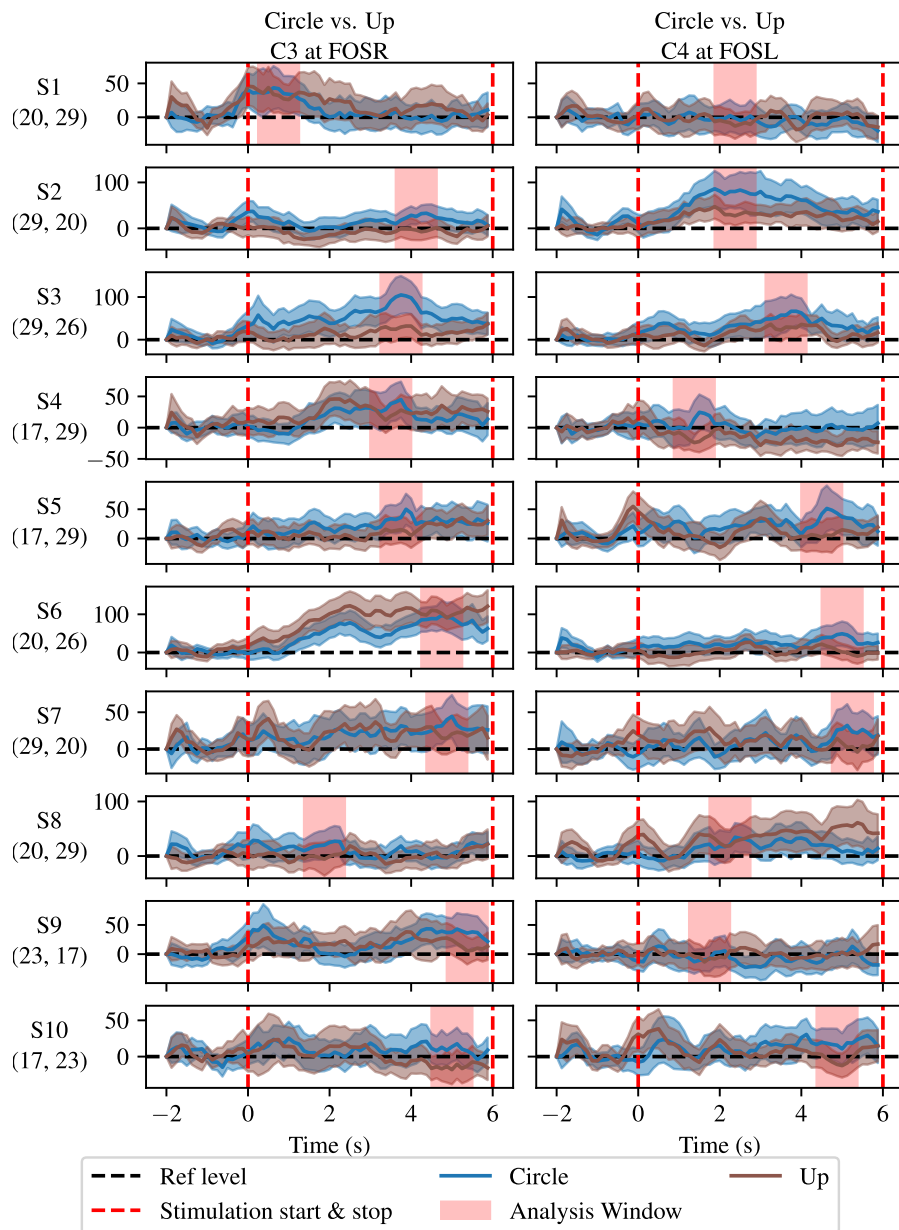


Figure B.3 : Comparison of the average relative band power increase (%) of Circle condition against Up condition. Identical y-scale between conditions for each subject. FOS are reminded in parenthesis (FOS on left wrist, FOS on right wrist). The analysis window is centred around the maximum difference between the start and end of stimulation.



---

In the next page we reproduce one poster presented during the CORTICO 2022 meeting (see below). The original work was done in A0 format, for printing purpose we integrate it in A4 format.

Reference:

Jimmy Petit, José Rouillard, and François Cabestaing. *Somatosensory Gating for an SSSEP-based BCI*. CORTICO 2022 : Invasive and non invasive Brain-Computer Interfaces - A handshake over the cliff. Poster. Mar. 2022. URL: <https://hal.archives-ouvertes.fr/hal-03651273>

# Somatosensory Gating for an SSSEP-based BCI

Jimmy Petit<sup>1</sup>, José Rouillard<sup>1</sup> & François Cabestaing<sup>1</sup>

1. Univ. Lille, CNRS, Centrale Lille, UMR 9189 CRISTAL, F-59000 Lille, France

## I What are SSSEP?

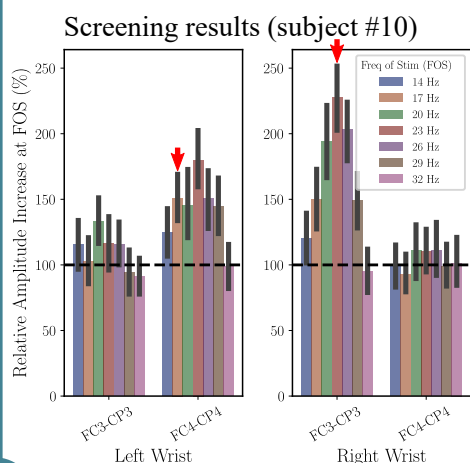
A sustained vibrotactile stimulus of the skin produces resonance-like evoked potentials named Steady-State Somatosensory-Evoked Potentials or SSSEP. They appear as an increase of activity at the frequency of stimulation.

## II What is Sensory Gating?<sup>1</sup>

Sensory gating, or gating, is the capacity of the brain to filter out stimuli perceived as irrelevant during a goal-oriented activity.

## IV Mandatory step: Screening procedure<sup>2,3</sup>

- Objective: Identify the stimulation frequency with the highest SSSEP.
- How: Train of stimulations of 2 s, at different frequencies: from 14 to 32 Hz.
- Amplitude estimation: fast Fourier Transform.



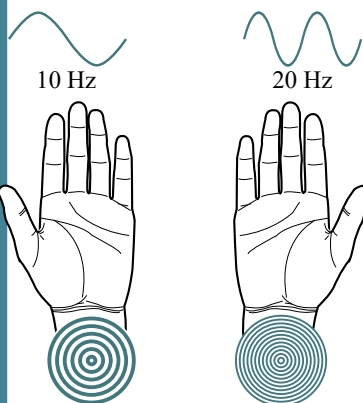
## III Idea of an SSSEP-based BCI exploiting Somatosensory Gating

- Performing Motor Imagery (MI) with one or two arms.
- Sustained vibrotactile stimuli on both wrists produces two SSSEP.
- The Gating resulting from the MI should decrease the amplitude of the respective SSSEP.
- The amplitude of the two SSSEP are used as classification features.

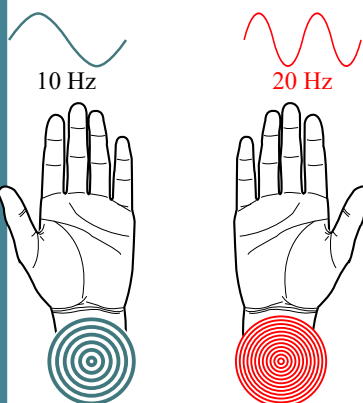
### Illustration of a command selection in this context

Initial State: IDLE

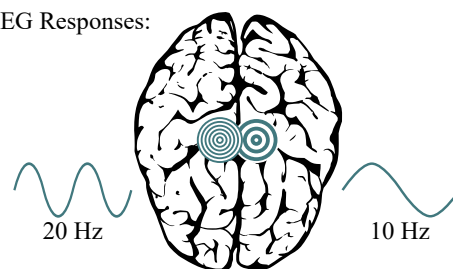
Mechanical stimulation frequencies



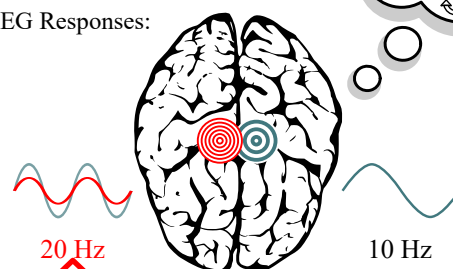
Motor Imagery with the right arm:  
Identical mechanical stimulation



EEG Responses:



EEG Responses:



SSSEP's amplitude decrease, caused by Sensory Gating

## V An experiment to test the Somatosensory Gating for an SSSEP-based BCI

### Setup:

- Subject is sitting in front of a computer.
- Frequency of Stimulation (FOS) identified during a screening session.
- C-2 Tactors tapped to both wrists<sup>4</sup>.
- EEG amplifier & Laptop: powered by batteries.

### Experimental Conditions:

- Stay IDLE.
- Performing Motor Imagery (MI) with one arm.

### Signal Processing:

#### Preprocessing:

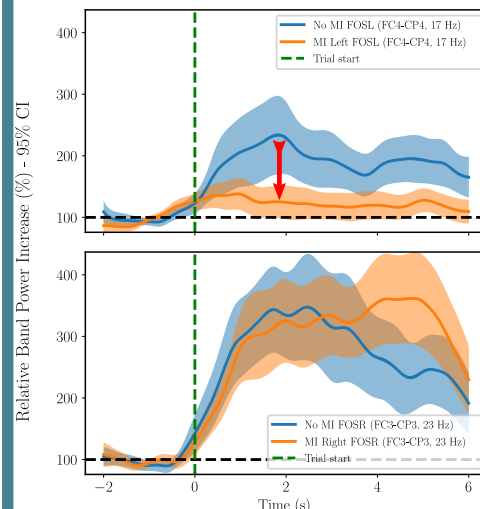
- Non-causal highpass filter at 5 Hz.
- Peak-to-peak signal amplitude for eye blinks detection. Trial removed, if significant.
- Subject #10:  $\approx$  15% of data rejection.

#### Amplitude estimation:

- Narrow non-causal bandpass filter.
- Signal squared.
- Smoothen by a moving average (window length = 30 x FOS periods).

## VI

### Observed effect (subject #10)



[1] J. I. A. Voisin, C. Mercier, P. L. Jackson, C. L. Richards, and F. Malouin. Is somatosensory excitability more affected by the perspective or modality content of motor imagery? *Neuroscience Letters* (2011)

[2] C. Breitwieser, V. Kaiser, C. Neuper, and G. R. Müller-Putz. Stability and distribution of steady-state somatosensory evoked potentials elicited by vibro-tactile stimulation. *Medical & Biological Engineering & Computing* (2012)

[3] J. Petit, J. Rouillard, and F. Cabestaing. EEG-based Brain-Computer Interfaces exploiting Steady-State Somatosensory-Evoked Potentials: A Literature Review. *Journal of Neural Engineering* (2021)

[4] C. Pokorny, A. Breitwieser, and G. R. Müller-Putz. A Tactile Stimulation Device for EEG Measurements in Clinical Use. *IEEE Transactions on Biomedical Circuits and Systems* (2014)

Une interface cerveau-ordinateur (ICO) est un système visant à différencier différents états mentaux d'un utilisateur pour les traduire en commandes transmises à un dispositif externe. Une catégorie d'ICO, appelée ICO réactive, utilise les réponses automatiques du cerveau provenant d'une stimulation sensorielle de l'utilisateur pour différencier plusieurs états mentaux. Un potentiel évoqué est la manifestation sous la forme d'une variation du potentiel électrique de la réponse du cerveau. Notre travail se concentre sur les potentiels évoqués apparaissant dans le cortex somatosensoriel, aussi appelé cortex somesthésique. Il s'agit d'un composant du système somatosensoriel, c'est-à-dire le réseau de structures neuronales qui permet la perception des sensations liées à la peau et à la proprioception. Une action mécanique appliquée sur la peau évoque une réponse cérébrale spécifique dans le cortex somesthésique primaire controlatéral à la stimulation. L'électroencéphalographie (EEG) de surface permet de mesurer cette réponse en produisant ce que l'on appelle un potentiel évoqué somesthésique (PES). Lorsque l'action mécanique est périodique et maintenue, comme c'est le cas lors d'une vibration, le PES est également périodique avec la même fréquence, il est alors appelé PES stationnaire (PESS).

Des activités mentales spécifiques, telles que la focalisation attentionnelle, modulent l'amplitude et/ou la phase du PESS. Cette modulation volontaire constitue un marqueur significatif de l'activité mentale communément utilisé dans les ICOs exploitant des PESSs. Dans cette thèse, nous étudions un nouveau marqueur basé sur le filtrage somesthésique du cortex. Le filtrage somesthésique est la capacité du cortex à filtrer les stimuli non pertinents ou répétitifs reçus par le système somatosensoriel, dans notre cas, issus des récepteurs mécaniques de la peau. Le filtrage somesthésique est une forme spécifique du filtrage sensoriel qui est plus général. Ce phénomène de filtrage sensoriel existe aussi avec la vue ou l'ouïe, mais dans ces travaux, nous nous concentrons sur le filtrage somesthésique. Ce dernier a été observé dans la littérature, par exemple, une diminution de l'amplitude d'un PESS provoquée électriquement pendant une tâche d'imagerie motrice (IM).

L'architecture des ICOs est souvent décrite comme une boucle. Dans un premier temps, l'utilisateur effectue une tâche mentale censée générer une activité cérébrale spécifique. Son activité cérébrale est alors mesurée continuellement par un instrument de mesure. Suit une étape de traitement du signal pour extraire les caractéristiques clés de l'activité cérébrale spécifique susmentionnée. Un classificateur identifie l'état mental généré parmi plusieurs modèles d'états mentaux étiquetés. Un retour d'information est enfin fourni à l'utilisateur sur la base des résultats de la classification. Ce dernier permet à l'utilisateur de réagir en conséquence, et la boucle d'interaction recommence. Dans cette thèse, nous étudions chaque étape de cette boucle pour une ICO combinant PESS et IM, ainsi que les caractéristiques des PESSs et les contraintes

méthodologiques résultant de leur utilisation. Nous étudions les aspects théoriques du PESS sur des données synthétiques afin d'identifier le traitement du signal adéquat pour notre application. Nous évaluons les aspects humains liés à l'interaction avec notre système. Nous nous concentrons également sur la relation entre la performance de l'ICO et l'utilisabilité ressentie du système ou la charge mentale de l'utilisateur.

Enfin, nous souhaitons que notre système soit utilisable par des individus affectés par une déficience motrice lourde, comme les personnes en situation d'enfermement disposant toujours du sens du toucher. L'approche somatosensorielle a été choisie car elle exploite le sens du toucher de l'utilisateur. En outre, contrairement à la focalisation attentionnelle, l'imagerie motrice peut facilement être réalisée avec plusieurs membres à la fois. Cette propriété de l'imagerie motrice nous a conduits à choisir une combinaison liant PESS et IM car elle pourrait augmenter le nombre de commandes disponibles pour notre système ICO.

#### VUE D'ENSEMBLE CHAPITRE PAR CHAPITRE

Nous avons rédigé un manuscrit de type thèse-article. En première page de chaque chapitre, la mention "*Related Work*" suivie d'un élément de bibliographie marque le fait que ce chapitre est un article soumis pour expertise avant publication ou déjà publié au cours de cette thèse. Nous insérons l'article le plus fidèlement possible à l'œuvre originale, qu'elle soit publiée ou en cours de révision. Afin d'uniformiser notre manuscrit, nous avons remis en page les articles et éventuellement apporté des modifications mineures : corrections de fautes de frappe, gestion de la taille des figures, insertion des références des figures dans le texte en utilisant le mot "*figure*" au lieu de la préférence de la revue ou du modèle de conférence, et harmonisation des polices de caractères à l'intérieur des figures.

Ci-après, nous présentons un résumé chapitre par chapitre du manuscrit.

#### *Chapitre 1 – Introduction générale*

Dans ce premier chapitre, nous présentons rapidement la définition des ICOs et les différentes catégories existantes. Nous nous attardons également sur les défis actuels des ICOs. Enfin, nous présentons l'objectif de cette thèse et nous mentionnons les contributions scientifiques qui résultent de nos travaux.

#### *Chapitre 2 – ICO à base d'EEG exploitant le PESS : une revue de la littérature*

Nous passons en revue la littérature sur les PESSs et leur utilisation dans les ICOs utilisant l'EEG. Cette revue nous permet de décrire les

principales caractéristiques des PESS. De plus, l'analyse des protocoles de calibration standards permettant de définir la fréquence de stimulation qui maximise l'amplitude des PESSs nous permet d'identifier et d'intégrer cette procédure à notre protocole. Ensuite, nous présentons les algorithmes standards en traitement du signal et en classification des données, ainsi que les performances de classification obtenues. En outre, l'amplitude des PESS à une fréquence de stimulation spécifique dépend fortement de l'individu, et aucune tendance des les distributions ne semble émerger. Par conséquent, nous insistons sur le fait qu'une procédure de calibration doit être effectuée pour obtenir une stimulation qui maximise l'amplitude des PESSs.

La littérature montre également que la plupart des ICO exploitant les PESSs le font en utilisant des signaux caractéristiques fondés sur des informations spatiales ou de large bande de fréquence. Ainsi, l'utilisation de la variation d'amplitude des PESSs dans la littérature est très sommaire. En conclusion, la revue de la littérature ne nous permet pas d'identifier l'algorithme le plus efficace pour mesurer les variations d'amplitude d'un PESS.

### *Chapitre 3 – Estimation de l'amplitude des composantes sinusoïdales dans les ICOs basés sur l'EEG et exploitant les PESSs*

Dans ce chapitre, nous complétons les résultats de la revue de la littérature en comparant plusieurs méthodes de traitement du signal pour estimer l'amplitude d'une oscillation sinusoïdale ciblée, *i. e.* les PESSs; Nous introduisons tout d'abord un modèle de formation d'EEG de surface adapté au cas spécifique d'une ICO exploitant les PESSs. Notre modèle considère un mélange de sources sinusoïdales d'intérêt et suppose une conduction volumique constante de la tête.

Nous mesurons ensuite, sur les EEG synthétiques, la précision de l'estimation de l'amplitude des PESSs par des algorithmes de traitement du signal couramment utilisés dans les ICOs. Nous étendons notre comparaison aux données EEG recueillies lors de nos expériences. Nos résultats montrent que le filtre spatial *current source density* combiné à une technique simple de démodulateur synchrone est la méthode la plus efficace par rapport à un filtre laplacien de faible étendue ou à des méthodes auto-adaptatives telles que l'analyse de corrélation canonique. Cette dernière est désormais le standard des ICOs utilisant les potentiels évoqués visuels stationnaires ou PEVSs\*. Nous comparons notamment les contraintes méthodologiques résultant de l'utilisation de PEVS ou de PESS.

\* comme un PESS, un PEVS est une augmentation de l'oscillation de l'activité cérébrale due à l'observation de stimulus clignotants. L'amplitude de l'oscillation augmente à la fréquence du stimulus sur le lobe occipital.



*Chapitre 4 – Imagerie motrice kinesthésique pour la modulation sélective de l’amplitude du PESS par filtrage somesthésique*

Nous décrivons en détail le protocole mis en place pour la procédure de calibration et la session de mesure de la taille d’effet du filtrage somesthésique. Plus précisément, nous mesurons l’effet du filtrage somesthésique dans une situation d’IM avec un ou deux bras lorsque le sujet reçoit des stimulations vibro-tactiles multiples. En accord avec les défis sous-jacents aux ICOs, concernant la contamination des données, nous proposons un protocole pour réduire le bruit dans les données. Nous testons notre hypothèse principale de “sélectivité” de la modulation d’un PESS en fonction du contenu de l’IM. En d’autres termes, l’IM effectuée avec le bras droit a-t-elle un impact uniquement sur le PESS résultant du même bras ? Cette hypothèse semble nécessaire pour mettre en place avec succès une ICO permettant d’obtenir plus de commandes qu’elle n’utilise de stimulations. De plus, dans cette première approche, nous souhaitons nous appuyer sur un algorithme simple qui utilise exclusivement les informations issues des variations d’amplitude des PESSs.

*Chapitre 5 – Filtrage somesthésique : Une tentative de classification en ligne et hors ligne*

Ce court chapitre présente une classification à 4 classes fondée uniquement sur l’effet généré par le filtrage somesthésique des données recueillies avec le protocole présenté au chapitre 4. En d’autres termes, nous cherchons à classer les états d’IM en utilisant uniquement la variation d’amplitude du PESS. Nous utilisons la méthode de traitement du signal identifiée dans les résultats du chapitre 3. Nous essayons également de réaliser une classification à 2 classes visant à différencier l’intention de mouvement, c’est-à-dire à reconnaître l’état de repos et un de nos états d’IM. Enfin, plusieurs pistes de recherche pour améliorer les performances de la classification sont discutées.

*Chapitre 6 – Conception et étude de deux applications contrôlées par une ICO exploitant le PESS*

Nous proposons et étudions deux applications contrôlées par ICO qui diffèrent sur deux aspects fondamentaux. La première est plus punitive en cas d’erreur, et la seconde implique l’inertie. Nous mesurons l’influence de ces facteurs à l’aide d’un protocole utilisant des retours d’informations fictives, ce qui signifie que la performance de classification est fixée à des valeurs spécifiques. Nous introduisons un modèle de la relation entre la performance de classification et l’utilisabilité perçue du système. Par ailleurs, les travaux de Bangor *et al.* [7] fournissent un modèle de la relation entre l’utilisabilité perçue d’un système et

son acceptabilité. Notre modèle nous permet, en extrapolant à partir des travaux de Bangor *et al.*, de prédire la performance de classification nécessaire pour atteindre un système “acceptable” pour chaque application.

#### *Chapitre 7 – Discussions, Conclusions & Perspectives*

Enfin, nous rappelons les contributions de cette thèse. Nous discutons également de leur limites et des améliorations possibles de notre travail.

D’un point de vue plus personnel, j’aborde les aspects que je souhaite approfondir. Je présente également certains aspects de notre travail réalisés pendant le doctorat mais qui ne sont pas inclus dans cette dissertation pour des raisons de cohérence du manuscrit. Ceci m’amène à discuter des perspectives à l’issue de cette thèse sur lesquelles je souhaite travailler davantage.



DISCLAIMER

Le protocole expérimental présenté en annexe a été envoyé au comité d'éthique de l'Université de Lille et validé le 24/09/2020 (numéro : 2020-417-S81). Quelques changements marginaux dans la conception des sessions ont été effectués. Pour des informations précises sur les détails de l'expérience, comme la durée de la période de référence lors de la session de calibration par exemple, veuillez vous référer au cœur de ce manuscrit.

DISCLAIMER – ENGLISH

*The experimental protocol given in this appendix was sent to the ethical comity of the University of Lille and validated the 24/09/2020 (record number: 2020-417-S81). Some marginal changes in the design of the sessions were made. For precise information about the details of the experiment, such as the baseline duration of the calibration session for example, please refer to the core of this manuscript.*

**Titre :** Étude et Développement d'une Interface Cerveau-Ordinateur exploitant des Potentiels Évoqués Somesthésiques.

**Acronyme de l'étude :** EDICOPES

**Organisme responsable de la recherche (Promoteur) :**  
Université de Lille

**Porteur du projet recherche :**

- Titre : Professeur
- Nom : Cabestaing
- Prénom : François
- Tel : 03 20 43 42 88
- Portable : Aucun
- Domaine scientifique : Science Pour l'Ingénieur (SPI)
- Sous-domaine scientifique : Automatique, Génie Informatique, Traitement du Signal et des Images (AGITSI)
- Domaine disciplinaire : 61 section CNU
- Numéro de l'Unité de recherche : UMR 9189
- Laboratoire : Centre de Recherche en Informatique, Signal et Automatique de Lille (CRISAL)
- Équipe : Brain-Computer Interface (BCI)

**Financier cas échéant (Organisme demandeur) :** Université de Lille

**Responsables scientifiques :** François Cabestaing

**Coordinateur de la recherche :**

- François Cabestaing (Professeur, équipe BCI, CRISAL)
- José Rouillard (Maître de conférence - HDR, équipe BCI, CRISAL)
- Jimmy Petit (Doctorant, équipe BCI, CRISAL)
- Camille Bordeau (Stagiaire, équipe BCI, CRISAL)
- Madli Bayot (Doctorante, Service de neurophysiologie clinique, CHRU Lille)

Version n°2 du 14/09/2020

**Clause de confidentialité :**

Les informations contenues dans ce document sont la propriété du promoteur. Les informations contenues dans ce document ne doivent pas être communiquées à des tiers sans l'autorisation écrite préalable du promoteur.

APPROBATION ET SIGNATAIRES DU PROTOCOLE

**Titre du protocole :** Étude et Développement d’une Interface Cerveau-Ordinateur exploitant des Potentiels Évoqués Somesthésiques.

**Nom du responsable scientifique de l’étude :** François Cabestaing  
**Fonction :** Professeur des universités

Je reconnais avoir pris connaissance de l’ensemble du protocole EDI-COPES et je m’engage à conduire ce protocole conformément à ce qui est décrit dans ce document.

Date : 14/09/2020

Signature :

Retrait de la signature lors de la publication du présent manuscrit pour raison de confidentialité.

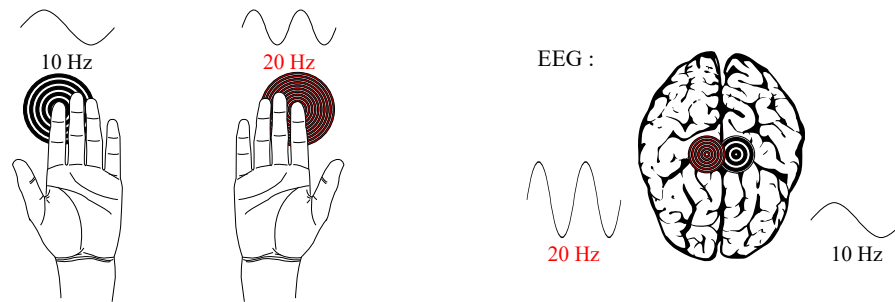


Figure E.1 : Illustration d'une variation d'amplitude d'un PESS modulée par l'attention.

## E.1 INTRODUCTION ET RATIONNEL

Ce protocole expérimental est porté par l'équipe BCI au sein du Centre de Recherche en Informatique, Signal et Automatique de Lille (CRISAL, UMR Univ. Lille / CNRS 9189). L'équipe BCI est spécialisée dans la spécification, la conception et la validation d'interfaces cerveau-ordinateur (ou Brain-Computer Interface, BCI). Ces interfaces ont pour vocation de permettre à un utilisateur de contrôler un objet via sa seule activité cérébrale. Pour l'équipe BCI, le but est plus précisément de pallier l'incapacité de déplacement ou de communication d'un utilisateur en situation de handicap.

L'objectif de l'expérience décrite dans ce protocole sera d'évaluer les possibilités offertes par une modalité d'interfaçage BCI très peu étudiée à ce jour, à savoir l'évocation puis la détection de potentiels évoqués somesthésiques stationnaires (PESS). Un « potentiel évoqué » désigne une variation de l'activité électrique cérébrale en réaction à un stimulus. Les « potentiels évoqués somesthésiques » ou « potentiels somesthésiques » désignent la catégorie particulière de potentiels évoqués par un stimulus faisant intervenir le sens du toucher. Ce sera, par exemple, une stimulation vibratoire dans notre étude. Quand la stimulation est périodique et de durée suffisante, les potentiels évoqués sont qualifiés de « stationnaires ».

La figure e.1 présente le principe d'une BCI utilisant les PESS et la modulation d'attention. Des vibrations, de fréquences différentes, stimulent les mécanorécepteurs des index gauche et droit. Une vibration appliquée sur l'index gauche évoque un PESS dans le cortex somatosensoriel droit et réciproquement. Une focalisation de l'attention sur l'une ou l'autre des vibrations entraîne une modulation d'amplitude des PESS qui peut être mise en évidence dans les signaux EEG. En simplifiant à l'extrême, on peut donc considérer qu'une mesure de variation d'amplitude permet d'identifier indirectement l'état attentionnel du sujet.

Notre protocole expérimental propose de reprendre et surtout d'étendre le protocole de Müller-Putz et al. de 2001 [60] et 2006 [62], en



intégrant les améliorations proposées par Pokorny et al. en 2014 [84] et 2016 [85].

Le premier protocole visant à étudier l'intérêt des PESS dans l'implémentation d'une BCI a été proposé par Müller-Putz et son équipe en 2006. Il comprenait plusieurs sessions expérimentales, dont la première servait à identifier une fréquence de « pseudo-résonance » pour chaque sujet. La fréquence de pseudo-résonance est la fréquence particulière de stimulation qui maximise l'amplitude des PESS dans l'EEG. Plus l'amplitude est importante, plus il est facile de mettre en évidence des variations de l'amplitude des PESS dans les signaux, améliorant ainsi les performances de l'interface. Lors des autres sessions d'expérimentation, les sujets recevaient des stimulations sur les deux index. La tâche consistait à diriger l'attention pendant 3 s sur l'une des deux stimulations, indiquée par une instruction. L'algorithme de traitement et de catégorisation devait ensuite retrouver l'intention en analysant l'EEG. L'expérience comprenait jusqu'à 5 sessions d'entraînement, en fonction de la disponibilité des sujets, avec *feedbacks* en temps-réel pour les 4 dernières sessions.

Cette BCI a montré un pouvoir discriminant globalement similaire à celui d'autres paradigmes d'interaction, exploitant par exemple des stimulations visuelles. Cependant, le sens du toucher est plus intéressant pour certaines applications, puisque moins contraignant pour le sujet que l'utilisation du regard. Par exemple, pour le contrôle d'un système de déplacement tel qu'un fauteuil roulant électrique, il peut être dommageable pour l'utilisateur d'utiliser son regard pour observer par un panneau de contrôle produisant des stimulations visuelles plutôt que l'environnement dans lequel il se déplace.

Dans le système de Müller-Putz, les vibrations mécaniques étaient produites par des matrices de pointes utilisées sur les anciennes imprimantes. Les fréquences des PESS correspondaient alors directement à celles des vibrations. En 2014 [84], Pokorny *et al.* ont développé un système de stimulation vibro-tactile visant à augmenter l'amplitude des PESS. Afin de mieux correspondre à la sensibilité maximale des corpuscules de Pacini, la fréquence de vibration est beaucoup plus élevée, aux alentours de 250 Hz. L'amplitude de ces vibrations est par contre modulée par une fréquence plus basse, qui sera celle caractéristique des potentiels stationnaires évoqués. En outre, le système de stimulation développé répond aux exigences de sécurité pour une utilisation en environnement médical (norme EN 60601-1:2006). Il est particulièrement intéressant de disposer d'un système de stimulation qui soit à la fois standardisé et compatible avec une utilisation clinique.

En définitive, le protocole décrit dans ce document diffère sensiblement de celui proposé par Müller-Putz. D'abord, nous utiliserons des vibrations de haute fréquence dont l'amplitude est modulée, comme proposé par Pokorny. Ensuite, nous appliquerons les stimulations sur les poignets plutôt que sur les index. Dans l'hypothèse d'une utilisa-

tion avec des sujets malades, cela nous semble plus pertinent. En effet, certaines pathologies empêchent les sujets d'avoir des mains ou les poignets détendus. Si les mains sont fermées ou recroquevillées vers les poignets, la mise en place du stimulateur sur l'index est impossible. Enfin, la littérature qui s'est un peu étoffée depuis 2006 concernant les fréquences de pseudo-résonance, montre que leur variabilité intersujet est très importante. Ainsi, nous considérons qu'il est nécessaire de réaliser une session de calibration pour chaque sujet et pour chaque main.

Notre expérience reprend malgré tout la méthodologie de Müller-Putz pour l'identification des fréquences de pseudo-résonance. Le sujet sera ainsi soumis à des trains de stimulations vibro-tactiles sur chaque poignet. Ces vibrations se produiront à différentes fréquences de modulation de la vibration, plus précisément entre 14 à 32 Hz avec un pas de 3 Hz. L'EEG enregistré devra permettre d'identifier l'amplitude des PESS produits. Les fréquences générant les PESS de plus grande amplitude seront définies comme fréquences de pseudo-résonance.

Notre objectif sera également d'étudier la capacité d'influencer l'amplitude des modulations des PESS par du *gating*. Le *gating* désigne les processus neurologiques filtrant les stimulus redondants ou superflus provenant de l'environnement [24]. Par exemple, lorsqu'une personne bouge un membre, elle perçoit moins des vibrations appliquées sur ce membre que lorsqu'il est au repos. Un *gating* se produit également lorsque la personne imagine réaliser un mouvement ou bien lorsqu'elle observe d'autres personnes qui réalisent ce mouvement, comme indiqué par Voisin *et al.* en 2011 [108].

Dans notre protocole, lorsque des vibrations appliquées sur le poignet gauche évoqueront des PESS dans le cortex droit, et que le sujet imaginera un mouvement du bras gauche, nous nous attendons à mesurer une diminution de l'amplitude des PESS causée par le *gating*, et inversement avec le bras droit. Par ailleurs, lorsque le sujet imaginera un mouvement des deux bras, nous nous attendons à mesurer une diminution des deux PESS simultanément. Nous essayerons de détecter ces variations d'amplitudes, afin de les traduire en commandes que le sujet pourrait envoyer à un système. A notre connaissance, une BCI exploitant le *gating* modulant l'amplitude de PESS n'a jamais été décrite dans la littérature.

Enfin, nous exploiterons ces marqueurs neurophysiologiques pour implémenter et évaluer une BCI complète. Celle-ci sera testée lors de notre dernière session de l'expérience. Les résultats préliminaires obtenus lors de ces expérimentations en Interaction Homme-Machine (IHM) sur des sujets témoins pourront nous ouvrir la voie vers des expériences avec des sujets malades et un système déjà éprouvé.

## E.2 OBJECTIFS

L'objectif principal de ce protocole expérimental est d'évaluer un système d'interaction cerveau-ordinateur exploitant des PESS. Dans un premier temps, nous vérifierons si une résonance est détectable dans les signaux EEG, lorsqu'une fréquence de stimulation<sup>1</sup> est appliquée sur le poignet de la personne. Ensuite, cette étude préliminaire évaluera la faisabilité de l'utilisation des PESS pour le contrôle d'une application BCI. L'impact avec des tâches cognitives de modulation d'attention et d'imagerie motrice sera également évalué (c.f. section 3.5 pour plus de détails sur les différentes sessions de l'expérience). À terme, la technique d'interaction testée dans ce protocole pourra constituer un moyen de communication exploitable par des patients lourdement handicapés ne pouvant plus utiliser les outils traditionnels d'interaction (clavier, joystick, reconnaissance vocale, etc.).

## E.3 MÉTHODE

### E.3.1 *Type d'étude*

Cette étude sera menée en collaboration entre CRISAL et le Service de neurophysiologie clinique du CHRU de Lille (contact : Pr. Arnaud Delval, Université de Lille, Faculté de médecine de Lille). Il s'agira d'une étude monocentrique. En effet tous les enregistrements seront effectués au CHRU de Lille par Jimmy Petit. Le recrutement pourra se faire au CHRU (personnes non-malades), au sein de CRISAL, ou plus généralement au sein du campus Cité Scientifique (étudiants de licence ou master, doctorants d'autres laboratoires, etc.). L'étude ne comportera pas de randomisation. Notre protocole est à groupes appariés, ainsi tous les sujets passeront toutes les conditions expérimentales. Les sujets participant à cette étude ne seront pas rémunérés.

### E.3.2 *Population*

Pourront être incluses dans l'expérience toutes les personnes respectant les critères d'inclusion mentionnés ci-dessous, consentant à ce que toutes les données non-nominatives, une fois anonymisées, soient mises à disposition de la communauté scientifique dans des bases de données appropriées (c.f. section 4. et 5.3).

#### **Critères d'inclusion :**

- Age : entre 18 et 75 ans

<sup>1</sup> Ici, comme dans la suite de la description, la « fréquence de stimulation » désigne la fréquence modulant l'amplitude des vibrations, lesquelles se produisent en fait à une fréquence constante beaucoup plus élevée afin d'activer efficacement les corpuscules de Pacini.

- Genre : homme ou femme
- Volontaire, ayant donné son consentement éclairé
- Personne disposée à se conformer à toutes les procédures de l'étude et à sa durée (4 séances de 2 heures)

**Critères non inclusion :**

- Antécédent neurologique : épilepsie, AVC, démence
- Femmes enceintes
- Personnes sous tutelle ou sous curatelle
- Comorbidité majeure considérée comme une contre-indication par l'investigateur (cancer, angor instable ...)
- Raisons administratives : impossibilité de recevoir une information éclairée, impossibilité de participer à la totalité de l'étude ou refus de signer le consentement

**E.3.3** *Lieu d'étude et matériel EEG*

Les enregistrements seront effectués dans les locaux du service de Neurophysiologie clinique du CHRU de Lille, au moyen d'un système EEG portatif à 64 électrodes : le eego sport de la compagnie néerlandaise ANT Neuro.

**E.3.4** *Procédure*

Un formulaire de consentement et une lettre d'information seront fournis aux sujets dès la première session. Ces documents expliqueront le déroulement de toute l'expérience (i.e. les quatre sessions) ainsi que le traitement des données, de leur pseudo-anonymisation à leur anonymisation complète. Ces documents seront aussi clairs et pédagogiques que possibles (documents fournis en annexe).

Nous souhaitons faire réaliser notre expérience à une vingtaine de sujets satisfaisant les critères d'inclusion susmentionnés. Ce nombre est un standard dans la littérature en BCI, et se révèle en général suffisant pour valider une hypothèse. Il devrait être suffisant pour pouvoir apporter des réponses statistiquement significatives aux questions soulevées par nos travaux.

En ce qui concerne la sécurité des sujets, le système de stimulation (notamment les transducteurs) respecte la norme de sécurité EN 60601-1 : 2006 pour matériel électrique médical [84].

En début et en fin de session, les sujets répondront à des questionnaires. Ces questionnaires seront de diverses natures. Il pourra s'agir, par exemple, de récupérer les avis des sujets sur le système proposé, leur niveau de motivation quant à leur participation à l'expérience ou bien leur niveau de fatigue. Ces questionnaires seront également anonymisés lors de l'expérimentation (c.f. section 4 à-propos du traitement des données).

L'expérience sera divisée en quatre sessions. Chaque session sera espacée de plusieurs jours (entre 7 et 14). Ce délai, de 7 à 14, a été choisi volontairement de façon flexible pour deux raisons principales :

- Nous pensons qu'il serait plus difficile de recruter des personnes pour une expérience sur 4 jours consécutifs.
- Le matériel étant partagé par le CHU, une certaine flexibilité est nécessaire quant à son utilisation.

Un délai légèrement supérieur à 14 jours n'entraînera pas l'exclusion du sujet. Cette information sera simplement prise en compte dans l'analyse et l'interprétation des résultats. Pour réaliser une meilleure comparaison, entre sessions et entre sujets, chaque session sera, idéalement, réalisée à la même heure. Cette contrainte sera cependant flexible et dépendra naturellement des disponibilités du sujet.

La première session sera une session de calibration, la deuxième une session de test, la troisième de *gating* et la quatrième sera une session d'application. La durée de chaque session sera d'environ 45 minutes. Les différentes pauses entre essais et blocs sont comptabilisées dans la durée des sessions décrites ci-après, mais pas le temps d'installation du casque EEG ni celui de vérification des impédances d'électrodes. En pratique, environ deux heures seront nécessaires pour la réalisation complète d'une session en tenant compte de l'installation du casque EEG. On estime la durée totale d'expérimentation « active » à 3 heures. Toutes les sessions se dérouleront au CHRU de Lille. La personne en charge des passations sera Jimmy Petit.

Les méthodes de recrutement seront les suivantes : listes de diffusion électroniques, bulletins d'information de l'université, affichage au niveau des R.U., MDE, tableaux d'affichage proches des amphis et recrutements en local (campus du V.A. et CHU). La lettre d'information sera également attachée aux courriels pour diffusion plus large et liée à l'affiche de recrutement via un QR Code. Les critères d'inclusion et de non-inclusion seront précisés sur tous les supports de communication. Nous ajoutons en annexe du protocole l'affiche qui sera utilisée pour diffusion de l'appel à recrutement.

### E.3.5 *Méthodologie utilisée*

Chacune des 4 sessions sera découpée en plusieurs blocs d'expérimentation. Chaque bloc sera d'une durée variable d'une session à l'autre, laquelle durera entre 47 et 57 minutes. Les blocs les plus longs seront ceux de la première session, qui dureront 9 minutes. Dans les autres sessions les blocs seront plus courts, mais plus nombreux. Durant toutes les sessions, des pauses d'au moins 3 minutes sont prévues entre deux blocs d'expérimentation. Ce design est flexible, si le sujet désire plus de temps de pause cela sera possible dans la mesure du raisonnable.

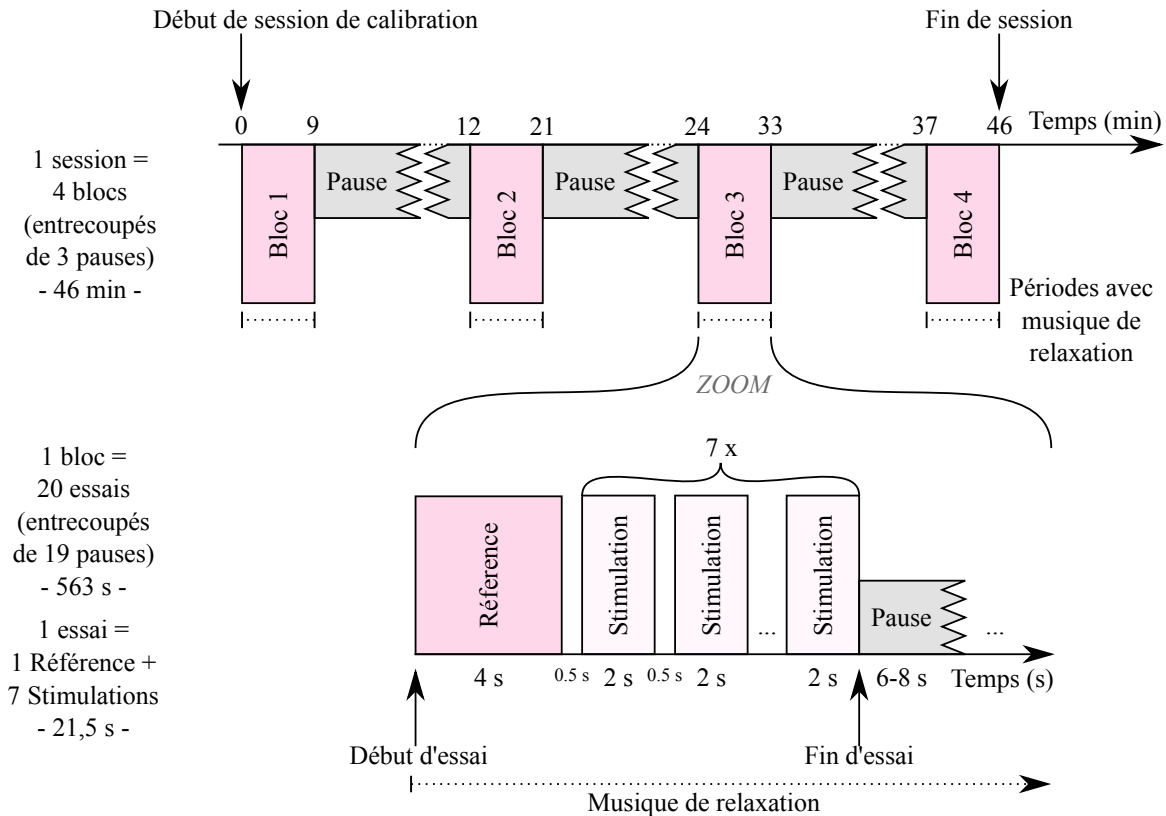


Figure E.2 : Présentation de la session de calibration. Déroulement des phases d'enregistrement lors d'un essai de la session de calibration, modifié depuis Pokorny *et al.* 2014 [84]. Un couple « poignet/fréquence de stimulation » est aléatoirement généré pour chaque stimulation. On vérifie que ce couple ne soit jamais utilisé deux fois successivement. Les fréquences testées varient de 14 Hz à 32 Hz avec un pas de 3 Hz. La durée d'un essai est de 21,5 s. Les durées en minutes relatives au déroulement de la session sont des approximations et sont données à titre indicatif.

### E.3.5.1 Première session : calibration

La première session a pour but de soumettre les poignets des sujets à différentes fréquences de stimulation pour déterminer une éventuelle fréquence de pseudo-résonance. Cette dernière est celle qui produit la plus forte activité cérébrale au niveau du cortex somatosensoriel, mesurée à la même fréquence que la fréquence de la stimulation.

Durant un essai de la première session, les 4 premières secondes d'enregistrement seront utilisées comme référence pour déterminer la ligne de base de l'EEG. Le sujet regardera le mur devant lui en étant détendu, en écoutant de la musique de relaxation (voir l'annexe pour avoir les détails concernant le choix des musiques). Il sera demandé au sujet de se détendre et de ne pas se concentrer sur les vibrations, pour éviter toute variation potentielle d'amplitude des réponses causée par une variation d'attention de la part du sujet. Pour cela, on diffusera

aux sujets de la musique de relaxation à l'aide d'un casque audio. La musique permettra également d'éviter que les sujets n'entendent les vibrations des transducteurs. Les sujets devront, autant que possible, limiter les activités musculaires parasites (clignement d'œil ou déglutition, par exemple) pendant les périodes d'enregistrement actif, i.e. un bloc (voir figure 2). Les fréquences des stimulations testées varieront de 14 Hz à 32 Hz, par pas de 3 Hz. Un couple « poignet/fréquence de stimulation » sera aléatoirement généré pour chaque stimulation. On vérifiera que ce couple ne soit jamais utilisé deux fois successivement. Il y aura au total 40 répétitions par fréquence et par poignet.

Grâce aux données de cette première session, nous déterminerons une fréquence de stimulation optimale pour chaque poignet. Si les fréquences de pseudo-résonance sont suffisamment différentes pour les deux poignets (plus de 5 Hz) alors elles seront retenues comme fréquences de stimulation. Sinon, l'une des deux sera remplacée par l'autre diminuée ou augmentée de 5 Hz de telle sorte que les deux restent dans l'intervalle 14-32 Hz.

#### E.3.5.2 Deuxième session : test

Durant la deuxième session, nous souhaitons tester la réponse du système sensoriel somatique à une stimulation mécanique répétée à une fréquence spécifique sur les poignets. De plus, nous étudierons l'influence de l'amplitude de la stimulation sur l'amplitude des PESS générés, mais également l'influence de la modulation attentionnelle sur l'amplitude des PESS, ceci permettant par la suite de faire un lien avec la session de *gating*.

Un essai de la session de test se déroulera comme suit :

- Pendant les deux premières secondes, le sujet posera son regard sur une croix à l'écran. Il s'agit d'un état de repos qui servira de référence lors de l'analyse.
- À  $t = 2$  s, les transducteurs commenceront à vibrer aux fréquences de stimulation déterminées pour ce sujet lors de sa session de calibration.
- À  $t = 3$  s, une flèche apparaîtra à l'écran. Elle indiquera le poignet sur lequel le sujet devra se concentrer lors de l'essai.

Nous diminuerons parfois l'amplitude des vibrations à  $t = 5$  s. D'une durée de 2 secondes, cette diminution devrait permettre de passer d'un régime établi des PESS à un autre, où les amplitudes sont plus faibles. Cette diminution ne sera présente que dans 50% des essais, et avec la même proportion sur les deux poignets. Le déroulement de l'expérience est résumé en figure 3. Cette session de test inclut deux conditions expérimentales : le poignet sur lequel le sujet doit concentrer son attention ainsi que la présence ou non d'une diminution d'amplitude sur ce poignet. Sur la session, il y aura donc un quart des essais où le sujet se



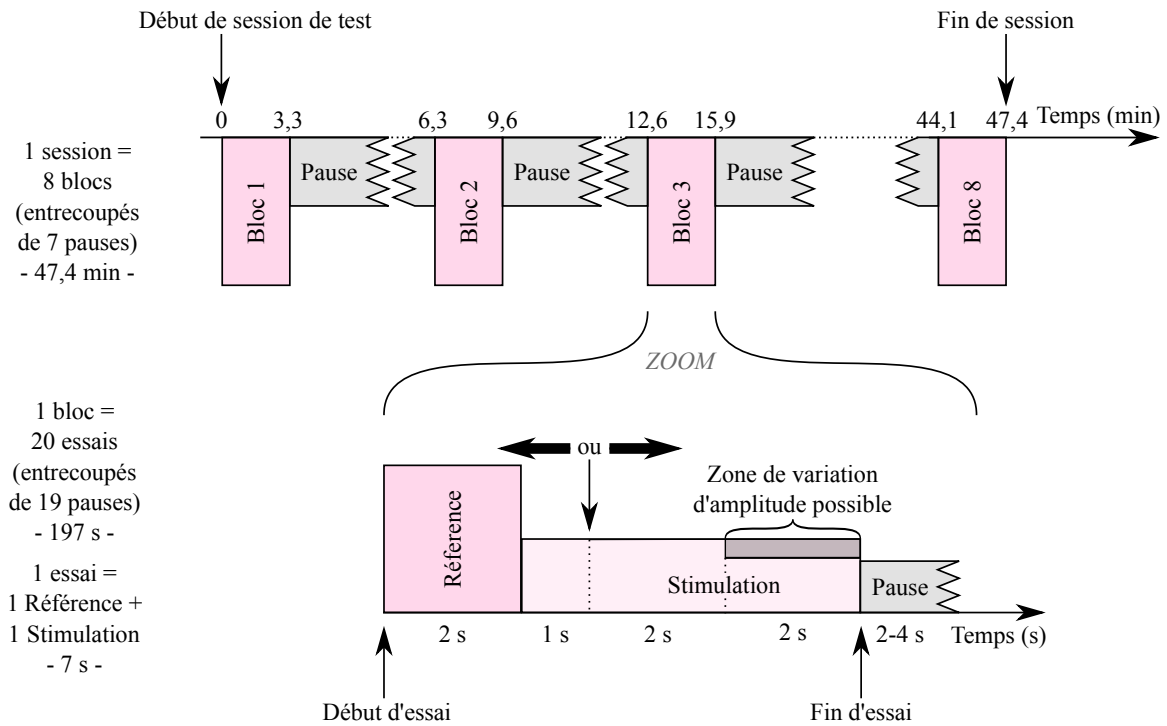


Figure E.3 : Présentation de la session de test. Déroulement des phases d'enregistrements lors d'un essai de la session de test, modifié depuis les travaux de Müller-Putz *et al.* de 2006 [62]. Les durées en minutes relatives au déroulement de la session sont des approximations et sont données à titre indicatif.

concentrera sur le poignet gauche et où l'amplitude diminuera sur ce même poignet. Un autre quart, où le sujet se concentrera sur le poignet gauche et sans diminution d'amplitude. Les deux quarts restants seront identiques pour le poignet droit.

#### E.3.5.3 Troisième session : *gating*

La troisième session consistera en des essais où le sujet imaginera réaliser un mouvement. Notre hypothèse est que cette tâche d'imagination motrice influencera l'amplitude des PESS par *gating*. Pendant chaque essai, il sera demandé au sujet d'imaginer déplacer le bras gauche ou droit, ou bien les deux bras en même temps. Après une pause de quelques secondes, un nouvel essai commencera. La tâche motrice à imaginer pourra être de toucher une cible rouge à l'écran avec le/les bras indiqué, par exemple.

Le déroulement de cette troisième session est présenté en figure 4. En début d'essai, un symbole définissant une consigne de mouvement sera affiché : une flèche vers la gauche ou la droite s'il faut bouger un seul des deux bras, une flèche vers le haut s'il faut bouger les deux bras simultanément, et un rond s'il faut rester immobile.

Dans les deux premiers blocs, le sujet ne recevra pas de *feedback* en fin d'essai (essais « A » dans la figure 4). Dans les blocs suivants, un *feedback* visuel sera fourni au sujet après chaque essai (essais « B » et « C » dans la figure 4). En cas de succès, un symbole similaire à celui ayant indiqué la consigne sera affiché en vert. En cas d'échec, ce symbole sera affiché en rouge. Ces *feedbacks* permettent de maintenir l'engagement du sujet dans l'expérience.

Dans les troisième et quatrième blocs, les *feedbacks* seront factices et simuleront un taux de classification correct à 80% (essais « B » dans la figure 4). Dans les deux derniers blocs d'expérimentation, les *feedbacks* seront calculés en temps-réel à partir des signaux EEG. L'algorithme de classification sera entraîné pendant la première partie de la session, c'est-à-dire sur les 4 premiers blocs.

#### E.3.5.4 Quatrième session : *application*

La dernière session, la session d'application, permettra aux sujets de contrôler un kart virtuel dans un environnement 3D. Le kart piloté par le sujet devra passer par différents points de passage dans l'environnement virtuel. Cette session aura pour but d'évaluer le système dans son ensemble en allouant aux sujets une plus grande liberté dans le contrôle des commandes.

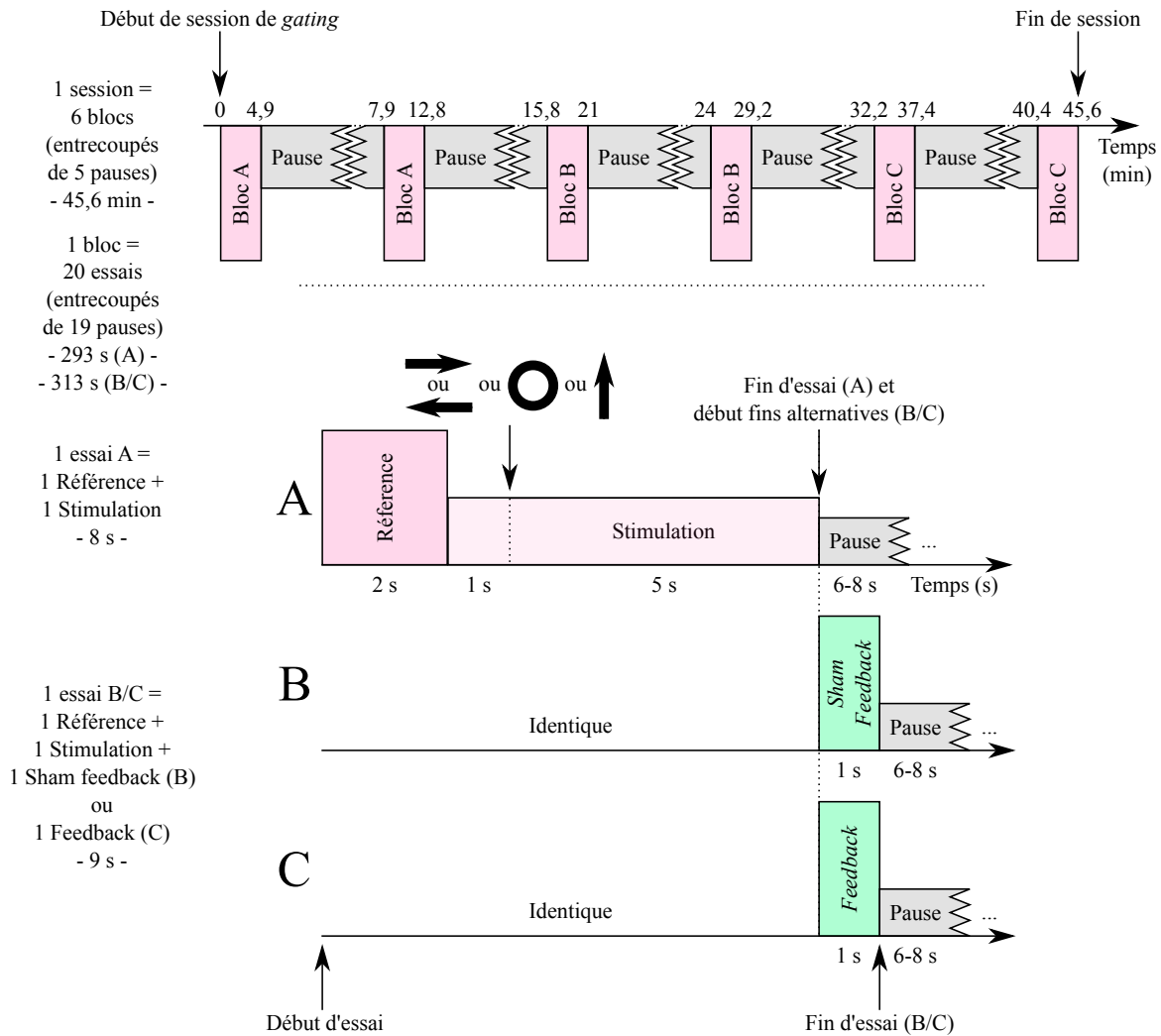


Figure E.4 : Présentation de la session de *gating*. Les durées en minutes relatives au déroulement de la session sont des approximations et sont données à titre indicatif. Cette session est séparée en 6 blocs, chacun d’une durée similaire. Tous les blocs sont composés de 20 essais chacun. Une pause d’une durée minimum de 3 minutes est imposée au sujet entre chaque bloc. Les blocs de type A ne sont composés que d’essais de type A. Il en va de même pour les blocs de type B ou C. Pour pouvoir fournir un *feedback* en temps-réel lors des blocs C, les enregistrements réalisés durant les quatre premiers blocs A et B seront utilisés comme données de calibration.

## E.4 TRAITEMENT DES DONNÉES

E.4.1 *Gestion des données*

Toutes les procédures de gestion des données décrites dans ce protocole ont été définies en collaboration avec Olivier AUVERLOT, DPO de CRISStAL. Les données des expérimentations seront anonymisées à l'aide d'un identifiant aléatoire pour chaque sujet d'expérience. Ces identifiants seront stockés sur un registre papier unique sous la forme d'une liste d'identification code-nom. Cette liste sera rédigée pour associer à chaque sujet un identifiant aléatoire pour maintenir l'anonymat de la personne. À ce stade, les données sont considérées pseudo-anonymes puisqu'une tierce personne, avec cette liste, pourrait obtenir l'identité du sujet d'expérimentation via l'étiquette apposée sur les données d'expérimentation. Cependant, ce stade est nécessaire, pour deux raisons :

- Il permet d'étiqueter les données expérimentales du même sujet d'une session à l'autre.
- Il permet aux sujets de faire valoir leurs droits sur ces données : i.e. accès, rectification ou même suppression si le sujet décide de quitter l'expérience.

Les sujets seront informés (par la lettre d'information, c.f. annexe) qu'ils disposent d'une durée de 3 mois après leur dernière session pour faire valoir leurs droits sur les données. Passé ce délai il ne sera plus techniquement possible de le faire. Puisque les sujets apparaîtront de façon chronologique sur la liste d'identification, il sera possible de détruire la liste progressivement, au fur et à mesure que les délais de 3 mois s'écoulent. Elle sera ainsi complètement détruite 3 mois après la dernière session du dernier sujet d'expérimentation. Passé ce stade, les données non-nominatives seront ainsi complètement anonymisées et donc facilement partageables au sein de la communauté scientifique. Nous avons l'intention de rendre publiques ces données d'expérimentation, notamment en accompagnement de publications des résultats scientifiques obtenus, pour assurer la reproductibilité de nos travaux de recherche. Cette liste et les formulaires de consentement signés par les sujets seront conservés de façon sécurisés, c.f. section 5.4.

E.4.2 *Analyse des données*

Le but de notre traitement du signal est de retrouver parmi les réponses PESS, celles qui ont la plus forte amplitude pour chaque sujet. Pour cela, on va d'abord reproduire les traitements implémentés par Müller-Putz en 2006 [62]: un *lock-in analyser* (ou *digital lock-in amplifier*) pour chaque électrode et une Analyse Discriminante Linéaire (ADL) de Fisher [11] (*Fisher's Linear Discriminant Analysis*).

L'analyse des données sera effectuée en suivant les traitements, analyses connues et standards du domaine des BCI [21, 53].

Lors de ces travaux, nos hypothèses concernent la variation d'amplitude de PESS dans l'EEG. Nous présentons ici une métrique canonique pour mesurer l'augmentation relative de l'amplitude d'un PESS à un état de repos [83]. L'amplitude,  $A$ , du PESS est estimée par un Lock-in Amplifier. L'amplitude, à la fréquence du PESS, est également estimée sur toute la durée de l'état de repos :  $R$ . L'augmentation relative de la bande de puissance (RBP), en pourcentage, est donnée par l'équation :  $RBP = (A-R)/R * 100$  [83]. Ainsi, une RBP de 0%, montrerait qu'il n'y a pas de variation d'amplitude induite par la stimulation, et donc que les PESS, même s'ils existent, ne sont pas mesurables par notre système.

Les critères d'évaluation / objectifs pour ce protocole pourront être comme suit :

- Proportion de sujets chez lesquels une stimulation tactile induit des PESS ;
- Proportion de sujets pouvant moduler l'amplitude des PESSs par *gating* ;
- Proportion de sujets pouvant moduler l'amplitude des PESSs par focalisation attentionnelle ;
- Proportion et qualité (taux de bonne classification) des sujets capables d'utiliser le système BCI final dans de bonnes conditions.

#### E.4.3 Finalité de l'étude

L'intérêt de cette expérience réside dans le but d'ouvrir la voie à de futures études sur les PESS avec des personnes atteintes d'amyotrophie spinale en étudiant leur capacité à utiliser ce paradigme d'interaction. Un protocole similaire à celui décrit dans ce document, mais adapté à des patients atteints d'une amyotrophie spinale, été soumis à la DRS du CHRU de Lille pour évaluation par un CPP. À terme, si ces expériences tendent à montrer que ces personnes réagissent et peuvent influencer leurs PESS, alors elles pourront potentiellement bénéficier des techniques BCI, avec des finalités diverses : assistance à la mobilité, contrôle domotique ou encore communication. Notre quatrième session propose d'explorer cet aspect.

### E.5 ASPECTS RÉGLEMENTAIRES ET ÉTHIQUES

#### E.5.1 Confidentialité

Toutes les personnes appelées à collaborer ou à prendre connaissance de l'étude sont tenues au secret professionnel.

### E.5.2 *Information et consentement*

Les participants seront informés de l'étude, des bénéfices, des contraintes, des risques possibles, du temps de passation... dans un langage clair. Ces informations sont reprises dans un document signé (la lettre d'information) qui sera paraphé par le participant. Les participants devront également signer un formulaire de consentement de participation nominatif. Ces deux documents sont disponibles en annexe du présent document.

### E.5.3 *Propriétés des données et publication*

Les données non-nominatives pseudo-anonymisées ont vocation à être publiées dans des bases de données exploitées par la communauté scientifique (par exemple : MOABB<sup>2</sup>). La principale raison de ce choix vient des impératifs de reproductibilité exigés à juste titre pour des travaux d'analyse de ce genre.

### E.5.4 *Archivage des données*

Les consentements et les données nominatives (i.e. la liste d'identification code-nom des participants) seront stockés dans un coffre-fort, prévu à cet effet, au sein de CRISAL. À ce jour, deux personnes ont accès à ce coffre-fort : Olivier COLOT (directeur de CRISAL) et Olivier AUVERLOT (DPO de CRISAL). Aucune copie numérique ne sera réalisée de ces documents. Les données non nominatives fournies par les participants (réponses aux questionnaires, données socio-démographiques, etc.) seront stockées sur une machine fixe chiffrée au sein de CRISAL. Les autres données non-nominatives, enregistrées lors des expérimentations, seront archivées sur un disque dur chiffré au sein de l'équipe BCI du CRISAL. Ces données seront mises à disposition de la communauté scientifique à l'aide de bases de données (par exemple : MOABB) une fois la liste d'identification code-nom détruite.

## E.6 DURÉE DE L'ÉTUDE ET ÉCHÉANCIER

Calendrier prévisionnel de l'étude :

- De Février 2020 à Octobre 2020 : montage du projet
- De Octobre 2020 à Décembre 2021 : inclusions et enregistrement des sujets
- De Octobre 2020 à Décembre 2021 : traitement et analyse des données

---

<sup>2</sup> « Mother of all BCI Benchmark »

E.7 DOCUMENTS SUPPLÉMENTAIRES

Dans les pages suivantes nous incluons tous les documents liés à l'expérience, c'est-à-dire:

- Consentement de participation
- Lettre d'information
- Feuilles d'instructions pré-sessions
- Questionnaires pré et post-sessions
- Affiche de recrutement
- Détails complémentaires au protocole expérimental



# Consentement de participation

Mr / Mme  
Nom :

Prénom :

Date de naissance :

Il m'a été proposé de participer à l'étude intitulée : "Étude et Développement d'une Interface Cerveau-Ordinateur exploitant des Potentiels Évoqués Somesthésiques" (EDICOPES). L'investigateur·rice ..... m'a précisé que je suis libre d'accepter ou de refuser.

Afin d'éclairer ma décision, j'ai reçu et compris les informations suivantes :

1. Je pourrai à tout moment interrompre ma participation si je le désire, sans avoir à me justifier.
2. Je pourrai prendre connaissance des résultats de l'étude dans sa globalité lorsqu'elle aura été publiée.
3. Les données nominatives recueillies demeureront strictement confidentielles.
4. Les données (mesures et réponses aux questionnaires) anonymisées pourront être partagées avec d'autres équipes de recherche via différents moyens.

Compte-tenu des informations qui m'ont été transmises :

*cocher les cases appropriées en fonction de votre volonté (OUI/NON)*

	OUI	NON
J'accepte librement et volontairement de participer à la recherche EDICOPES.		

Conformément à la loi Informatique et Libertés du 6 janvier 1978 modifiée et au Règlement (UE) 2016/679 du Parlement européen et du Conseil du 27 avril 2016, vous pouvez exercer votre droit d'accès aux données vous concernant et les faire rectifier ou effacer en contactant le délégué à la protection des données : cristal-dpo@univ-lille.fr

Date : ... / ... / .....

Signature du participant·e :

Date : ... / ... / .....

Signature de l'investigateur·rice :

# Lettre d'information

Études et Développement d'une Interface Cerveau-Ordinateur exploitant  
des Potentiels Évoqués Somesthésiques (EDICOPES)

Jimmy Petit, José Rouillard et François Cabestaing

Univ. Lille, CNRS, Centrale Lille, UMR 9189 - CRISTAL - Centre de Recherche  
en Informatique, Signal et Automatique de Lille,  
F-59000 Lille, France

Vous êtes sur le point de prendre part à une étude du Centre de Recherche en Informatique, Signal et Automatique de Lille (CRISTAL). Le responsable scientifique de cette étude est François Cabestaing<sup>1</sup>. Veuillez lire attentivement les informations ci-dessous avant de prendre une décision quant à votre participation à cette étude.

## Objectifs et déroulement de l'étude

Cette étude a pour objectif d'étudier une nouvelle possibilité de contrôle d'un système artificiel par une personne.

Durant l'expérience, l'activité cérébrale est mesurée à l'aide d'un ElectroEncéphaloGramme (EEG). L'EEG permet de recueillir les signaux électriques générés par le cerveau grâce à des électrodes posées à la surface du cuir chevelu. Pour que le casque à EEG soit en contact avec votre cuir chevelu, nous déposerons du gel entre le cuir chevelu et les électrodes du casque. Lors de cette étape, vous pourrez être amené · e à sentir une légère sensation de froid sur les zones où nous poserons le gel. Le gel se retire très facilement avec du shampoing. Vous aurez la possibilité de vous nettoyer les cheveux après chaque session (lavabo, shampoing, serviettes de toilette et sèche-cheveux à disposition). De plus, vous serez équipé · e d'un stimulateur vibrant sur chacun de vos poignets (voir Figure 1). Au bout d'un certain temps, certaines personnes peuvent trouver les vibrations désagréables ou bien apaisantes. Cependant, cet équipement est sans risque et les vibrations sont non douloureuses.

L'étude se déroule en 4 sessions, chacune espacée de plusieurs jours (idéalement : entre 7 et 14), nous établirons un calendrier avec vous, en fonction de vos disponibilités, pour préparer tout cela. Toutes les sessions se déroulent à l'Hôpital Salengro du CHU de Lille. Durant chaque session vous aurez à réaliser différentes tâches en restant confortablement assis sur un fauteuil en bougeant le moins possible. Vous pourrez aussi bien être équipé d'un casque supplémentaire et écouter

---

1. François Cabestaing - mail : francois.cabestaing@univ-lille.fr - téléphone : 03 20 43 42 88

de la musique, que rester assis devant un écran à suivre des consignes. Une feuille d'instruction vous sera fournie à chaque début de session pour vous expliquer la tâche à réaliser.

Chaque session dure approximativement 2h30, pose du casque à EEG et remplissage des questionnaires compris. **Chaque session a pour objectif de répondre à une question particulière. Elles sont complémentaires les unes des autres. Il est donc très important de réaliser toutes les sessions.**

À terme, le système développé ici pourra constituer un moyen de communication exploitable par des patient(e)s lourdement handicapés ne pouvant plus utiliser les outils traditionnels (clavier, joystick, reconnaissance vocale, etc).

#### Critères d'inclusion

- Age : entre 18 et 75 ans
- Genre : homme ou femme
- Volontaire, ayant donné son consentement éclairé
- Personne disposé à se conformer à toutes les procédures de l'étude et à sa durée (4 séances de 2h30)

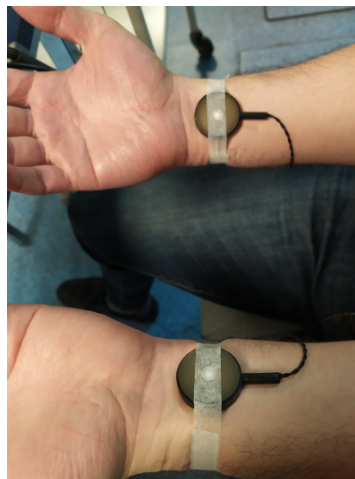


FIGURE 1 – Photo du système de stimulation attaché au poignet.

#### Critères non inclusion

- Antécédents neurologique : épilepsie, AVC, démence
- Femmes enceintes
- Personnes sous tutelle ou sous curatelle
- Comorbidité majeure considérée comme une contre-indication par l'investigateur (cancer, angor instable ...)
- Raisons administratives : impossibilité de recevoir une information éclairée, impossibilité de participer à la totalité de l'étude ou refus de signer le consentement

## Pour information

Vous pouvez à tout moment et sans vous justifier vous désengager du projet.

## Confidentialité des données

Lors de ces expériences, de nombreuses données personnelles vont être recueillies. Tout d'abord, en arrivant nous vous demanderons de signer un formulaire de consentement. D'autre part, toutes les données relatives aux résultats d'expériences, c'est-à-dire EEG et réponses aux questionnaires, seront anonymisées par un code aléatoire qui vous sera attribué. Seules les données anonymisées seront susceptibles d'être partagées à la communauté scientifique. Trois mois après votre dernière session, le document faisant l'appariement entre votre nom et le code aléatoire sera détruit, rendant les données relatives aux résultats d'expériences complètement anonymes. Il ne nous sera donc plus possible de faire valoir vos droits sur vos données une fois ce délai dépassé.

## Loi Informatique et Libertés

Conformément à la loi Informatique et Libertés du 6 janvier 1978 modifiée et au Règlement (UE) 2016/679 du Parlement européen et du Conseil du 27 avril 2016, vous pouvez exercer votre droit d'accès aux données vous concernant et les faire rectifier ou effacer en contactant le délégué à la protection des données.

Le traitement EDICOPES est porté au registre du délégué à la protection des données de CRISAL. Pour plus d'informations ou toute demande concernant l'accès à vos données, vous pouvez contacter le délégué à la protection des données par mail : [crystal-dpo@univ-lille.fr](mailto:crystal-dpo@univ-lille.fr).

---

Date et signature  
du participant : e :

3/3

Date et signature de  
l'investigateur : rice :

# Instructions Session 1

Nous vous remercions d'avoir accepté de prendre part à l'étude EDICOPES. Cette étude a pour but d'étudier un nouveau moyen de communication entre une personne et une machine, avec pour finalité de pallier les handicaps moteurs sévères.

Pour rappel, cette étude comprend 4 sessions d'environ deux heures, chacune espacée d'environ 2 semaines. **Les tâches à réaliser dans les 4 sessions sont différentes mais dépendantes et complémentaires les unes des autres. Il est donc très important de réaliser les 4 sessions.**

Cette première session sera divisée en plusieurs parties. D'abord, il vous sera demandé de remplir des questionnaires. Ensuite, nous vous équiperons d'un casque ÉlectroEncéphaloGraphique (EEG) pour mesurer l'activité électrique générée par votre cerveau. Vous serez également équipé.e de deux stimulateurs vibrants attachés à vos poignets, qui vibreront par moments pendant la session. Après avoir installé ces équipements, vous pourrez commencer l'expérience. Vous serez alors assis.e sur un siège et vous porterez des écouteurs dans lesquels de la musique sera diffusée. Votre tâche sera simplement d'écouter la musique. Pendant ce temps, vous recevrez des vibrations sur les poignets droit ou gauche. **Ne faites pas attention à ces vibrations, vous devez juste rester décontracté.e et concentré.e sur la musique tout le long de sa diffusion.** Pendant la tâche, il est très important que vous restiez décontracté.e, sans bouger, pour que votre activité musculaire ne bruite pas le signal EEG que l'on mesure. Des activités musculaires qui peuvent sembler dérisoires polluent en réalité fortement les données, c'est le cas des mouvements oculaires par exemple. Essayez, dans la mesure du possible, de ne pas parler, déglutir ou cligner des yeux lors des stimulations tactiles.

L'expérience est divisée en 4 séquences d'environ 9 minutes. Entre chaque séquence, nous éteindrons la musique et vous aurez une petite pause d'au moins 3 minutes. Vous pourrez alors enlever les écouteurs, bouger un peu et nous poser des questions si besoin. À la fin de ces 4 séquences, nous vous ferons remplir un rapide dernier questionnaire. Ensuite, vous pourrez vous rincer les cheveux et la session sera terminée. Avant de commencer, avez-vous des questions ?

## Instructions Session 2

La deuxième session de cette étude dure environ 2 heures, remplissage des questionnaires et installation du matériel compris (casque EEG et stimulateurs).

**Votre tâche sera de vous concentrer sur les vibrations délivrées sur un des poignets, en ignorant celles délivrées sur l'autre poignet.**

L'expérience comprend 8 séquences d'environ 3 minutes, et chaque séquence est elle-même divisée en 20 essais.

Au début de chaque essai, une croix sera affichée à l'écran : vous devrez la fixer, en restant aussi détendu que possible.

Après quelques secondes, les stimulateurs attachés à vos poignets commenceront à vibrer en même temps. Au bout de 1 seconde, une flèche apparaîtra à l'écran :

- une flèche pointant à gauche signifie que vous devrez vous concentrer sur la vibration du poignet gauche (et ignorer celle du poignet droit).
- une flèche pointant à droite signifie que vous devrez vous concentrer sur la vibration du poignet droit (et ignorer celle du poignet gauche).

Au bout de quelques secondes, les stimulateurs arrêteront de vibrer et l'écran redeviendra tout noir, marquant la fin de l'essai. Vous pourrez alors arrêter de faire la tâche, vous reposer, bouger un peu si besoin et vous préparer à l'essai suivant qui débutera quelques secondes plus tard avec l'apparition de la croix rouge à l'écran. Au cours de certains essais, l'intensité de la vibration du stimulateur indiqué par la flèche sera diminuée. À la fin de l'essai, si vous avez perçu la diminution, indiquez-le verbalement par un "oui" ou "non" à l'expérimentateur.

Nous vous rappelons que pendant la tâche, il est très important que vous restiez décontracté.e, sans bouger, pour que votre activité musculaire ne bruite le signal EEG que l'on mesure. Des activités musculaires qui peuvent sembler dérisoires polluent en réalité fortement les données, c'est le cas des mouvements oculaires par exemple. Essayez, dans la mesure du possible, de ne pas parler, déglutir ou cligner des yeux durant les essais, mais faites-le durant les quelques secondes de pause entre les essais.

Entre chaque séquence, vous aurez une courte pause d'environ 3 minutes. Vous

pourrez alors bouger un peu et nous poser des questions si besoin.

Nous allons commencer par un entraînement pour vérifier que les instructions ont été claires. Avant l'entraînement, avez-vous des questions ?



## Instructions Session 3

Dans cette session, vous devrez réaliser des tâches **d'imagerie mentale**. **Votre tâche sera de vous imaginer mentalement réaliser un mouvement du ou des bras pour toucher une cible à l'écran.**

L'expérience comprend 6 séquences d'environ 5 minutes, et chaque séquence est elle-même divisée en 20 essais. Au début de chaque essai, une croix sera affichée à l'écran : vous devrez la fixer tout en restant détendu.e. Après quelques secondes, la consigne au sujet de la tâche que vous devrez effectuer apparaîtra sous la forme d'une icône :

- une flèche pointant à gauche signifie que vous devrez imaginer le mouvement avec le bras gauche.
- une flèche pointant à droite signifie que vous devrez imaginer le mouvement avec le bras droit.
- une flèche pointant en haut signifie que vous devrez imaginer le mouvement avec les deux bras en même temps.
- un cercle signifie qu'il s'agit d'une période de repos. Dans cette condition, vous ne devrez effectuer aucune tâche en particulier, restez détendu.e.

Dans chaque essai, à partir du moment où vous verrez apparaître la consigne (une flèche ou un cercle), vous devrez commencer à faire la tâche demandée, et vous devrez la faire en continu jusqu'à la fin de l'essai (c'est-à-dire jusqu'à ce que l'écran redevienne tout noir, soit environ 5 secondes). **Il est très important que vous fassiez la tâche en continu. Pour le mouvement du ou des bras, il faudra donc s'imaginer le répéter en boucle jusqu'à la fin de l'essai.**

À partir de la séquence 3, à la fin de chaque essai, il vous sera indiqué si la tâche que vous réalisiez dans l'essai a bien été reconnue par le système. Lorsque le système a reconnu le mouvement demandé, alors la flèche affichée (ou le cercle) vire au vert. Sinon, elle vire au rouge. Ensuite, l'écran redeviendra tout noir. Vous pourrez alors arrêter de faire la tâche, vous reposer, et vous préparer à l'essai suivant qui débutera quelques secondes plus tard.

**Il est plus efficace de faire ce que l'on appelle de l'imagerie motrice**

**kinesthésique, plutôt que simplement visualiser une main qui bouge. Il s'agit de s'imaginer réaliser le mouvement d'une façon plus réelle. Cela passe notamment par l'imagination des sensations au niveau des muscles et tendons, de la même façon que lorsque vous réalisez réellement le mouvement, mais toujours sans bouger.**

Entre chaque séquence, vous aurez une courte pause d'environ 3 minutes. Vous pourrez alors bouger un peu et nous poser des questions si besoin.

Nous rappelons que pendant la tâche, il est très important que vous restiez décontracté.e, sans bouger, pour que votre activité musculaire ne bruite pas le signal EEG que l'on mesure. Des activités musculaires qui peuvent sembler dérisoires polluent en réalité fortement les données, c'est le cas des mouvements oculaires par exemple. Essayer, dans la mesure du possible, de ne pas parler, déglutir ou cligner des yeux, mais faites-le durant les quelques secondes de pause entre les essais.

Nous allons commencer par un entraînement pour vérifier que les instructions ont été claires.

Avant l'entraînement, avez-vous des questions ?

# Questionnaires pré-session 1

<b>ID participant :</b> ..... <b>Date :</b> ..... / ..... / ..... <b>Session :</b> 1
--

Veillez indiquer vos préférences d'utilisation des mains dans les activités suivantes en mettant + dans la colonne correspondante. Lorsque la préférence est si marquée que vous n'utiliserez l'autre main que si vous ne pouvez faire autrement, mettez ++. Dans le cas où une tâche ou un geste sont réalisés indifféremment par les deux mains, mettre + dans les deux colonnes.

Certaines activités nécessitent les deux mains. Dans ce cas, la partie de la tâche, ou de l'objet, pour lequel une préférence manuelle est nécessaire est indiquée entre parenthèses.

Veillez essayer de répondre à toutes les questions, et laissez un blanc seulement dans le cas où vous n'avez aucune expérience de l'activité ou de l'usage de l'objet.

**Femme**      **Homme**

--	--

**ans**

--

	Oui
TDA-H	
Syndrome des jambes sans repos	
Épilepsie	
Schizophrénie	
AVC	

**3 : Si vous présentez (ou avez présenté) un de ces troubles, veuillez cocher la case associée**

**1 : Sexe**

**2 : Âge**

--	--

**Oui**      **Non**

**4 : Avez-vous subi une intervention chirurgicale du système nerveux central ?**

--	--

**Oui**      **Non**

**5 : Avez-vous déjà participé à une expérience sur une interface cerveau-ordinateur ?**

Items	Gauche	Droite
Ecrire		
Dessiner		
Lancer (un objet ou une balle)		
Tenir des ciseaux (et découper)		
Se brosser les dents		
Se servir d'un couteau (sans fourchette)		
Se servir d'une cuillère		
Se servir d'un balai (main au dessus)		
Allumer une allumette		
Ouvrir le couvercle d'une boîte (main sur le couvercle)		
<b>Total croix</b>		

**QL : .....**

Pour chacune des questions, merci de répondre en accord avec votre état actuel, en cochant la case associée ou en renseignant la valeur approximative correspondante.

**1 : Dans quel état d'éveil estimez-vous vous trouver ?**

Très peu en forme		Très en forme		
<input type="checkbox"/>	<input type="checkbox"/>	<input type="checkbox"/>	<input type="checkbox"/>	<input type="checkbox"/>
1	2	3	4	5

**2 : Dans quel état de fatigue estimez-vous vous trouver ?**

Très peu fatigué.e		Très fatigué.e		
<input type="checkbox"/>	<input type="checkbox"/>	<input type="checkbox"/>	<input type="checkbox"/>	<input type="checkbox"/>
1	2	3	4	5

**3 : Comment qualifieriez-vous l'orientation de votre humeur ?**

Très négative		Très positive		
<input type="checkbox"/>	<input type="checkbox"/>	<input type="checkbox"/>	<input type="checkbox"/>	<input type="checkbox"/>
1	2	3	4	5

**4 : Comment qualifieriez-vous l'intensité de vos émotions ?**

Très peu intenses		Très intenses		
<input type="checkbox"/>	<input type="checkbox"/>	<input type="checkbox"/>	<input type="checkbox"/>	<input type="checkbox"/>
1	2	3	4	5

**5 : Combien d'heures avez-vous dormi la nuit dernière ?**

**6 : Habituellement, combien d'heures dormez-vous la nuit ?**

**7 : Combien de doses de stimulants avez-vous consommé dans les 12 dernières heures ?**

**8 : Dont combien de doses dans les 2 dernières heures ?**

Plutôt inhabituel (j'en prends moins)	Habituel	Plutôt inhabituel (j'en prends plus)
<input type="checkbox"/>	<input type="checkbox"/>	<input type="checkbox"/>

**9 : Est-ce normal par rapport à votre consommation habituelle ?**

Aujourd'hui	Hier	Ni l'un ni l'autre
<input type="checkbox"/>	<input type="checkbox"/>	<input type="checkbox"/>

**10 : Quand avez-vous consommé des drogues ou traitements médicamenteux pour la dernière fois ?**

Moins de 2h	<input type="checkbox"/>
Entre 2h et 3h	<input type="checkbox"/>
Entre 3h et 4h	<input type="checkbox"/>
Entre 4h et 5h	<input type="checkbox"/>
Plus de 5h	<input type="checkbox"/>

**11 : À quand remonte votre dernier repas ?**

# Questionnaires pré-session 2

ID participant : .....  
 Date : ..... / ..... / .....  
 Session : 2

Pour chacune des questions, merci de répondre en accord avec votre état actuel, en cochant la case associée ou en renseignant la valeur approximative correspondante.

--

8 : Dont combien de doses dans les 2 dernières heures ?

	Très peu en forme		Très en forme		
	1	2	3	4	5

1 : Dans quel état d'éveil estimez-vous vous trouver ?

	Très peu fatigué.e		Très fatigué.e		
	1	2	3	4	5

2 : Dans quel état de fatigue estimez-vous vous trouver ?

	Très négative		Très positive		
	1	2	3	4	5

3 : Comment qualifieriez-vous l'orientation de votre humeur ?

	Très peu intenses		Très intenses		
	1	2	3	4	5

4 : Comment qualifieriez-vous l'intensité de vos émotions ?

--

5 : Combien d'heures avez-vous dormi la nuit dernière ?

--

6 : Habituellement, combien d'heures dormez-vous la nuit ?

--

7 : Combien de doses de stimulants avez-vous consommé dans les 12 dernières

Plutôt inhabituel (j'en prends moins)	Habituel	Plutôt inhabituel (j'en prends plus)

9 : Est-ce normal par rapport à votre consommation habituelle ?

Aujourd'hui	Hier	Ni l'un ni l'autre

10 : Quand avez-vous consommé des drogues ou traitements médicamenteux pour la dernière fois ?

Moins de 2h	
Entre 2h et 3h	
Entre 3h et 4h	
Entre 4h et 5h	
Plus de 5h	

11 : À quand remonte votre dernier repas ?

# Questionnaires pré-session 3

Pour chacune des questions, merci de répondre en accord avec votre état actuel, en cochant la case associée ou en renseignant la valeur approximative correspondante.

ID participant : .....  
 Date : ..... / ..... / .....  
 Session : 3

8 : Dont combien de doses dans les 2 dernières heures ?

Très peu en forme		Très en forme	
1	2	3	4
			5

1 : Dans quel état d'éveil estimez-vous vous trouver ?

Très peu fatigué.e		Très fatigué.e	
1	2	3	4
			5

2 : Dans quel état de fatigue estimez-vous vous trouver ?

Très négative		Très positive	
1	2	3	4
			5

3 : Comment qualifieriez-vous l'orientation de votre humeur ?

Très peu intenses		Très intenses	
1	2	3	4
			5

4 : Comment qualifieriez-vous l'intensité de vos émotions ?

5 : Combien d'heures avez-vous dormi la nuit dernière ?

6 : Habituellement, combien d'heures dormez-vous la nuit ?

7 : Combien de doses de stimulants avez-vous consommé dans les 12 dernières heures ?

Plutôt inhabituel (j'en prends moins)	Habituel	Plutôt inhabituel (j'en prends plus)

9 : Est-ce normal par rapport à votre consommation habituelle ?

Aujourd'hui	Hier	Ni l'un ni l'autre

10 : Quand avez-vous consommé des drogues ou traitements médicamenteux pour la dernière fois ?

Moins de 2h	
Entre 2h et 3h	
Entre 3h et 4h	
Entre 4h et 5h	
Plus de 5h	

11 : À quand remonte votre dernier repas ?

# Questionnaires pré-session 4

Pour chacune des questions, merci de répondre en accord avec votre état actuel, en cochant la case associée ou en renseignant la valeur approximative correspondante.

ID participant : .....  
 Date : ..... / ..... / .....  
 Session : 4

8 : Dont combien de doses dans les 2 dernières heures ?

Très peu en forme		Très en forme		
1	2	3	4	5

1 : Dans quel état d'éveil estimez-vous vous trouver ?

Très peu fatigué.e		Très fatigué.e		
1	2	3	4	5

2 : Dans quel état de fatigue estimez-vous vous trouver ?

Très négative		Très positive		
1	2	3	4	5

3 : Comment qualifieriez-vous l'orientation de votre humeur ?

Très peu intenses		Très intenses		
1	2	3	4	5

4 : Comment qualifieriez-vous l'intensité de vos émotions ?

5 : Combien d'heures avez-vous dormi la nuit dernière ?

6 : Habituellement, combien d'heures dormez-vous la nuit ?

7 : Combien de doses de stimulants avez-vous consommé dans les 12 dernières heures ?

Plutôt inhabituel (j'en prends moins)	Habituel	Plutôt inhabituel (j'en prends plus)
<input type="text"/>	<input type="text"/>	<input type="text"/>

9 : Est-ce normal par rapport à votre consommation habituelle ?

Aujourd'hui	Hier	Ni l'un ni l'autre
<input type="text"/>	<input type="text"/>	<input type="text"/>

10 : Quand avez-vous consommé des drogues ou traitements médicamenteux pour la dernière fois ?

Moins de 2h	<input type="text"/>
Entre 2h et 3h	<input type="text"/>
Entre 3h et 4h	<input type="text"/>
Entre 4h et 5h	<input type="text"/>
Plus de 5h	<input type="text"/>

11 : À quand remonte votre dernier repas ?

# Questionnaire post-session 1

ID participant : ..... Date : ..... / ..... / ..... Session : 1
---

Pour chacune des questions, merci de répondre en accord avec votre état actuel, en cochant la case associée.

1 : Dans quel état d'éveil estimez-vous vous trouver ?	Très peu en forme				Très en forme
	1	2	3	4	5

2 : Dans quel état de fatigue estimez-vous vous trouver ?	Très peu fatigué.e				Très fatigué.e
	1	2	3	4	5

3 : Comment qualifieriez-vous l'orientation de votre humeur ?	Très négative				Très positive
	1	2	3	4	5

4 : Comment qualifieriez-vous l'intensité de vos émotions ?	Très peu intenses				Très intenses
	1	2	3	4	5

5 : Pensez-vous avoir cligné des yeux, ou avalé pendant les essais ?	Non	Oui, rarement	Oui, souvent
	1	2	3

6 : Pensez-vous avoir bougé les bras ou mains pendant les essais ?	Non	Oui, rarement	Oui, souvent
	1	2	3

7 : De façon générale, qu'avez-vous pensé du volume des musiques diffusées	Il était beaucoup trop faible	Il me convenait			Il était beaucoup trop élevé
	1	2	3	4	5

8 : À quel point avez-vous apprécié les musiques diffusées ?	Pas du tout				Énormément
	1	2	3	4	5

9 : Que vous ont évoqué les musiques diffusées ?	Commentaire libre : ..... ..... ..... ..... .....
--	---

10 : À quel point vous étiez-vous concentré.e sur la musique au lieu des stimulations sur les poignets ?	Pas du tout				Énormément
	1	2	3	4	5



**11 : Les stimulations sur les poignets vous ont-elles dérangé.e pour vous concentrer sur la musique ?**

	<b>Pas du tout</b>		<b>Énormément</b>	
	1	2	3	4
				5

**12 : À quel point vous a-t-il été difficile d'ignorer les stimulations sur les poignets ?**

	<b>Pas du tout</b>		<b>Énormément</b>	
	1	2	3	4
				5

**13 : À quel point les stimulations sur les poignets vous ont été désagréables ?**

	<b>Pas du tout</b>		<b>Énormément</b>	
	1	2	3	4
				5

**14 : À quel point les stimulations sur les poignets vous ont été douloureuses ?**

	<b>Pas du tout</b>		<b>Énormément</b>	
	1	2	3	4
				5

**15 : Si vous avez des commentaires sur la session qui vient de se dérouler, merci de les indiquer ici :**

<b>Commentaire libre :</b> ..... ..... ..... ..... .....
--

# Questionnaire post-session 2

ID participant : .....
Date : ..... / ..... / .....
Session : 2

Pour chacune des questions, merci de répondre en accord avec votre état actuel, en cochant la case associée.

**1 : Dans quel état d'éveil estimez-vous vous trouver ?**

Très peu en forme					Très en forme
1	2	3	4	5	

**2 : Dans quel état de fatigue estimez-vous vous trouver ?**

Très peu fatigué.e					Très fatigué.e
1	2	3	4	5	

**3 : Comment qualifieriez-vous l'orientation de votre humeur ?**

Très négative					Très positive
1	2	3	4	5	

**4 : Comment qualifieriez-vous l'intensité de vos émotions ?**

Très peu intenses					Très intenses
1	2	3	4	5	

**5 : Pensez-vous avoir cligné des yeux, ou avalé pendant les essais ?**

Non	Oui, rarement	Oui, souvent

**6 : Pensez-vous avoir bougé les bras ou mains pendant les essais ?**

Non	Oui, rarement	Oui, souvent

**7 : À quel point les stimulations sur les poignets vous ont été désagréables ?**

Pas du tout					Énormément
1	2	3	4	5	

**8 : À quel point les stimulations sur les poignets vous ont été douloureuses ?**

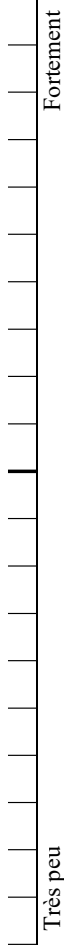
Pas du tout					Énormément
1	2	3	4	5	

**9 : Si vous avez des commentaires sur la session qui vient de se dérouler, merci de les indiquer ici :**

<b>Commentaire libre :</b> .....
.....
.....
.....
.....

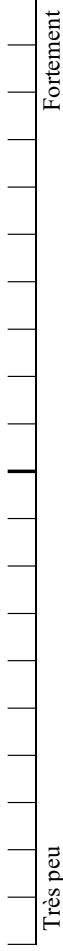
Demande mentale

À quel point la tâche était-elle exigeante mentalement ?



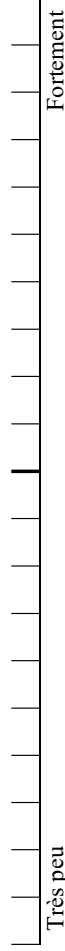
Demande physique

À quel point la tâche était-elle exigeante physiquement ?



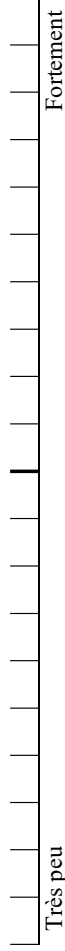
Demande temporelle

À quel point le rythme de la tâche était-il hâtant ou pressant ?



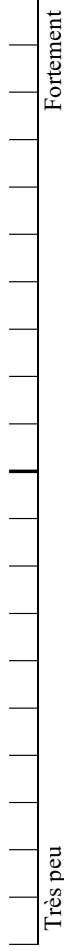
Performance

Quel était votre degré de réussite lorsque vous accomplissiez ce qu'il vous était demandé ?



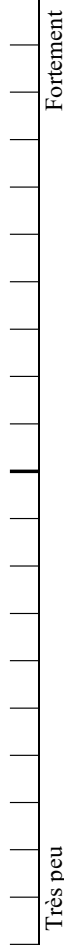
Effort

Quel était le degré d'intensité de l'effort que vous avez fourni pour atteindre ce niveau de performance ?



Frustration

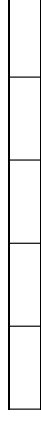
À quel point vous sentiez-vous dans la précarité, découragé.e, exaspéré.e, stressé.e ou contrarié.e ?



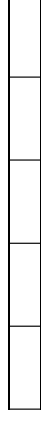
Pas du tout d'accord



1 : Je n'ai pas trouvé ces instructions très contraignantes à suivre



2 : J'ai trouvé ces instructions inutilement complexes



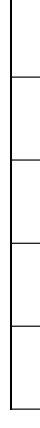
3 : J'ai trouvé ces instructions difficiles à suivre



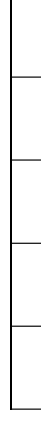
4 : Je pense que j'aurais besoin d'aide pour être capable de suivre ces instructions



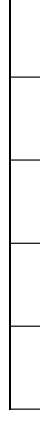
5 : Je suppose que la plupart des personnes apprendraient très rapidement à suivre ces instructions



6 : J'ai trouvé qu'il y avait trop d'incohérence dans ces instructions



7 : Je me suis senti.e très confiant.e en suivant ces instructions



8 : J'ai dû poser des questions pour comprendre ces instructions

Tout à fait d'accord

# Questionnaire post-session 3

<b>ID participant : .....</b> <b>Date : ..... / ..... / .....</b> <b>Session : 3</b>
--

Pour chacune des questions, merci de répondre en accord avec votre état actuel, en cochant la case associée.

<b>1 : Dans quel état d'éveil estimez-vous vous trouver ?</b>	<b>Très peu en forme</b>	<b>Très en forme</b>			
	1	2	3	4	5

<b>2 : Dans quel état de fatigue estimez-vous vous trouver ?</b>	<b>Très peu fatigué.e</b>	<b>Très fatigué.e</b>			
	1	2	3	4	5

<b>3 : Comment qualifieriez-vous l'orientation de votre humeur ?</b>	<b>Très négative</b>	<b>Très positive</b>			
	1	2	3	4	5

<b>4 : Comment qualifieriez-vous l'intensité de vos émotions ?</b>	<b>Très peu intenses</b>	<b>Très intenses</b>			
	1	2	3	4	5

<b>5 : Pensez-vous avoir cligné des yeux, ou avalé pendant les essais ?</b>	<b>Non</b>	<b>Oui, rarement</b>	<b>Oui, souvent</b>

<b>6 : Pensez-vous avoir bougé les bras ou mains pendant les essais ?</b>	<b>Non</b>	<b>Oui, rarement</b>	<b>Oui, souvent</b>

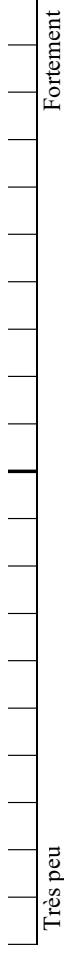
<b>7 : À quel point les stimulations sur les poignets vous ont été désagréables ?</b>	<b>Pas du tout</b>	<b>Énormément</b>			
	1	2	3	4	5

<b>8 : À quel point les stimulations sur les poignets vous ont été douloureuses ?</b>	<b>Pas du tout</b>	<b>Énormément</b>			
	1	2	3	4	5

<b>9 : Si vous avez des commentaires sur la session qui vient de se dérouler, merci de les indiquer ici :</b>	<b>Commentaire libre :</b> .....
	.....
	.....
	.....
	.....

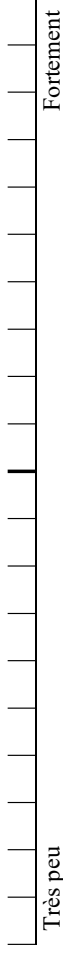
Demande mentale

À quel point la tâche était-elle exigeante mentalement ?



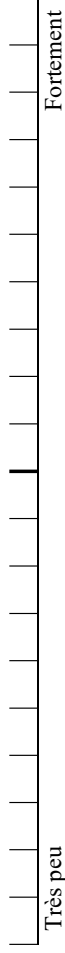
Demande physique

À quel point la tâche était-elle exigeante physiquement ?



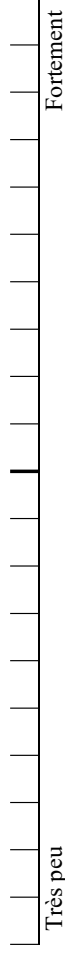
Demande temporelle

À quel point le rythme de la tâche était-il hâtant ou pressant ?



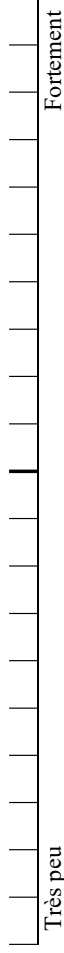
Performance

Quel était votre degré de réussite lorsque vous accomplissiez ce qu'il vous était demandé ?



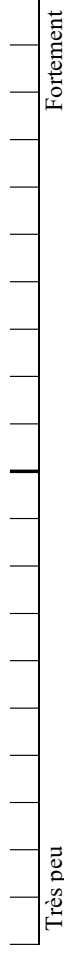
Effort

Quel était le degré d'intensité de l'effort que vous avez fourni pour atteindre ce niveau de performance ?

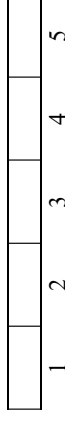


Frustration

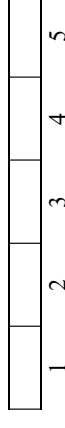
À quel point vous sentiez-vous dans la précarité, découragé.e, exaspéré.e, stressé.e ou contrarié.e ?



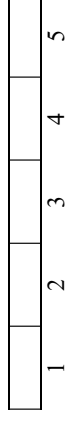
Pas du tout d'accord



1 : Je n'ai pas trouvé ces instructions très contraignantes à suivre



2 : J'ai trouvé ces instructions inutilement complexes



3 : J'ai trouvé ces instructions difficiles à suivre



4 : Je pense que j'aurais besoin d'aide pour être capable de suivre ces instructions



5 : Je suppose que la plupart des personnes apprendraient très rapidement à suivre ces instructions



6 : J'ai trouvé qu'il y avait trop d'incohérence dans ces instructions



7 : Je me suis senti.e très confiant.e en suivant ces instructions



8 : J'ai dû poser des questions pour comprendre ces instructions

Tout à fait d'accord

# Questionnaire post-session 4

ID participant : .....
Date : ..... / ..... / .....
Session : 4

Pour chacune des questions, merci de répondre en accord avec votre état actuel, en cochant la case associée.

**1 : Dans quel état d'éveil estimez-vous vous trouver ?**

Très peu en forme					Très en forme
1	2	3	4	5	

**2 : Dans quel état de fatigue estimez-vous vous trouver ?**

Très peu fatigué.e					Très fatigué.e
1	2	3	4	5	

**3 : Comment qualifieriez-vous l'orientation de votre humeur ?**

Très négative					Très positive
1	2	3	4	5	

**4 : Comment qualifieriez-vous l'intensité de vos émotions ?**

Très peu intenses					Très intenses
1	2	3	4	5	

**5 : Pensez-vous avoir cligné des yeux, ou avalé pendant les essais ?**

Non	Oui, rarement	Oui, souvent

**6 : Pensez-vous avoir bougé les bras ou mains pendant les essais ?**

Non	Oui, rarement	Oui, souvent

**7 : À quel point les stimulations sur les poignets vous ont été désagréables ?**

Pas du tout					Énormément
1	2	3	4	5	

**8 : À quel point les stimulations sur les poignets vous ont été douloureuses ?**

Pas du tout					Énormément
1	2	3	4	5	

**9 : Si vous avez des commentaires sur la session qui vient de se dérouler, merci de les indiquer ici :**

<b>Commentaire libre :</b> .....
.....
.....
.....
.....

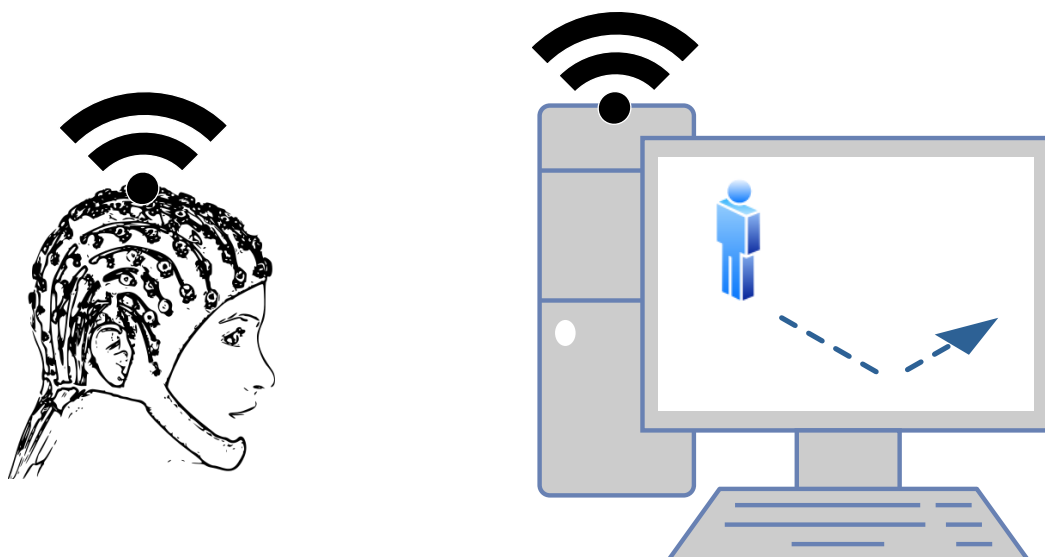


# Recherche de participant.e.s

## Expérience Interface Cerveau-Ordinateur

L'équipe BCI du laboratoire CRIStAL recherche des participant.e.s pour une **expérience** sur les **interfaces cerveau-ordinateur** exploitant le **sens du toucher** pour pallier les **handicaps moteurs sévères**.

Objectif d'une Interface Cerveau-Ordinateur ?  
**Contrôle sans activité musculaire !**



**Quand :** dans l'année scolaire 2020 - 2021

4 sessions de 2h, espacées d'une à deux semaines.

Un agenda sera mis en place avec vous, pour plus de flexibilité.

**Où :** CHRU de Lille (Terminus métro ligne 1 - CHU Eurasanté)

**Rémunération :** non, mais vous faites avancer la science \\_(ツ)\_/

Plus d'information :



**Vous pouvez participer si :**

- Vous avez entre 18 et 75 ans.
- Vous vous engagez à participer à l'entièreté de l'étude (4 sessions).
- Vous donnez votre consentement éclairé (signature d'un formulaire).

(\*) à noter que certaines situations médicales ou administratives interdisent la participation à ce type d'étude.

Contact :

jimmy.petit@  
univ-lille.fr





## E.8 DÉTAILS COMPLÉMENTAIRES AU PROTOCOLE EXPÉRIMENTAL

E.8.1 *Détails à propos de la stimulation utilisée*

La stimulation est générée par un transducteur mécanique, identique à celui utilisé dans [84]. Ces transducteurs respectent la norme de sécurité EN 60601-1:2006 pour matériel électrique médical. Ils ont une surface de contact vibrante et circulaire de 7 mm de diamètre, et sont positionnés sur les poignets droit et gauche des sujets. La stimulation sera effectuée à une fréquence proche de 275 Hz, pour maximiser la réponse des corpuscules de Pacini [94] tout en utilisant la fréquence de résonance de nos transducteurs. Cette stimulation est également modulée en amplitude par un signal carré d'une fréquence inférieure, entre 14 Hz et 32 Hz. Ainsi, la stimulation réelle peut-être décrite comme une succession de pulsations mécaniques à 275 Hz modulées par une enveloppe de fréquence située entre 14 Hz et 32 Hz.

E.8.2 *Matériels et méthodes utilisés pour les sessions*

- 64 électrodes au chlorure d'argent (Ag\AgCl)
- Les 64 positions permises par le système, avec référence et *ground*.
- Vérification des impédances avant et après chaque sessions d'enregistrement, pour toutes les sessions.
- Solution EEG : eego™sports (ANT Neuro, Netherlands)
- Fréquence d'échantillonnage 512 Hz
- Filtre analogique passe-haut à 0.5 Hz et filtre numérique passe-haut à 0.5 Hz, filtre passe-bas à 35 Hz
- Transducteurs (C-2 tactors, Engineering Acoustics, Inc.)
- Bracelets de montre et une impression 3D (utilisant un polymère biodégradable, le PLA - *PolyLactic Acid*) pour maintenir les transducteurs aux poignets, cf figure e.5.
- Les sujets ne bénéficieront pas de compensation financière pour leur participation.



Figure E.5 : Photo du transducteur et de son support sur un poignet, au repos.

## E.9 DÉTAILS CONCERNANT LE CHOIX DES MUSIQUES DE RELAXATION UTILISÉES

Comme précisés précédemment, nos choix expérimentaux pour la session de calibration se basent sur un protocole proposé et implémenté dans [84]. Cependant, les auteurs ne précisent pas les musiques utilisées. Nous utiliserons donc un ensemble de musique de relaxation issu des travaux de Tan *et al.* [99]. Dans leurs travaux, les auteurs ont demandé à un groupe de 5 praticiens de musicothérapie de proposer 6 musiques de relaxation. Ces thérapeutes venaient de différents états des États-Unis et de différents milieux professionnels : certains pratiquent dans des hôpitaux et d'autres sont des professeurs de musicothérapie, par exemple. Toutes les musiques provenaient d'un usage fréquent dans leurs pratiques cliniques au cours desquelles un effet de relaxation a été observé. Ainsi, un corpus de 30 musiques a été réuni. Les auteurs ont par la suite conduit d'autres études pour mesurer la relaxation engendrée par l'écoute de ces musiques ainsi que de leurs propriétés psychoacoustiques par 9 thérapeutes en musicothérapie, tous certifiés par un comité : le *Certification Board for Music Therapist (CBMT)*. Après évaluation des musiques selon différents critères : préférence, familiarité, degrés de relaxation, tempo, rythme, complexité mélodique, ... un total de 10 musiques parmi les 30 n'ont pas été gardées pour la suite de leurs travaux parce qu'elles ont obtenu une note médiane en relaxation produite inférieure ou égale à 5 (sur 10), ce qui correspond à des musiques modérément ou faiblement relaxantes.

Ce sont ces 20 musiques restantes que nous utiliserons en tant que musique de relaxation dans notre expérience. Le nom des musiques, des auteurs, des albums et leurs durées sont reportés dans le tableau e.3. La durée totale de toutes les musiques est de 209 minutes et 19 secondes, la durée de notre session de calibration ne dépassera pas les 50 minutes. Sur ces 20 musiques, nous ne garderons que les musiques les plus courtes pour composer une sélection de musique d'une durée de 50 minutes; ces musiques sont annotées par un astérisque. Dans leurs expériences, Pokorny *et al.* [84], ont utilisé des extraits représentatifs de 3 minutes des musiques. En ne gardant que les musiques les plus courtes, nous nous rapprochons des extraits ayant été évalués.

	Müller-Putz <i>et al.</i> [62]	Notre protocole	Idtq.
Matériel			
Nombre d'électrodes (sans Référence ni <i>Ground</i> )	6	64	Non
Position des électrodes	2,5 cm antérieur et postérieur à C3, Cz et C4	64 positions permise par le système, avec référence et <i>ground</i>	Non
Composition des électrodes	Or	Chlorure d'argent (Ag\AgCl)	Non
Fréquence d'échantillonnage	200 Hz	512 Hz	Non
Vérification des impédances	Temps réelle : $\leq 5 \text{ k}\Omega$	Avant et après chaque sessions	Non
Solution EEG	Bipolar amplifier (Raich, Graz, Austria)	eego <sup>TM</sup> sports (ANT Neuro, Netherlands)	Non
Compensation financière	Oui (NS)	Non	Non
Transducteur mécanique	12 mm, QMB-105 Star Micronics America, Inc., Edison, NJ	C-2 factors (Engineering Acoustics, Inc.)	Non
Matériels sur batterie	Non	Oui, tout est sur batterie (amplificateur, transducteur, ...)	Non
Session de calibration			
Partie du corps stimulé	Index	Poignets	Non
Rapide entretiens pré-expérience	Oui	Oui	Oui
Référence à chaque essai	Oui, quatre première secondes	Oui, quatre première secondes	Oui
Fréquences testées	17 à 35 Hz, par pas de 2 Hz	14 à 32 Hz, par pas de 3 Hz	Non
Assignation des fréquences	Croissant	Aléatoire	Non
Demandé aux sujets de limiter leurs activités musculaires	Oui	Oui	Oui
Durée d'un essai	24 s	21,5 s	Non
Nombre de bloc	8	4	Non
Nombre d'essai par bloc	20	20	Oui
Durée moyenne d'un bloc	480 s	563 s	Non
Assignation index/poignet	8 blocs sur l'index droit	Autant de stimulation sur les deux poignets	Non
Durée des pauses entre les blocs	Courte pause entre les blocs 4 et 5 (NS)	Minimum de 3 minutes	Non
Durée de la session	64 min d'enregistrement	1 720 s d'enregistrement et minimum de 1 072 s de pause (minimum total 46 min)	Non
Session de test			
Partie du corps stimulé	Index	Poignets	Non
Référence à chaque essai	Oui, deux première secondes	Oui, deux première secondes	Oui
Débuts des vibrations à $t = 2 \text{ s}$	Oui	Oui	Oui
Indication du poignet cible à $t = 3 \text{ s}$	Oui, flèche à l'écran	Oui, flèche à l'écran	Oui
Tâche secondaire pour aide à la concentration	Oui	Oui	Oui
Détail tâche secondaire	A $t = 5,7 \text{ s}$ , présence aléatoire d'une variation dans l'amplitude de la vibration pendant 0,125 s. Le sujet doit indiquer si a ressenti le changement en fin d'essai	Depuis $t = 5 \text{ s}$ , présence aléatoire d'une diminution dans l'amplitude de la stimulation, sur le poignet d'intérêt pour l'essai.	Non
Attribution des fréquences pseudo-résonante	Index droit, l'index gauche à la même fréquence que l'index droit mais réduite de 5 Hz.	Poignet droit (50%) ou gauche (50%), l'autre poignet reçoit la même fréquence réduite de 5 Hz (dépendent des résultats de la calibration).	Non
Délai de durée aléatoire entre les essais	Oui (NS)	Oui, $U(2, 4)$ secondes	NS
Nombre de session	Entre 3 et 4, en fonction du sujet	1	Non
Durée d'un essai	6,2 s (sans délai)	7 s (sans délai), $U(9, 11)$ avec délai.	NS
Feedback auditif	Oui (sauf première session)	Non	Non

Table E.1 : Différences et similitudes dans les protocoles expérimentaux, entre les travaux de Müller-Putz *et al.* [62] et le protocole proposé. NS pour « Non Spécifié » relatif à un montant ou à une durée.

	Notre protocole
Session de <i>gating</i>	
Partie du corps stimulé	Poignets
Référence à chaque essai	Oui, deux premières secondes
Débuts des vibrations	Oui, à $t = 2$ s
Indication du/des poignet cible	Oui, flèche à l'écran, à $t = 3$ s
Délai de durée aléatoire entre les essais	Oui, $\mathcal{U}(6, 8)$ secondes
Nombre de session	1
Durée d'un essai A	8 s (sans délai), $\mathcal{U}(14, 16)$ avec délai.
Durée d'un essai B/C	9 s (sans délai), $\mathcal{U}(15, 17)$ avec délai.
<i>Feedback</i> (Bloc A)	Non
<i>Sham Feedback</i> (Bloc B)	80% correct et 20% incorrect
<i>Feedback</i> (Bloc C)	Oui
Nombre d'essais par bloc	20, pour chaque type de bloc
Durée moyenne d'un bloc	293 s (A) et 313 s (B/C)
Durée moyenne d'une session	1 040 s d'enregistrement et 1 698 s de pause, soit 2 738 s ( $\approx 46$ min).
Session d'application	
Partie du corps stimulé	Poignets
Application	Contrôle de Kart virtuel
Nombre de session	1
Durée de la session	$\approx 45$ min, sans le temps d'installation
<i>Feedback</i>	Oui

Table E.2 : Détails expérimentaux pour nos sessions de *gating* et d'application. La partie matériel est identique au tableau e.1.

Titre	Artistes	Album	Durée
Concerto In C Minor For Oboe And Orchestra	Philadelphia Orchestra	Old Album title: First Chair Encores	10:26
<b>Air From Orchestral Suite No. 3</b>	<b>Philadelphia Orchestra</b>	<b>Bach Favorites</b>	<b>05:43</b>
<b>Bach Prelude I (The Well-Tempered Clavier)</b>	<b>Christopher Parkening</b>	<b>Parkening Plays Bach</b>	<b>01:59</b>
Dreaming And Sleep	Steven Roach	Quiet Music 3	29:30
Going Home Medley	Daniel Kobialka	Going Home Again	15:34
Into the Silence of My Being	Chuck Wild	Liquid Mind VII: Reflection	12:33
Jesu, Joy of Man's Desiring	Daniel Kobialka	Velvet Dreams	17:29
<b>Kaluhyanu:Wes</b>	<b>Joanne Shenandoah</b>	<b>Peace &amp; Power</b>	<b>03:28</b>
Mirror Veil	Chuck Wild	Liquid Mind: Slow World	16:54
Pachelbel Kanon	Daniel Kobialka	Timeless Motion	22:52
(Pachalbel's) Canon in D	Dan Gilbson	Exploring Nature with Music: The Classics	08:02
<b>Salvation Is Created (Spaséniye sodélal), for choir, Op. 25/5</b>	<b>Cathedral Choral Society of the National Cathedral</b>	<b>Millennium: Russian Choral Music</b>	<b>05:20</b>
<b>Santa Ynez</b>	<b>John Erickson</b>	<b>Contemplation</b>	<b>06:09</b>
<b>Soul Mates</b>	<b>Danny Wright</b>	<b>Soul Mates (from 2001)</b>	<b>03:06</b>
<b>Spectrum Suite</b>	<b>Steven Halpern</b>	<b>Among Friends: Collection, Vol. 1</b>	<b>03:05</b>
<b>Prelude on Welsh Hymn Tunes for organ No. 2 (G major) and 3 (C major)</b>	<b>Northern Sinfonia of England</b>	<b>Hickox conducts Vaughan Williams</b>	<b>06:24</b>
<b>Cantique de Jean Racine, for 4-part chorus</b>	<b>organ (or orchestra), Op. 11</b>	<b>The Choir of new College Oxford &amp; Agnus Dei Vol. 1</b>	<b>04:56</b>
Satie: Trois Gymnopedies	Daniel Kobialka	Fragrances of a Dream	23:16
<b>When you wish upon a star</b>	<b>Daniel Kobialka</b>	<b>When you Wish Uppon a Star</b>	<b>07:16</b>
<b>Winds of Peace</b>	<b>Lisa Lynne Franco</b>	<b>New Morning</b>	<b>05:17</b>

Table E.3 : Corpus de musiques de relaxation, classées par ordre alphabétique. Celles utilisées dans notre session de calibration sont affichées en gras. Modifié depuis [99]. Nous avons dû actualiser certains noms. La plus grosse incertitude réside avec les *Prelude on Welsh Hymn Tunes*, dans le papier d'origine ils sont mentionnés comme « Three prelude on Welsh Hymn », or dans l'album *Hickox conducts Vaughan Williams*, il n'y a que deux préludes *On Welch Hymn* pour orgue. Nous les avons donc reportés dans le tableau. Les informations supplémentaires apportées au tableau proviennent de deux sites internet : *allmusic.com* et *discogs.com*, consulté le 31 octobre 2019.

## LIST OF FIGURES

---

- Figure 1.1 Illustration of the interaction loop of the proposed active and reactive BCI. 5
- Figure 1.2 Thesis contributions overview. This figure will be used as a roadmap for this dissertation [43, 75]. 6
- Figure 2.1 Histogram of the number of publications per year from the PubMed database with the keywords “steady-state somatosensory” in “all fields” the 24th of August 2021. 13
- Figure 2.2 PRISMA-based article inclusion: identification, screening and inclusion stages. 14
- Figure 2.3 Temporal characteristics of an theoretical SEP reaching its steady-state. (a) The “stimulus” plot is the representation of the periodical somatosensory stimulus amplitude *vs.* time, considered here as a windowed sine function. (b) Representation of an ideal SEP elicited by the stimulus, *i. e.* an amplitude modulated sine function without noise. (c) Zoom on the plots (a) and (b) around the beginning of the SEP. It shows the phase difference between the SEP and the stimulus. 19
- Figure 2.4 Temporal characteristics of an SEP reaching its steady-state. (a) Grand average over 14 subjects and 40 min of 20 Hz stimulus train on the right index finger for 2 s, with a 5 s inter-trial interval. (b) Zoom on the first half second of the grand average, clear component of the SEP are annotated. (c) Zoom on an SSSEP-established period, 4 periods of the 20 Hz-SSSEP are well visible over 0.2 s of signal. All data is presented from CP1 and as mean  $\pm$  SEM. Figure reproduced with the appreciated authorisation of the authors from [15]. 19
- Figure 2.5 Grand average of SSSEP amplitudes, calculated across subjects and attention-related experimental condition (one-hand attended, one-hand ignored and both-hand attended). Figure reproduced with the appreciated authorisation of the authors from [71]. 31
- Figure 3.1 Illustration of CCA computation 46

- Figure 3.2 Influence of sinusoids amplitude on the ratio of amplitudes at target frequency estimated during active and idle periods for a fixed Gaussian noise level. The targeted sinusoidal signal has a frequency of 20 Hz and a random phase in  $]-\pi, \pi]$ . The second sinusoidal component, treated as noise in the simulation, is at 25 Hz with a random phase in  $]-\pi, \pi]$ . The Gaussian noise standard deviation is fixed at  $6.3 \times 10^{-7} V$  to have an SNR of 1 dB over  $C_3$  when  $A_{0,active} = 1 \mu V$  – see (3.10). One relative standard deviation is displayed in a colour lighter than the one of the average curve, computed as  $\frac{1}{\ln(10)} \frac{Std(x)}{\bar{x}}$ . The light grey area displays the x-axis interval where the linear regressions are calculated in order to find the divergence point. 50
- Figure 3.3 Examples of spatial filters computed by the CCA and PLS as the SNR level increases. They are estimated on a single noise realisation and are normalised to have a maximum coefficient of 1.0. 51
- Figure 3.4 Spatial filters resulting from the electrode selection, Small Laplacian, and computed by the Current Source Density at  $C_3$ . 51
- Figure 3.5 Attention Focusing session timeline. Each block lasts approximately 5 minutes. Blocks are interspersed with three-minutes breaks. One block consists of 20 trials. One trial contains a 2-second long idle period (no stimulation, idle) and a 5-second long active attention focusing period (with stimulations at different frequencies on both wrists). 52
- Figure 3.6 Comparison of amplitude estimators on real EEG data. Legend – RAI: Relative Amplitude Increase, FOSR: Frequency Of Stimulation of Right wrist. 55
- Figure 4.1 (a) Vibro-tactile tactors tapped on the subject’s wrists. (b) Stimulation box: a micro-controller that powers vibro-tactile tactors and connected to a computer. 64
- Figure 4.2 Timeline of the screening session. Each block contains 20 trials and blocks are separated by 3-minute breaks. 65

- Figure 4.3 Grand Average of RAI according to two different referencing modes. The first line shows the RAI to the Reference period (*i. e.* without stimulation). The second line shows the RAI to the non-condition (NC) period. Error bars show 95% confidence interval (computing using 1000 bootstraps). 68
- Figure 4.4 Relative amplitude increase to the Reference period (first row) and non-condition (second row) from the screening procedure of subject #10. Error bars show 95% confidence interval (computing using 1000 bootstraps). 70
- Figure 4.5 Timeline of the somatosensory gating session. Each block contains 20 trials. Blocks are separated by 3-minute breaks. There are three possible trial types. In trials of A blocks, no feedback is given to the subject before a break lasting from 6 to 8 s. In trials of B blocks, the subject receives sham feedback 1 second before the break. In trials of C blocks, the subject receives a real feedback 1 second before the break. 71
- Figure 4.6 Subject #2: comparison of the average RAI (%) between conditions: Circle *vs.* Right, Left, and Up. Analysis windows are centred around the maximum difference between start and stop of stimulation. Lighter colours show the 95% confidence interval. 73
- Figure 4.7 (a) Distribution of the Raw-TLX scores. (b) Distribution of the individual dimension of the Raw-TLX questionnaire. 74
- Figure 4.8 Results from the behavioural data on the 5-point Likert scale item: Awakeness, Tiredness, Mood Orientation, and Mood Intensity, for the screening and somatosensory gating session, before and after the recordings. 75
- Figure 5.1 Mean classification accuracy from a thousand train-test split of the dataset with a ratio of 75%-25%. Error bars show one standard deviation. The threshold at 40% represents the chance level for a risk  $\alpha$  at 0.05 for 10 test-trials per class in a 4-class classification problem [61]. 80
- Figure 5.2 Average confusion matrices from a thousand LDA, for every subject. There are 10 test-trials per class. Predicted labels are displayed on the x-axis while True labels are on the y-axis. 80



- Figure 5.3 (a) 2-class classifications, from top to bottom: Circle *vs.* Left, Right, and Up. (b) Evolution of the mean accuracy on selected subjects versus a length increase of the analysis window. Error bars show one standard deviation. Chance level is at 70% in these conditions (risk  $\alpha$  at 0.05) [61]. 81
- Figure 6.1 Screenshots of the kart (a) on a straight line (b) at the cross section of the eight shaped. 87
- Figure 6.2 User view at the beginning of a level 2 (Turn Left induced-design). 88
- Figure 6.3 Top view of the SokoBCI levels. (a) shows level 1. Depending on the number of TL or TR used to solve the level 1, one level 2 is chosen (b) or (c). The blue squares show the possible location of the avatar, accessible with the Forward command while facing the proper direction. The red squares show the targets. The user has to orient the avatar towards a target and use the command MF to plant a tree. 89
- Figure 6.4 Stacked bar plots showing the distribution and evolution of Behavioural data over the subjects. 93
- Figure 6.5 Box plots of the Raw TLX results, grouped by the application type. The six first lines show the individual dimension of the questionnaire, while the seventh line show the score of it. 94
- Figure 6.6 Mean and 95% Confidence Interval, computed by bootstrap, of the SUS Score in regard to sham accuracy. 95
- Figure 6.7 Relationship between the adjective ratings, acceptability scores, and school grading scales, in relation to the average SUS score. From [6]. 95
- Figure A.1 Results for subject # 1. 111
- Figure A.2 Results for subject # 2. 111
- Figure A.3 Results for subject # 3. 111
- Figure A.4 Results for subject # 4. 112
- Figure A.5 Results for subject # 5. 112
- Figure A.6 Results for subject # 6. 112
- Figure A.7 Results for subject # 7. 113
- Figure A.8 Results for subject # 8. 113
- Figure A.9 Results for subject # 9. 113
- Figure A.10 Results for subject # 10. 114
- Figure A.11 Results from all subjects for easier comparison. Reference to **Reference period**. It displays only the electrodes contralateral to the stimulation side. 114

- Figure A.12 Results from all subjects for easier comparison. Reference to **Non-Condition period**. It displays only the electrodes contralateral to the stimulation side. 114
- Figure B.1 Comparison of the average relative band power increase (%) of Circle condition against Left condition. Identical y-scale between conditions for each subject. FOS are reminded in parenthesis (FOS on left wrist, FOS on right wrist). The analysis window is centred around the maximum difference between the start and end of stimulation. 115
- Figure B.2 Comparison of the average relative band power increase (%) of Circle condition against Right condition. Identical y-scale between conditions for each subject. FOS are reminded in parenthesis (FOS on left wrist, FOS on right wrist). The analysis window is centred around the maximum difference between the start and end of stimulation. 116
- Figure B.3 Comparison of the average relative band power increase (%) of Circle condition against Up condition. Identical y-scale between conditions for each subject. FOS are reminded in parenthesis (FOS on left wrist, FOS on right wrist). The analysis window is centred around the maximum difference between the start and end of stimulation. 117
- Figure E.1 Illustration d'une variation d'amplitude d'un PESS modulée par l'attention. 130
- Figure E.2 Présentation de la session de calibration. Déroulement des phases d'enregistrement lors d'un essai de la session de calibration, modifié depuis Pokorny *et al.* 2014 [84]. Un couple « poignet/fréquence de stimulation » est aléatoirement généré pour chaque stimulation. On vérifie que ce couple ne soit jamais utilisé deux fois successivement. Les fréquences testées varient de 14 Hz à 32 Hz avec un pas de 3 Hz. La durée d'un essai est de 21,5 s. Les durées en minutes relatives au déroulement de la session sont des approximations et sont données à titre indicatif. 136

- Figure E.3 Présentation de la session de test. Déroulement des phases d'enregistrements lors d'un essai de la session de test, modifié depuis les travaux de Müller-Putz *et al.* de 2006 [62]. Les durées en minutes relatives au déroulement de la session sont des approximations et sont données à titre indicatif. 138
- Figure E.4 Présentation de la session de *gating*. Les durées en minutes relatives au déroulement de la session sont des approximations et sont données à titre indicatif. Cette session est séparée en 6 blocs, chacun d'une durée similaire. Tous les blocs sont composés de 20 essais chacun. Une pause d'une durée minimum de 3 minutes est imposée au sujet entre chaque bloc. Les blocs de type A ne sont composés que d'essais de type A. Il en va de même pour les blocs de type B ou C. Pour pouvoir fournir un *feedback* en temps-réel lors des blocs C, les enregistrements réalisés durant les quatre premiers blocs A et B seront utilisés comme données de calibration. 140
- Figure E.5 Photo du transducteur et de son support sur un poignet, au repos. 168

## LIST OF TABLES

---

Table 1a	<b>User-specific frequencies identifications: Methodology.</b> Legend and Acronyms: Vibration: vibrotactile stimulation (carrier frequency at X Hz); Pulses: short mechanical pulses; FOS: frequency of stimulation; Subj.: number of subjects; SS: spherical shell; NP: dot matrix needle printer; KoP: Knock-out Pin; C2: C-2 factor; LRA: Linear Resonant Actuator; ERM: Eccentric Rotating Mass; N/A: not available; *: skin contact assumed to be perfect; †: N/A but likely as in [60], <i>i.e.</i> short mechanical pulses; ? : unclear or ambiguous. <a href="#">21</a>
Table 1b	<b>User-specific frequencies identifications: Results.</b> Legend and Acronyms: RLF: resonance-like frequency; TC: tuning curve; N/A: not available. <a href="#">22</a>
Table 2a	<b>EEG-based BCI exploiting SSSEP: Methods and Algorithms.</b> All reported works use mechanical stimulation of the skin unless mentioned differently as an observation in table 2b. Legend and Acronyms: BM: bipolar montage; CS ( $x$ ): channel selection $x$ being the number of kept bipolar channel (if BM) monopolar channel otherwise; cc: concatenate; SPow.: power of selected frequencies (FOS) computed with FFT; Pow.: power computed with FFT; LAS: lock-in amplifier system; Amp.: amplitude output of a LAS; LV: log-variance of spatially filtered data from a CSP; ISPC: inter-stimulus phase coherence; nBP: narrow band-pass filter around stimulation frequencies ( $\pm 1$ Hz); wBP: wide band-pass filters whose range can vary from 16-25 Hz [1] to 8-30 Hz [2]; N/A: not available; *: irrespective of the paradigms or the algorithms; ? : unclear or ambiguous. <a href="#">27</a>
Table 2b	<b>EEG-based BCI exploiting SSSEP: Performances.</b> All of the reported works uses mechanical stimulation of the skin unless mentioned differently as an observation. Legend and Acronyms: N/A: not available; *: irrespective of the paradigms or the algorithms; †: extracted from a figure. <a href="#">28</a>

Table 3.1	Compared amplitude estimation methods, each one combining a spatial filter and an amplitude estimator 49
Table 3.2	Divergence point for each method, signal amplitude and equivalent SNR. 51
Table 4.1	Results from one-sample one-tailed Wilcoxon signed-rank test over the RAI to the non-condition referencing mode. The colour code shows the p-values lower than a risk threshold $\alpha$ at 0.05, 0.01 and 0.001, with the colour red, orange, and green respectively. The threshold $\alpha$ is Bonferroni-corrected, so the threshold $\alpha$ at 0.001 becomes $7.1 \times 10^{-5}$ , and so on. 69
Table 4.2	Expert-based selection of FOS for each subject based on distribution RAI, statistical test, and visual inspection of the subject-wise topomaps. FOS for subjects in bold are results from the selection procedure. 69
Table 4.3	Statistical analysis results: are RAI distributions significantly lower during MI than during idle state? Results from one-tailed Mann-Whitney U-tests over the distributions of RAI within the analysis window shown in figure 4.6. The colour code outlines p-values lower than a risk threshold $\alpha$ at 0.05, 0.01 and 0.001, with red, orange, and green, respectively. The threshold $\alpha$ is Bonferroni-corrected, so the threshold $\alpha$ at 0.05 becomes 0.0083, and so on. 74
Table 6.1	Interview guide for the experimenter 92
Table E.1	Différences et similitudes dans les protocoles expérimentaux, entre les travaux de Müller-Putz <i>et al.</i> [62] et le protocole proposé. NS pour « Non Spécifié » relatif à un montant ou à une durée. 170
Table E.2	Détails expérimentaux pour nos sessions de <i>gating</i> et d'application. La partie matériel est identique au tableau e.1. 171

Table E.3 Corpus de musiques de relaxation, classées par ordre alphabétique. Celles utilisées dans notre session de calibration sont affichées en gras. Modifié depuis [99]. Nous avons dû actualiser certains noms. La plus grosse incertitude réside avec les *Prelude on Welsh Hymn Tunes*, dans le papier d'origine ils sont mentionnés comme « Three prelude on Welsh Hymn », or dans l'album *Hickox conducts Vaughan Williams*, il n'y a que deux préludes *On Welch Hymn* pour orgue. Nous les avons donc reportés dans le tableau. Les informations supplémentaires apportées au tableau proviennent de deux sites internet : *allmusic.com* et *discogs.com*, consulté le 31 octobre 2019. 172



## LIST OF ACRONYMS (USED MORE THAN TWICE)

---

AF	Attention Focusing
BCI	Brain–Computer Interface
CS	Channel Selection
CCA	Canonical Correlation Analysis
CSD	Current Source Density
CSP	Common Spatial Pattern
DFT	Discrete Fourier Transform
EEG	ElectroEncephaloGraphy
ERD	Event-Related Desynchronisation
ERS	Event-Related Synchronisation
FOS	Frequency Of Stimulation
FFT	Fast Fourier Transform
FOSR	Frequency Of Stimulation of the Right wrist
ISPC	Inter-Stimulus Phase Coherence
KMI	Kinaesthetic Motor Imagery
LAS	Lock-in Amplifier System (only in chapter 2)
LDA	Linear Discriminant Analysis
LiA	Lock-in Amplifier System
MF	Move Forward
MI	Motor Imagery
NC	Non-Condition
PLS	Partial Least Squares
PSD	Power Spectral Density
PRISMA	Preferred Reporting Items for Systematic reviews and Meta-Analysis
RAI	Relative Amplitude Increase
Raw-TLX	Raw Task Load Index
SE	Standard Error
SL	Small Laplacian
SS	Selective Sensation
SEP	Somatosensory-Evoked Potential
SMR	SensoriMotor Rhythm
SNR	Signal-to-Noise Ratio
SUS	System Usability Scale
SSSEP	Steady-State Somatosensory-Evoked Potential
SSVEP	Steady-State Visually-Evoked Potential
TL	Turn Left
TR	Turn Right





## PUBLICATIONS

---

Please find below a list of our publications, sorted by type and date.

### INTERNATIONAL JOURNAL

- Jimmy Petit, José Rouillard, and François Cabestaing. “EEG-based brain–computer interfaces exploiting steady-state somatosensory-evoked potentials: a literature review.” *Journal of Neural Engineering* 18.5 (Oct. 2021). Number: 5 Publisher: IOP Publishing, p. 051003. ISSN: 1741-2552. DOI: [10.1088/1741-2552/ac2fc4](https://doi.org/10.1088/1741-2552/ac2fc4)

### INTERNATIONAL CONFERENCE (IN PROCEEDINGS) – WITH ORAL PRESENTATION

- Jimmy Petit, José Rouillard, and François Cabestaing. “Design and study of two applications controlled by a Brain-Computer Interface exploiting Steady-State Somatosensory-Evoked Potentials.” *Human Interaction & Emerging Technologies (IHIET 2022): Artificial Intelligence & Future Applications*. Vol. 68. ISSN: 27710718 Issue: 68. 2022. DOI: [10.54941/ahfe1002787](https://doi.org/10.54941/ahfe1002787)

### NATIONAL CONFERENCE – POSTER & ORAL PRESENTATION

- Jimmy Petit, José Rouillard, and François Cabestaing. *Somatosensory Gating for an SSSEP-based BCI*. CORTICO 2022 : Invasive and non invasive Brain-Computer Interfaces - A handshake over the cliff. Poster. Mar. 2022. URL: <https://hal.archives-ouvertes.fr/hal-03651273>\*
- Jimmy Petit, José Rouillard, and François Cabestaing. “Towards Brain-Computer Interfaces based on Steady-State Somatosensory-Evoked Potentials.” *Journées CORTICO 2020*. Autrans (en virtuel), France, Oct. 2020. URL: <https://hal.archives-ouvertes.fr/hal-03034713>

\* this poster is available in appendix c.

### SUBMITTED PAPERS OR IN PREPARATION –

- Jimmy Petit, François Cabestaing, and José Rouillard. “Amplitude Estimation of Sinusoidal Components in EEG-based Brain–Computer Interfaces exploiting Steady-State Somatosensory-Evoked Potentials” (submitted)
- Jimmy Petit, José Rouillard, François Cabestaing, and Arnaud Delval. “Kinaesthetic Motor Imagery for Selective Amplitude Modulation of SSSEPs by Somatosensory Gating” (in preparation)



## BIBLIOGRAPHY

---

- [1] Sangtae Ahn, Minkyu Ahn, Hohyun Cho, and Sung C. Jun. "Achieving a hybrid brain–computer interface with tactile selective attention and motor imagery." *Journal of Neural Engineering* 11.6 (Oct. 2014). Number: 6, p. 066004. ISSN: 1741-2552. DOI: [10.1088/1741-2560/11/6/066004](https://doi.org/10.1088/1741-2560/11/6/066004).
- [2] Sangtae Ahn and Sung. C. Jun. "Feasibility of hybrid BCI using ERD- and SSSEP- BCI." *2012 12th International Conference on Control, Automation and Systems*. Oct. 2012, pp. 2053–2056.
- [3] Sangtae Ahn, Kiwoong Kim, and Sung C. Jun. "Steady-State Somatosensory Evoked Potential for Brain–Computer Interface–Present and Future." *Frontiers in Human Neuroscience* 9 (2016), p. 716. ISSN: 1662-5161. DOI: [10.3389/fnhum.2015.00716](https://doi.org/10.3389/fnhum.2015.00716).
- [4] Brendan Z. Allison, Andrea Kübler, and Jing Jin. "30+ years of P300 brain–computer interfaces." *Psychophysiology* 57.7 (July 2020). Number: 7. ISSN: 0048-5772, 1469-8986. DOI: [10.1111/psyp.13569](https://doi.org/10.1111/psyp.13569).
- [5] Santiago Arroyo, Ronald P. Lesser, Barry Gordon, Sumio Uematsu, Darryl Jackson, and Robert Webber. "Functional significance of the mu rhythm of human cortex: an electrophysiologic study with subdural electrodes." *Electroencephalography and Clinical Neurophysiology* 87.3 (Sept. 1993), pp. 76–87. ISSN: 0013-4694. DOI: [10.1016/0013-4694\(93\)90114-B](https://doi.org/10.1016/0013-4694(93)90114-B).
- [6] Aaron Bangor. "Determining What Individual SUS Scores Mean: Adding an Adjective Rating Scale." *Journal of Usability Studies* 4.3 (2009), p. 10.
- [7] Aaron Bangor, Philip T. Kortum, and James T. Miller. "An Empirical Evaluation of the System Usability Scale." *International Journal of Human–Computer Interaction* 24.6 (July 2008). Number: 6 Publisher: Taylor & Francis, pp. 574–594. ISSN: 1044-7318. DOI: [10.1080/10447310802205776](https://doi.org/10.1080/10447310802205776).
- [8] Sabyasachi Bhattacharyya, Ragib N. Ahmed, Basab B. Purkayastha, and Kaustubh Bhattacharyya. "Implementation of Digital Lock-in Amplifier." *Journal of Physics: Conference Series* 759 (Oct. 2016), p. 012096. ISSN: 1742-6588, 1742-6596. DOI: [10.1088/1742-6596/759/1/012096](https://doi.org/10.1088/1742-6596/759/1/012096).
- [9] Niels Birbaumer, Thomas Elbert, Anthony Canavan, and Brigitte Rockstroh. "Slow potentials of the cerebral cortex and behavior." *Physiological Reviews* 70.1 (Jan. 1990). Publisher: American

- Physiological Society, pp. 1–41. ISSN: 0031-9333. DOI: [10.1152/physrev.1990.70.1.1](https://doi.org/10.1152/physrev.1990.70.1.1).
- [10] Niels Birbaumer, Cornelia Weber, Christa Neuper, Ethan Buch, Klaus Haapen, and Leonardo Cohen. “Physiological regulation of thinking: brain–computer interface (BCI) research.” *Progress in Brain Research*. Ed. by Christa Neuper and Wolfgang Klimesch. Vol. 159. Event-Related Dynamics of Brain Oscillations. Elsevier, Jan. 2006, pp. 369–391. DOI: [10.1016/S0079-6123\(06\)59024-7](https://doi.org/10.1016/S0079-6123(06)59024-7).
- [11] Christopher M. Bishop. *Pattern recognition and machine learning*. Information science and statistics. New York: Springer, 2006. ISBN: 978-0-387-31073-2.
- [12] Christian Breitwieser, Vera Kaiser, Christa Neuper, and Gernot R. Müller-Putz. “Stability and distribution of steady-state somatosensory evoked potentials elicited by vibro-tactile stimulation.” *Medical & Biological Engineering & Computing* 50.4 (Apr. 2012). Number: 4, pp. 347–357. ISSN: 0140-0118, 1741-0444. DOI: [10.1007/s11517-012-0877-9](https://doi.org/10.1007/s11517-012-0877-9).
- [13] Christian Breitwieser, Christoph Pokorny, and Gernot R. Müller-Putz. “A hybrid three-class brain–computer interface system utilizing SSSEPs and transient ERPs.” *Journal of Neural Engineering* 13.6 (Dec. 2016). Number: 6, p. 066015. ISSN: 1741-2560, 1741-2552. DOI: [10.1088/1741-2560/13/6/066015](https://doi.org/10.1088/1741-2560/13/6/066015).
- [14] Christian Breitwieser, Christoph Pokorny, Christa Neuper, and Gernot R. Müller-Putz. “Somatosensory evoked potentials elicited by stimulating two fingers from one hand — Usable for BCI?” *Conference proceedings : ... Annual International Conference of the IEEE Engineering in Medicine and Biology Society. IEEE Engineering in Medicine and Biology Society. Conference 2011* (Aug. 2011), pp. 6373–6. DOI: [10.1109/IEMBS.2011.6091573](https://doi.org/10.1109/IEMBS.2011.6091573).
- [15] Marion Brickwedde, Marie D. Schmidt, Marie C. Krüger, and Hubert R. Dinse. “20 Hz Steady-State Response in Somatosensory Cortex During Induction of Tactile Perceptual Learning Through LTP-Like Sensory Stimulation.” *Frontiers in Human Neuroscience* 14 (2020), p. 257. ISSN: 1662-5161. DOI: [10.3389/fnhum.2020.00257](https://doi.org/10.3389/fnhum.2020.00257).
- [16] John Brooke. “SUS-A quick and dirty usability scale.” *Usability evaluation in industry* (P. W. Jordan, B. Thomas, B. A. Weerdmeester, & A. L. McClelland (Eds.)) 21. CRC Press, June 1996, p. 276. ISBN: 978-0-7484-0460-5.
- [17] John Brooke. “SUS: A Retrospective.” *Journal of Usability Studies* (Feb. 2013), pp. 29–40.

- [18] Xiaogang Chen, Yijun Wang, Masaki Nakanishi, Xiaorong Gao, Tzyy-Ping Jung, and Shangkai Gao. "High-speed spelling with a noninvasive brain-computer interface." *Proceedings of the National Academy of Sciences* 112.44 (Nov. 2015). Number: 44 Publisher: National Academy of Sciences Section: PNAS Plus, E6058–E6067. ISSN: 0027-8424, 1091-6490. DOI: [10.1073/pnas.1508080112](https://doi.org/10.1073/pnas.1508080112).
- [19] Alain de Cheveigné and Israel Nelken. "Filters: When, Why, and How (Not) to Use Them." *Neuron* 102.2 (Apr. 2019). Number: 2 Publisher: Elsevier, pp. 280–293. ISSN: 0896-6273. DOI: [10.1016/j.neuron.2019.02.039](https://doi.org/10.1016/j.neuron.2019.02.039).
- [20] Inchul Choi, Kyle Bond, Dean Krusienski, and Chang S. Nam. "Comparison of Stimulation Patterns to Elicit Steady-State Somatosensory Evoked Potentials (SSSEPs): Implications for Hybrid and SSSEP-Based BCIs." *2015 IEEE International Conference on Systems, Man, and Cybernetics*. Oct. 2015, pp. 3122–3127. DOI: [10.1109/SMC.2015.542](https://doi.org/10.1109/SMC.2015.542).
- [21] Maureen Clerc, Laurent Bougrain, and Fabien Lotte. *Brain-Computer Interfaces 1: Methods and Perspectives*. 1st ed. Wiley-ISTE, July 2016.
- [22] James G. Colebatch. "Bereitschaftspotential and movement-related potentials: Origin, significance, and application in disorders of human movement." *Movement Disorders* 22.5 (2007), pp. 601–610. ISSN: 1531-8257. DOI: [10.1002/mds.21323](https://doi.org/10.1002/mds.21323).
- [23] Elisabeth Colon, Valéry Legrain, and André Mouraux. "Steady-state evoked potentials to study the processing of tactile and nociceptive somatosensory input in the human brain." *Neurophysiologie Clinique = Clinical Neurophysiology* 42.5 (Oct. 2012). Number: 5, pp. 315–323. ISSN: 1769-7131. DOI: [10.1016/j.neucli.2012.05.005](https://doi.org/10.1016/j.neucli.2012.05.005).
- [24] Howard C. Cromwell, Ryan P. Mears, Li Wan, and Nash N. Boutros. "Sensory Gating: A Translational Effort From Basic to Clinical Science." *Clinical EEG and neuroscience* 39.2 (Apr. 2008). Number: 2, pp. 69–72. ISSN: 1550-0594. DOI: [10.1177/155005940803900209](https://doi.org/10.1177/155005940803900209).
- [25] Arnaud Delorme, Jason Palmer, Julie Onton, Robert Oostenveld, and Scott Makeig. "Independent EEG Sources Are Dipolar." *PLOS ONE* 7.2 (Feb. 2012). Publisher: Public Library of Science, e30135. ISSN: 1932-6203. DOI: [10.1371/journal.pone.0030135](https://doi.org/10.1371/journal.pone.0030135).
- [26] Jan B. F. van Erp and Anne-Marie Brouwer. "Touch-based Brain Computer Interfaces: State of the art." *2014 IEEE Haptics Symposium (HAPTICS)*. Feb. 2014, pp. 397–401. DOI: [10.1109/HAPTICS.2014.6775488](https://doi.org/10.1109/HAPTICS.2014.6775488).

- [27] Lawrence A. Farwell and Emanuel Donchin. "Talking off the top of your head: toward a mental prosthesis utilizing event-related brain potentials." *Electroencephalography and Clinical Neurophysiology* 70.6 (Dec. 1988), pp. 510–523. ISSN: 0013-4694. DOI: [10.1016/0013-4694\(88\)90149-6](https://doi.org/10.1016/0013-4694(88)90149-6).
- [28] Mathis Fleury, Giulia Lioi, Christian Barillot, and Anatole Lécuyer. "A Survey on the Use of Haptic Feedback for Brain-Computer Interfaces and Neurofeedback." *Frontiers in Neuroscience* 1 (June 2020). Publisher: Frontiers. DOI: [10.3389/fnins.2020.00528](https://doi.org/10.3389/fnins.2020.00528).
- [29] Ove Franzén and Kurt Offenloch. "Evoked response correlates of psychophysical magnitude estimates for tactile stimulation in man." *Experimental Brain Research* 8.1 (Apr. 1969), pp. 1–18. ISSN: 1432-1106. DOI: [10.1007/BF00234922](https://doi.org/10.1007/BF00234922).
- [30] Ola Friman, Jonny Cedefamn, Peter Lundberg, Magnus Borga, and Hans Knutsson. "Detection of neural activity in functional MRI using canonical correlation analysis." *Magnetic Resonance in Medicine* 45.2 (2001), pp. 323–330. ISSN: 1522-2594. URL: <https://pubmed.ncbi.nlm.nih.gov/11180440/>.
- [31] Michel Georgesco, Antoine Salerno, and William Camu. "Somatosensory evoked potentials elicited by stimulation of lower-limb nerves in amyotrophic lateral sclerosis." *Electroencephalography and Clinical Neurophysiology/ Evoked Potentials Section* 104.4 (July 1997). Number: 4, pp. 333–342. ISSN: 01685597. DOI: [10.1016/S0168-5597\(97\)00018-X](https://doi.org/10.1016/S0168-5597(97)00018-X).
- [32] Claire-Marie Giabbiconi, Chris Dancer, Regine Zopf, Thomas Gruber, and Matthias M. Müller. "Selective spatial attention to left or right hand flutter sensation modulates the steady-state somatosensory evoked potential." *Cognitive Brain Research* 20.1 (June 2004). Number: 1, pp. 58–66. ISSN: 0926-6410. DOI: [10.1016/j.cogbrainres.2004.01.004](https://doi.org/10.1016/j.cogbrainres.2004.01.004).
- [33] I. I. Goncharova, Dennis J. McFarland, Theresa M. Vaughan, and Jonathan R. Wolpaw. "EMG contamination of EEG: spectral and topographical characteristics." *Clinical Neurophysiology* 114.9 (Sept. 2003), pp. 1580–1593. ISSN: 1388-2457. DOI: [10.1016/S1388-2457\(03\)00093-2](https://doi.org/10.1016/S1388-2457(03)00093-2).
- [34] Moritz Grosse-Wentrup and Bernhard Schölkopf. "A Review of Performance Variations in SMR-Based Brain–Computer Interfaces (BCIs)." *Brain-Computer Interface Research: A State-of-the-Art Summary*. Ed. by Christoph Guger, Brendan Z. Allison, and Günter Edlinger. SpringerBriefs in Electrical and Computer Engineering. Berlin, Heidelberg: Springer, 2013, pp. 39–51. ISBN: 978-3-642-36083-1. DOI: [10.1007/978-3-642-36083-1\\_5](https://doi.org/10.1007/978-3-642-36083-1_5).

- [35] Christoph Guger, Günter Edlinger, Werner Harkam, I. Niedermayer, and Gert Pfurtscheller. "How many people are able to operate an EEG-based brain-computer interface (BCI)?" *IEEE transactions on neural systems and rehabilitation engineering: a publication of the IEEE Engineering in Medicine and Biology Society* 11.2 (June 2003), pp. 145–147. ISSN: 1534-4320. DOI: [10.1109/TNSRE.2003.814481](https://doi.org/10.1109/TNSRE.2003.814481).
- [36] Masashi Hamada, Ritsuko Hanajima, Yasuo Terao, Fumio Sato, Tomoko Okano, Kaoru Yuasa, Toshiaki Furubayashi, Shingo Okabe, Noritoshi Arai, and Yoshikazu Ugawa. "Median nerve somatosensory evoked potentials and their high-frequency oscillations in amyotrophic lateral sclerosis." *Clinical Neurophysiology* 118.4 (Apr. 2007). Number: 4, pp. 877–886. ISSN: 13882457. DOI: [10.1016/j.clinph.2006.12.001](https://doi.org/10.1016/j.clinph.2006.12.001).
- [37] Jonathan C. Hansen and Steven A. Hillyard. "Selective attention to multidimensional auditory stimuli." *Journal of Experimental Psychology. Human Perception and Performance* 9.1 (Feb. 1983), pp. 1–19. ISSN: 0096-1523. DOI: [10.1037//0096-1523.9.1.1](https://doi.org/10.1037//0096-1523.9.1.1).
- [38] Sandra G. Hart. "Nasa-Task Load Index (NASA-TLX); 20 Years Later." *Proceedings of the Human Factors and Ergonomics Society Annual Meeting* 50.9 (Oct. 2006). Publisher: SAGE Publications Inc, pp. 904–908. DOI: [10.1177/154193120605000909](https://doi.org/10.1177/154193120605000909).
- [39] Christoph S. Herrmann. "Human EEG responses to 1–100 Hz flicker: resonance phenomena in visual cortex and their potential correlation to cognitive phenomena." *Experimental Brain Research* 137.3 (Apr. 2001), pp. 346–353. ISSN: 1432-1106. DOI: [10.1007/s002210100682](https://doi.org/10.1007/s002210100682).
- [40] Richard W. Homan, John Herman, and Phillip Purdy. "Cerebral location of international 10–20 system electrode placement." *Electroencephalography and Clinical Neurophysiology* 66.4 (Apr. 1987), pp. 376–382. ISSN: 0013-4694. DOI: [10.1016/0013-4694\(87\)90206-9](https://doi.org/10.1016/0013-4694(87)90206-9).
- [41] Harold Hotelling. "Relations Between Two Sets of Variates." *Biometrika* 28.3-4 (Dec. 1936), pp. 321–377. ISSN: 0006-3444. DOI: [10.1093/biomet/28.3-4.321](https://doi.org/10.1093/biomet/28.3-4.321).
- [42] Christopher Hughes, Angelica Herrera, Robert Gaunt, and Jennifer Collinger. "Chapter 13 - Bidirectional brain-computer interfaces." *Handbook of Clinical Neurology*. Ed. by Nick F. Ramsey and José del R. Millán. Vol. 168. Brain-Computer Interfaces. Elsevier, Jan. 2020, pp. 163–181. DOI: [10.1016/B978-0-444-63934-9.00013-5](https://doi.org/10.1016/B978-0-444-63934-9.00013-5).



- [43] Camille Jeunet. "Understanding & Improving Mental-Imagery Based Brain-Computer Interface (Mi-Bci) User-Training : towards A New Generation Of Reliable, Efficient & Accessible Brain- Computer Interfaces." These de doctorat. Bordeaux, Dec. 2016. URL: <http://www.theses.fr/2016B0RD0221> (visited on 06/15/2020).
- [44] Dorothee Kasteleijn-Nolst Trenité, Guido Rubboli, Edouard Hirsch, Antonio Martins da Silva, Stefano Seri, Arnold Wilkins, Jaime Parra, Athanasios Covanis, Maurizio Elia, Giuseppe Capovilla, Ulrich Stephani, and Graham Harding. "Methodology of photic stimulation revisited: Updated European algorithm for visual stimulation in the EEG laboratory." *Epilepsia* 53.1 (2012), pp. 16–24. ISSN: 1528-1167. DOI: [10.1111/j.1528-1167.2011.03319.x](https://doi.org/10.1111/j.1528-1167.2011.03319.x).
- [45] Jürgen Kayser and Craig E. Tenke. "On the benefits of using surface Laplacian (Current Source Density) methodology in electrophysiology." *International journal of psychophysiology : official journal of the International Organization of Psychophysiology* 97.3 (Sept. 2015), pp. 171–173. ISSN: 0167-8760. DOI: [10.1016/j.ijpsycho.2015.06.001](https://doi.org/10.1016/j.ijpsycho.2015.06.001).
- [46] Young-Jin Kee, Dong-Ok Won, and Seong-Whan Lee. "Classification of left and right foot movement intention based on steady-state somatosensory evoked potentials." *2017 5th International Winter Conference on Brain-Computer Interface (BCI)*. Gangwon Province, South Korea: IEEE, Jan. 2017, pp. 106–108. ISBN: 978-1-5090-5096-3. DOI: [10.1109/IWW-BCI.2017.7858174](https://doi.org/10.1109/IWW-BCI.2017.7858174).
- [47] Keun-Tae Kim and Seong-Whan Lee. "Steady-state somatosensory evoked potentials for brain-controlled wheelchair." *2014 International Winter Workshop on Brain-Computer Interface (BCI)*. Gangwon province, Korea (South): IEEE, Feb. 2014, pp. 1–2. ISBN: 978-1-4799-2588-9. DOI: [10.1109/iww-BCI.2014.6782570](https://doi.org/10.1109/iww-BCI.2014.6782570).
- [48] Keun-Tae Kim and Seong-Whan Lee. "Wheelchair Control Based on Steady-State Somatosensory Evoked Potentials." *2015 IEEE International Conference on Systems, Man, and Cybernetics*. Oct. 2015, pp. 1504–1507. DOI: [10.1109/SMC.2015.266](https://doi.org/10.1109/SMC.2015.266).
- [49] Keun-Tae Kim and Seong-Whan Lee. "Towards an EEG-based intelligent wheelchair driving system with vibro-tactile stimuli." *2016 IEEE International Conference on Systems, Man, and Cybernetics (SMC)*. Oct. 2016, pp. 002382–002385. DOI: [10.1109/SMC.2016.7844595](https://doi.org/10.1109/SMC.2016.7844595).
- [50] Keun-Tae Kim, Heung-Il Suk, and Seong-Whan Lee. "Commanding a Brain-Controlled Wheelchair Using Steady-State Somatosensory Evoked Potentials." *IEEE transactions on neural systems and rehabilitation engineering: a publication of the IEEE Engineering in Medicine and Biology Society* 26.3 (2018). Num-

- ber: 3, pp. 654–665. ISSN: 1558-0210. DOI: [10.1109/TNSRE.2016.2597854](https://doi.org/10.1109/TNSRE.2016.2597854).
- [51] Zhonglin Lin, Changshui Zhang, Wei Wu, and Xiaorong Gao. “Frequency Recognition Based on Canonical Correlation Analysis for SSVEP-Based BCIs.” *IEEE Transactions on Biomedical Engineering* 53.12 (Dec. 2006). Number: 12, pp. 2610–2614. ISSN: 0018-9294, 1558-2531. DOI: [10.1109/TBME.2006.886577](https://doi.org/10.1109/TBME.2006.886577).
- [52] Fabien Lotte. “Etude des techniques de traitement et de classification de signaux électroencéphalographiques pour l’utilisation d’interfaces cerveau-ordinateur dans des applications de réalité virtuelle.” These de doctorat. Rennes, INSA, Jan. 2008. URL: <http://www.theses.fr/2008ISAR0026> (visited on 06/22/2020).
- [53] Fabien Lotte, Laurent Bougrain, Andrzej Cichocki, Maureen Clerc, Marco Congedo, Alain Rakotomamonjy, and Florian Yger. “A review of classification algorithms for EEG-based brain–computer interfaces: a 10 year update.” *Journal of Neural Engineering* 15.3 (June 2018). Number: 3, p. 031005. ISSN: 1741-2560, 1741-2552. DOI: [10.1088/1741-2552/aab2f2](https://doi.org/10.1088/1741-2552/aab2f2).
- [54] Fabien Lotte, Laurent Bougrain, and Maureen Clerc. “Electroencephalography (EEG)-Based Brain-Computer Interfaces.” *Wiley Encyclopedia of Electrical and Electronics Engineering*. Hoboken, NJ, USA: John Wiley & Sons, Inc., Sept. 2015, pp. 1–20. ISBN: 978-0-471-34608-1. DOI: [10.1002/047134608X.w8278](https://doi.org/10.1002/047134608X.w8278).
- [55] Steven J. Luck. *An Introduction to the Event-Related Potential Technique, second edition*. MIT Press, May 2014. ISBN: 978-0-262-52585-5.
- [56] Dennis J. McFarland. “The advantages of the surface Laplacian in brain–computer interface research.” *International Journal of Psychophysiology*. On the benefits of using surface Laplacian (current source density) methodology in electrophysiology 97.3 (Sept. 2015), pp. 271–276. ISSN: 0167-8760. DOI: [10.1016/j.ijpsycho.2014.07.009](https://doi.org/10.1016/j.ijpsycho.2014.07.009).
- [57] Dennis J. McFarland, Lynn M. McCane, Stephen V. David, and Jonathan R. Wolpaw. “Spatial filter selection for EEG-based communication.” *Electroencephalography and Clinical Neurophysiology* 103.3 (Sept. 1997), pp. 386–394. ISSN: 0013-4694. DOI: [10.1016/S0013-4694\(97\)00022-2](https://doi.org/10.1016/S0013-4694(97)00022-2).
- [58] Jianjun Meng, John H. Mundahl, Taylor D. Streitz, Kaitlin Maile, Nicholas S. Gulachek, Jeffrey He, and Bin He. “Effects of Soft Drinks on Resting State EEG and Brain–Computer Interface Performance.” *IEEE Access* 5 (2017), pp. 18756–18764. ISSN: 2169-3536. DOI: [10.1109/ACCESS.2017.2751069](https://doi.org/10.1109/ACCESS.2017.2751069).

- [59] David Moher, Alessandro Liberati, Jennifer Tetzlaff, and Douglas G. Altman. "Preferred reporting items for systematic reviews and meta-analyses: the PRISMA statement." *BMJ* 339 (July 2009). Publisher: British Medical Journal Publishing Group Section: Research Methods & Reporting, b2535. ISSN: 1756-1833. DOI: [10.1136/bmj.b2535](https://doi.org/10.1136/bmj.b2535).
- [60] Gernot R. Müller-Putz, Christa Neuper, and Gert Pfurtscheller. "'Resonance-like' Frequencies of Sensorimotor Areas Evoked by Repetitive Tactile Stimulation - Resonanzeffekte in sensomotorischen Arealen, evoziert durch rhythmische taktile Stimulation." *Biomedizinische Technik - BIOMED TECH* 46 (Jan. 2001), pp. 186–190. DOI: [10.1515/bmte.2001.46.7-8.186](https://doi.org/10.1515/bmte.2001.46.7-8.186).
- [61] Gernot R. Müller-Putz, Reinhold Scherer, Clemens Brunner, Robert Leeb, and Gert Pfurtscheller. "Better than random? A closer look on BCI results." *International journal of bioelectromagnetism* 10.1 (2008). Number: 1, pp. 52–55. URL: <https://graz.pure.elsevier.com/en/publications/better-than-random-a-closer-look-on-bci-results> (visited on 09/17/2020).
- [62] Gernot R. Müller-Putz, Reinhold Scherer, Christa Neuper, and Gert Pfurtscheller. "Steady-state somatosensory evoked potentials: suitable brain signals for brain-computer interfaces?" *IEEE Transactions on Neural Systems and Rehabilitation Engineering* 14.1 (Mar. 2006). Number: 1, pp. 30–37. DOI: [10.1109/TNSRE.2005.863842](https://doi.org/10.1109/TNSRE.2005.863842).
- [63] Yunjun Nam, Andrzej Cichocki, and Seungjin Choi. "Common spatial patterns for steady-state somatosensory evoked potentials." *Conference proceedings: ... Annual International Conference of the IEEE Engineering in Medicine and Biology Society. IEEE Engineering in Medicine and Biology Society. Annual Conference 2013* (2013), pp. 2255–2258. ISSN: 1557-170X. DOI: [10.1109/EMBC.2013.6609986](https://doi.org/10.1109/EMBC.2013.6609986).
- [64] Norman S. Namerow, Robert J. Scwabassi, and Nelson F. Enns. "Somatosensory responses to stimulus trains: normative data." *Electroencephalography and Clinical Neurophysiology* 37.1 (July 1974). Number: 1, pp. 11–21. ISSN: 0013-4694. DOI: [10.1016/0013-4694\(74\)90241-7](https://doi.org/10.1016/0013-4694(74)90241-7).
- [65] Christa Neuper, Michael Wörtz, and Gert Pfurtscheller. "ERD/ERS patterns reflecting sensorimotor activation and deactivation." *Progress in Brain Research*. Ed. by Christa Neuper and Wolfgang Klimesch. Vol. 159. Event-Related Dynamics of Brain Oscillations. Elsevier, Jan. 2006, pp. 211–222. DOI: [10.1016/S0079-6123\(06\)59014-4](https://doi.org/10.1016/S0079-6123(06)59014-4).

- [66] Roger S. Noss, Colby D. Boles, and Charles D. Yingling. "Steady-state analysis of somatosensory evoked potentials." *Electroencephalography and Clinical Neurophysiology* 100.5 (Sept. 1996). Number: 5, pp. 453–461. ISSN: 0013-4694.
- [67] Paul L. Nunez, Richard B. Silberstein, Peter J. Cadusch, Ranjith S. Wijesinghe, Andrew F. Westdorp, and Ramesh Srinivasan. "A theoretical and experimental study of high resolution EEG based on surface Laplacians and cortical imaging." *Electroencephalography and Clinical Neurophysiology* 90.1 (Jan. 1994), pp. 40–57. ISSN: 0013-4694. DOI: [10.1016/0013-4694\(94\)90112-0](https://doi.org/10.1016/0013-4694(94)90112-0).
- [68] Paul L. Nunez and Ramesh Srinivasan. *Electric Fields of the Brain: The neurophysics of EEG*. 2nd ed. New York: Oxford University Press, 2006. ISBN: 978-0-19-505038-7. DOI: [10.1093/acprof:oso/9780195050387.001.0001](https://doi.org/10.1093/acprof:oso/9780195050387.001.0001).
- [69] Marc R. Nuwer, Edgar G. Dawson, Linda G. Carlson, Linda E. A. Kanim, and John E. Sherman. "Somatosensory evoked potential spinal cord monitoring reduces neurologic deficits after scoliosis surgery: results of a large multicenter survey." *Electroencephalography and Clinical Neurophysiology/ Evoked Potentials Section* 96.1 (Jan. 1995). Number: 1, pp. 6–11. ISSN: 0168-5597. DOI: [10.1016/0013-4694\(94\)00235-D](https://doi.org/10.1016/0013-4694(94)00235-D).
- [70] Richard C. Oldfield. "The assessment and analysis of handedness: The Edinburgh inventory." *Neuropsychologia* 9.1 (Mar. 1971), pp. 97–113. ISSN: 0028-3932. DOI: [10.1016/0028-3932\(71\)90067-4](https://doi.org/10.1016/0028-3932(71)90067-4).
- [71] Cheuk Y. Pang and Matthias M. Müller. "Test-retest reliability of concurrently recorded steady-state and somatosensory evoked potentials in somatosensory sustained spatial attention." *Biological Psychology* 100 (July 2014), pp. 86–96. ISSN: 1873-6246. DOI: [10.1016/j.biopsycho.2014.05.009](https://doi.org/10.1016/j.biopsycho.2014.05.009).
- [72] Sangin Park, Jihyeon Ha, Da-Hye Kim, and Laehyun Kim. "Improving Motor Imagery-Based Brain-Computer Interface Performance Based on Sensory Stimulation Training: An Approach Focused on Poorly Performing Users." *Frontiers in Neuroscience* 15 (2021). ISSN: 1662-453X. DOI: [10.3389/fnins.2021.732545](https://doi.org/10.3389/fnins.2021.732545).
- [73] Wilder Penfield and Theodore Rasmussen. *The cerebral cortex of man : A clinical study of localization of function*. New York: MacMillan Company, 1950.
- [74] Francois Perrin, Olivier Bertrand, and Jacques Pernier. "Scalp Current Density Mapping: Value and Estimation from Potential Data." *IEEE Transactions on Biomedical Engineering* BME-34.4 (Apr. 1987). Conference Name: IEEE Transactions on Biomed-

- ical Engineering, pp. 283–288. ISSN: 1558-2531. DOI: [10.1109/TBME.1987.326089](https://doi.org/10.1109/TBME.1987.326089).
- [75] Lorraine Perronnet. “Combinaison de l’électroencéphalographie et de l’imagerie par résonance magnétique fonctionnelle pour le neurofeedback.” These de doctorat. Rennes 1, Sept. 2017. URL: <http://www.theses.fr/2017REN15043> (visited on 06/15/2020).
- [76] Jimmy Petit, François Cabestaing, and José Rouillard. “Amplitude Estimation of Sinusoidal Components in EEG-based Brain-Computer Interfaces exploiting Steady-State Somatosensory-Evoked Potentials” (submitted).
- [77] Jimmy Petit, José Rouillard, and François Cabestaing. *Somatosensory Gating for an SSSEP-based BCI*. CORTICO 2022 : Invasive and non invasive Brain-Computer Interfaces - A handshake over the cliff. Poster. Mar. 2022. URL: <https://hal.archives-ouvertes.fr/hal-03651273>.
- [78] Jimmy Petit, José Rouillard, and François Cabestaing. “Design and study of two applications controlled by a Brain-Computer Interface exploiting Steady-State Somatosensory-Evoked Potentials.” *Human Interaction & Emerging Technologies (IHET 2022): Artificial Intelligence & Future Applications*. Vol. 68. ISSN: 27710718 Issue: 68. 2022. DOI: [10.54941/ahfe1002787](https://doi.org/10.54941/ahfe1002787).
- [79] Jimmy Petit, José Rouillard, and François Cabestaing. “Towards Brain-Computer Interfaces based on Steady-State Somatosensory-Evoked Potentials.” *Journées CORTICO 2020*. Autrans (en virtuel), France, Oct. 2020. URL: <https://hal.archives-ouvertes.fr/hal-03034713>.
- [80] Jimmy Petit, José Rouillard, and François Cabestaing. “EEG-based brain-computer interfaces exploiting steady-state somatosensory-evoked potentials: a literature review.” *Journal of Neural Engineering* 18.5 (Oct. 2021). Number: 5 Publisher: IOP Publishing, p. 051003. ISSN: 1741-2552. DOI: [10.1088/1741-2552/ac2fc4](https://doi.org/10.1088/1741-2552/ac2fc4).
- [81] Jimmy Petit, José Rouillard, François Cabestaing, and Arnaud Delval. “Kinaesthetic Motor Imagery for Selective Amplitude Modulation of SSSEPs by Somatosensory Gating” (in preparation).
- [82] Gert Pfurtscheller, Christa Neuper, Doris Flotzinger, and Martin Pregenzer. “EEG-based discrimination between imagination of right and left hand movement.” *Electroencephalography and Clinical Neurophysiology* 103.6 (Dec. 1997), pp. 642–651. ISSN: 0013-4694. DOI: [10.1016/S0013-4694\(97\)00080-1](https://doi.org/10.1016/S0013-4694(97)00080-1).

- [83] Gert Pfurtscheller and Fernando H. Lopes da Silva. "Event-related EEG/MEG synchronization and desynchronization: basic principles." *Clinical Neurophysiology* 110.11 (Nov. 1999). Number: 11, pp. 1842–1857. ISSN: 1388-2457. DOI: [10.1016/S1388-2457\(99\)00141-8](https://doi.org/10.1016/S1388-2457(99)00141-8).
- [84] Christoph Pokorny, Christian Breitwieser, and Gernot R. Müller-Putz. "A Tactile Stimulation Device for EEG Measurements in Clinical Use." *IEEE Transactions on Biomedical Circuits and Systems* 8.3 (June 2014). Number: 3, pp. 305–312. ISSN: 1932-4545, 1940-9990. DOI: [10.1109/TBCAS.2013.2270176](https://doi.org/10.1109/TBCAS.2013.2270176).
- [85] Christoph Pokorny, Christian Breitwieser, and Gernot R. Müller-Putz. "The Role of Transient Target Stimuli in a Steady-State Somatosensory Evoked Potential-Based Brain-Computer Interface Setup." *Frontiers in Neuroscience* 10 (2016), p. 152. ISSN: 1662-4548. DOI: [10.3389/fnins.2016.00152](https://doi.org/10.3389/fnins.2016.00152).
- [86] Yunyong Punsawat and Yodchanan Wongsawat. "Multi-command SSAEP-based BCI system with training sessions for SSVEP during an eye fatigue state." *IEEJ Transactions on Electrical and Electronic Engineering* 12 (June 2017), s72–s78. DOI: [10.1002/tee.22441](https://doi.org/10.1002/tee.22441).
- [87] "Recommendations for the practice of clinical neurophysiology: guidelines of the International Federation of Clinical Neurophysiology." *Electroencephalography and Clinical Neurophysiology. Supplement* 52 (1999), pp. 1–304. ISSN: 0424-8155.
- [88] David Regan. "Some characteristics of average steady-state and transient responses evoked by modulated light." *Electroencephalography and Clinical Neurophysiology* 20.3 (Mar. 1966). Number: 3, pp. 238–248. ISSN: 00134694. DOI: [10.1016/0013-4694\(66\)90088-5](https://doi.org/10.1016/0013-4694(66)90088-5).
- [89] David Regan. "Comparison of Transient and Steady-State Methods\*." *Annals of the New York Academy of Sciences* 388.1 (1982), pp. 45–71. ISSN: 1749-6632. DOI: [10.1111/j.1749-6632.1982.tb50784.x](https://doi.org/10.1111/j.1749-6632.1982.tb50784.x).
- [90] David Regan. *Human brain electrophysiology: evoked potentials and evoked magnetic fields in science and medicine*. Open Library ID: OL2044400M. New York: Elsevier, 1989. ISBN: 978-0-444-01324-8.
- [91] Yann Renard, Fabien Lotte, Guillaume Gibert, Marco Congedo, Emmanuel Maby, Vincent Delannoy, Olivier Bertrand, and Anatole Lécuyer. "OpenViBE: An Open-Source Software Platform to Design, Test, and Use Brain-Computer Interfaces in Real and Virtual Environments." *Presence: Teleoperators and Virtual Environments* 19.1 (Feb. 2010), pp. 35–53. DOI: [10.1162/pres.19.1.35](https://doi.org/10.1162/pres.19.1.35).



- [92] "Report of the committee on methods of clinical examination in electroencephalography: 1957." *Electroencephalography and Clinical Neurophysiology* 10.2 (May 1958), pp. 370–375. ISSN: 0013-4694. DOI: [10.1016/0013-4694\(58\)90053-1](https://doi.org/10.1016/0013-4694(58)90053-1).
- [93] José Rouillard, François Cabestaing, Marie-Hélène Bekaert, and Jean-Marc Vannobel. "Toward a SSSEP-Based BCI Using the Sensory Gating Phenomenon." *Journal Of Clinical Neurology, Neurosurgery And Spine* (Feb. 2021). Publisher: Scientific Literature. URL: <https://hal.archives-ouvertes.fr/hal-03232373> (visited on 09/16/2022).
- [94] Robert F. Schmidt, ed. *Fundamentals of Sensory Physiology*. 3rd ed. Springer Study Edition. Berlin Heidelberg: Springer-Verlag, 1986. ISBN: 978-3-642-82598-9. (Visited on 10/14/2019).
- [95] Marianne Severens, Jason Farquhar, Jacques Duysens, and Peter Desain. "A multi-signature brain-computer interface: Use of transient and steady-state responses." *Journal of neural engineering* 10 (Feb. 2013), p. 026005. DOI: [10.1088/1741-2560/10/2/026005](https://doi.org/10.1088/1741-2560/10/2/026005).
- [96] Abraham Z. Snyder. "Steady-state vibration evoked potentials: descriptions of technique and characterization of responses." *Electroencephalography and Clinical Neurophysiology* 84.3 (June 1992). Number: 3, pp. 257–268. ISSN: 0013-4694. DOI: [10.1016/0168-5597\(92\)90007-x](https://doi.org/10.1016/0168-5597(92)90007-x).
- [97] Shiyong Su, Guohong Chai, Xiaokang Shu, Xinjun Sheng, and Xiangyang Zhu. "Electrical stimulation-induced SSSEP as an objective index to evaluate the difference of tactile acuity between the left and right hand." *Journal of Neural Engineering* 17.1 (Feb. 2020). Number: 1, p. 016053. ISSN: 1741-2552. DOI: [10.1088/1741-2552/ab5ee9](https://doi.org/10.1088/1741-2552/ab5ee9).
- [98] William H. Talbot, Ian Darian-Smith, Hans H. Kornhuber, and Vernon B. Mountcastle. "The sense of flutter-vibration: comparison of the human capacity with response patterns of mechanoreceptive afferents from the monkey hand." *Journal of Neurophysiology* 31.2 (Mar. 1968). Publisher: American Physiological Society, pp. 301–334. ISSN: 0022-3077. DOI: [10.1152/jn.1968.31.2.301](https://doi.org/10.1152/jn.1968.31.2.301).
- [99] Xueli Tan, Charles J. Yowler, Dennis M. Super, and Richard B. Fratianne. "The Interplay of Preference, Familiarity and Psychophysical Properties in Defining Relaxation Music." *Journal of Music Therapy* 49.2 (July 2012). Number: 2, pp. 150–179. ISSN: 0022-2917. DOI: [10.1093/jmt/49.2.150](https://doi.org/10.1093/jmt/49.2.150).
- [100] Xuewen Tao, Weibo Yi, Kun Wang, Feng He, and Hongzhi Qi. "Inter-stimulus phase coherence in steady-state somatosensory evoked potentials and its application in improving the performance of single-channel MI-BCI." *Journal of Neural Engineering*

- 18.4 (June 2021). Number: 4. ISSN: 1741-2552. DOI: [10.1088/1741-2552/ac0767](https://doi.org/10.1088/1741-2552/ac0767).
- [101] Craig E. Tenke and Jürgen Kayser. "Generator localization by current source density (CSD): Implications of volume conduction and field closure at intracranial and scalp resolutions." *Clinical Neurophysiology* 123.12 (Dec. 2012), pp. 2328–2345. DOI: [10.1016/j.clinph.2012.06.005](https://doi.org/10.1016/j.clinph.2012.06.005).
- [102] Shozo Tobimatsu, You M. Zhang, and Motohiro Kato. "Steady-state vibration somatosensory evoked potentials: physiological characteristics and tuning function." *Clinical Neurophysiology* 110.11 (Nov. 1999). Number: 11, pp. 1953–1958. DOI: [10.1016/S1388-2457\(99\)00146-7](https://doi.org/10.1016/S1388-2457(99)00146-7).
- [103] Shozo Tobimatsu, You M. Zhang, Rie Suga, and Motohiro Kato. "Differential temporal coding of the vibratory sense in the hand and foot in man." *Clinical Neurophysiology* 111.3 (Mar. 2000). Number: 3, pp. 398–404. DOI: [10.1016/S1388-2457\(99\)00278-3](https://doi.org/10.1016/S1388-2457(99)00278-3).
- [104] J. Richard Toleikis. "Intraoperative Monitoring Using Somatosensory Evoked Potentials." *Journal of Clinical Monitoring and Computing* 19.3 (June 2005). Number: 3, pp. 241–258. DOI: [10.1007/s10877-005-4397-0](https://doi.org/10.1007/s10877-005-4397-0).
- [105] Jaimie F. Veale. "Edinburgh Handedness Inventory - Short Form: a revised version based on confirmatory factor analysis." *Laterality* 19.2 (2014), pp. 164–177. ISSN: 1464-0678. DOI: [10.1080/1357650X.2013.783045](https://doi.org/10.1080/1357650X.2013.783045).
- [106] Jacques J. Vidal. "Toward Direct Brain-Computer Communication." *Annual Review of Biophysics and Bioengineering* 2.1 (1973), pp. 157–180. DOI: [10.1146/annurev.bb.02.060173.001105](https://doi.org/10.1146/annurev.bb.02.060173.001105).
- [107] Julien I. A. Voisin, Catherine Mercier, Philip L. Jackson, Carol L. Richards, and Francine Malouin. "Is somatosensory excitability more affected by the perspective or modality content of motor imagery?" *Neuroscience Letters* 493.1 (Apr. 2011). Number: 1, pp. 33–37. ISSN: 0304-3940. DOI: [10.1016/j.neulet.2011.02.015](https://doi.org/10.1016/j.neulet.2011.02.015).
- [108] Julien I. A. Voisin, Erika C. Rodrigues, Sébastien Héту, Philip L. Jackson, Claudia D. Vargas, Francine Malouin, C. Elaine Chapman, and Catherine Mercier. "Modulation of the response to a somatosensory stimulation of the hand during the observation of manual actions." *Experimental Brain Research* 208.1 (Jan. 2011). Number: 1, pp. 11–19. ISSN: 0014-4819, 1432-1106. DOI: [10.1007/s00221-010-2448-3](https://doi.org/10.1007/s00221-010-2448-3).



- [109] Hui Wang, Yunjian Ge, Aiguo Song, Bowei Li, and Baoguo Xu. "The vibro-tactile stimulations experiment to verify the optimal resonance frequency of human's tactile system." *2015 IEEE International Conference on Information and Automation*. Aug. 2015, pp. 2960–2964. DOI: [10.1109/ICInfA.2015.7279795](https://doi.org/10.1109/ICInfA.2015.7279795).
- [110] Jacob Wegelin. "A Survey of Partial Least Squares (PLS) Methods, with Emphasis on the Two-Block Case." *Technical report* (Apr. 2000).
- [111] Sidney Weinstein. "Invitational Lecture: Fifty years of somatosensory research." *Journal of Hand Therapy* 6.1 (Jan. 1993). Number: 1, pp. 11–22. ISSN: 08941130. DOI: [10.1016/S0894-1130\(12\)80176-1](https://doi.org/10.1016/S0894-1130(12)80176-1).
- [112] Herman Wold. "11 - Path Models with Latent Variables: The NIPALS Approach\*\*NIPALS = Nonlinear Iterative Partial Least Squares." *Quantitative Sociology*. Ed. by H. M. Blalock, A. Aganbegian, F. M. Borodkin, Raymond Boudon, and Vittorio Capocchi. International Perspectives on Mathematical and Statistical Modeling. Academic Press, Jan. 1975, pp. 307–357. ISBN: 978-0-12-103950-9. DOI: [10.1016/b978-0-12-103950-9.50017-4](https://doi.org/10.1016/b978-0-12-103950-9.50017-4).
- [113] Jonathan R. Wolpaw, Niels Birbaumer, Dennis J. McFarland, Gert Pfurtscheller, and Theresa M. Vaughan. "Brain–computer interfaces for communication and control." *Clinical Neurophysiology* 113.6 (June 2002), pp. 767–791. ISSN: 1388-2457. DOI: [10.1016/S1388-2457\(02\)00057-3](https://doi.org/10.1016/S1388-2457(02)00057-3).
- [114] Lin Yao, Jianjun Meng, Dingguo Zhang, Xinjun Sheng, and Xiangyang Zhu. "Combining motor imagery with selective sensation toward a hybrid-modality BCI." *IEEE transactions on biomedical engineering* 61.8 (Aug. 2014). Number: 8, pp. 2304–2312. ISSN: 1558-2531. DOI: [10.1109/TBME.2013.2287245](https://doi.org/10.1109/TBME.2013.2287245).
- [115] Thorsten O. Zander and Sabine Jatzev. "Detecting affective covert user states with passive brain-computer interfaces." *2009 3rd International Conference on Affective Computing and Intelligent Interaction and Workshops*. ISSN: 2156-8111. Sept. 2009, pp. 1–9. DOI: [10.1109/ACII.2009.5349456](https://doi.org/10.1109/ACII.2009.5349456).
- [116] Lujia Zhou, Xuewen Tao, Feng He, Peng Zhou, and Hongzhi Qi. "Reducing false triggering caused by irrelevant mental activities in brain-computer interface based on motor imagery." *IEEE journal of biomedical and health informatics* PP (Mar. 2021). ISSN: 2168-2208. DOI: [10.1109/JBHI.2021.3066610](https://doi.org/10.1109/JBHI.2021.3066610).

#### COLOPHON

This document was typeset using the typographical look-and-feel `classicthesis` developed by André Miede and Ivo Pletikosić\*. The style was inspired by Robert Bringhurst's seminal book on typography "*The Elements of Typographic Style*". `classicthesis` is available for both  $\LaTeX$  and  $\text{LyX}$ :

<https://bitbucket.org/amiede/classicthesis/>

Happy users of `classicthesis` usually send a real postcard to the author, a collection of postcards received so far is featured here:

<http://postcards.miede.de/>

Thank you very much for your feedback and contribution.

*\* the author of the present document has modified various part of the typographical style.*